



**Molecular-Genetics Studies of Organophosphate
Induced Neurodegeneration in Differentiating
Mammalian Cell lines and Neural Progenitor
Stem Cells**

Najiah Alyamani

A thesis submitted in partial fulfilment of the requirements of
Nottingham Trent University for the degree of Doctor of
Philosophy

March 2018

In loving memory of my true love my Dad

Copyright statement

This work is the intellectual property of the author.

Najiah Alyamani

Declaration

I certify that all the work submitted of this thesis was carried out by me, except the publish reports of other works which have been clearly stated in the text. Acknowledgement has been made for assistance received under the supervision of my supervisors and guidance of colleagues helped. I further declare that this research has not previously accepted to ward of any other degree.

Signed (Candidate) Date 14/ 03/ 2018

Signed (Director of Studies) Date 14/ 03/ 2018

"In the name of God, the Most Gracious, the Most Merciful" ...

Acknowledgments

From bottom of my heart I would like to thank Allah for being with me all way and all his gifts that made me the person I am today.

I would like to express my sincere gratitude to my supervisors Dr. Alan J. Hargreaves, and Dr. Cristina Montiel-Duarte for all their help and support during my studies. They made this experience, in which I felt the development in my way of thinking and personality, very special. Their presence and support were very valuable and made this work more interesting and accomplished.

I would also like to acknowledge King Abdulaziz University and Saudi Cultural Bureau in London, who sponsored my scholarship.

At this stage, I would like to thank Wayne for his help especially in my first year. Special thanks to Biola and Reham for all the help and support. Many thanks for my lab mate Rmaya for her guides and comments. Special thanks to all my friends and colleagues in King Abdulaziz University in Jeddah and Nottingham Trent University who made this experience more enjoyable.

Finally, words cannot express my deepest feelings and emotions to my mom, who surrounded me with all her love, her prayer and support throughout my entire life. My deepest thanks to my sisters who were always surrounding me with all their love.

Thanks Allah for passed all difficulties I faced to achieve my dream.

Abstract

Organophosphorus (OP) pesticides are widely used despite evidence they cause neurotoxicity after exposure. The primary target for OPs is acetylcholinesterase, but there is evidence they can inhibit other cellular proteins including cytoskeletal and axon growth associated proteins, which are implicated in nervous system development. Furthermore, little is known about the ability of OPs to cause genotoxicity.

The objectives of this study were to evaluate the effects of selected OPs on neurite outgrowth, expression of cytoskeletal proteins and associated gene expression levels, and to investigate histone deacetylation (HDAC) activity in three types of differentiating cell models. The initial findings indicated that cell viability was unaffected by exposure to 1, 3 and 10 μ M CPF, CPO and PSP in N2a and C6 cells. A high content assay was sensitive enough to rapidly detect and quantify morphological changes, including inhibition of neurite number and length.

Western blot and ELISA analysis in N2a and C6 cells revealed reduced levels of the selected cytoskeletal and associated regulatory proteins (MAP-2, Tau, β III-tubulin, GAP-43, NFH and GFAP) following the treatment with at least one concentration of CPF, CPO and PSP, which could be linked to the inhibition of neurite outgrowth. Using quantitative RT-PCR analysis on the total RNA of the genes *MAP-2*, *TUBB3*, *MAPT*, *NEFH*, *GAP-43*, and *GFAP* showed a good correlation between the altered protein expression and regulation of gene levels for most markers, which suggests these OPs can cause genotoxic effects. Increased levels of HDAC activity were observed for all OPs in rodent cell lines, suggesting that epigenetic effects may be at least partly involved in some gene expression changes.

RT-PCR analysis of *TUBB3*, *NEFH*, and *GFAP* was also carried out in ReNcell CX cells, a co-culture of neuronal and glial cells, and showed down-regulation of gene levels for at least one concentration of all the OPs, as well as increasing the level of HDAC activity in a similar pattern to the results for N2a and C6 cells.

Taken together, the data in this thesis suggest a novel action of OPs altering HDAC activity, which can be correlated to some of the observed changes in gene and protein levels of selected cytoskeletal and associated regulatory proteins that can be linked to the observed disruption of neurite outgrowth and neural development. Further work is needed to identify other molecular targets involved in these phenomena, particularly when there is no correlation with HDAC activity changes.

List of Abbreviations

Ach	Acetylcholine
AChE	Acetylcholinesterase
ACP	Advisory Committee of Pesticides
AD	Alzheimer's disease
ADF	Actin depolymerizing factor (cofilin)
AIDA	Advanced Image Data Analyser software
APS	Ammonium persulphate
ATP	adenosine triphosphate
BCA	Bicinchoninic acid
Bp	Base pair
BSA	Bovine serum albumin
BW	body weight
CNS	the central nervous system
COPIND	chronic OP induced neuropsychiatric disorder
CPF	Chlorpyrifos
CPO	chlorpyrifos oxon
CYP	Cytochrome
Ct	cycle threshold
dbcAMP	dibutyl cyclic 3',5'-monophosphate
DDT	Dichlorodiphenyltrichloroethane
DEP	Diethylphosphate
DETP	Diethylthiophosphate
DMEM	Dulbecco's modified Eagle's medium
DMSO	Dimethylsulphoxide
DNA	Deoxyribonucleic acid
ECACC	European Collection of Animal Cell Cultures
ECL	Enhanced chemiluminescence reagent
ECM	extracellular matrix
ECM	extracellular matrix protein
EGF	Recombinant human epidermal growth factor
ELISA	enzyme linked immunosorbent assay
EPA	U.S. Environmental Protection Agency
ER	Endoplasmic reticulum
FBS	Foetal bovine serum
FGFb	Recombinant human fibroblast growth factor b
GAP-43	Growth associated protein-43
GAPDH	Glyceraldehyde 3-phosphate dehydrogenase
GDNF	Glial-derived neurotrophic factor
GFAP	Glial fibrillary acidic proteins
GTP	Guanosine triphosphate
H ₂ O ₂	Hydrogen peroxide
H ₂ SO ₄	Sulphuric acid
HDAC	Histone deacetylases assay
HRP	Horseshoe peroxidase secondary antibody conjugate
HTS	High throughput screening

I.P	Intra peritoneal
IC50	Half maximum inhibitory concentration
IFs	Intermediate filaments
KCl	Potassium chloride
kDa	Kilo Dalton
KH ₂ PO ₄	Monopotassium phosphate
LD	Lethal dose
Lys40	lysine at position 40
MAPK	Mitogen-activated protein kinase
MAPs	Microtubule associated proteins
MBP	Myelin-basic protein
MFs	Microfilaments
MN	Micronuclei
MS	Multiple sclerosis
MTOCs	Microtubule organising centres
MTs	Microtubules
MTT	3-(4,5-Dimethylthiazol-2-yl)-2,5 diphenyltetrazolium bromide
N2a	Mouse neuroblastoma 2A
Na ₂ HPO ₄	Disodium phosphate
NaB	Sodium butyrate
NaCl	Sodium chloride
NaOH	Sodium hydroxide
NCFAP	National Centre for Food and Agriculture Policy
NF	Neurofilament proteins
NFH	Neurofilament heavy chains protein
NFL	Neurofilament light chains
NFM	Neurofilament medium chains
NTE	Neuropathy target esterase
OP	Organophosphate
OPIDN	Organophosphate-induced delayed neuropathy
OPs	Organophosphates
PBS	Phosphate buffered saline
PC12	Rat PC12 pheochromocytoma cell line
PCE	polychromatic erythrocyte
PI-3K/PKB	phosphoinositide-3-kinase/protein kinase B
PMSF	Phenylmethylsulfonyl fluoride
PNS	Peripheral nervous system
PON1	Paraoxonase 1
PSP	Phenyl saligenin phosphate
PMSF	Phenylmethylsulfonyl fluoride
qPCR	Quantitative real time polymerase chain reaction
RB	Electrophoresis running buffer
ReNcell CX	Human neural progenitor cell line
RNA	Ribonucleic acid
ROS	Reactive oxygen species
Rps18	RPS18 ribosomal protein S18
RT-PCR	Reverse transcription polymerase chain reaction
SCE	Sister chromatid exchange

SCOTP	Saligenin cyclic-o-tolyl phosphate
SDS	Sodium dodecyl sulphate
SEM	Standard error of mean
Ser-444	Serine at residue 444
SENSOR	Sentinel Event Notification System for Occupational Risks
TAE	Tris- Acetate-EDTA buffer
TBS	Tris-buffered saline
TCP	3,5,6-trichloro-2-pyridinol
TEMED	N,N,N,N-Tetramethylethylene diamine
TEPP	Tetraethyl pyrophosphate
the USA	The United States
TMB	3,3',5,5'-Tetramethylbenzidine
TOCP	Tri-ortho cresyl phosphate
TOTP	Tri- <i>ortho</i> -tolyl phosphate
Tween	Polyoxyethylene sorbiton monolaurate
UK	The United Kingdom
WHO	World Health Organisation
β III-tubulin	The class III β -tubulin isotype
β -ME	β -mercaptoethanol

Research publications and scientific meetings arising from this thesis

Publications:

1. Alyamani, N., Montiel-Duarte, C. and Hargreaves, A. J. (2016) Molecular studies of organophosphate toxicity in cultured neural cells, *FEBS Journal* , 283 (1), abstract no: 90, pp.405-406. doi:10.1111/febs.13808.

Scientific meetings:

1. Molecular studies of organophosphate toxicity in cultured neural cell (Oral presentation and poster), abstract no: 8, pp.21. 9thannual research (STAR) conference, 6-7 May 2015, Nottingham Trent University, Nottingham, UK.
2. Genotoxic effects of organophosphorous compounds on the expression of neural marker genes in differentiating neural cells (poster). London Chromatin Meeting, Organizers: Andy Bannister (University of Cambridge) and Abcam, 10th November 2017. University College London, London, UK.
3. Organophosphorous Compounds-Induced Neurodegeneration in Differentiating Mammalian Neural Cell Lines (poster), abstract no: 6, pp.34. *In vitro* toxicology society (IVTS), Senate House Building of University of London, 23-24 November 2017, London, UK.
4. Phenyl Saligenin Phosphate Induced Neurodegeneration in Differentiating Mouse N2a cells (poster), abstract no: 1, pp.58. ESACT-UK's 28th Annual Meeting of the UK Society for Cell Culture and Biotechnology, at 10th - 11th January 2018, Leeds, UK.

Table of Contents

Chapter 1 Introduction	
1.1 Major cell types in the nervous system	1
1.1.1 Neurons	1
1.1.2 Glial cells	1
1.2 Historical overview of organophosphates	5
1.3 Organophosphorus insecticides and pesticides	5
1.4 Chlorpyrifos	7
1.4.1 Chemical structure and physical properties	7
1.4.2 Routes of exposure to chlorpyrifos	8
1.4.3 Metabolic pathway of chlorpyrifos to chlorpyrifos-oxon	10
1.5 Phenyl saligenin phosphate	11
1.6 The acute toxicity of organophosphates in the nervous system	12
1.7 Acute cholinergic syndrome	15
1.8 Intermediate syndrome	18
1.9 Organophosphate-induced delayed neuropathy (OPIDN)	18
1.10 Other chronic neurological conditions associated with OP exposure	21
1.11 Effects of OPs on cytoskeletal proteins	22
1.11.1 Cellular and cytoskeletal proteins as molecular targets of CPF, CPO and PSP toxicity	22
1.11.2 Microtubules	23
1.11.3 Intermediate filaments	28
1.11.4 Glial fibrillary acidic proteins	31
1.11.5 Microfilaments and GAP-43	32
1.12 Genotoxic effects of organophosphorus compounds	33
1.12.1 CPF, CPO and PSP associated genotoxicity	34
1.13 The use of <i>in vitro</i> mammalian cell line models for assessment of organophosphate induced neurotoxicity	37
1.13.1 N2a neuroblastoma cell line	39
1.13.2 C6 rat glioma cell lines	40
1.13.3 Human neural progenitor stem cells (ReNcell CX)	41
1.14 Summary	42
1.15 Project Aims	44
Chapter 2 Material and Methods	
2.1 Materials	45
2.1.1 General laboratory reagents	45
2.1.2 Plastic ware	47
2.1.3 Test compounds	48
2.1.4 Cell lines	48
2.2 Methods	49
2.2.1 Cell culture and maintenance of N2a neuroblastoma cells and rat C6 glioma cells	49
2.2.2 Human neural ReNcell CX stem cell culture and maintenance	50
2.2.3 Cryopreservation of cell lines	51
2.2.4 Cell recovery from liquid nitrogen storage	51
2.2.5 Cell plating for experimentation	52
2.2.6 Induction of cell differentiation	54
2.2.7 Measurement of cell viability in cells exposed to OPs	55
2.2.8 Morphological measurements of fixed differentiated N2a and C6 cells	56
2.2.9 Indirect immunofluorescence staining	57
2.2.10 Image acquisition and analysis	59

2.2.11 Preparation of N2a and C6 cell lysates for one dimensional polyacrylamide gel electrophoresis (SDS-PAGE).....	60
2.2.12 One dimensional polyacrylamide gel electrophoresis (SDS-PAGE).....	62
2.2.13 Western blotting.....	66
2.2.14 Enzyme linked immunosorbent assay (ELISA).....	70
2.2.15 Reverse transcription polymerase chain reaction (RT-PCR).....	71
2.2.16 Quantitative PCR (qPCR).....	77
2.2.17 Histone deacetylases assay (HDAC).....	79
2.2.18 Statistical analysis.....	81
Chapter 3 Cytotoxic Effects of Organophosphate Compounds on Differentiating Mouse N2a Neuroblastoma and C6 Glioma Cells	
3.1 Introduction.....	82
3.2 Aims.....	85
3.3 Effects of CPF, CPO and PSP on the viability of differentiating N2a cells	86
3.4 Effects of CPF, CPO and PSP on the viability of differentiating C6 cells	86
3.5 Effects of CPF, CPO and PSP on N2a and C6 cell growth.....	89
3.6 Effects of CPF, CPO and PSP on N2a cell morphology.....	92
3.7 Development of high content screening assay of neurite outgrowth	95
3.8 Monitoring multi-parameters of neurite outgrowth in differentiating N2a cells	98
3.9 Monitoring multi-parameters of neurite outgrowth in differentiating C6 cells	103
3.10 Effect of CPF, CPO and PSP on cytoskeletal organization in cultured differentiating N2a and C6 cells.....	107
3.11 Discussion.....	117
Chapter 4 Effects of Organophosphates on Cytoskeletal and Associated Regulatory Proteins in Differentiating N2a Neuroblastoma and C6 glial Cells.....	
4.1 Introduction.....	122
4.2 Aims.....	124
4.3 Effects of CPF, CPO and PSP on the expression level of GAPDH in N2a and C6 cell line.....	125
4.4 Effects of CPF, CPO and PSP on the expression levels of microtubule proteins in differentiating N2a cells.....	126
4.5 Effects of CPF, CPO and PSP on the expression levels of neurofilament and growth associated proteins in N2a cells.....	128
4.6 Effects of CPF, CPO and PSP on the expression levels of glial fibrillary acid protein in C6 cells.....	131
4.7 Determination of concentration-response effects of CPF, CPO and PSP on cytoskeletal and associated regulatory proteins using cell ELISA	133
4.8 Discussion.....	138
Chapter 5 Genotoxicity of Organophosphate Compounds Chlorpyrifos, Chlorpyrifos Oxon and Phenyl Saligenin Phosphate on Differentiating Mammalian Cell Lines.....	
5.1 Introduction.....	143
5.2 Aims.....	145
5.3 Results.....	146
5.3.1 Primer validation.....	146
5.3.2 Housekeeping genes.....	149
5.3.3 Effect of CPF, CPO and PSP on neural markers in mammalian cell lines.....	151
5.3.4 Effect of CPF, CPO and PSP on <i>GFAP</i> expression in differentiating C6 cells.....	158
5.3.5 Histone deacetylase (HDAC) activity upon exposure to CPF, CPO and PSP in differentiating neuronal cells.....	161
5.4 Discussion.....	164
Chapter 6 Organophosphate Toxicity in a Human Neural Progenitor Stem Cell Model.....	
6.1 Introduction.....	171
6.2 Results.....	173
6.2.1 Cell viability in the presence of organophosphates.....	173

6.2.2 Primer validation.....	176
6.2.3 Effect of CPF, CPO and PSP on neuronal markers in ReNcell CX cell line.	178
6.2.4 Glial fibrillary acidic protein (GFAP).....	180
6.2.5 Histone deacetylases (HDAC) activity upon exposure to CPF, CPO and PSP in differentiating RenCellCX cells.....	183
6.3 Discussion.....	184
Chapter 7	
7.1 General Discussion	188
7.2 Conclusions.....	198
7.3 Future work.....	198
References	202
Appendix	229

List of Figures

Figure 1.1. Schematic representation of neural cell types.	3
Figure 1.2. Chemical structure of (A) general organophosphate structure, (B) chlorpyrifos.	8
Figure 1.3. Representation of the metabolism of CPF.	11
Figure 1.4. Inhibition of AChE by organophosphates.	14
Figure 1.5. Classification of organophosphate toxicity.	15
Figure 1.6. Representation of interactions between esterases and OPs.	17
Figure 1.7. Microtubule structure and composition.	23
Figure 1.8. Structure of intermediate filament protein subunits.	30
Figure 1.9. Schematic representation of neural stem cell differentiation.....	42
Figure 2.1. Graphical protocol of the steps involved in RNA extraction.....	74
Figure 2.2. Phase contrast microscopy images of homogenised cells for nuclear extraction.	80
Figure 3.1. Effects of CPF, CPO and PSP on MTT reduction in differentiating N2a cells after 24 h.	87
Figure 3.2. Effects of CPF, CPO and PSP on MTT reduction in differentiating C6 cells after 24 h.	88
Figure 3.3. Effects of CPF, CPO or PSP on the cell number and viability of differentiating N2a cells.	90
Figure 3.4. Effects of CPF, CPO or PSP on the number and viability of differentiating C6 cells...91	
Figure 3.5. Effects of CPF, CPO or PSP on the morphology of differentiating N2a cells.	94
Figure 3.6. Segmentation of stained differentiating N2a and C6 cells using high throughput screening assay.....	97
Figure 3.7. Effects of CPF, CPO and PSP on cell number and cell body area in differentiating N2a cells as assessed by high throughput assays.....	99
Figure 3.8. Effects of CPF CPO or PSP on average intensity of staining and percentage of cells with significant outgrowth in co-differentiated N2a cells as assessed by high throughput analysis.	100
Figure 3.9. Effects of CPF, CPO or PSP on maximum and average neurite length/cell in differentiating N2a cells as assessed by high throughput analysis.	102
Figure 3.10. Effects of CPF CPO or PSP on multiple parameters in co-differentiated C6 cells as assessed by high throughput analysis.....	105
Figure 3.11. Effects of CPF CPO or PSP on multiple parameters in co-differentiated C6 cells as assessed by high throughput analysis.....	106
Figure 3.12. Indirect immunofluorescence staining of CPF effects on β III tubulin staining of differentiating N2a cells as detected by EVOS cell imaging system.....	108
Figure 3.13. Indirect immunofluorescence staining of CPO effects on β III tubulin staining of differentiating N2a cells as detected by EVOS cell imaging system.....	109
Figure 3.14. Indirect immunofluorescence staining of PSP effects on β III tubulin staining of differentiating N2a cells as detected by EVOS cell imaging system.....	110
Figure 3.15. Indirect immunofluorescence staining of CPF effects on NFH staining of differentiating N2a cells as detected by EVOS cell imaging system.....	111
Figure 3.16. Indirect immunofluorescence staining of CPO effects on NFH staining of differentiating N2a cells as detected by EVOS cell imaging system.....	112
Figure 3.17. Indirect immunofluorescence staining of PSP effects on NFH staining of differentiating N2a cells as detected by EVOS cell imaging system.....	113
Figure 3.18. Indirect immunofluorescence of CPF effects on anti-GFAP staining co-differentiated C6 cells as detected by EVOS cell imaging system.....	114
Figure 3.19. Indirect immunofluorescence of CPO effects on anti-GFAP staining co-differentiated C6 cells as detected by EVOS cell imaging system.....	115
Figure 3. 20. Indirect immunofluorescence of PSP effects on anti-GFAP staining co-differentiated C6 cells as detected by EVOS cell imaging system.....	116

Figure 4.1. Detection of microtubule proteins by Western blots of differentiating N2a cell lysates.	127
Figure 4.2. Detection of neurofilament and growth associated proteins by Western blots of differentiating N2a cell lysates.	129
Figure 4.3. Detection of Glial fibrillary acidic protein by Western blots of differentiating C6 cell lysates.....	131
Figure 4.4. Effects of CPF, CPO and PSP on microtubule proteins in differentiating N2a cells as determined by cell ELISA.	134
Figure 4.5. Effects of CPF, CPO and PSP on neurofilament and growth associated proteins in differentiating N2a cells as determined by cell ELISA.	136
Figure 4.6. Effects of CPF, CPO and PSP on glial fibrillary acidic protein in differentiating N2a cells as determined by cell ELISA.	137
Figure 5.1. Analysis of genes of interest in mitotic and differentiating N2a cells by PCR.	148
Figure 5.2. Analysis of other neurofilament genes of interest in mitotic and differentiating N2a cells by PCR.	149
Figure 5.3. GFAP expression in mitotic and differentiating C6 cells.	149
Figure 5.4. Ct values obtained for GAPDH and Rps18 expression (qPCR) in differentiating N2a cells after different OP treatments.	150
Figure 5.5. Ct values obtained for GAPDH and Rps18 expression in C6 cell line.....	151
Figure 5.6. Relative expression of <i>MAP-2</i> mRNA in differentiating N2a cells after CPF, CPO and PSP exposure as determined by quantitative PCR.....	152
Figure 5.7. Relative expression of <i>TUBB3</i> mRNA in differentiating N2a cells after CPF, CPO and PSP exposure as determined by quantitative PCR.....	154
Figure 5. 8. Relative expression of <i>MAPT</i> (Tau) mRNA in differentiating N2a cells after CPF, CPO and PSP exposure as determined by quantitative PCR.	155
Figure 5. 9. Relative expression of <i>NEFH</i> mRNA in differentiating N2a cells after CPF, CPO and PSP exposure as determined by quantitative PCR.....	156
Figure 5. 10. Relative expression of <i>GAP43</i> mRNA in differentiating N2a cells after CPF, CPO and PSP exposure as determined by quantitative PCR.....	158
Figure 5. 11. Relative expression of <i>GFAP</i> mRNA in differentiating C6 cells after CPF, CPO and PSP exposure as determined by quantitative PCR.....	159
Figure 5.12. Effects of CPF, CPO and PSP on HDAC activity in differentiating N2a cells.	162
Figure 5.13. Effects of CPF, CPO and PSP on total HDAC activity differentiating C6 cells	163
Figure 6.1. Effects of CPF (A), CPO (B) and PSP (C) on MTT reduction in differentiating ReNcell CX cells.....	174
Figure 6.2. Effects of CPF, CPO or PSP on the morphology of differentiating ReNcell CX cells.....	175
Figure 6.3. Confirmation of PCR for genes of interest in mitotic and differentiating ReNcell CX cells.	178
Figure 6.4. Expression of <i>TUBB3</i> mRNA in differentiating ReNcell CX cells after CPF, CPO and PSP exposure, as determined by quantitative qPCR.	179
Figure 6. 5. Expression of <i>NEFH</i> mRNA in differentiating ReNcell CX cells after CPF, CPO and PSP exposure as determined by quantitative qPCR.....	180
Figure 6.6. Expression of <i>GFAP</i> mRNA in differentiating ReNcell CX cells after CPF, CPO and PSP exposure as determined by quantitative qPCR.....	181
Figure 6.7. Effects of CPF, CPO and PSP on HDAC activity in differentiating ReNcell CX cells.	183
Figure 7.1. Schematic diagram of common CPF, CPO and PSP impacts on neural cells.	200

Figure 8.1. Dose estimation of the effects of CPF,CPO and PSP on MTT reduction in differentiating N2a cells after 24 h.	229
Figure 8.2. Dose estimation of the effects of CPF,CPO and PSP on MTT reduction in differentiating C6 cells after 24 h.	230
Figure 8.3. Electropherogram data for MAP2 (panel A), TUBB3 (panel B), MAPT (panel C), NEFH (panel D) and GAP43 (panel E) PCR sequenced product in N2a cell lines.	231
Figure 8.4. Electropherogram data for GFAP PCR sequenced product in C6 cell lines.....	232
Figure 8.5. Sequences alignments.	232
Figure 8.6. Sequences alignments.	233
Figure 8.7. Electropherogram data for NEFM (panel A) and NEFL (panel B) PCR sequenced product in N2a cell lines.	233
Figure 8.8. Sequences alignments.	233

List of Tables

Table 1.1. Acetylcholine receptors, subtypes and location (Adopted from Tata <i>et al.</i> , 2014).....	13
Table 1.2. Major microtubule cytoskeleton proteins of the nervous system and their regulation (Adopted from Luduena, 1993).	25
Table 1.3. Intermediate filament classification.	29
Table 2.1. List of cell culture reagents.....	45
Table 2.2. List of other reagents and materials.	46
Table 2.3. The cell density of N2a, C6 and ReNcell CX cell lines for the experiments of current study.	54
Table 2.4. List of primary antibodies used for indirect immunofluorescence staining.....	57
Table 2.5. Secondary antibodies for indirect immunofluorescence staining	58
Table 2.6. BSA protein standards for protein estimation.....	62
Table 2.7. Reagent volumes required for preparation of SDS-PAGE resolving gel for two mini gels	65
Table 2.8. Reagent volumes required for preparation of SDS-PAGE stacking gel for two mini gels	65
Table 2.9. List of primary antibodies used for Western Blot and ELISA assay	67
Table 2.10. Secondary antibodies for probing Western blot.....	67
Table 2.11. List of reverse transcription polymerase chain reaction reagents	72
Table 2.12. Final volumes and amounts of cDNA synthesis components	75
Table 2.13. Volumes and final concentrations of the components for RT-PCR.....	76
Table 2.14. Settings of thermal cycler for PCR.	76
Table 2.15. Volumes and amounts of the components used in qPCR.	78
Table 2.16. Quantitative RT-PCR protocol	78
Table 2.17. List of nuclei extraction buffers for HDAC assay	79
Table 2.18. Assay incubation setup	81
Table 3.1. Quantification of neurite outgrowth in differentiating N2a cells.....	93
Table 4.1. Densitometric analysis of Western blots probed with antibody to GAPDH protein in N2a and C6 cell lines.....	126
Table 4.2. Densitometric analysis of Western blots probed with antibodies to microtubule proteins in N2a cell lines.	128
Table 4.3. Densitometric analysis of Western blots probed with antibodies to neurofilament and growth associated proteins in N2a cell lysates.....	130
Table 4.4. Densitometric analysis of Western blots probed with antibodies to glial fibrillary acid protein (GFAP) in C6 cells.	132
Table 5.1. Designed primers targeting N2a and C6 cell lines neuronal markers.	147
Table 5.2. Summary of OP effects on neural marker gene expression relative to <i>GAPDH</i>	160
Table 6.1. Primer sequences and standardised PCR optimisation protocols for the amplification of specific neural markers genes	177
Table 6.2. Summary of OP effects on human neural marker genes relative to <i>GAPDH</i>	182

Chapter 1

Introduction

1.1 Major cell types in the nervous system

The nervous system in mammals is composed of two main cell types, the glial and neuronal cells, both of which play important roles in the regulation of neural function. Neuronal cells are involved in the transmission of information to neighbouring cells, which may be either neurons or effector cells, via electrical impulses that travel along axons (Alberts *et al.*, 1983). Glial cells do not play a direct role in such information processing; their main roles include providing structural, homeostatic, and defensive support to neurons (Barone *et al.*, 2000). These functionally and morphologically distinct cells act together to sustain the correct functioning of the nervous system; it is therefore important to understand the basic properties of these cells in order to better understand the effects of neurotoxins *in vivo* (Brown, 1991).

1.1.1 Neurons

As neurons regulate neurotransmission, any effect of a neurotoxin on this cell type may have a large effect on the nervous system. Neurons are responsible for the perception of and response to stimuli, and they also transmit cellular signals to other neighbouring cells through synaptic transmission (Barres and Barde, 2000). Neurons are highly polarised cells that produce dendrites and axons upon differentiation. The structural and morphological features of axons reflect their role in neurotransmission and the need for a system to mediate axonal transport (Barres and Barde, 2000).

The structure of the differentiated neuronal cells displays three key features: the growth cone, axon and cell body. Within the cell body are located the nucleus and the cytoplasmic organelles including ribosomes and the endomembrane system (Wilson and Hunt, 2014). The axon is a long projection that extends from the cell body; this structure is vital for neurotransmission and axonal transport. The actual length of the axon varies and can measure up to one thousand times longer than the cell body (Alberts *et al.*, 1983). Further information about these morphological features can be determined by studying cultured neuronal cells induced to differentiate in a controlled environment (Henschler *et al.*, 1992; Flaskos *et al.*, 1994; 1998; Schmuck and Ahr, 1997).

1.1.2 Glial cells

The second most important type of cells, and the most numerous in the nervous system is the glial cell. Glial cells include all neural cells that do not transmit electrical signals (Compston *et al.*, 1997). They are not directly involved in signal transduction, but the

interest in glia has increased due to their multiple roles, including providing defensive, homeostatic, structural, and nutritional support to neurons (Barone *et al.*, 2000). The actual number of glial cells in the nervous system is much greater than neuronal cells; approximately 90 % of the cells in the human brain are glial cells (Allen and Barres, 2009).

Glia comprises a heterogenous array of cell types from different origins that have specific functions and morphologies (Compston *et al.*, 1997). The cell types include microglia, oligodendrocytes and astrocytes in the central nervous system (CNS), and enteric glia and Schwann cells in the peripheral nervous system (PNS) (Figure 1.1) (Allen and Barres, 2009).

Glial cells, except microglia, originate from the neuroectoderm, and mainly develop after neurogenesis. Microglial cells are derived from the immune system and reach the brain via blood circulation during development (Allen and Barres, 2009). Astrocytes and oligodendrocytes can be found in differentiating neural stem cell cultures, which allows them to be studied *in vitro* (Compston *et al.*, 1997; Rice and Barone, 2000).

In the PNS, Schwann cells consist of two types, myelinating and non-myelinating cells. The myelinating cells have a similar function and structure to oligodendrocytes in the CNS; they produce an insulating sheath around axons. The non-myelinating Schwann cells provide metabolic and mechanical support for neurons. Enteric glia have an essential role in synaptic transmission and are located in the autonomic ganglia (Jessen, 2004).

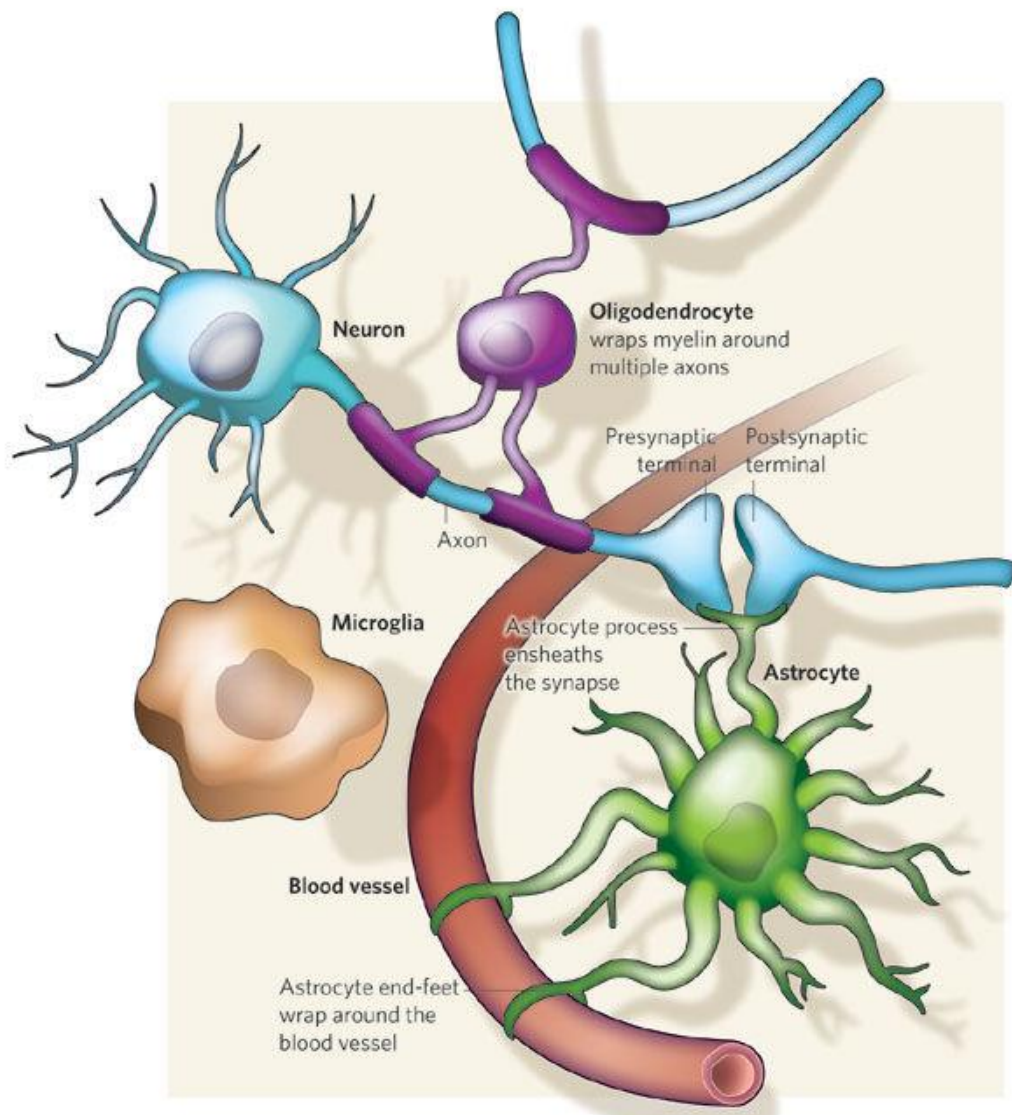


Figure 1.1. Schematic representation of neural cell types.

The interaction between glia cells and neurons with blood vessels. Adopted from Allen and Barres (2009).

1.1.2.1 Microglia

Microglia is prenatally derived from mesodermal (myeloid) tissue (Chan *et al.*, 2007). They have a protective role as specialised brain macrophages, in that they clean up cellular debris, check the brain for damage or infections, eliminate inadequate synapses and digest dead neurons that have undergone apoptosis (Compston *et al.*, 1997; Allen and Barres, 2009).

In some neurodegenerative disorders, for example Alzheimer's disease (AD), microglia become activated, which changes the phenotype to amoeboid and this increases their phagocytic function (de la Torre, 2002; Grammas *et al.*, 2002; Nakamura, 2002; Allen and Barres, 2009).

1.1.2.2 Oligodendrocytes

Oligodendrocytes synthesise the myelin sheath around axons, which is an insulating membrane that provides support and improves electrical signal transmission efficiency and speed (Compston *et al.*, 1997; Allen and Barres, 2009). Due to their important role, any toxicity towards these cells could greatly affect the development of insulated neurons in mammals (Sachana *et al.*, 2008). In some neurodegenerative disorders, such as multiple sclerosis (MS), the myelin sheath produced by the oligodendrocyte undergoes an autoimmune attack, resulting in demyelination of the axons (Antel, 2006). Other studies have suggested that loss of this type of glial cell can be linked to clinical depression (Allen and Barres, 2009).

1.1.2.3 Astrocytes

Originally, it was thought the main function of astrocytes was to regulate the levels of extracellular potassium ions in neurons (Orkand *et al.*, 1966). However, it is now known that astrocytes carry out several important roles that support the functionality of neurons; they can guide neuronal migration, differentiation and proliferation, help in assembly and formation of synapses during central nervous development, neurite outgrowth generation, supply the neurons with energy, guidance for axons, and help to maintain the trophic and ionic balance of neurons and the extracellular environment (Guerri and Renau-Piqueras, 1997; Aschner *et al.*, 1999; Allen and Barres, 2009). Astrocytes also help to regulate the formation of the blood-brain barrier and they can respond to neural injury by secreting neurotrophic factors, including glial-derived neurotrophic factor (GDNF) (Barres and Barde, 2000).

Astrocytes can also act as physical barriers; they separate synaptic connections between neighbouring neurons, and they can recycle neurotransmitters, which protects the neurons from excitotoxicity (Hassel *et al.*, 1997; Hertz *et al.*, 1999). Astrocytes are in contact with neurons and blood vessels, which means that the calcium response that activates the astrocytes after neuronal activity, can be used to modulate the ability of blood vessels to regulate blood flow (Zonta *et al.*, 2003). This allows for more oxygen and glucose to be transported to the neurons (Allen and Barres, 2009). The intake of glutamate by astrocytes can induce glycolysis leading to elevated lactate production, which can be used by neurons as an energy source (Tsacopoulos and Magistretti, 1996). Astrocytes can also protect neurons from oxidative stress by releasing antioxidants including glutathione (Sagara *et al.*, 1993). Thus, the different types of neuronal and glial cells act cooperatively in the

regulation of neural function and the targeting of any one of them by neurotoxins such as organophosphates could have a detrimental effect on the nervous system.

1.2 Historical overview of organophosphates

Organophosphorous compounds (OPs) are a group of synthetic chemical compounds formed by a reaction between a phosphoric acid and alcohol. They were first synthesised in the 19th century (Singh and Khurana, 2009). Historically, OPs have been used in a range of agricultural, industrial and domestic settings, with a wide range of applications, but as more investigations were carried out it became clear that these types of compounds were toxic to mammals, causing different levels of neurotoxicity depending on the dose, age and route of exposure. OPs were developed as insecticides and pesticides in 1940 when Schrader's group developed around 2000 compounds, including chemical warfare agents like sarin and tabun and pesticides such as parathion (Antonijevic and Sojiljkovic, 2007).

1.3 Organophosphorus insecticides and pesticides

Pesticides are mainly used to control insect damage in agricultural crops; they are mixtures of chemicals and the OP insecticides are the most widely used (Gupta, 2006; Gennari *et al.*, 2015). The worldwide consumption of pesticides is significant; it is estimated to be more than five billion pounds per year (Gupta, 2006; Gennari *et al.*, 2015).

Although the main use of OPs is in agriculture, they are not restricted to this category; they are also used in many residential, medical, and industrial settings, including use as solvents, lubricants, and fire retardants as well as insecticides (Hargreaves, 2012). In the year 2005, it was estimated that 2 billion tonnes of OP insecticides, including chlorpyrifos (CPF), were applied to agricultural fields across the world; only a small proportion of this actually targeted pests, and the rest ended up polluting the environment (Gavrilescu *et al.*, 2015).

A European study has helped to highlight how widespread the problem of OP pollution is; it is reported that different food products including processed food and baby food were contaminated with more than 250 different OPs (EC, 2005). In addition, the study found that approximately 50 % of the cereals, fruits, and vegetables from Europe contained OP residues (EC, 2005). These findings of overuse and pollution were supported by a study from the USA, which reported that in 1995, approximately 11 million kg of OP compounds (primarily diazinon, malathion, and CPF) were used to produce agricultural crops, with commercial and residential properties using 6 to 9 million kg of insecticidal OP compounds in the same year (Aspelin, 1997).

The widespread overuse of OPs and their potential adverse effects pose a significant risk to public health; it is not only agricultural workers that are at risk of exposure to these insecticides; due to pollution, the general population are also at risk (Mearns *et al.*, 1994; Stephens *et al.*, 1995). Different epidemiological studies have all shown that there is repeated exposure in the majority of people to low concentrations of OPs, due to interaction with the environment and also through food sources. Over the long-term this exposure may cause chronic nervous system damage (Mearns *et al.*, 1994; Stephens *et al.*, 1995).

This prolonged low level exposure to OPs, together with increased reports of acute pesticide poisoning is a major public health concern. Globally, around three million people suffer accidental acute pesticide poisoning, which results in around 346,000 deaths per year (WHO, 2008). A report by the World Health Organisation (WHO) highlighted that each year there are 2 million cases of pesticide poisoning which results in approximately 370,000 deaths worldwide (Gunnell *et al.*, 2007). The US Sentinel Event Notification System for Occupational Risks (SENSOR) pesticide program has shown that nearly 50 % of the acute pesticide related illnesses were caused by OP insecticides (Calvert *et al.*, 2004). The incidence of acute poisoning related deaths in the UK and other western countries is relatively low (Jamal, 1995), but this is in contrast to developing countries, where the rate is significantly higher, with estimates of over 300,000 deaths/year. The increased rate is influenced by the higher use of OP pesticides, combined with a lack of strict regulations, and limited knowledge of safety procedures in developing countries (Carlton *et al.*, 2004; WHO, 2008).

Due to their widespread use and potential impacts on public health, there have been suggestions by regulatory authorities in some developed countries that OP compounds should be tightly regulated, including imposition of restrictions or bans on their uses. For example, in the USA the Environmental Protection Agency (EPA) in 2000 completely banned CPF for domestic use due to its proven developmental neurotoxicity (EPA, 2000). The Advisory Committee of Pesticides (ACP) in the UK also raised concerns over the potential toxicity of CPF and its impact on public health and food safety (ACP, 2002). Based on these recommendations, the use of CPF in a household setting has been stopped and it was restricted to agricultural application only in some countries (Colborn, 2006). As mentioned previously, a recent study by the EPA recommended that the use of most of OPs should be banned not only in household but in agriculture as well due to the toxicity of OPs (EPA, 2016), but the suggested ban has not been carried out (EPA, 2017). Despite the

potential dangers to health and the imposed restrictions, CPF remains a popular pesticide to use especially in many developing countries (Salyha, 2010).

1.4 Chlorpyrifos

CPF was first synthesised and then manufactured commercially in 1965 by the Dow Elanco Company, and it is still one of the most extensively used OPs to control insects in homes, gardens and agricultural fields worldwide (Cox, 1994; Hargreaves, 2012). It has become widely distributed in the world market under different brand names, including Scout, Eradex, Empire, Brodan, Lorsban, Dursban, and Reldan (Salyha, 2010). In 1997, there were approximately 850 commercial CPF products registered in the USA, according to the EPA (EPA, 1999). Currently CPF use is still authorised in around 50 countries, including Japan, New Zealand, Australia, USA, France, UK, Canada, Spain, and Italy (Salyha, 2010).

CPF has been used in many applications in different locations; within residential settings it has been used to control pests and insects including cockroaches, mosquitos, fleas, flies, and lice, whereas in farming and industrial settings it is applied directly to storage bins, farm buildings, golf courses, lawns, animal sites, and even sheep and turkeys (Eaton *et al.*, 2008; Salyha, 2010). One of the largest areas of use is arable farming; CPF is applied to several major crops, including corn, fruits, vegetables, tree nuts, wheat, soybeans, and citrus fruit (Eaton *et al.*, 2008; Salyha, 2010). The National Centre for Food and Agriculture Policy (NCFAP), reported that the USA used approximately 1.4 million kg of CPF in the home and garden every year (NCFAP, 2000). This high level of use is also typical in other countries; for example, the annual usage of CPF in 2011 in China was approximately 20 million kg (AgroNews, 2013).

CPF is classified as an EPA class II toxicant as it induces the same toxic effects as most acetylcholinesterase (AChE) inhibiting pesticides, but there are conflicting data on the carcinogenic and mutagenic potential of CPF in the literature (Dreiherr *et al.*, 2005; Cui *et al.*, 2006).

1.4.1 Chemical structure and physical properties

OPs are phosphoric acid derived esters (Figure 1.2, panel A), which contain an X group (leaving group) and two lipophilic groups R1 and R2 (Eddleston *et al.*, 2008; Hargreaves, 2012). The X group is usually displaced when an OP binds forming a stable bond through an organophosphorylation reaction (Costa, 2006). The chemical name of CPF, which is one of the compounds of interest to the current study, is O,O-diethyl O-3,5,6-trichloropyridin-2-

yl phosphonothioate, O,O-diethyl O-3,5,6-trichloro-2-pyridyl phosphothionate, chlorpyrifos-ethyl; it is normally found as a white to colourless crystalline solid, which gives off a strong mercaptan-like odour (Figure 1.2). CPF is the active ingredient in many insecticide formulations, available in different forms, including capsules, suspensions, granules, powder, gel-based products, and emulsifiable concentrates (Wauchope *et al.*, 1992). CPF is lipophilic meaning it is poorly soluble in water but it does dissolve into most organic solvents; therefore, before application on to crops or animals, it needs to be mixed with solvents, for example acetone, benzene, xylene, diethyl ether, methanol or carbon disulphide (Wauchope *et al.*, 1992; Eaton *et al.*, 2008).

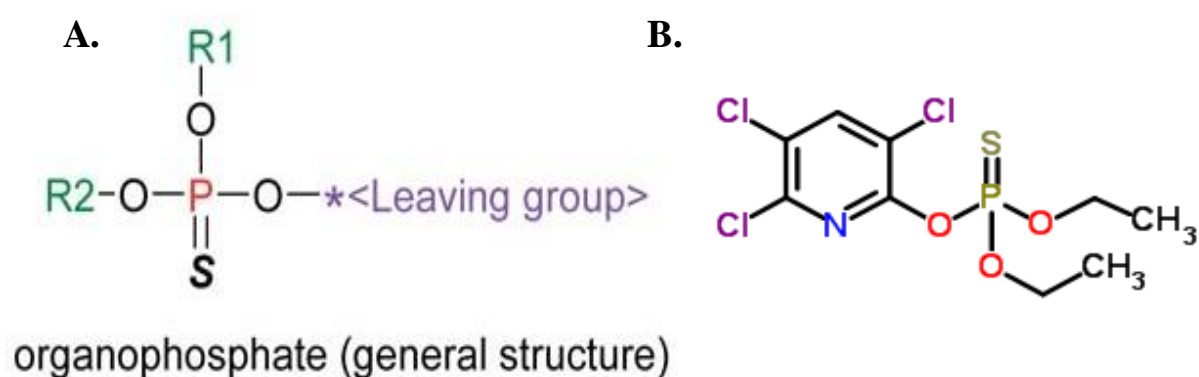


Figure 1.2. Chemical structure of (A) general organophosphate structure, (B) chlorpyrifos.

OPs contain a central phosphorus atom with a double bond to either sulphur or oxygen, R1 and R2 groups that are typically (but not always) ethyl or methyl in structure, and a leaving group which is specific to the individual organophosphate. Adopted from Reigart and Roberts (1999).

1.4.2 Routes of exposure to chlorpyrifos

There are different routes that can lead to exposure CPF; it can enter the body through ingestion, dermal contact, or inhalation, and this leads to it being rapidly absorbed through the airways, oral mucosa, and skin (Karki *et al.*, 2004; Munoz-Quezada *et al.*, 2012). Common exposure routes in animals and humans are from inhaling contaminated dust, breathing polluted air, contact during application or preparation of OPs in the workplace, and eating or drinking food and water that are contaminated with OPs (WHO, 2001).

In the USA one of the major sources of CPF exposure is application of pesticides and other insect treatments indoors; the EPA reported over 17,000 cases between 1993 and 1996 (EPA, 1997), and between 1998 and 2002 there were 2,593 incidents of acute CPF poisoning reported in school children in the USA (Alarcon *et al.*, 2005). Even after the

introduction of restrictions in CPF use, there were still more than 300 cases of acute CPF toxicity reported between 2002 and 2011 (EPA, 2013).

Outside of the home, occupational exposure is one of the most common sources of CPF poisoning; CPF exposure affects agricultural workers, such as pesticide sprayers, sheep dippers, and farmers, and their families (Gupta, 2006; Munoz-Quezada *et al.*, 2012). Even children and other people living on or near a farm that uses OP insecticides can be at risk of OP exposure due to the amounts of insecticides applied (Gupta, 2006; Munoz-Quezada *et al.*, 2012). There is also a risk that the treatment of a workplace with insecticides, such as CPF, to remove termites or other insects could lead to significant exposure of the employees; indeed, over 1300 cases of workplace exposure to CPF were reported between 1985 and 1992 to the US poison control centre (EPA, 1994). Another common source of CPF exposure is during manufacturing; a prospective cohort study evaluated the level of occupational exposure in manufacturing workers. The results of the study showed there was a significant increase in CPF metabolites in the urine of those workers tested, which raised major concerns about the guidelines for occupational exposure to CPF (Albers *et al.*, 2004).

One of the other key exposure routes is through inhalation of CPF contaminated air and water, with CPF contamination of groundwater having been reported in nine states in the USA (EPA, 1992), South Africa and Spain (Thoma and Nicholson, 1989). Significant CPF air contamination has been detected at application sites; studies that analysed air samples taken from approximately one metre above a cornfield that had been sprayed, showed that half of the CPF applied was vaporized, and that this contaminated the air for over 25 days (Whang *et al.*, 1993). CPF can also be carried up into the atmosphere and move some distance away from the application site; for example, studies of air samples detected CPF contamination up to about 24 km away from the site of CPF application (Zabik and Seiber, 1993).

As soon as CPF is applied and is in the environment, it can be rapidly absorbed through all possible routes of exposure (oral, dermal, inhalation) due to the fact it is a lipophilic compound which crosses biological membranes, including the blood brain barrier and the placenta (Timchalk *et al.*, 2002). As CPF enters the bloodstream it can distribute into the tissues at significant concentrations, which are able to inhibit AChE, a key enzyme in the regulation of cholinergic neuron activity, and induce neural damage (Timchalk *et al.*, 2002).

1.4.3 Metabolic pathway of chlorpyrifos to chlorpyrifos-oxon

Within humans, many different enzymes contain polymorphisms which means that individuals can have variations in enzyme activity, and therefore will react differently after exposure to toxins such as OPs, resulting in differences in activation and detoxification of the xenobiotic in question (Costa *et al.*, 2005). CPF is metabolically converted into its oxygen form chlorpyrifos oxon (CPO), by replacing the sulphur group with oxygen. CPF biotransformation is mostly mediated by cytochromes. Generally, CPF is oxidized by CYP450 to diethylthiophosphate (DETP) and 3,5,6-trichloro-2-pyridinol (TCP) formation (Figure 1.3). CYP450 are present in several isoforms in the liver; studies have shown CYP2B6 and CYP3A4 are the most effective enzymes for CPO formation from CPF (Mutch and Williams, 2006; Croom *et al.*, 2010). Then, the metabolites are filtered through the kidneys to be excreted in the urine (Eaton *et al.*, 2008). In the liver, CPO is hydrolysed by diethylphosphate (DEP) and 3,5,6-trichloro-2-pyridinol (TCP) to become a less toxic product. CPO detoxification also involves plasma A-esterases, such as paraoxonase 1 (PON1). It has been highlighted by several *in vivo* studies which showed that low levels of these enzymes can increase the OP neurotoxicity susceptibility (Costa *et al.*, 2013). Studies in humans have shown that PON1 has a polymorphic distribution in plasma samples, which means there is a large variation in concentrations and activity in individuals (Costa *et al.*, 2013).

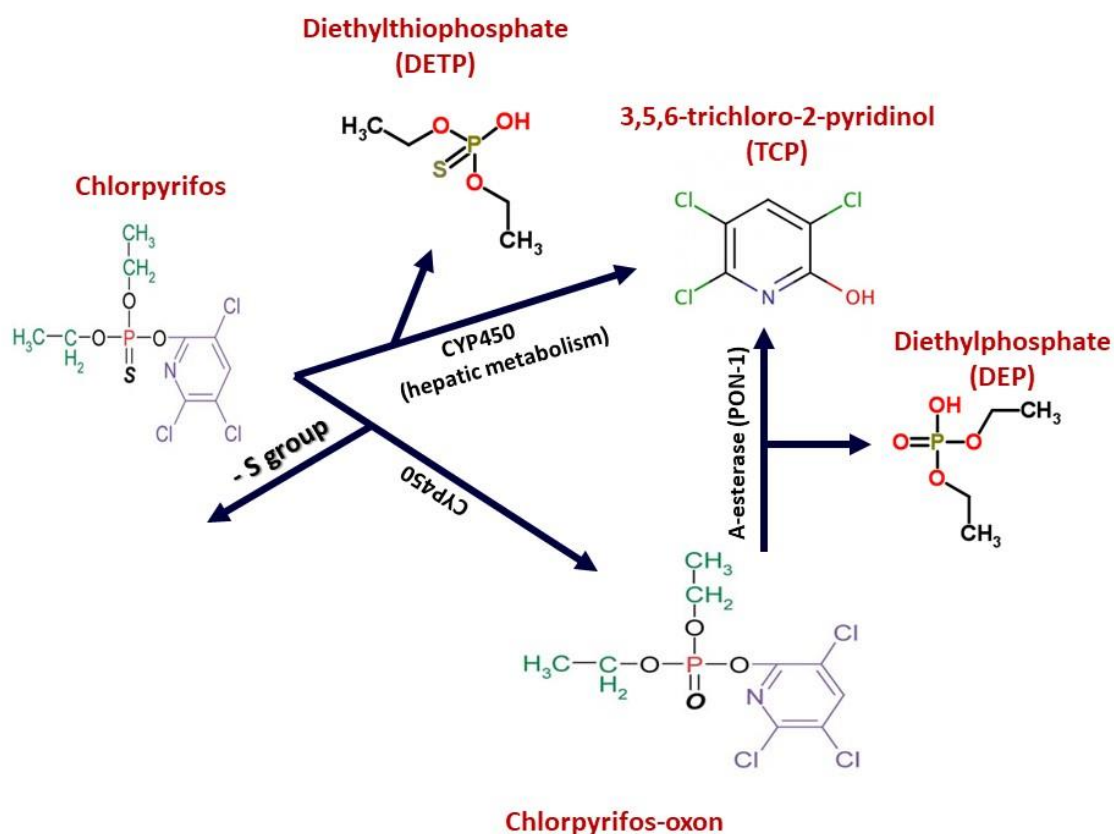


Figure 1.3. Representation of the metabolism of CPF.

1.5 Phenyl saligenin phosphate

Phenyl saligenin phosphate (PSP) is a structural analogue of saligenin cyclic-o-tolyl phosphate (SCOTP), which is the active metabolite of tri-ortho cresyl phosphate (TOCP) (Fowler *et al.*, 2001). Studies of this non-pesticide OP and its ‘parent’ compound show that they produce their toxic effect by NTE organophosphorylation, which leads to inhibition of enzyme activity and can cause organophosphate-induced delayed neuropathy (OPIDN) (Nomeir and Abou-Donia, 1986; Zhao *et al.*, 2006). Occupational exposure to toxic aerosols of TOCP via its use in aviation fluids, can result in cognitive dysfunction, neurodegenerative poisoning, and memory loss (Winder and Balouet, 2001; Michaelis, 2011; Hargreaves, 2012).

Studies of PSP have shown that it has several key targets within the body, such as neuropathy target esterase (NTE), mitogen-activated protein kinase (MAPK) signalling, cytoskeletal proteins, transglutaminase enzyme activity and neurotrophin receptors (Carlson and Ehrich, 2001; Harris *et al.*, 2009a; Pomeroy-Black and Ehrich, 2012; Baker *et al.*, 2013). PSP is a classical inhibitor of NTE; after exposure to PSP, NTE is inhibited by organophosphorylation. In differentiating neuronal cells, this is followed by reduced neurite

outgrowth associated with modification of axonal morphology and neuronal degeneration, which are critical events in the development of OPIDN (Flaskos *et al.*, 1994; Ehrich and Jortner, 2001).

Studies investigating PSP-induced toxicity have focused on the effects of MAPK and phosphoinositide-3-kinase/protein kinase B (PI-3K/PKB) signalling, as these play a vital role in the neuronal response to OP exposure (Kaplan, 1995; Hargreaves *et al.*, 2006; Pomeroy-Black and Ehrich, 2012). The studies found increased phosphorylation of PKB and MEK1/2 protein kinases in human SH-SY5Y neuroblastoma cells by low concentrations of PSP (e.g. 0.01-1.0 μM), and that 2.5 μM PSP for 4 h in mouse N2a neuroblastoma cells caused activation of extracellular-signal-regulated kinases 1/2 (ERK1/2) associated with the inhibition of NTE and neurite outgrowth (Nostrandt *et al.*, 1992; Carlson *et al.*, 2000; Hargreaves *et al.*, 2006; Pomeroy-Black and Ehrich, 2012).

Other studies have focused on the effects of PSP on cytoskeletal proteins and myelin basic protein; generally, the studies have found that sub-lethal concentrations of PSP induced NF and microtubule degradation, in association with in myelin degeneration, abnormal neurite growth and axonal damage (Abou-Donia and Lapadula, 1990; Ehrich and Jortner, 2001; Massicotte *et al.*, 2003; Hargreaves *et al.*, 2006; El-Fawal and McCain, 2008).

Overall, these results indicate that PSP and TOCP can cause significant neurotoxicity by disrupting the activity of cytoskeletal proteins and MBP, but the molecular basis of these effects has not been fully investigated; therefore, further research is required to fully elucidate the mechanisms involved (Baker *et al.*, 2013).

1.6 The acute toxicity of organophosphates in the nervous system

The enzyme AChE is the primary target of OPs in the nervous system, and its inhibition produces the best-known effect of OP acute toxicity. AChE is found at neuromuscular junctions, is involved in termination of neurotransmission, and is a serine hydrolase that catalyses the degradation of acetylcholine (ACh), a neurotransmitter that is present in the CNS and PNS, to produce acetate and choline (Campbell *et al.*, 1997; Steevens and Benson, 1999; Ray and Richards, 2001). The inhibition of AChE results in the accumulation of ACh in the synaptic cleft, thereby overstimulating nicotinic and muscarinic receptors (Table 1.1) (Hasan *et al.*, 1979; Pope, 1999; Costa, 2006). This overstimulation causes neurotoxic effects, for example neuromuscular paralysis (such as continuous muscle contraction), throughout the entire body (Gupta, 2006).

Table 1.1. Acetylcholine receptors, subtypes and location (Adopted from Tata *et al.*, 2014).

ACh receptors	Subtypes	Location
Nicotinic receptors	N1 or Nm	Neuromuscular junction
	N2 or Nn	Autonomic ganglia, central nervous system
Muscarinic receptors	M1	Cortex and hippocampus regions of the brain
	M2	Heart, brain, spinal cord, exocrine gland
	M3	Exocrine glands and smooth muscles
	M4	Central nervous system
	M5	Central nervous system

OPs inhibit AChE by forming a covalent bond with a serine residue in the active site; as a consequence of this reaction, a transient intermediate complex is generated, which is partially hydrolysed through the loss of the X substituent group, resulting in the formation of a stable, organophosphorylated and inhibited AChE enzyme (Figure 1.4) (Betancourt and Carr, 2004; Eaton *et al.*, 2008). CPF can target AChE both in the CNS and PNS, however in its non-oxidised state, it does not inhibit AChE very strongly *in vivo*, whereas the oxidised state (CPO) powerfully inhibits AChE. As mentioned previously, cytochrome P-450 catalyses the conversion of CPF to CPO through oxidative desulphuration, allowing CPF to become a powerful inhibitor of AChE *in vivo* (Betancourt and Carr, 2004; Eaton *et al.*, 2008).

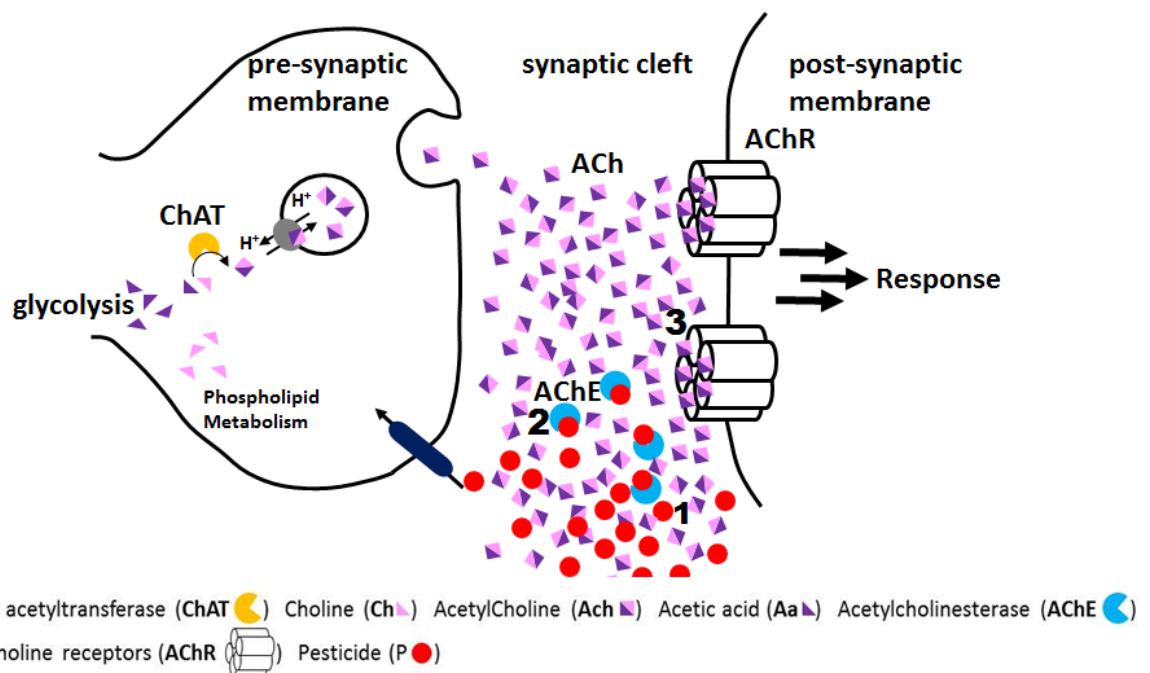


Figure 1.4. Inhibition of AChE by organophosphates.

This leads to accumulation of ACh in the synaptic cleft which results in impeded neurotransmission. Obtained from Vargas-Bernal *et al.* (2012).

Another vital target for some OPs is the serine hydrolase enzyme known as NTE. NTE is a B-esterase, and its inhibition and ageing (in a similar manner as AChE (Section 1.6) is associated with the onset of the disorder called OPIDN (Johnson, 1970; Costa, 2006). In vertebrates, NTE is an integral membrane protein which is expressed in the endoplasmic reticulum (ER) of all neuronal cells, and some non-neuronal tissues, such as testicles, kidney, and lymphocytes (Glynn *et al.*, 1998; Glynn, 1999). NTE belongs to the esterase family of enzymes and plays a critical role in neural development.

Other functions of NTE include the hydrolysis of lipids to form lysolecithin, a membrane phospholipid that possesses demyelination properties and is linked with cell signalling between glial cells and neurons in nervous system development (Glynn 1999; Costa, 2006). NTE expression increases in the early stages of embryo development, where it may be involved in nervous system development and signal transduction (Lotti and Moretto, 1993; Moser *et al.*, 2000; Road, 2010). Genetic studies have suggested the absence of NTE in the brain causes neuronal degeneration as associated with the loss of ER, and vacuolation in cell bodies, which cause defects in cellular function (Van Tienhoven *et al.*, 2002; Akassoglou *et al.*, 2004). To date, the precise molecular mechanism underlying OPIDN has not been fully elucidated; it has been established that, besides inhibition and ageing of

NTE, some cytoskeletal rearrangements as well as disruption of calcium homeostasis, are involved in the disorder (El-Fawal and Ehrich, 1993; Hargreaves, 2012).

The clinical manifestations that form as a result of CPF poisoning can be divided into four main categories, including acute cholinergic syndrome, intermediate syndrome, delayed neuropathy and other neurological disorders (Figure 1.5) (Abou-Donia, 2003). The development of the specific neurological syndromes is dependent on different factors, including the onset of clinical symptoms, the chemical nature of the compound, and time and extent of exposure (Abou-Donia, 2003).

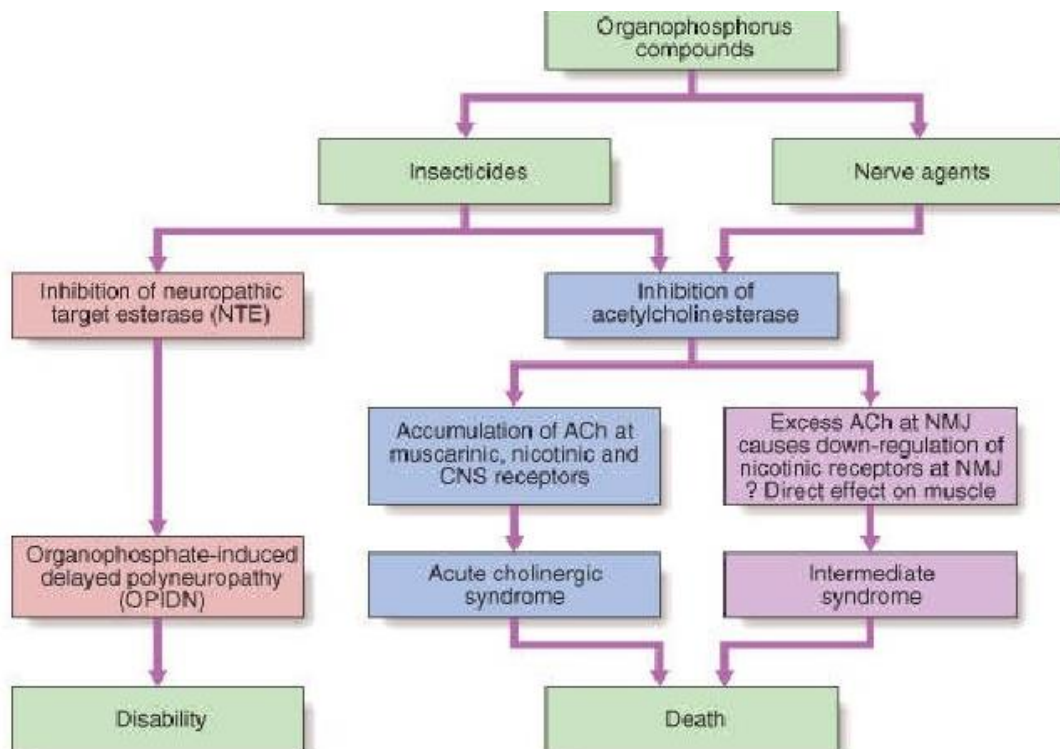


Figure 1.5. Classification of organophosphate toxicity.

Representation of the pathways involved in forming the different types of OP toxicity. Adopted from Jones and Karalliedde (2006).

1.7 Acute cholinergic syndrome

The main cause of acute CPF toxicity in mammals is the bioactivation of CPF to CPO in the liver as, at the molecular level, the P=O moiety of CPO can act as a potent inhibitor of AChE, whereas the P=S moiety of CPF lacks the inhibitory effect (Richardson, 1995; Bjorling-Poulsen *et al.*, 2008; Eaton *et al.*, 2008). CPO binds to the active site of by forming a stable covalent bond between the hydroxyl group of the serine in AChE and the phosphate group of the OP compound, which usually remains stable for hours to weeks (Karalliedde, 1999). This organophosphorylation of AChE results in the inhibition of its

normal function, degrading the major neurotransmitter of ACh at the ending of cholinergic nerve in the CNS and PNS, which leads to accumulation of ACh (Koelle, 1992).

The accumulation of excess ACh at the synapses in the PNS and CNS results in hyperstimulation of the cholinergic receptors and causes what is known as 'cholinergic syndrome' (Abou-Donia, 2003). It is characterised by different clinical symptoms depending on the site where ACh accumulation occurs; the excess ACh binds to muscarinic receptors and different muscarinic effects can develop depending on the route of toxic exposure, including visual disorders, miosis, bronchoconstriction, hypersalivation, hypotension, bronchorrhoea, increased sweating and lacrimation, diarrhoea, vomiting, increased gastrointestinal mobility, abdominal cramps, and lowered heart beat (Elersek and Filipic, 2011).

After CPF exposure, development of acute cholinergic syndrome usually occurs within a few minutes or up to a few hours (Eaton *et al.*, 2008; Hargreaves, 2012). The extent and severity of the symptoms depends on the nature of the OP and the level of OP-AChE binding (Chambers, 2004). During onset, nicotinic receptors are stimulated, which causes hypertension and uncontrolled muscle contractions subsequently leading to paralysis (Singh and Sharma, 2000; Elersek and Filipic, 2011). The well-established symptoms of cholinergic crisis occur when there is severe inhibition of AChE (i.e. > 70 % of the normal levels) (Clegg and van Germet, 1999a). After the development neuromuscular paralysis (such as neuromuscular block) in the body, death can occur within a short time, by respiratory-failure and/or cardiac arrest (Lauder and Schambra, 1999; Costa, 2006; Gupta, 2006; Easton *et al.*, 2008; Flaskos, 2012; Hargreaves, 2012). Different CNS symptoms can arise after severe CPF intoxication, including confusion, headache, blurred vision, spasms, speaking disorders, insomnia, ataxia, coma, and convulsions (Clegg and van Germet, 1999b; Lotti and Moretto, 2005; Elersek and Filipic, 2011).

The reactivation of AChE after inhibition by many different OP compounds usually occurs within several hours by the spontaneous hydrolysis of the AChE-OP bond (Abou-Donia and Lapadula, 1990). However, when the inhibition is caused by CPO, the AChE-CPO complex undergoes an 'ageing' mechanism where a non-enzymatic hydrolysis or dealkylation process results in loss of one or two of the alkoxy labile groups (R₁, R₂) (Figure 1.6). After this ageing process has occurred, the inhibition of AChE becomes irreversible as the enzyme is more resistant to reactivation, and this inhibition can only be

overcome by the synthesis of new enzyme molecules and clearance of the xenobiotic (Abou-Donia and Lapadula, 1990; Karalliedde, 1999; Costa, 2006).

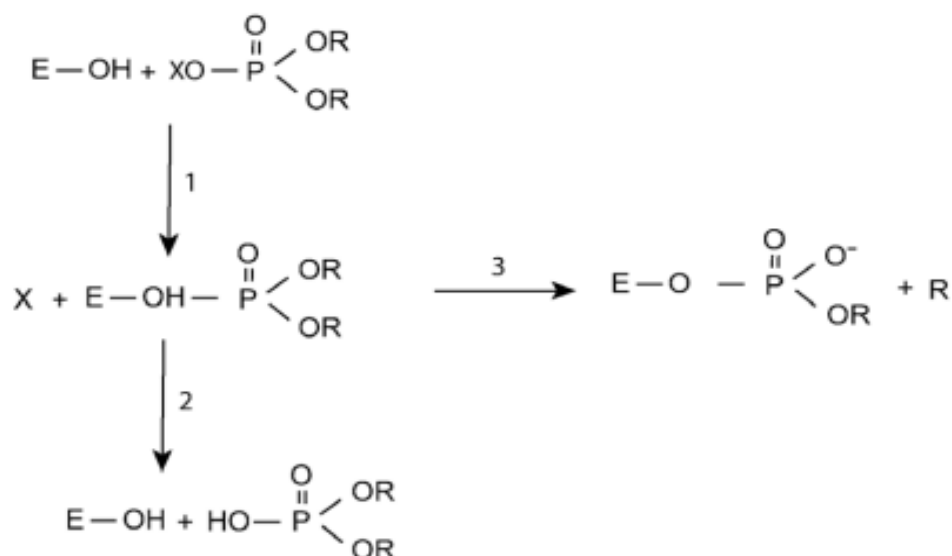


Figure 1.6. Representation of interactions between esterases and OPs.

The first reaction (1) leads to reversible organophosphorylation of AChE; the second (2) to hydrolysed OP and spontaneous reactivation of AChE, and the third (3) forms the 'aged' organophosphorylated AChE which is inactive, stable and carries an increased negative charge. Adopted from Costa (2006).

There are two main approaches to the treatment of acute CPF toxicity; the first is to block the over stimulation of the muscarinic receptors and the second is to reactivate AChE activity. The first of these aims can be achieved by administering atropine that is a cholinergic muscarinic antagonist and prevents the ACh accumulation at the receptors. For the second approach, which promotes ACh breakdown, AChE enzyme reactivation is induced by the administration of an oxime, such as pralidoxime (Thiermann *et al.*, 1999; Eaton *et al.*, 2008; Eddleston *et al.*, 2008). However, if the AChE-CPO complex has already undergone ageing, oximes are unable to reactivate the inhibited AChE (Eaton *et al.*, 2008). Anticonvulsant drugs such as diazepam are another potential treatment for CPF intoxication; these drugs are used to relieve anxiety and the convulsions, which are caused by acute poisoning after the exposure to CPF (Thiermann *et al.*, 1999; Eaton *et al.*, 2008; Eddleston *et al.*, 2008).

1.8 Intermediate syndrome

Intermediate syndrome is another neurotoxic effect associated with OP toxicity, characterised by symptoms that begin with respiratory insufficiency, and continue to produce weakness in limbs, neck and respiratory muscles (Senanayake and Karalliedde, 1987; Eaton *et al.*, 2008). This condition develops after the symptoms of cholinergic syndrome, but prior to the signs of OPIDN (Senanayake and Karalliedde, 1987; Costa, 2006). Following OP exposure, it is estimated that 20 % of people will go on to develop intermediate syndrome, and the symptoms usually occur within 24 to 96 hours after exposure (Karalliedde, 2006; Yang and Deng, 2007). This was seen in a clinical case study of intermediate syndrome described in a 16-month old child who ingested CPF and developed flaccid paralysis and respiratory arrest after 27 hours (Mattingly *et al.*, 2003).

The precise underlying mechanism for the development of intermediate syndrome remains unclear, but there have been a number of mechanisms proposed, including failure of ACh release at neuromuscular junctions, the down regulation of ACh receptors, damage to muscles (myopathy), and prolonged inhibition of AChE (Yang and Deng, 2007; Abdollahi and Karami-Mohajeri, 2012).

The treatment of intermediate syndrome depends on the progression and symptoms involved; the clinical signs (e.g. severe respiratory muscle weakness) can be treated by monitoring respiratory functions and giving mechanical ventilation if necessary (Karalliedde, 2006). Other symptoms can be treated in a similar way to acute cholinergic syndrome by the administration of oximes; however, timing is critical, as these drugs were found to prevent myopathy in animal studies if they were administered immediately after CPF exposure, but they had no effect if they were administered more than two hours or more after poisoning (Karalliedde, 2006).

1.9 Organophosphate-induced delayed neuropathy (OPIDN)

OPIDN is another delayed peripheral neuropathy caused by OP poisoning. It is a rare neuropathic condition which can result following a single or repeated exposure to certain OPs such as diisopropylfluorophosphate, o-tolyl saligenin phosphate dioctyl dichlorovinyl phosphate, mipafox, and dibutyl dichlorovinyl phosphate, (Abou-Donia and Lapadula, 1990; Ehrich *et al.*, 1997). OPIDN is characterised by shaking in hands and feet, an initial delay in the onset of ataxia, which is followed by degeneration of the distal end of long axons and large peripheral nerves, and finally there is degeneration of the myelin sheath in

both the CNS and PNS (Abou-Donia and Lapadula, 1990; Lotti, 1992; Ehrich and Jortner, 2001).

Studies into the prediction of the ability of OPs to induce OPIDN have been carried out *in vitro* in cell lines, and also *in vivo* using hens, as these have proved to be reliable animal model as they readily show lesions and other clinical signs of OPIDN (Glynn, 1999).

Studies have shown that it is possible to use cell cultures to screen for OPIDN inducing OPs, as NTE activity is found in both human and mouse differentiated and undifferentiated neuronal cell lines (Fedalei and Nardone, 1983; Carrington *et al.*, 1985). There have been several studies measuring NTE inhibition in cultured neuronal cells, with mixed results when compared to animal studies (Nostrandt and Ehrich, 1992; El-Fawal and Ehrich, 1993). The majority of the early studies of OPIDN in cell cultures that measured parameters other than NTE, used the cell lines to try to predict the ability to induce OPIDN, instead of using them to investigate the underlying mechanism of OPIDN (Veronesi, 1992). By using a controlled environment such as a cell line it is possible to study how the molecular initiating and other key events occur, beginning with phosphorylation, then 'ageing' of NTE and finally the production of axonal degeneration, which has been described *in vivo* (Johnson, 1990; Abou-Donia *et al.*, 1988; 1990; 1993). To investigate these important details, it is necessary to use a relevant cell model, which will allow for the clarification of the biochemical mechanisms involved in development of OPIDN, especially as this could lead to the identification of novel endpoints for applied testing purposes (Flaskos, 1995).

After CPF exposure, OPIDN clinical effects usually manifest after cholinergic toxicity and intermediate syndrome, but the progression may not be immediate; clinical onset of OPIDN can occur 6 to 14 days after OP exposure (Abou-Donia, 2003; Eaton *et al.*, 2008; Jokanovic *et al.*, 2011). With some OPs, the clinical onset can take even longer to occur; for the poor AChE inhibitor TOCP, it can take several weeks for the metabolism to the active SCOTP to produce clinical symptoms of OPIDN (Nomeir and Abou-Donia, 1986; Abou-Donia and Lapadula, 1990). The early signs of OPIDN in humans include vomiting and diarrhoea, which is followed by progressive weakness of the lower limbs after the latency period (Abou-Donia, 1981; Abou-Donia and Lapadula, 1990; Abou-Donia, 1993; Jokanovic *et al.*, 2011). In the later stages of OPIDN, weakness of the limbs may affect the arms and hands, resulting in reflex deterioration of certain limbs and abnormal balance; OPIDN eventually causes a flaccid paralysis, which means there is nerve damage in the muscles

and this results in prolonged spasms (Abou-Donia, 1981; Abou-Donia and Lapadula, 1990; Abou-Donia, 1993; Jokanovic *et al.*, 2011).

Studies of the clinical onset of OPIDN in hens have revealed that this process occurs in two main steps; the first involves the inhibition of NTE enzymatic activity by phosphorylation, which significantly decreases enzyme hydrolysis, and the second step is the ageing of the phosphorylated NTE, which allows OPIDN to be initiated (Glynn, 1999). Studies have shown that the NTE inhibition alone is not associated with neural degeneration; OPs which can inhibit NTE but do not induce ageing of phosphorylated NTE cannot generate neuropathic effects (Costa, 2006). The NTE ageing process occurs when a negatively charged group of an OP covalently binds to the OH group in the side chain of the serine residue in the NTE active site. This ageing of the NTE means the enzyme's activity becomes permanently (irreversibly) inhibited, and this allows OPIDN to occur (Johnson, 1990; Glynn, 1999). The importance of NTE ageing has also been shown in the work of du Toit *et al.* (1981) and Johnson (1969), who demonstrated that NTE inhibition in the spinal cord resulted in only spinal syndrome with no associated neuropathy, whereas the development of an axonopathy such as OPIDN also required NTE ageing (Johnson, 1969; du Toit *et al.*, 1981). This suggests that only OPs that can inhibit and age NTE enzymatic activity can induce OPIDN. After NTE inhibition and ageing, there are then several alterations in the peripheral nerves, including myelin sheath loss, degeneration of long axons, accumulation of macrophage in nerves, and proliferation of Schwann cells (Singh and Sharma, 2000). Studies have also suggested that the susceptibility of NTE towards different OPs is associated with the age of the subject, as younger animals have a higher resistance to OPs than adults (Peraica *et al.*, 1993).

Further work in hen experimental models has suggested that CPF can induce OPIDN if there was over 50 % inhibition of NTE activity (Johnson, 1990; Lotti, 1992), which agrees with the known CPF-induced OPIDN cases in humans, mainly from accidental exposure (Eaton *et al.*, 2008). This can be seen in the study by Osterloh *et al.* (1983) which demonstrated there were only low levels of NTE activity and plasma cholinesterase in a patient who had ingested CPF; in addition the patient presented with minimal acute cholinergic syndrome, cardiac arrhythmia, coma, and they eventually died 30 h after poisoning (Osterloh *et al.*, 1983; Lotti *et al.*, 1986) studied a male patient who had accidental oral CPF poisoning (<300 mg/kg); the patient developed mild axonal neuropathy after 43 days, and the authors concluded that, in this case, CPF induced OPIDN with a lower inhibition of NTE than is usually required in animals (Lotti *et al.*, 1986).

The administration of PSP has also been shown to induce OPIDN in animal models (Nomeir and Abou-Donia, 1986). Studies have shown that PSP exposure can cause an increase in phosphorylation of the neurofilament heavy chain and tubulin and inhibit neurite outgrowth (Hargreaves *et al.*, 2006; Flaskos *et al.*, 2006). This suggests the phosphorylation of cytoskeletal proteins is a crucial process in the development of OPIDN (Abou-Donia, 1993).

1.10 Other chronic neurological conditions associated with OP exposure

Alongside the classical neurological syndromes, certain OPs including CPF, are able to cause other long lasting, persistent, and chronic neuropsychiatric and neurobehavioral disorders, which are collectively known as chronic OP induced neuropsychiatric disorder (COPIND), and these are commonly observed after an acute single dose or repeated sub-chronic exposure to an OP (Sanchez-Santed *et al.*, 2004). The key characteristics of COPIND are behavioural changes, including irritability, confusion, anxiety, drowsiness, insomnia, depression, anorexia, fatigue, emotional lability, and lethargy (Salvi *et al.*, 2003). Symptoms that could be classified as COPIND have been observed after accidental exposure of agricultural workers to a single dose of CPF; the workers had impaired cognitive functions, memory and attention deficits, and abnormalities in neuropsychological tests (Savage *et al.*, 1988; Rosenstock *et al.*, 1991; Steenland *et al.*, 1994).

Studies of long term OP use have shown there are neurological changes in adults; for example, Stephens *et al.* (1995) studied the performance of farm workers after repeated OP exposure; they found in neurobehavioral tests that there was a relatively slow speed for information processing, memory problems, greater susceptibility to psychiatric disorders, and an impaired attention span. These results were supported by the work of Fiedler *et al.* (1997), who observed schizophrenia and dystonic reactions in people who had been exposed to CPF over long periods. Studies have also shown that low level exposure to CPF can induce neurobehavioral effects; there have been high levels of anxiety observed in insecticide sprayers, but these results were not found in farmers (Levin *et al.*, 1976). This is further supported by studies which have shown there was impaired cognitive function after exposure of weaning rats to sub-acute doses of CPF (Jett *et al.*, 2001).

There have also been investigations into the impact of CPF insecticides on children to determine whether they cause cognitive defects; several epidemiological studies on children and adolescents that have worked as pesticide applicators on crops including cotton, have

established that they have a significantly lower neurobehavioral performance and more neurological symptoms compared to non-OP workers (Rohlman *et al.*, 2001; 2005; Rasoul *et al.*, 2008). The results of these studies confirm the previously detected association between the duration and period of CPF application in an agriculture setting and the extent of developmental and cognitive disorders, but research is yet to determine the precise mechanisms that cause COPIND clinical symptoms in humans (Kamel *et al.*, 2003; Rohlman *et al.*, 2007).

1.11 Effects of OPs on cytoskeletal proteins

Although there are many studies highlighting the fact that CPF can cause poisoning effects based on CPO mediated AChE activity inhibition, there are several other cellular proteins that are proposed targets for CPF, CPO and PSP neurotoxicity, including cytoskeletal proteins, axon growth associated proteins and those involved in cell signalling pathways (Flaskos, 2014).

As the disruption of cytoskeletal proteins can result in serious damage at different phases of neural development, how these key proteins are involved will be considered in the next sections.

1.11.1 Cellular and cytoskeletal proteins as molecular targets of CPF, CPO and PSP toxicity

Some of the developmental processes of the nervous system are controlled by the neuronal cytoskeleton, including cell migration, proliferation, morphogenesis, differentiation, neurite outgrowth, branching of dendrites, elongation of axons, steering of growth cones, and also apoptosis (Hargreaves, 1997; Flaskos, 2014). Due to their involvement in all these processes, disruption of cytoskeletal proteins can result in serious damage to neural development (Flaskos, 2014). The cytoskeleton itself is a complex structure, which is made up of three main classes of filamentous proteins, microfilaments (MFs), microtubules (MTs), and intermediate filaments (IFs). These cytoskeletal networks play an important role in axon growth regulation and stability and so they represent potential targets of neurotoxicity (Hargreaves, 1997). Different OPs produce a variety of effects on cytoskeleton filaments in human neuroblastoma cells, depending on the OP structure and potency (Carlson and Ehrich, 2001). Therefore, future studies need to focus on the identification of non-cholinergic targets of these OP compounds, as this will help to identify the molecular mechanisms involved in OP-induced toxicity.

1.11.2 Microtubules

Microtubules (MTs) have been shown to have important roles in growth and physiology; they are cytoplasmic elements composed of tubulin heterodimers and microtubule associated proteins (MAPs); they are involved in the regulation of intracellular transport, neuronal morphology, and the outgrowth of dendrites and axons (Cambray-Deakin, 1991; Ginzburg, 1991; Lodish *et al.*, 2000a). MTs are the largest cytoskeletal structures in diameter being made of hollow, straight cylindrical polymers that are made of a ring of thirteen protofilaments, with an internal diameter of approximately 14 nm, and an external diameter of approximately 25 nm (Figure 1.7) (Okabe and Hirokawa, 1988; Hargreaves, 1997). Protofilaments are formed by the assembly of heterodimers of the two tubulin subunits (α - and β -tubulin) in a staggered fashion (Figure 1.7), assisted by the interaction with MAPs (Tilney *et al.*, 1973; Hargreaves, 1997). The evidence for the presence of MAPs in MTs comes from the fact that they co-purify with tubulin *in vitro*, the ability of MAPs to stimulate MT assembly *in vitro* and the observation that MTs are stained by indirect immunofluorescence with anti-MAP antibodies (Shelanski *et al.*, 1973; Murphy and Borisy, 1975; Sloboda, 1976; Lodish *et al.*, 2000a).

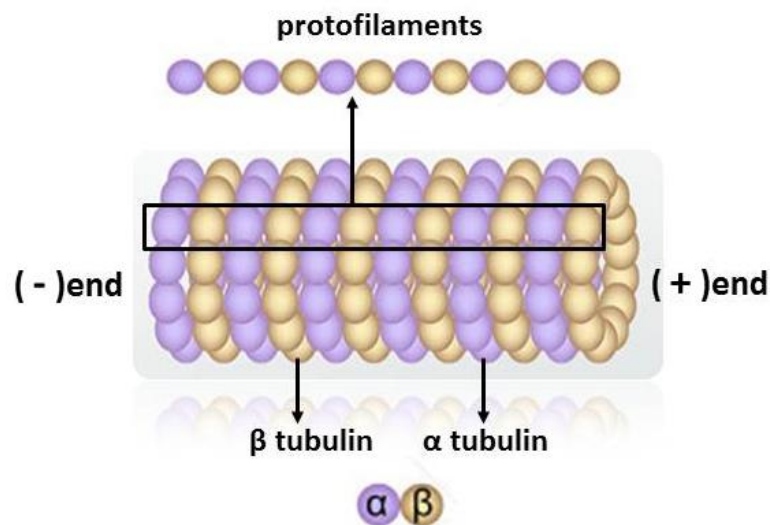


Figure 1.7. Microtubule structure and composition.

Schematic diagram of a microtubule showing how the tubulin polypeptides pack together to form a cylindrical wall of protofilaments.

MTs originate from specific regions in most mammalian cell types; these are called the centrosomes or microtubule organising centres (MTOCs) (Heidemann *et al.*, 1981). They are organised in a polar orientation, with depolymerisation and polymerisation occurring at the ends of the structure (Heidemann *et al.*, 1981). The name for the ends of the MTs are

defined by the rate of growth in vitro; the ‘minus end’ is known slow growing end and the ‘plus end’ is known as the fast-growing end (Figure 1.7) (Heidemann *et al.*, 1981). In neuronal cells, axonal MTs are oriented with their minus ends anchored at the MTOCs of the axon, with the plus end extending along the axon toward the tip (Heidemann *et al.*, 1981; Bamberg *et al.*, 1986; Lodish *et al.*, 2000b). In non-neuronal cells, for example glia, centrioles, basal bodies, and centrosomes of chromosomes, the MTOCs are associated with the minus ends, and it is from here that MTs assemble, which means the polarity of MTs become fixed with the plus end extending outwards to the extremities of the cell (Lodish *et al.*, 2000b). In dendrites the polarity of the MTs is mixed, with both ends being distal to the cell body (Lodish *et al.*, 2000a).

1.11.2.1 Biochemical properties of MTs

1.11.2.1.1 Tubulin

Tubulin is the main component of MTs and it contains α - and β - subunits, with the molecular weight each subunit being approximately 50 kDa. Each tubulin subunit has several isoforms encoded by different genes. A third subunit, γ -tubulin, is not part of MTs but instead is present in the MTOC, where it plays an important role in MT polar orientation and nucleation (Martin *et al.*, 1997; Tischfield and Engle, 2010). Tubulin is a highly acidic, conserved protein and can bind a variety of MAPs (Hargreaves, 1997).

Both α - and β - tubulin isoforms play important roles during the development of the nervous system. For example, the class III β -tubulin isotype (β III-tubulin) has an essential role in neurite growth and cell differentiation; it is almost exclusively distributed in neuronal cells and is also one of earliest cytoskeletal proteins expressed in neural development (Easter *et al.*, 1993).

The presence of a strongly acidic carboxyl terminal domain allows both α - and β -subunits of tubulin to bind a variety of MAPs (Hargreaves, 1997). Within this domain there is an acidic region of 40 amino acids that contains phosphorylation sites (serine residues) for regulation, and binding sites for calcium and proteins such as MAPs that stabilise the MTs (Cleveland, 1993) (Table 1.2).

The regulation of tubulin polymer formation is also controlled by several post-translational modifications, including phosphorylation of a serine at residue 444 (Ser-444) in the β -tubulin subunit, acetylation of the lysine at position 40 (Lys40) in α -tubulin, detyrosination/tyrosination (removal/addition) of C-terminal tyrosine (Tyr) residues in α -subunits, and the

addition of multiple glutamate residues in both α - and β -subunits (LeDizet and Piperno, 1987; Barra *et al.*, 1989; Diaz-Nido *et al.*, 1990; Alexander *et al.*, 1991; Ludueña, 1993; Fourest-Lieuvain *et al.*, 2006; Janke, 2014) (Table 1.2). Such modifications may affect MT stability and locations (Janke and Kneussel, 2010).

Tubulin synthesis can also be auto-regulated by a pool of unpolymerized tubulin, which is used up during MT assembly and in turn, then stimulates tubulin synthesis to increase (Cleveland, 1993).

Table 1.2. Major microtubule cytoskeleton proteins of the nervous system and their regulation (Adopted from Luduena, 1993).

Protein	Expression pattern and distribution	Post-translational modification
α-tubulin	In all cells, but some isoforms preferentially expressed in brain	Acetylation, tyrosination, polyglutamylation
β-tubulin	In all cells, but some isoforms preferentially expressed in brain	Phosphorylation, polyglutamylation
γ-tubulin	In MTOC of all cells	Phosphorylation
MAP 1a	Appears late, widely distributed	Phosphorylation
MAP 1b	Appears early, then declines; enriched in axons	Phosphorylation
MAP 2a	High molecular weight; expressed in dendrites in mature neurons	Phosphorylation
MAP 2b	High molecular weight; expressed in dendrites	Phosphorylation
MAP 2c	Low molecular weight; expressed in dendrites in developing neurons	Phosphorylation
Tau	Enriched in axons	Phosphorylation

OPs have been found to target tubulin, interfering with assembly and causing impairment of MT function (Prendergast *et al.*, 2007). Studies have shown low concentrations (0.005 and 0.01 mM) of CPO bound to tubulin and prevented polymerization, and dichlorvos increased tubulin phosphorylation, which resulted in synaptic dysfunction and axon dissociation (Choudhary *et al.*, 2006; Grigoryan and Lockridge, 2009).

1.11.2.1.2 Microtubule-associated proteins

The stability and assembly of MTs has been shown to be strongly dependent upon MAPs, as they regulate the dynamics of tubulin heterodimer formation, and help determine the balance between plasticity and rigidity in neuronal processes (Doering, 1993; Lodish *et al.*, 2000a; 2000b). MAPs are known to modulate MT dynamics, assembly and disassembly and are also involved in the interaction of MTs with IFs, actin filaments and other organelles (Matus, 1988; Nixon *et al.*, 1990; Hargreaves, 1997). The MAP family members which are important in central nervous system development include MAP 1, MAP 2, Tau and stathmin (Schoenfeld and Obar, 1994). The main function of these proteins during neuronal development are to maintain the growth cone's stability, by precise modulation of axonal and dendritic MT dynamics (Schoenfeld and Obar, 1994). For example, MAP 1, MAP 2 and Tau stimulate MT assembly, cross-link MTs with other cytoskeletal elements, and modulate interactions of MTs with IFs and actin filaments (Murphy *et al.*, 1977; Griffith and Pollard, 1978; Sattilaro *et al.*, 1981; Leterrier *et al.*, 1982; Olmsted, 1986; Nixon *et al.*, 1990). Other groups of MAPs, for example dynein and kinesin, can function as motor proteins (ATPases) and drive the intracellular transport of proteins and organelles from the cell body to the extending synapses and axons (Vallee and Bloom, 1991).

MAPs 1 and 2 have three different isoforms each (MAP 1a, 1b, 1c, and MAP 2a, 2b, 2c), which can be detected based on their molecular weights; MAP 1a, MAP 1b, and MAP 1c have molecular weights of 350 kDa, 330 kDa, and 230 kDa, respectively (Olmsted, 1986; Nixon *et al.*, 1990). MAP 2a and 2b are thermostable, elongated molecules that are expressed through the life of the neuron (MAP 2b), or during synaptic formation (MAP 2a), have a molecular weight of 280 kDa, and an estimated length of 185 nm (Vallee, 1980; Caceres *et al.*, 1984; De Camili *et al.*, 1984; Olmstead, 1986). MAP 1 and 2 are found in neuronal cell bodies and dendrites (Table 1.2), where they protect radially from the MT surface and form cross-bridges between MTs and NFs (Vallee, 1980; Leterrier *et al.*, 1982; Heimann *et al.*, 1985).

1.11.2.1.3 Kinesin

Kinesins are important motor proteins that mediate the transport of organelles, vesicles and other cellular proteins through the axon along microtubules (Pernigo *et al.*, 2013). Studies of OP toxicity have shown significant effects on axonal transport through inhibition of motor proteins such as kinesin, for example administration of 10 μ M CPF and 0.59 nM diisopropylfluorophosphate in bovine brain cortex cells reduced kinesin function and

axonal transport and increased axonal swelling (Inui *et al.*, 1993; Massicotte *et al.*, 2003; Gearhart *et al.*, 2007). Axonal swelling results in decreased transportation, resulting in protein aggregation along the axon (Abou-Donia, 1993).

1.11.2.1.4 Tau

Tau is primarily found in axons (Cleveland, 1993) (Table 1.2), so it is considered as an axonal marker (Binder *et al.*, 1985). It is formed of several polypeptides with molecular weights ranging between 45-60 kDa (Nixon *et al.*, 1990). These proteins have calmodulin binding sites and can be phosphorylated, which modulates their role in promoting assembly of MTs, and stabilizing MTs (Weingarten *et al.*, 1975; Black and Greene, 1982; Drubin and Kirschner, 1986; Olmsted, 1986; Kosik *et al.*, 1988). Evidence for these roles of Tau comes from the work of Drubin and Kirschner (1986); they microinjected Tau into fibroblasts and observed that Tau could stabilize existing MTs and induce assembly of new MTs, which fits with the proposed roles of Tau in axonal MTs stability (Drubin and Kirschner, 1986). Studies have also shown that Tau abnormalities strongly correlate to the pathophysiology of neurodegenerative diseases, including AD (Kolarova *et al.*, 2012).

MT assembly dynamics are controlled by processes such as treadmilling and dynamic instability which maintain a constant polymer mass (Margolis and Wilson, 1978; Kirschner and Mitchison, 1986; Kerssemakers *et al.*, 2006). Treadmilling involves producing a net gain or loss at the plus end of the MTs, with the minus being stabilised at the MTOC (Bergen and Borisy, 1980). The growing end of an MT can be stabilized by different factors including MAP binding, the presence of a GTP cap, or interaction with other cytoskeletal membrane elements (Kirschner and Mitchison, 1986; Gelfand and Bershadsky, 1991).

The stability and assembly of MTs is highly dependent upon MAPs, which help regulate the dynamics of the tubulin heterodimers (Lodish *et al.*, 2000a; 2000b). MAPs can stimulate MT assembly and they are involved in the interaction of MTs with actin filaments and IFs (Cleveland, 1993).

The ability of MTs to help organise axonal development and growth is well established; as the developing neurites begin to extend, MTs are assembled and begin to be modulated by specific post-translational modifications of the tubulin subunits (Cambray-Deakin, 1991). MAPs play essential roles in this process, as they help to maintain the structure, function, and orientation of MTs involved (Heidemann *et al.*, 1981; Craig and Banker, 1994; Mandell and Banker, 1995). Due to the important roles of MTs in different aspects of neuronal development and functions, any disruption or alterations to MT protein

phosphorylation by toxic agents can lead to problems with brain development, and these types of changes may also be involved in the pathophysiological mechanisms of some neurodegenerative diseases (Millecamps and Julien, 2013).

A number of studies have investigated the ability of CPF and CPO to disrupt the MT cytoskeleton and therefore cause developmental neurotoxicity. One study exposed differentiating rat C6 glioma cells to sub-cytotoxic (1-10 μM) doses of CPF and CPO that inhibited neurite outgrowth, and these doses reduced the protein levels of α -tubulin and MAP 1b in this cell line (Sachana *et al.*, 2008). These results are further supported by the *in vivo* work of Abou-Donia (1993), who found after exposure to OPs, hens exhibited increased phosphorylation of cytoskeletal proteins including MAPs and tubulin, which would result in lower active protein levels, and also an increase in autophosphorylation of calcium/calmodulin kinase II (Abou-Donia, 1993). In addition, work in cultured rat brain slices showed exposure to doses of CPO between 0.1 to 10 μM induced alterations in the MAP-2 immunoreactivity (Prendergast *et al.*, 2007). All of this suggests that alterations to MTs could be a useful biomarker of CPF-induced neurodegeneration.

1.11.3 Intermediate filaments

Intermediate filaments (IFs) are important components of the eukaryotic cytoskeleton, and they can be useful markers of cell differentiation (Omary *et al.*, 2006). They include an array of proteins expressed in different cell types and are classified as type I to VI based on gene sequence homology (Table 1.3) (Lewis and Cowan, 1986; Osborn and Weber, 1986; Robson, 1989; Strelkov *et al.*, 2003; Eriksson *et al.*, 2009). IFs are more biochemically stable and smaller in diameter than MTs, which allows them to provide structural support to many different types of cells, including neurons (Omary *et al.*, 2006).

Table 1.3. Intermediate filament classification.

(Lewis and Cowan, 1986; Osborn and Weber, 1986; reviewed by Robson, 1989; Strelkov *et al.*, 2003; Eriksson *et al.*, 2009).

Type	Name	Tissue/Cell
I	Acidic cytokeratins	Epithelial cells
II	Basic cytokeratins	Epithelial cells
III	Vimentin Glial fibrillary acidic protein (GFAP) Desmin Paranemin Synemin Peripherin	Mesenchymal cells Glial cells Muscle cells Muscle cells Muscle cells Neuronal cells
IV	Neurofilaments Internexin Nestins Syncoilin	Neuronal cells Neuronal cells Pluripotent cells Muscle cells
V	Nuclear lamins	All cell types
VI	Phakinin Filensin	Eye lens cells Eye lens cells

All IF proteins have a conserved α -helical rod domain, which is flanked by a carboxy-terminal tail, and an amino-terminal hypersensitive head domain (Figure 1.8) (Cooper and Hausman, 2000). The central rod domain contains a highly homologous 310 aa residue region that is conserved amongst the main IF types, and the variations in molecular interactions and molecular weight of all the IF subunits are determined by the sequence of the two end domains (Cooper and Hausman, 2000). IFs are constructed initially from two polypeptide chains that are wound together in a parallel form that then make a helical coiled-coil dimer; two of these then form a staggered tetramer (two anti-parallel dimers), which then form octamers, then protofilaments, and finally large complex IFs that contain 16 to 32 polypeptides (Lodish *et al.*, 2000b).

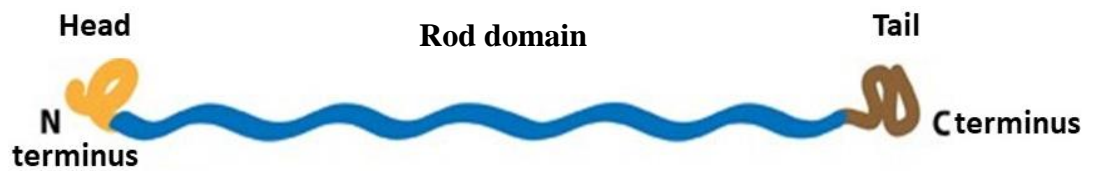


Figure 1.8. Structure of intermediate filament protein subunits.

The diagram demonstrates the structure of IF protein monomer that contains an α -helical rod domain composed of 310 amino acid residues, an amino-terminal head domain and the carboxy-terminal domain at the tail.

Within the family of IF proteins, more than 50 different proteins have been identified that can be classified into six main groups based on aa sequence homology (Cooper and Hausman, 2000). There are types classes of IFs specific to the nervous system and these include neurofilament (NF) proteins, glial fibrillary acidic proteins (GFAP) and nestins, which are mainly expressed in astroglial and neuronal cells, respectively (Cooper and Hausman, 2000; Eriksson *et al.*, 2009).

1.11.3.1 Neurofilaments

The axonal cytoskeleton contains MTs, MFs and NFs that form ordered networks of interconnected filaments linked by cross-bridges (Black and Lasek, 1980). After synthesis, NFs are initially assembled and transported from the neuronal cell body into the axonal space slowly, in a non-diffuse manner, then they are rapidly incorporated into the axonal cytoskeleton (Black and Lasek, 1980).

NFs are made of three polypeptides chains called neurofilament light (NFL), medium (NFM), and heavy (NFH) chains, that can be categorised based on their molecular weights, which are approximately 70, 145 and 200 kDa, respectively (Ackerley *et al.*, 2003). In mammals, these three protein types are found in mature neurons, and they are also highly expressed in axons (Lee and Cleveland, 1994). During axonal extension NFs can provide support, and they also have major roles in the regulation of axonal development and growth which is carried out in a complex series of interactions (Lee and Cleveland, 1994).

NFs have a similar structure to the other IF proteins; each subunit of NF contains a head, a central rod and a tail domain (Yuan *et al.*, 2012). During NF polymerization, the central rod domain (310 amino acids) plays an important role, whereas in NFM and NFH the tail domains have an important role in fine lateral projection formation (Yuan *et al.*, 2012). NFs can form filaments 10 nm in diameter via the central rod domain of each NF being co-assembled with the other NFs (Rao *et al.*, 2003). NFM and NFH subunits are found on the

surface of the filament and form radial projections to interconnect NFs with other cytoskeletal elements, and NFL forms the central core (Rao *et al.*, 2003). This filament structure allows cross bridges to form between extensions of the NF tail domains and other cytoplasmic organelles, and this stabilizes the axonal outgrowth (Hirokawa *et al.*, 1984).

Studies on the effect of OPs on IFs have found an alteration in expression or activity of different types of IFs, all of which can affect neural development. Studies in differentiating N2a cells that used exposure of CPF at levels that were sub-cytotoxic, but still inhibitory to neurite outgrowth (3 μ M), showed there was a significant reduction in the concentration of total NFH (Sachana *et al.*, 2001). This change in NFH is further supported by the work of by Flaskos *et al.* (2011), who used neurite inhibitory concentrations of CPO in differentiating N2a cells and then detected changes in protein levels using densitometric analysis of Western blots; they found there was a reduction in total NFH levels, which occurred in a concentration-dependant manner (Flaskos *et al.*, 2011). These results are also similar to those found by Hargreaves *et al.* (2006), who showed that using PSP at neurite inhibitory sub-cytotoxic concentrations resulted in reduced total NFH concentrations, after exposure of differentiating N2a cells for 4 and 24 hours, and Sindi *et al.*, (2016) that found CPO and CPF induced transient changes in NFH phosphorylation after differentiation (Hargreaves *et al.*, 2006; Sindi *et al.*, 2016). Overall, these alterations in NFH levels suggest that OP compounds, such as CPF and CPO, can interfere with the expression of important axonal cytoskeletal proteins, and this can affect the arrangement within the cell of the cytoskeletal networks (Flaskos *et al.*, 2007; Harris *et al.*, 2009a).

1.11.4 Glial fibrillary acidic proteins

Within mature astrocytes in the nervous system the major IF protein is GFAP (Yang and Wang, 2015). It is also found in other types of cells, including the non-myelinating Schwann cells in the PNS (similar to astrocytes), and the glial cells of the digestive system (Yang and Wang, 2015). GFAP plays important roles in providing structural support to astrocytes, and it helps to modulate their motility and shape during their different processes (Eng *et al.*, 2000). Astrocytes can be activated via reactive astrocytosis or astrogliosis in response to neuronal toxicity, brain injury, neural damage, or in genetic disorders (O'Callaghan, 1988). OP intoxication of astrocytes can be detected by the characteristics of increased GFAP expression levels and astroglial cells number; early studies into the effect of OP toxicity on astrocytes suggested GFAP expression and astro-glial cell levels were both increased in response to exposure (O'Callaghan, 1988). This was supported by studies

into the production of GFAP-deficient-mice, which showed there was an association with behavioural and neurological abnormalities, reduced spinal cord myelin thickness, and abnormal myelination (Gomi *et al.*, 1995; Liedtke *et al.*, 1996).

During brain development, glial development and differentiation can be detected by an increase in GFAP expression; they start as neural precursor cells and form astrocytes, and this process usually reaches a peak in the second or third postnatal week (Bramanti *et al.*, 2010). Due to this change GFAP is recognised as a biomarker for astrocyte differentiation, and as glial development continues into adolescence, the effects of CPF and CPO exposure on developing glia may contribute to developmental neurotoxicity (Bramanti *et al.*, 2010).

In vivo studies in developing rats by Garcia *et al.* (2002) showed that after 4 days of subcutaneous CPF administration, which corresponded to the peak of glial differentiation and gliogenesis, there was a decrease in GFAP levels (Garcia *et al.*, 2002). Studies in differentiating rat C6 glioma cells have found similar results of a decrease in GFAP expression after treatment with sub-cytotoxic concentrations (1-10 μM) of diazinon oxon (DZO) for 24 hours, which suggests that the OPs can interfere with the development of astro-glial cells (Sidiropoulou *et al.*, 2009b).

Further evidence of the importance of GFAP in neurodevelopment and neurotoxicity comes from studies that have detected increased levels of this protein in the brains of humans suffering from neurodegenerative conditions including Parkinson's and Alzheimer's disease (Zhang *et al.*, 2014). Overall, the results of these studies suggest that GFAP could be a useful protein marker for detecting alterations in neurological pathophysiology and developmental neurotoxicity (Liu *et al.*, 2012).

1.11.5 Microfilaments and GAP-43

Another class of cytoskeletal network proteins are the MFs; the core filament is formed by polymerisation of actin, which has an approximate molecular weight of 43 kDa (Theriot, 1994; Hargreaves, 1997). The polymerisation of two globular strands of actin (G-actin) monomers forms MFs; the actin strands twisted around each other to produce F-actin, and this occurs through adenosine triphosphate (ATP) binding (Theriot, 1994; Hargreaves, 1997).

The dynamics of MF production occur through the exchange (incorporation and release) of G-actin monomers at the polymer ends (Zhang *et al.*, 2005). The process of exchange is

regulated by the binding/hydrolysis of ATP and interactions with specific actin binding proteins including growth associated protein-43 (GAP-43) and actin depolymerizing factor (ADF, also known as cofilin) (McGough and Chiu, 1999).

GAP-43 has been suggested to also play an important role in neurite outgrowth regulation (Skene, 1989; Pekiner *et al.*, 1996). It is found mainly in the elongating axons and growth cones in neurons (Das *et al.*, 2004). GAP-43 regulates a number of processes during neuronal development, including the plasticity of synapses, the development of axons, and the formation of growth cones (Benowitz and Routtenberg, 1997). During axonal outgrowth, studies have shown an increase in GAP-43 synthesis, which means disruption of neurite outgrowth could be indicated by an altered expression of GAP-43 (Skene, 1989; Pekiner *et al.*, 1996; Das *et al.*, 2004).

Studies on the effects of OPs on MFs have suggested that OP toxicity may be linked to a disruption in MF regulation. For example, a study by Harris *et al.* (2009b) in N2a cells found there was increased levels of cofilin after the cells were induced to differentiate in the presence of 10 μ M diazinon (DZ) for 24 hours. These changes in the observed cofilin levels could indicate a disruption in MF polymerisation and dynamics, which would affect the organisation of the MF network (Harris *et al.*, 2009b).

Numerous studies have evaluated the effect of exposing differentiating N2a cells to neurite inhibitory concentrations of CPF, CPO and other OPs, and the results show an association with reduced levels of GAP-43 (Fowler *et al.*, 2001; Sachana *et al.*, 2001; 2003; 2005; Sidiropoulou *et al.*, 2009a; Flaskos *et al.*, 2011). These findings indicate that a reduction in GAP-43 synthesis may lead to a loss of transport of GAP-43 from the cell body to dendrites and axons, which would inhibit neurodevelopment. Overall, this suggests GAP-43 could be used as a molecular marker to detect OPs-induced inhibition neurite outgrowth (Sachana *et al.*, 2005).

1.12 Genotoxic effects of organophosphorus compounds

Studies on the long-term effects of OP pesticide use suggest there is an association with increased incidence of certain cancers, such as non-Hodgkin's lymphoma, in individuals who are occupationally exposed to OPs (Dreiherr *et al.*, 2005). This suggestion of OPs causing DNA damage is supported by the work of Atherton *et al.* (2006), who used the *in vitro* comet assay to demonstrate the ability of the concentration 2.7 nM of dichlorvos to cause DNA damage in freshly isolated human lymphocytes from six healthy individuals.

Additional studies of OP exposed workers, such as that by Atherton *et al.* (2009), who studied lymphocytes from horticultural farm workers in Spain immediately after application of OP to crops, provide a better picture of the extent of DNA damage. The results of this study showed there was an increase in oxidative stress linked to DNA damage, and increased levels of 8-oxodeoxyguanosine which correlated with increased concentrations of urinary OP metabolites, even though the sample number was low (Atherton *et al.*, 2009). Further studies of OP exposed workers and studies on OP exposed cultured cells is needed to fully understand the mechanisms of OP associated DNA damage or altered gene expression (Paz-y-Mino *et al.*, 2002). Of particular interest to the present study were the effects of CPF, CPO and PSP on gene expression and its regulation.

1.12.1 CPF, CPO and PSP associated genotoxicity

Early studies in the developing rodent brain, suggested that CPF exposure is associated with inhibition of protein and DNA synthesis, thereby affecting the normal brain development after the treatment by subcutaneous administration of 2 mg CPF/kg body weight (Whitney *et al.*, 1995). Moreover, CPF exposure has also been associated with the inhibition of DNA synthesis, neuronal cell replication as well as neurite outgrowth in studies with neural cell lines (Song *et al.*, 1998; Das and Barone, 1999; Qiao *et al.*, 2001; Sachana *et al.*, 2001).

Exposure to *in vivo* (neonatal rats and female Sprague-Dawley rats) and *in vitro* (N2a, PC12 and HeLa cells) CPF can also stimulate increased ROS production, in a reversible manner, which may affect DNA and proteins within cells (Bagchi *et al.*, 1995; Bagchi *et al.*, 1996; Crumpton *et al.*, 2000a).

In vitro studies in PC12 and C6 mammalian cell lines have suggested that CPF may also interfere with the cell replication and differentiation of glial cells in the brain (Qiao *et al.*, 2001). Other studies have indicated that CPF and CPO at sub lethal concentrations 1-10 μM can inhibit the induction of glial cell differentiation in the presence of sodium butyrate (Sachana *et al.*, 2008). Exposure of glial cells to CPF is linked with increased ROS production; however, the ROS production is not a result of a direct chemical action, rather it is associated with the ability of CPF to interfere with cell metabolism (Crumpton *et al.*, 2000b).

In vitro studies have suggested that CPF does not cause DNA damage; for example, the work by Gollapudi *et al.* (1995) in rat lymphocytes and Chinese hamster cells (CHO) using

the chromosome aberration test showed 0.35 to 35.0 $\mu\text{g/ml}$ CPF for 24 h did not cause DNA damage. Muscarella *et al.* (1984) also worked with CHO cells exposing them to 1, 10 and 100 $\mu\text{g/ml}$ of CPF, and a no increase in the rate of chromosome aberration or sister chromatid exchange. This is further supported by the work of Cui *et al.* (2006) who used mouse hepatocytes to evaluate the potential of cypermethrin and CPF to form DNA adducts, and their results suggested CPF caused an increase in micronuclei incidence but that CPF could not form DNA adducts. In contrast, Rahman *et al.* (2002) used the alkaline comet assay to measure DNA damage in mice leucocytes, and concluded that CPF could cause damage in a dose-dependent manner. They also found that any damage to the DNA was repaired 48 hours after exposure, which could explain why it was not detected in the other studies.

However, it is important to consider both CPF and CPO for *in vivo* studies, as CPF is readily metabolised to the active oxon form in animals, due to the abundance of cytochrome P450s (Costa, 2006). There is some evidence from *in vivo* studies that CPF does have an effect, for example Amer *et al.* (1982) demonstrated significant increase micronuclei in the bone marrow of mice after repeated or dietary administration of CPF. They found that after two injections in one week of 45 mg/kg body weight (interval between dosing not stated), mice had a mean of 23 micronuclei (MN) per 1000 polychromatic erythrocyte (PCE), compared to 10.8 MN-PCE for the control. This MN-PCE background has been questioned as being quite high, with suggestions of a normal background being approximately 4 MN-PCE, suggesting the results may not be valid. The same group in 1996 found that dosing mice with and intra peritoneal injection of CPF at 4 mg/kg resulted in 57 chromosomal aberrations (aberrant metaphase 22.8 ± 0.79 % including gaps ($P < 0.01$), 14.8 ± 1.35 % excluding gaps ($P < 0.05$)) 24 hours after exposure (Amer *et al.*, 1996). In contrast Gollapudi *et al.* (1995) found there was no significant increase in MN in bone marrow after using a dose of 111 mg/kg that was 80 % of the estimated lethal dose (LD₅₀) for CPF. Further *in vivo* studies in mice have been carried out by Rahman *et al.* (2002), who used Swiss albino mice to investigate the DNA damaging capacity of CPF, using cyclophosphamide as a positive control. The mice were administered 24, 48, 72, and 96 hours using whole blood samples. They found a dose related statistically significant increase in DNA damage after 24 hours, when compared to the positive control, and the DNA damage decreased over time due to DNA repair pathways.

Other groups have used *Drosophila melanogaster* to study DNA damage and apoptosis caused by CPF, for example Gupta *et al.* (2010) treated third instar *Drosophila* larvae with

different concentrations of CPF (0.015-15.0 $\mu\text{g/L}$) for 24-48 hours. To determine the damage caused, oxidative stress markers, ROS generation, apoptotic cell death and DNA damage end points were measured, and they found that in 15.0 $\mu\text{g/L}$ CPF-treated organisms, there was a significant increase in DNA damage, which was associated with the apoptotic mode of cell death for both 24 and 48 hour treatments. The study also found that CPF exposure induced depolarisation of the mitochondrial membrane potential, and an increase in the activity of caspase-9 and caspase-3, suggesting that ROS may be involved in inducing DNA damage and apoptosis in *Drosophila* larvae (Gupta *et al.*, 2010).

Another type of study to evaluate the DNA damaging potential of CPF was carried out by Salazar-Arredondo *et al.* (2008), who evaluated the effect of different OPs on sperm DNA using the sperm chromatin structure assay. The damage was assessed in human spermatozoa from healthy volunteers after incubation with the non-cytotoxic (evaluated by eosin-Y exclusion) doses of 50-750 μM CPF and CPO. The results showed that CPO was 15 % more toxic than CPF to sperm DNA.

Other studies have investigated the toxicity of TOTP and PSP in SH-SY5Y human neuroblastoma cell cultures, using the fluorescent stain Hoechst 33342 to investigate whether OP-induced cell death was via apoptosis or necrosis (Carlson *et al.*, 2000). The results showed that exposure to PSP (10 and 100 μM) resulted in significant ($p < 0.05$) increases in apoptosis in a time-dependent manner, with increases in budding and nuclear condensation at 1 mM (Carlson *et al.*, 2000). This study also investigated caspase-3 activity and found that exposure to all 3 concentrations of PSP resulted in significant ($p < 0.05$) increases in caspase-3 activation, again in a time-dependent manner (Carlson *et al.*, 2000). To further elucidate the mechanisms involved, the cells were pre-treated with cyclosporin A (to inhibit apoptosis) or the serine esterase inhibitor PMSF (to help detect the method of inhibition) resulting in significantly ($p < 0.05$) decreased caspase-3 activation after treatment with 1 mM PSP and TOTP, which suggested that the OP-induced cytotoxicity could be modulated through different mechanisms, such as receptor-mediated caspase. In addition, they found that the exposure to 1 mM PSP induced random DNA fragmentation, and necrotic morphological changes (Carlson *et al.*, 2000).

Overall, these results suggest OPs like CPF, CPO and PSP do have the ability to induce DNA damage, but the questions remain as to the exact mechanisms involved in different cell types. The previous studies into OP, and specifically CPF, toxicity have highlighted changes in key neuronal proteins, which are good starting point for determining the actual

mechanism behind the toxicity. Moreover, as the effects of OPs on gene expression are still not fully understood, further study is needed to elucidate the actual mechanisms of toxicity, which will help to prevent and detect toxicity of OP.

1.13 The use of *in vitro* mammalian cell line models for assessment of organophosphate induced neurotoxicity

Animal experimentation is now associated with a high economic and ethical impact, combined with the time consuming, laborious, and complex processes required for neurological experiments due to the complexity and relative inaccessibility of the nervous system, which has meant that investigators are keen to identify alternative methods for use to assess both pathological and physiological processes. One such method is the use of *in vitro* cellular models; the main advantages of mammalian cell lines comes from their ability to grow and reproduce quickly. They form homogenous cells in large numbers using relatively simple preparation methods, which means they can be grown and maintained for extended periods, cryopreserved, and reanimated easily to re-test at different intervals with the same cells (Radio and Mundy, 2008; Flaskos, 2012). In addition, *in vitro* models can provide invaluable information as they are a simplified tool that can be used for studying OP induced neurotoxicity at both molecular and cellular levels in a specific cell type (Silva *et al.*, 2006). There are some limitations for neurotoxicity assessment with cell culture models including partial involvement of pharmacokinetic factors, lack of cell to cell interaction, such as between glial and compromise their ability to reliably predict or model *in vivo* toxicity (Rice and Barone, 2000; Flaskos, 2012). However, there are important advantages of these culture systems which make them an appropriate approach in this project.

The advantages of cell lines over *in vivo* studies include the ability to screen or study the effects of multiple doses of toxins or mixtures of toxins on specific cell models at relatively low cost compared to animal models, which has led to an increasing number of publications using different cell lines to study the effects of OPs. Another key advantage for the current study is the ability to allow different concentrations of CPF and CPO to be tested on glial cells and neuronal separately, which means the different contributions of the toxicity on these cells types can be determined (Flaskos, 2012). Using cell lines can result in not only qualitative assessment of cytotoxic effects, but also the quantitative detection of any cellular alterations, such as molecular changes within specific neuronal cells expressing specific neurite morphological features, such as dendrites and axons. This level of control

means the research methodology can be adjusted by controlling the onset and timing of development to fit the requirements of the study (Banker and Goslin, 1998). These advantages of cell lines mean that are suitable models for using in high throughput screening methods, which allows studies into the primary screening of compounds (Giacomotto and Ségalat, 2010). One of the key disadvantages of the using a cell culture system is the lack of replication of systemic effects, such as cell-cell interactions in tissues, the input of other organs including the liver where toxic agents are degraded or bioactivated, bio-eliminated, and excreted from the body, or appropriate supply and balance of growth factors (Sprague and Castles, 1985; Sachana and Hargreaves, 2012). The availability of growth factors can be partially addressed by inclusion of suitable growth factors in the media, and cell-cell interactions can be tackled to some extent by using organ culture or co-culture systems (Sachana and Hargreaves, 2012). Some of the effects of the liver can be mimicked by using processes to bioactivate or inactivate the toxin being investigated using microsomal activation (Sprague and Castles, 1985). The systemic effects can also be addressed by using other metabolic activation systems, such as hepatic cells or microsomes that are nicotinamide adenine dinucleotide phosphate hydrogen (NADPH) activated contained in a cell culture well with a filtered-insert (Sachana and Hargreaves, 2012). The insert allows the toxin to be introduced to the cells or microsomes and then the non-metabolized and metabolized toxin diffuses into the growth medium below where it can be accessed by the cell line of interest (Sachana and Hargreaves, 2012).

A large proportion of OP neurotoxicity studies have used neuroblastoma cell lines from different species, including mouse N2a neuroblastoma, rat PC12 pheochromocytoma, and human neuroblastoma clones SH-SY5Y, IMR32, C-1300, and N-18, and there have also been many studies using the rat C6 glioma cell line. Some of these studies have used the cell lines to evaluate NTE inhibition after OP exposure, as a potential replacement for the use of homogenates from hen brains after OP exposure in vivo (Fedalei and Nardone, 1983; Ehrich, 1995; Ehrich *et al.*, 1994).

Other studies have focused on the effects of OPs on the cellular mechanisms in both glioma and neuroblastoma cell lines; for example, studies by Henschler *et al.* (1992) and Schmuck and Ahr (1997) both investigated a large number of OPs in rat C6 glioma and human N-18 neuroblastoma cell lines. These cell lines were cultured, differentiated and then treated with a panel of OPs for up to three weeks. One of the major drawbacks of this experimental design was the lengthy incubation period, which would have resulted in high levels of cytotoxicity, which could affect the usefulness of the results observed. These culture

conditions were also very different from the conditions seen for OPIDN induction *in vivo*, studies have shown NTE and cytoskeletal protein inhibition occurs within 24 hours of OP exposure, which suggests these studies may have missed key early cellular changes based on their design (Abou-Donia 1993; 1995).

A more mechanistic approach was developed by Flaskos *et al.* (1994; 1998), which used sub-lethal concentrations of OPs given to cultured cell lines, which were then studied for short time periods. As PC12 cells can be effectively cultured for several weeks before cell loss, they used them to study axon maintenance and found sub-cytotoxic levels of TCP (1 µg/ml) inhibited neurite maintenance (Flaskos *et al.*, 1994). The studies also used glioma and neuroblastoma cell lines to investigate the early OP effects, and they found there was no effect on cell viability even after 48 hours with the doses used (Flaskos *et al.*, 1994; 1998). These sub-cytotoxic conditions were also used in cell lines to investigate the effects of OPs on the nervous system, mainly the glial and neurons, neurite outgrowth, and the effects on expression of cytoskeletal proteins. The studies found CPF, CPO and PSP caused alterations neurite outgrowth, cytoskeletal protein expression, axon growth associated proteins and those involved in cell signalling pathways (Sachana *et al.*, 2001; Sachana *et al.*, 2008; Flaskos *et al.*, 2011; Flaskos, 2014; Sindi *et al.*, 2016).

The use of human derived neural stem cells may enhance the ability to predict CPF and CPO neurotoxicity with more human relevant results, but currently there is not enough evidence to clearly show an advantage of these stems cells over rodent derived cell lines in terms of predicting human neurotoxicity (Radio and Mundy, 2008). Three mammalian cell lines that are commonly used to investigate CPF and CPO developmental neurotoxicity are further described below.

1.13.1 N2a neuroblastoma cell line

One of the most widely used cell lines for studying OP toxicity is the N2a cell line, especially for studies to investigate neurite outgrowth and neuronal differentiation (Henschler *et al.*, 1992; Flaskos *et al.*, 1998; 2011; Sachana *et al.*, 2001; 2003; 2005; 2014; Hargreaves *et al.*, 2006; Sidiropoulou *et al.*, 2009a). The N2a cell line was originally derived from a C1300 mouse tumour (neuroblastoma); these cells are able to be differentiated into cells with a neuron-like morphology, and they can then express many neuronal markers, including cholinergic and adrenergic markers, and AChE, which is important for studying OP toxicity (Klebe and Ruddle, 1969). N2a cells grow under normal mitotic conditions as round neuroblasts. The differentiation process for N2a cells starts by

serum removal from the medium; this helps to form the non-dividing differentiating cells which have the morphological characteristics of neurons. This serum free medium is supplemented by the addition of dibutyl cyclic 3',5'-monophosphate (dbcAMP), which mimics cAMP action to promote N2a cell differentiation (Schubert *et al.*, 1969; Haffke and Seeds, 1975). During differentiation, N2a cells undergo morphological changes including the formation of dendrite- and axon-like processes contain have high concentrations of cytoskeletal proteins, including MTs and NFs, which makes them an ideal cell line for studying the effect of OPs on these types of proteins (Schubert *et al.*, 1969).

One of the main disadvantages of using the N2a cell line for OP toxicity studies is the fact that the dendrites and axons produced by these cells may not be able to reproduce some of the more complex characteristics that are observed in neurites from primary neurons, meaning that some effects of the toxicity may be missed or reduced due to the lack of connections (Radio and Mundy, 2008). Overall, these cells are a suitable model for investigating CPF neurotoxicity as they express some of the key targets for toxicity, including AChE, MTs and NFs, they grow quickly and reproducibly, and they are commercially available, which outweighs the disadvantages.

1.13.2 C6 rat glioma cell lines

The C6 rat glioma cell line has also been widely used to study the effect of OPs, with differing results between the studies (Sachana *et al.*, 2008). The C6 cell line was originally derived from glioma cell line was originally derived from an N-nitrosomethyl-urea-induced rat brain tumour, and have been used as an *in vitro* model for the investigation of glial properties for many years, including expression of GFAP, 2':3'-cyclic nucleotide 3'-phosphohydrolase, glycerol phosphate dehydrogenase by glucocorticoid hormones, and S-100 protein (Wolfe *et al.*, 1980).

Schmuck and Ahr (1997) and Henschler *et al.* (1992) used C6 glioma and human N-18 neuroblastoma cell lines to investigate the effects of many OPs by treating the cells for three weeks, and the results showed high levels of cytotoxicity due to the long exposure period. The C6 cell line has been used to study the effect of OPs neurite outgrowth, and the results of the studies have shown that sub-cytotoxic concentrations, OPs including CPF and CPO, inhibit neurite outgrowth (Henschler *et al.*, 1992; Schmuck and Ahr, 1997; Flaskos *et al.*, 1998). These cell lines are suitable for use in conjunction with the N2a cell line as they provide more information about how OPs cause neurotoxicity in different key cell types within the brain.

1.13.3 Human neural progenitor stem cells (ReNcell CX)

Although N2a and C6 cell lines have many advantages for investigation the process of OP toxicity, they are both monocultures that lack neuronal-glia interactions and both of them are rodent cell lines. There is, however, a neural progenitor stem cell line that could offer different advantages for these types of studies, namely the ReNcell CX cell line. This cell line, is can be induced to differentiate to form a co-culture of different neuronal and glial cell types, such as cholinergic and dopaminergic neurons, astrocytes and oligodendrocytes, and is commercially available (Merck Millipore) (Seaberg and van der Kooy, 2003). The origin of the ReNcell X cells was a 14-week gestation human foetus with a normal male karyotype, specifically the cortical region of brain, which was then immortalized using c-myc oncogene retroviral transduction and this produced unlimited growth of clonal human neural stem cells (Donato *et al.*, 2007; Kornblum, 2007). The morphology of these cells on uncoated tissue culture flasks starts as round neurospheres when they are undifferentiated, but when they are grown on laminin coated surfaces as a monolayer, with the appropriate growth factors, they produce a normal diploid karyotype, which is maintained even after prolonged passage (Jakel *et al.*, 2004). When grown on a laminin coated surface in the absence of mitogens these cells differentiate into a mixed population of three main nervous system cell types, astrocytes, oligodendrocytes, and neurons (Figure 1.9), which are identical to those found in the human nervous system (Kornblum, 2007). One key advantage of these cells over N2a and C6 cells is the fact the dendrites and axons produced in this cell line form the same level of complex interactions as neurons in humans, making them an ideal choice for studying OP toxicity in a more relevant human model (Bal-Price *et al.*, 2008; Radio and Mundy, 2008).

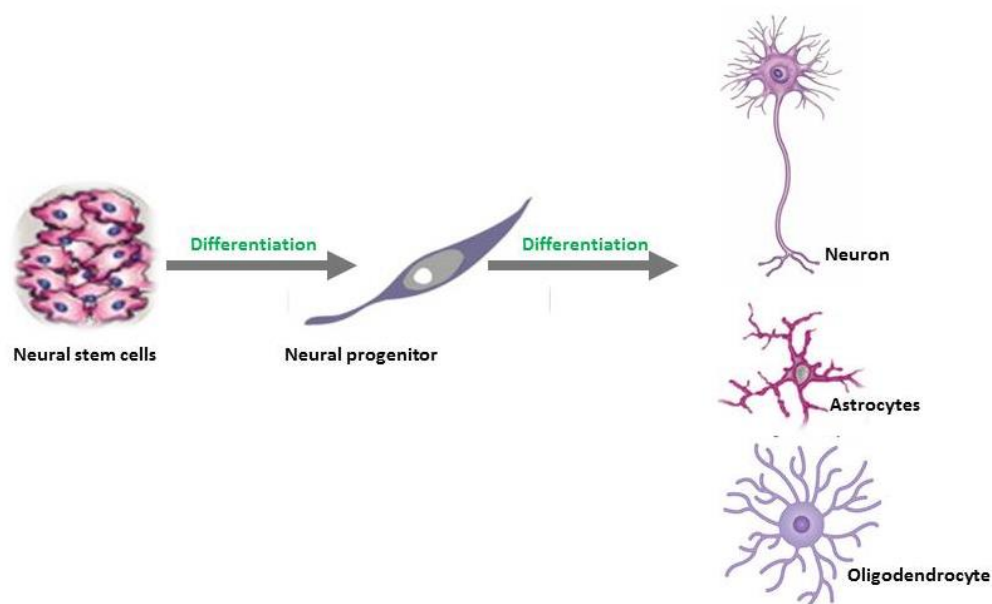


Figure 1.9. Schematic representation of neural stem cell differentiation.

1.14 Summary

Historically, OPs have been used in a number of industrial, agricultural and domestic settings, with a wide range of applications, but as more investigations were carried out it became clear that these types of compounds are toxic, causing different levels of neurotoxicity depending on the dose, age of patient and route of exposure. Due to this toxicity, many countries have put restrictions on their use in residential settings and limitations in place for their agricultural use, but these pesticides are still very widely used in developing countries. Despite the potential dangers to health and the imposed restrictions, CPF remains a popular pesticide to use especially in many developing countries (Salyha, 2010). The main OPs selected for this study were CPF, CPO and PSP; these were chosen because they are widely used, have been studied for toxicity, and can induce the different stages of OP toxicity (acute cholinergic syndrome, intermediate syndrome, OPIDN, and COPIND) depending on dose, age of the patient, and the duration of exposure. CPF has been shown to affect different parts of nervous system, including glial cells, neurons, key cellular and cytoskeletal proteins, neurite outgrowth, and it can also affect DNA, therefore studying the effects on gene expression could provide key insights into its method of action.

Studies of OP toxicity have shown that *in vitro* methods are suitable for studying the processes involved, and they have some advantages over *in vivo* methods, such as being able to produce large numbers of identical cells which will allow many OPs, or different

doses, to be screened at the same time. The main disadvantage of *in vitro* methods is that they lack the processing that occurs in the rest of the body, such as the bioprocessing that occurs in the liver, but some of these processed can be added into the methodology which will mimic the action of the liver, making the process more accurate.

There have been many studies showing that CPF, CPO and PSP can all disrupt cytoskeletal protein formation and inhibit outgrowth in differentiating neural cell lines. Studies have also shown that the toxicity produced by OPs depends on when exposure occurs; exposure in different developmental stages can result in different effects. Previous *in vitro* studies have mainly involved OP administration at the induction of cell differentiation, meaning the results do not explore the full range of potential toxicities that could be produced. Currently, not many investigations have involved studying the genotoxic effects of OPs on cells, therefore this thesis has investigated this aspect of toxicity to increase the knowledge in this area, by examining the toxic effects of the selected OPs at different time points in 3 different models of neural cell differentiation.

1.15 Project Aims

Studies conducted by research colleagues have shown that treatments of sub-lethal concentration of CPF and CPO in differentiating mouse N2a neuroblastoma cells inhibited axon outgrowth and disrupted the cytoskeleton (Sachana *et al.*, 2001; Sindi *et al.*, 2016). Therefore, by replicating these culture conditions, the aims of this thesis were to:

1. Determine the effects of CPF, CPO and PSP (1, 3 and 10 μM) on cell viability in differentiating N2a, C6 and human ReNcell CX stem cells, after treatment for 24 h.
2. Determine the effects of sub-lethal exposure to all 3 OPs on different parameters of neurite outgrowth and the underlying effects on cytoskeletal proteins by high content analysis, cell ELISA and quantitative Western blotting.
3. Generate oligonucleotide probes for neural marker genes for quantitative PCR in order to quantify the effects of sub-lethal concentrations of OPs on the expression of genes encoding key cytoskeletal proteins affected by OP exposure in these cell models.
4. Investigate the effects of sub-lethal concentrations of CPF, CPO and PSP on the epigenetic regulation of gene expression focussing on histone deacetylase activity

Chapter 2

Materials and Methods

2.1 Materials

2.1.1 General laboratory reagents

All laboratory reagents were of the highest grade and purchased from Sigma-Aldrich Chemical Company (UK) unless otherwise specified in the text. They are listed in tables 2.1 and 2.2.

Table 2.1. List of cell culture reagents

Reagents	Code number	Supplier
Dulbecco's Modified Eagle's Medium (DMEM) with 4.5 g/L glucose and 2 mM L-glutamine	BE12-614F	Lonza (Slough, UK)
Penicillin/streptomycin (penicillin 10,000 units/ml, streptomycin 10,000 units/ml)	DE17-602F	
Trypsin 10x	17-160E	
Foetal bovine serum (FBS) South American origin	FB-1001	Biosera
N6,2'-ODibutyryl adenosine 3',5'-cyclic monophosphate sodium salt (dbcAMP)	D0627	Sigma-Aldrich
Sodium butyrate (NaB)	B5887	
Dimethylsulphoxide (DMSO) sterile-filtered, BioReagent, suitable for cell culture - hybridoma tested	D2650	
Trypan Blue Solution 0.4% (w/v)	1450021	Bio-Rad
Laminin from Engelbreth-Holm-Swarm murine sarcoma basement membrane	L2020	Sigma-Aldrich
StemPro [®] Accutase [®] cell dissociation reagent	A11105-01	Thermo Fisher Scientific
StemPro [®] Neural supplement	A10508-01	
KnockOut [™] DMEM/F-12 (1X)	12660-012	

Neurobasal® -A medium, no L-glutamine, L-glutamic acid or aspartic acid	10888-022	
Recombinant human epidermal growth factor (EGF) (10 µg)	1380077C	
Recombinant human fibroblast growth factor b (FGFb) (10 µg)	1424760B	

Table 2.2. List of other reagents and materials.

Reagents	Code number	Supplier
3,3',5,5'-Tetramethylbenzidine (TMB)	T0440	Sigma-Aldrich
3-(4,5-Dimethylthiazol-2-yl)-2,5 diphenyltetrazolium bromide (MTT)	M2128	
AccuGel 29:1 acrylamide (40% (w/v) acrylamide/bisacrylamide 29:1)	EC852	Geneflow
StemPro Accutase Cell Dissociation Reagent	A1110501	Thermo Fisher Scientific
Acetone	121403/0031	Thermo Fisher Scientific
Amersham Protran 0.2 µm pore size nitrocellulose membrane	10600001	General Electric
Ammonium persulphate (APS)	A3678	Sigma-Aldrich
Bicinchoninic acid (BCA)	23223	
Bovine serum albumin (BSA)	A1302	Melford
Copper (II) phthalocyanine	C2284	Sigma-Aldrich
Dimethylsulphoxide (DMSO)	CHE1854	Thermo Fisher Scientific
Enhanced chemiluminescence reagent (ECL)	ME157124	Thermo Fisher Scientific
Ethanol	652261	Sigma-Aldrich
Glacial acetic acid	200.580-7	Thermo Fisher Scientific
Glycerol 10% (v/v)	15892001C	ACROS organics

Hydrochloric acid	H1000PB17	Thermo Fisher Scientific
Hydrogen peroxide (H ₂ O ₂)	H1009	Sigma-Aldrich
Methanol	M400/17	Thermo Fisher Scientific
β-Mercaptoethanol	M3148	Sigma-Aldrich
N,N,N,N-Tetramethylethylene diamine (TEMED)	T9281	Sigma-Aldrich
Paraformaldehyde 4% (w/v)	HT501128	Sigma-Aldrich
Protogel® resolving buffer (4x) (1.5 M Tris-HCl buffer pH 8.8, 0.4% (w/v) SDS)	EC892	Geneflow
Protogel® stacking buffer (4x) (0.5 M Tris-HCl buffer pH 6.8, 0.4% (w/v) SDS)	EC893	
Sodium acetate	S2889	Sigma-Aldrich
Sodium azide	S2002	Thermo Fisher Scientific
Sodium chloride	B22297	Sigma-Aldrich
Sodium dodecyl sulphate (SDS)	18299	Melford
Sodium hydroxide (NaOH)	1823	Sigma-Aldrich
Sulphuric acid (H ₂ SO ₄)	339741	
Tris (hydroxymethyl) aminomethane	C22561	
Tween 20	P1379	
VectaShield® mounting medium for fluorescence containing 4',6-diamidino-2-phenylindole (DAPI)	H1400	Vector Laboratories Ltd

2.1.2 Plastic ware

All sterile cell culture flask sizes (T25 and T75) were supplied by Scientific Laboratory Supplies Nottingham, UK. Nunc brand Cryotube vials were purchased from Merck Ltd., Leicester, UK. NUNC-immuno 96-well and 24-well cell culture plates were purchased from Thermo Scientific, UK. IbidiTreat 8-well 15μ-slides were purchased from Thistle Scientific, UK. Counting slides with dual chambers (Cat#1450015) were from Bio-Rad Laboratories Inc., UK. Serological pipettes (5 ml, 10 ml and 20 ml), Gilson pipettes (P10, P1000, P200, P100, P20, P10, P2 and Integra pipettes were obtained from Scientific Laboratory Supplies, Nottingham, UK.

2.1.3 Test compounds

Chlorpyrifos (CPF) and its metabolite, chlorpyrifos oxon (CPO) (purity 97.6 %) from Chem Service Inc. (West Chester, PA, USA), were supplied by Greyhound Chromatography (Birkenhead, UK). Phenyl saligenin phosphate (PSP) was synthesized by Dr Chris Garner (Department of Chemistry) at Nottingham Trent University and obtained at 98 % purity. Sterile filtered DMSO was used as control (purity 97.7 %). The final concentrations of the compounds 1, 3 and 10 μ M were prepared freshly from the stocks 0.2, 0.6 and 2 mM.

2.1.4 Cell lines

Three different cell lines were used in the current study and these were mouse neuroblastoma 2A (N2a), Rat C6 glioma and human neural progenitor stem cells (ReNcell CX).

2.1.4.1 Mouse neuroblastoma 2A

N2a is a well-established fast growing mouse neuroblastoma cell line derived from mouse neural crest (Klebe and Ruddle, 1969). N2a cells have been cultured and extensively used in research to study neural differentiation, neurofilament characteristics including neurite outgrowth and morphology, as well as signalling pathways involved in neurotoxicity, Alzheimer's disease and asymmetric division of mammalian cells (Ogrodnik *et al.*, 2014; Salto *et al.*, 2015). It was purchased from the American Type Culture Collection (product no. CCL-131TM, Middlesex, UK).

2.1.4.2 Rat C6 glioma

The C6 glioma cell line was established after culturing a clone of a rat glial tumour induced by N-nitrosomethylurea (Benda *et al.*, 1968). The C6 astrocyte cell line is fibroblast-like in morphology. It was purchased from the European Collection of Animal Cell Cultures (ECACC). The C6 astrocyte cell line, stains strongly positive for glial fibrillary acidic protein (GFAP). After 100 passages they can be used to study astrocytic functions including parameters of oxidative stress (Quincozes-Santos *et al.*, 2009).

2.1.4.3 Human ReNcell CX

The human neural progenitor stem cell line (ReNcell CX) was established by retroviral transduction of stem cells obtained from the cortical region of the brain from a 14-week gestating human foetus following normal termination and in accordance with nationally approved UK ethical and legal guidelines as described (Donato *et al.*, 2007). It was purchased from Merck Millipore (catalogue no. SCC007, UK). ReNcell CX is an immortalized multipotent human neural progenitor cell line with the ability to differentiate into neurons, astrocytes and oligodendrocytes (Breier *et al.*, 2010). ReNcell CX can be used for a variety of research applications including studies of neurotoxicity, neurogenesis, electrophysiology, neurotransmitter and receptor functions (Choi *et al.*, 2014).

2.2 Methods

2.2.1 Cell culture and maintenance of N2a neuroblastoma cells and rat C6 glioma cells

Mouse N2a and C6 glioma cell lines were grown and maintained as monolayer cultures in growth medium consisting of Dulbecco's modified Eagle's medium (DMEM) containing 4.5 g/L glucose and 2 mM L-glutamine, and supplemented with 10% (v/v) foetal bovine serum (FBS), penicillin (100 units/ml) and streptomycin (100 units/ml) at 37 °C, in a humidified atmosphere of 95% air /5% CO₂. All experiments were performed using plastic tissue culture treated flasks, dishes, microplates or chamber slides. Culture medium was changed every 2-3 days.

2.2.1.1 Sub culture and maintenance of N2a neuroblastoma cells and rat C6 glioma cells

Mouse N2a neuroblastoma and rat C6 glioma cells were passaged when growth was 80 % confluent (i.e. every 3-5 days) as follows. In N2a cell monolayers, half of the growth medium was carefully removed from the culture flask without disturbing the attached cell monolayer. Cells were mechanically detached from the flask surface using a sterile extra-long plastic Pasteur pipette to aspirate the rest of the growth medium and squirting it out on over the monolayer surface of the cell culture flask. C6 cells were mechanically detached from the flask by using the scraper in 5 ml of growth medium, and this method was shown to be effective and fast. In addition, there was an alternative method to maintain C6 cells,

after cell growth reached 80 % confluence in T75 culture flask before passage (i.e. every 3-4 days). The spent medium was discarded from the culture flask, then the cell monolayer was washed with phosphate buffered saline (PBS; 137 mM NaCl, 2.7 mM KCl, 10 mM Na₂HPO₄, 2 mM KH₂PO₄ pH 7.4) to remove all traces of serum. Cells were chemically detached from the flask surface by adding 2 ml of 1 % (v/v) trypsin solution to cover the cell monolayer and the flask was then placed in the 37 °C incubator for approximately 2 min. The enzymatic reaction was stopped by adding 5 ml of pre-warmed fresh growth medium.

N2a or C6 cells were then harvested by centrifugation at 300 × g at room temperature for 5 min. The supernatant was carefully discarded and the resultant pellet was re-suspended in 1 ml of growth medium by passing it 21 times through a P1000 micropipette tip to break up the pellet. About 1/5 of the cell suspension was then placed in a new T75 flask containing 40 ml fresh growth medium and incubated in a humidified atmosphere containing 5 % CO₂/95 % air at 37 °C until the growth reached 80 % confluent. All experiments were replicated at least 4 times, and controlled for passage number (less than 21), in order to avoid genetic drift, which may occur at higher passage.

2.2.2 Human neural ReNcell CX stem cell culture and maintenance

2.2.2.1 ReNcell CX maintenance medium

ReNcell CX cells were maintained in KnockOut™ DMEM: nutrient mixture F-12 (DMEM/F-12) low osmolality medium without HEPES buffer. The growth medium (500 ml) was supplemented with recombinant human epidermal growth factor (EGF) (20 ng/ml; Gibco), basic fibroblast growth factor (FGFb) (20 ng/ml; Gibco), StemPro neuro supplement (2 % v/v; Gibco), L-glutamine (0.5 mM), penicillin (100 units/ml) and streptomycin (100 units/ml).

2.2.2.2 ReNcell CX culture

All plastic tissue culture ware used for ReNcell CX cells culture was pre-coated with laminin from Engelbreth-Holm-Swarm murine sarcoma basement membrane (Sigma-Aldrich) prior to use. Laminin is an extracellular matrix (ECM) protein, which enhances neural progenitor stem cell adhesion, proliferation differentiation and neurite outgrowth (Flanagan *et al.*, 2006). In brief, 1 mg/ml laminin was thawed at room temperature and

diluted to 20 µg/ml final concentration in Neurabasal medium (Gibco) that contained no L-glutamine, L-glutamic acid, or aspartic acid. Laminin solution was added to cover the surface of the required tissue culture vessels and left on a shaker for 4 h at room temperature if required to use on the same day, or afterwards stored at 4 °C until needed. The laminin solution was removed and the flask was rinsed with sterile PBS just before using a coated flask for culturing ReNcell CX cells. Cells were chemically detached from the flask surface by adding 1 ml of Accutase™ cell detachment solution which contains 1x Accutase enzyme in Dulbecco's PBS (0.2 g/l KCl, 0.2 g/l KH₂PO₄, 8 g/l NaCl, and 1.15 g/l Na₂HPO₄) containing 0.5 mM EDTA-4Na and 3 mg/l Phenol Red). The flask was allowed to stand for 5min at room temperature. The enzymatic reaction was stopped by adding 4 ml of pre-warmed fresh growth medium and the cell suspension was centrifuged at 300 g for 5 min at 22°C. The pellet was resuspended by 10 passes up and down through a 1000 µl pipette tip in 1 ml of fresh growth medium. About 200 µl (i.e. ~ 1/5 of the total cells) of cell suspension were then placed in a new laminin coated T75 flask containing 40 ml fresh growth medium and incubated in a humidified atmosphere containing 5 % CO₂/95 % air at 37 °C until the growth reached 80 % confluence.

2.2.3 Cryopreservation of cell lines

For cell storage and preservation, cells were stored under liquid nitrogen in cryovessels until needed. Briefly, the confluent cells from a T75 flask were detached, harvested and resuspended in 1 ml of freezing medium (DMEM for C6 and N2a or knockout DMEM/F-12 medium for ReNcell CX, supplemented with 5 % (v/v) DMSO). Addition of DMSO to media prevents intracellular and extracellular crystals from forming in cells during the freezing process (Chen *et al.*, 2017). This cell suspension was placed into 1 ml cryo vials, which were transferred to cell freezing container and incubated overnight at -80°C for a minimum of 8 h. The cryo vials were then transferred to a liquid nitrogen container (-196°C) and stored until needed.

2.2.4 Cell recovery from liquid nitrogen storage

For continuous growing, cells were thawed from liquid nitrogen and added to pre-warmed growth medium in culture flasks. In brief, a vial of cells was removed from the liquid nitrogen storage and held in a 37 °C water bath for 1-2 min. The outside of the vial was quickly wiped with 70 % v/v ethanol in distilled water to sterilise and the cells were

transferred into centrifuge tube using a 1 ml sterile pipette. A volume of 9 ml maintenance medium (pre-warmed to 37 °C) was gently added to avoid osmotic shock which may result in decreased viability. The cell suspension was centrifuged at 300 g for 5 min. The supernatant was completely discarded following centrifugation in order to remove any residual cryopreservation medium. The resultant pellet was resuspended in 1 ml of pre-warmed growth medium. The cell suspension was then plated onto T75 tissue culture flask containing 40 ml of pre-warmed fresh maintenance medium for N2a and C6 glioma cell lines or onto a laminin coated T75 flask containing 20 ml of pre-warmed fresh growth medium for ReNcell CX.

2.2.5 Cell plating for experimentation

All experiments were preceded by cell seeding and counting in order to determine a specific cell density. In brief, cell monolayers were grown to reach 80 - 90 % confluence, then detached and harvested at 300 g by centrifugation for 5 min as described (sections 2.2.1.1 and 2.2.2.2). Cell pellets were resuspended in 1 ml of growth medium. Cell dilutions were prepared depending on the pellet size and cell counting method. The initial cell count was performed either manually using a haemocytometer chamber slide, or automatically using an automated cell counter.

2.2.5.1 Manual cell counting

A volume of 10 µl was transferred to the chamber from a dilution of 10 µl cell suspension with (1:20 dilution) 190 µl of growth medium, and the cell number determined by using a haemocytometer. Chamber cell counts were performed in five fields of a Neubauer haemocytometer (each field has a volume of 10^{-4} cm³) by using an inverted light microscope (Inverso 3650 Fisher Scientific Ltd., UK). Cell density was calculated as follows:

Cells / ml = cell number (average from five fields) $\times 10^4$ (volume correction factor) \times dilution factor

The formula was used to calculate the volume necessary to achieve a specific cell density. The cells were allowed to recover for 24 h in a humidified atmosphere of 95 % air / 5 % CO₂ at 37°C.

2.2.5.2 Automated cell counting

Automated cell counting has recently become the robust alternative method to manual haemocytometer cell counting because it can provide total cell count and assess cell viability in one simple step. Moreover, automated cell counting produces an accurate, reproducible result with rapid performance. The results of the current study were achieved by using the Trypan blue exclusion procedure coupled with a TC20™ automated cell counter (BioRad, USA). The TC20™ automated cell counter can count cells with a 6-50 µm diameter and within a broad concentration range of 5×10^4 to 1×10^7 cells/ml, which often eliminates the need to dilute cells, thus reducing the error associated with sample dilutions prior to counting. The device utilises already made Trypan blue dye (BioRad, USA) composed of 0.4 % (w/v) Trypan blue in 0.8 % (w/v) sodium chloride and 0.06 % (w/v) potassium phosphate dibasic solution. Trypan blue is a vital stain that differentiates between live and dead cells (Tran *et al.*, 2011). The principle of this staining is based on the blue acid dye chromophores which are taken up by dead cells and excluded from viable cells.

Briefly, depending on the size of the cells pellets which were resuspended in 2 ml pre-warmed fresh growth medium and a volume of 10 µl from the suspended cells was added onto the same equal volume of Trypan blue solution in an Eppendorf tube and mixed gently by 10 passes through a P10 pipette tip. This was then left to stand for 4 min for cells to be exposed to the stain. A volume of 10 µl of the mixture was then loaded onto a dual-chambered cell counting slide (BioRad, Watford, UK) using a pipette tip. The slide was inserted into the TC20 cell counter and counting was automatically initiated as soon as the presence of slide and Trypan blue dye were detected by the cell counter. When Trypan blue is detected in a sample, TC20 takes the dilution into account and multiplies results by 2. The result was adjusted to account for 1 to 1 cell dilution and was reported on the monitor as estimated concentration of the undiluted sample. For example, a 1×10^6 cells/ml mixed 1 to 1 with Trypan blue was at a concentration of 5×10^5 cells/ml. The total cell counts, live cell counts and the percentage of live cells appear on the count screen. The live cell counts per ml were used to determine the volume of cell suspension necessary to seed the cells at a required cell density in growth medium. A cell density of 50,000 cells/ml was used to plate out mouse N2a cells, rat C6 glioma cells and 100,000 cells/ml was used to plate out ReNcell CX cell according to the required size of flask or plate (Table 2.3).

Flasks were incubated in a humidified atmosphere containing 5 % CO₂/95 % air at 37°C for 24 h to allow for cell recovery.

Table 2.3. The cell density of N2a, C6 and ReNcell CX cell lines for the experiments of current study.

Type of cell culture ware	N2a		C6		ReNcell CX	
	Medium volume	Total cell number	Medium volume	Total cells number	Medium volume	Total cell number
T75 flask	40 ml/flask	2,000,000	40 ml/flask	2,000,000	40 ml/flask	4,000,000
T25 flask	10 ml/flask	500,000	10 ml/flask	500,000	10 ml/flask	1,000,000
8 well slide	300µl/well	15,000	300µl/well	15,000	300µl/well	30,000
24 well plate	500µl/well	25,000	500µl/well	25,000	500µl/well	50,000
96 well plate	200µl/well	10,000	200µl/well	10,000	200µl/well	20,000

2.2.6 Induction of cell differentiation

For differentiation, cells were cultured in maintenance medium devoid of mitogens or serum. Prior to differentiation, all cells were passaged as described previously. Cells were plated out according to the required plating density (Table 2.3) in culture flasks or plates and incubated for 24 h to allow for recovery, after which growth medium was carefully removed without disturbing the monolayer and replaced with an equal volume of serum free medium. In N2a and C6 cells, differentiation was induced by replacing growth medium with serum free medium (i.e. DMEM containing 4.5 g/l glucose, 2 mM L-glutamine, supplemented with penicillin (100 units/ml) and streptomycin (100 units/ml) and 0.3mM dibutyryl dbcAMP (for N2a) or 2mM sodium butyrate (for C6), which was diluted in serum free medium (Flaskos *et al.*, 1998). For this study, a volume of 100 µl of dbcAMP stock solution (30 mM) or sodium butyrate (200 mM stock solution) were dissolved in 10 ml serum free medium and sterile-filtered to give final concentrations of 0.3 mM and 2 mM respectively.

ReNcell CX differentiation was initiated by replacing the growth medium with mitogen free medium, consisting of knockout DMEM/F-12 medium plus all supplements except the

growth factors EGF and FGFb (section 2.2.2). The removal of growth factor EGF and FGFb from the maintenance culture medium induces ReNcell CX cells differentiation by stopping cell proliferation (Donato *et al.*, 2007). All cell lines were being treated with or without the OP compounds at the same time when they were induced to differentiate at 37°C in a humidified atmosphere of 95 % air / 5 % CO₂ for 24 h.

2.2.7 Measurement of cell viability in cells exposed to OPs

The measurement of cell viability plays a fundamental role in most *in vitro* studies of cellular response to toxic substance and sometimes forms the main purpose of the experiment, such as in toxicity assays. The effects of CPF, CPO and PSP on the viability of N2a cells, C6 cells and ReNcell CX in the present study were determined by the 3-(4,5-dimethylthiazol-2-yl)-2,5-diphenyltetrazolium bromide (MTT) reduction assay which was previously described by Mosmann (1983). The MTT assay is a test for enzymatic activity characteristic of a viable cell based on the ability of cellular dehydrogenase enzymes (mainly succinate dehydrogenase) from viable cells to cleave the tetrazolium rings of the pale yellow MTT and form purple formazan crystals that can be seen in a bright field microscope (Nikkhah *et al.*, 1992; Liu *et al.*, 1997). As these crystals are largely impermeable to the cell membrane, they accumulate within healthy cells. Addition of DMSO to the cells causes solubilisation of crystals resulting in their liberation which can be detected and quantified using a microliter plate reader. The ability of the cells to reduce MTT provides an indication of metabolic activity and the quantified level of the formazan product is directly proportional to the number of surviving cells; when compared to the amount produced by a control cell population, it can be used as a measure of cell viability. However, although often associated with the activity of mitochondrial dehydrogenases, it has also been shown that MTT can be reduced by other cellular dehydrogenases such as those found in cytoplasmic vesicles (Liu *et al.*, 1997). Reduction of MTT can also be mediated by NADH or NADPH within other cellular compartments (Berridge and Tan, 1992; Fotakis and Timbrell, 2006).

2.2.7.1 Assay buffers and reagents

PBS was prepared in a total volume of 1L containing 137 mM NaCl, 2.7 mM KCl, 8.1 mM Na₂HPO₄, 2 mM NaH₂PO₄ at pH 7.4.

MTT was prepared by dissolving 5 mg of MTT per ml of PBS. Aliquots (1 ml) were stored frozen at -20°C until required.

2.2.7.2 Assay procedure

Cells were plated out at the required density in Corning 24 well plates (Table 2.3) in 0.5 ml growth medium, and then incubated for 24 h to allow recovery before the induction of differentiation. Differentiating cells were treated without or with CPF, CPO or PSP. Briefly, growth medium was carefully aspirated from the wells and replaced with fresh differentiation medium (sections 2.2.1 and 2.2.2) containing different concentrations (0, 1, 3, 10 μ M) of CPF, CPO or PSP for 24 h. A volume of 50 μ l of MTT was added to each well 30 min prior to the end of the experimental incubation time and cells were incubated for a further 30 min at 37°C. Differentiation medium was then carefully aspirated from the well, 500 μ l of DMSO were added to each well and the plates were gently agitated on a flat-bed shaker to dissolve the reduced formazan product. A total of 200 μ l of each of the resulting solutions was transferred into a 96-well plate and the absorbance of the solubilised reduced MTT was then read at a wavelength of 570 nm using an ASYS Expert 96 microliter plate reader (Biochrom, UK). The absorbance was expressed as a percentage of MTT reduction relative to the corresponding control \pm SEM.

2.2.8 Morphological measurements of fixed differentiated N2a and C6 cells

The cells were induced to differentiate in 8-well chamber slides and then fixed in pre-warmed 4 % (w/v) paraformaldehyde (Sigma-Aldrich, UK) for 15 min at room temperature. They were then stained for one min with Coomassie Brilliant Blue stain (1.25 g Coomassie blue-R250, 10 % (v/v) glacial acetic acid, 40 % (v/v) methanol, 50 % (v/v) distilled water). Stained cells were washed with distilled water and left to dry overnight. Next day, the stained cells were checked by inverted light microscopy.

After staining, the total number of the cells and the amount of round versus flat cells were determined in five fields of each well. Neurites (cellular processes produced on differentiated cells) were also measured as mentioned below. The microscope used was an Olympus CKx41 inverted light microscope (Olympus Optical Company Ltd, London, UK).

In the case of N2a cell lines, neurites were divided into two categories which were (a) extensions of 0.5-2 cell body diameters in length, and (b) axon-like processes, defined as processes more than 2 cell body diameters in length with an extension foot (Keilbaugh *et al.*, 1991).

2.2.9 Indirect immunofluorescence staining

Morphological changes and the distribution of the structural proteins of cell lines were monitored by indirect immunofluorescence staining. This technique is based on the principle of the antibody-antigen binding when fluorescently labelled antibodies are used to detect particular target antigens by two steps. First, cells are stained with unconjugated primary antibody which binds to the antigen. Then a fluorescently labelled secondary antibody is used to detect the primary antibody (Odell and Cook, 2013). The fluorescent probe allows visualisation and study of the intracellular distribution of structures and proteins including neurofilament and microtubule proteins. Further analysis of such structures and proteins can be done by using fluorescence or confocal microscopy.

2.2.9.1 Immunofluorescence materials

2.2.9.1.1 Primary antibody

Table 2.4. List of primary antibodies used for indirect immunofluorescence staining

Target antigen	Clone	Dilution	Species	Approximate molecular weight of interest (kDa)	Code	Supplier
Primary Antibodies for N2a cell lines						
β III tubulin	2G10	1:500	Mouse	55	T8578	Sigma-Aldrich
Neurofilament heavy polypeptide (NFH)	SMI 33	1:500	Mouse	200	N0142	Merck-Millipore
Primary Antibodies for C6 cell lines						
Glial fibrillary acidic protein (GFAP)	GA5	1:500	Mouse	50	G3893	Sigma-Aldrich

2.2.9.1.2 Secondary antibody

Table 2.5. Secondary antibodies for indirect immunofluorescence staining

Secondary Antibody	Species	Dilution	Code	Supplier
Alexa Fluor [®] 568 IgG	Rabbit	1:500	A21069	Invitrogen
Alexa Fluor [®] 488 IgG(H+L)	Mouse	1:500	A21204	Invitrogen

2.2.9.2 Immunofluorescence methods

Both N2a and C6 cells were plated out at 50,000 cells/ml in 8-well chamber Ibidi μ -slides (Ibidi^(R), Thistle Scientific Ltd, UK) in 0.3 ml growth medium and left for 24 h to recover. Cells were induced to differentiate in the presence (1, 3 and 10 μ M) and absence of CPF, CPO and PSP for 24 h as described in section 2.1.3. After 24 h exposure time, the medium was carefully removed from each well and cells were fixed to keep the shape and locations of all cellular proteins by using 500 μ l/well of pre-warmed 4 % (w/v) paraformaldehyde (Sigma-Aldrich, UK) for 15 min at room temperature. Then, cells were washed three times with PBS for 5 min each rinse. Cell permeabilization was performed by incubating the cells for 15 min at room temperature with 0.05 % (v/v) Tween-20 in PBS, after which cells were washed 3 times with PBS allowing 10 min each rinse. The Tween-20 detergent solution permeabilized fixed cell membrane, which allowed the antibody to access the cytoplasm. After rinsing, blocking with 3 % (w/v) BSA in PBS was used to prevent non-specific binding for 1 h at room temperature. After blocking, cells were then incubated overnight at 4 °C in humidified chamber with 200 μ l of primary antibodies (diluted 1: 500 in BSA/TBS) against β III tubulin and NFH in N2a, GFAP in C6 cells. Negative control cells were also included to confirm the specificity of the primary antibody and this involved incubating non organophosphate-treated cell with the secondary antibody only. Unbound primary antibodies were removed by three subsequent washes (10 min each wash) with TBS/Tween 20. Cells were then incubated for 2 h at room temperature with either Alexa fluor 488 goat anti-mouse IgG, or fluorescein isothiocyanate (FITC)-conjugated secondary antibody (both diluted 1:500 in blocking buffer) (Invitrogen), after which a second series of washes was performed. For nuclei visualisation, cells were labelled with 4', 6-diamidino-2-phenylindole (DAPI) counterstain for 1 min after careful aspiration of excess TBS, followed by a further TBS wash. Slides were filled with TBS containing 0.01 % (w/v) sodium azide as a preservative and stored at 4 °C prior to image acquisition and analysis.

2.2.10 Image acquisition and analysis

The effects of CPF, CPO and PSP on neurite outgrowth of N2a and C6 were further determined by using the ImageXpress Micro Widefield High Content Analysis System (Molecular Devices, USA). This is a high throughput system that allows rapid evaluation of the effects of a wide range of toxins at different concentrations on multiple parameters of neurite outgrowth. The screening system uses an inverted fluorescence microscope which combined with automated image acquisition and analysis software to quantify different measurements of neurite outgrowth such as cell count, cell body area, neurite count, neurite length (Smith and Eisenstein, 2005; Dragunow, 2008).

For image analysis, the slides were loaded into the high content screening system plate holder for image acquisition and analysis. The system in the host laboratory is equipped with an automated microscope capable of fluorescence imaging of fixed-cells. Images were automatically focused and recorded from four different sites in each individual well. The size of each well was 9.4 x 9.4 mm, and the acquired image field was 741.6 x 587.6 μm . Fluorescence images were produced using matched laser excitation filters and multiple emission filter for two different channels, DAPI for nuclei (ex=377/50 nm, em=447/60 nm) and FITC for cell body and neurites (ex=482/35 nm, em=536/40 nm). Images were acquired using a Nikon 10x objective lens and 1.4 megapixel cooled CCD camera, with a stand-alone illuminator (Lambda LS) connected to the system, which involves a 175W Xenon-arc lamp (Sutter Instrument, USA). The 10x objective lens was used in order to acquire all cell bodies and neurites in one field of view, hence enabling more reliable morphological analysis. The acquired images were segmented by multi-coloured tracing masks on neurites and cell bodies, where each neurite segment was given the same coloured mask as that of their parent neuronal cell bodies. Segmentation masks were produced using the MetaXpress imaging and analysis software (version 5.1.0.46; Molecular devices, USA). The segmentation images were analysed by the MetaXpress imaging and analysis software, using integrated neurite outgrowth settings to measure a number of morphological parameters including average number of cells/field, average cell body area/field, neurite length/cell, percentage of cells with significant outgrowth and average intensity of staining within the stained cells. Particles from each image were identified as cells if the cell body width ranged from 15 to 20 μm and valid nuclei width between 5 to 10 μm were detected. Neurite outgrowth was recorded as significant when

minimum cell outgrowth was more than 10 μm (approximately half a cell body diameter in length). The measurement ranges for cell bodies and outgrowth were determined in preliminary studies using untreated cells from multiple cultures to develop the settings to exclude non-cellular particles from the analysis. Using a 10x objective, 4 fields/well from four independent experiments were acquired for the analysis of at least 200 cells/well. The obtained results by the image analysis software were then analysed by using a Graphpad Prism spread sheet and results were presented as mean \pm standard error of mean (SEM) for each OP treatment and compared statistically to its corresponding control.

2.2.11 Preparation of N2a and C6 cell lysates for one dimensional polyacrylamide gel electrophoresis (SDS-PAGE)

Molecular changes to both cell lines were studied in total protein extracts. Initially, cells were plated out in T75 flasks at a density of 50,000 cells/ml in 40 ml growth medium and allowed 24 h recovery. Growth medium was carefully removed from the flask and replaced with 40 ml fresh differentiation medium, containing 0, 1, 3 or 10 μM CPF, CPO or PSP. Cells were re-incubated for 24 h. At the end of the exposure time, differentiation medium was carefully discarded from the flasks and cell monolayers washed twice gently with pre-warmed PBS. A volume of 2 ml of boiling PBS containing 0.5 % (w/v) sodium dodecyl sulphate (SDS) was added to the flask to solubilise the cell monolayers. The resultant suspension was transferred to micro centrifuge tubes, heated at 100°C for 5 min and then allowed to cool at room temperature for 5-15 min. The insoluble materials such as nucleic acids that could affect the performance of the gel electrophoresis assay were then extracted from each lysate by placing 500 μl of cell lysate into a spin column (Dutscher Scientific, catalogue no. 789068) and centrifuged for few seconds at 10,000 g at room temperature. The filter with the captured DNA was carefully removed and discarded. The supernatants were collected from the lower chamber, placed into a clean micro centrifuge tube and stored at -20°C for future electrophoretic and western blotting analysis. The amount of protein available in the samples was then estimated by bicinchoninic acid (BCA) assay, as described in the following section.

2.2.11.1 Sample protein determination

The protein concentration of the samples was measured by the BCA assay, using BSA as the standard (Walker, 2002). The principle of the BCA assay is based on the formation of

a Cu^{2+} -protein complex under alkaline conditions, followed by reduction of the Cu^{2+} ions from cupric sulphate to Cu^+ by the peptide bonds in a protein. The molecules of BCA then bind with Cu^+ forming a purple-blue product, which can be detected and its absorbance measured at 570 nm. The absorbance is equivalent to the amount of protein present in the sample.

2.2.11.1.1 Assay materials

Microtitre 96-well plates were obtained from Sarstedt, (Leicester, UK). BCA Kits which comprised of reagents A (1 % (w/v) bicinchoninic acid sodium salt, 2 % (w/v) sodium carbonate, 0.16 % (w/v) sodium tartrate and 0.95 % (w/v) sodium bicarbonate in 0.1 M sodium hydroxide at pH 11.5) and reagent B (4 % (w/v) copper (II) sulphate pentahydrate solution) were obtained from Sigma-Aldrich.

2.2.11.1.2 Assay procedure

Using a BCA assay kit, a linear range of BSA standard concentrations from 0 to 1 mg/ml (Table 2.6) was prepared in the same buffer as with cell lysates, to produce a calibration curve to ensure that the relationship between protein content and absorbance was linear. A volume of 25 μl from each concentration of standard or from each cell lysate was pipetted into a clean, dry 96-well plate in four replicates and mixed with 200 μl of BCA working reagent. BCA working reagent was obtained by mixing BCA assay kit reagent A with reagent B in a volume ratio of 50:1. The samples were then incubated for 30 min at 37°C in an LEEC incubator (LSC 2933) and absorbance was read at a wavelength of 570 nm. The concentration of protein in the samples was then estimated from the linear correlation obtained from the BSA standard curve.

Table 2.6. BSA protein standards for protein estimation.

Volume of 1 mg/ml BSA (μ l)	Volume of assay buffer (μ l)	Final concentration of BSA (mg/ml)
0	1000	0
200	800	0.2
400	600	0.4
600	400	0.6
800	200	0.8
1000	0	1

When cell lysates showed very low protein concentration, the samples were precipitated by ice-cold acetone. This was achieved by mixing 9 volumes of acetone with 1 volume of protein sample in a micro centrifuge tube, which was vortex-mixed and incubated at -20°C overnight. Precipitated proteins were pelleted by centrifugation at $12,000 \times g$ for 30 min at 4°C . The supernatant was then carefully decanted and the resultant pellet air dried at room temperature for 30 min. Following complete acetone evaporation, the pellets were dissolved and resuspended with $100 \mu\text{l}$ of 0.5 % (w/v) SDS in TBS. BCA assays was also performed on the samples obtained after acetone precipitation in order to estimate the amount of protein present.

Once the protein concentration was determined, samples were prepared for polyacrylamide gel electrophoresis in the presence of sodium dodecyl sulphate (SDS-PAGE) and Western blotting.

2.2.12 One dimensional polyacrylamide gel electrophoresis (SDS-PAGE)

Protein samples from whole cell lysates were separated according to their molecular weight by Sodium dodecyl sulphate polyacrylamide gel electrophoresis (SDS-PAGE).

2.2.12.1 SDS-PAGE materials

Sample loading buffer (4x Laemmli buffer) was prepared in a total volume of 10.2 ml containing 40 % (v/v) glycerol, 8 % (w/v) SDS, 20 % (w/v) β -mercaptoethanol, 0.01 % (w/v) Bromophenol blue and 0.1 M Tris HCl, at pH 6.8.

Ammonium persulphate (APS) was purchased from Sigma-Aldrich and prepared by dissolving 0.1 mg of APS in 1 ml of dH₂O.

Electrophoresis running buffer (RB) was obtained from Geneflow Ltd. (UK) and was prepared in a total volume of 1 L containing 25 mM Tris base; 192 mM glycine; 0.1 % (w/v) SDS, pH 8.3.

Tris-buffered saline (TBS) was prepared in a total volume of 1 L containing 10 mM Tris and 140 mM NaCl at pH 7.4.

Blocking buffer was prepared in TBS containing 3 % (w/v) BSA and 0.01 % (w/v) sodium azide.

AccuGel™ 29:1 was purchased from Geneflow Ltd. (UK) and contains 40 % (w/v) acrylamide:bisacrylamide (29:1).

4x Protogel® Resolving buffer was purchased from Geneflow Ltd. (UK) and contains 1.5 M Tris-HCl buffer pH 8.8 and 0.4 % (w/v) SDS.

Protogel® Stacking buffer was purchased from Geneflow Ltd. (UK) and contains 0.5 M Tris-HCl buffer pH 6.8 and 0.4 % (w/v) SDS.

N,N,N',N'- tetramethylethylenediamine (TEMED) was obtained from Geneflow Ltd. (UK).

Precision Plus Protein™ Blue Colour Standards was acquired from Bio-Rad.

2.2.12.2 SDS-PAGE methods

2.2.12.2.1 Preparation of polyacrylamide gels

Typically, protein samples were separated by 10 % (w/v) polyacrylamide resolving gel (Table 2.7) overlaid with a 4 % (w/v) polyacrylamide stacking gel (Table 2.8) before being blotted onto nitrocellulose membranes (Towbin *et al.*, 1979). Resolving gels of 10 % polyacrylamide were selected for use as they provided optimal separation over a broad range of molecular weights from 10 to 250 kDa. The protein separation was performed on 1.5 mm thick polyacrylamide gels, in a Bio-Rad mini PROTEAN III™ Cell electrophoresis chamber. Two glass plates of 1.5 mm thickness and spacer combs were

wiped first with dH₂O and then with 70 % (v/v) ethanol prior to assembly. Glass plates were assembled evenly into the plate holders and then mounted on the casting stands. While on the casting stands, the plates were first filled with dH₂O to check for any leakage and the water was then removed and replaced with the gel mixture. The 10 % (w/v) acrylamide resolving gel mixture was prepared according to the number of gels that were going to be used as indicated in table 2.7. This was made by mixing AccuGel™ 29:1 acrylamide, 4x Protogel® Resolving buffer and distilled water as indicated in table 2.7. Acrylamide polymerisation was initiated by adding the indicated volume of APS and TEMED to the gel casting solution, mixed gently. Then 8 ml of the resolving gel casting solution were transferred into the gel casting cassette. Distilled water was carefully overlaid on top of the freshly poured resolving gel solution to create a smooth interface and prevent gel shrinkage. Resolving gels were allowed to polymerise at room temperature for approximately 30 to 40 min.

In the meantime, the required amount of 4 % (w/v) polyacrylamide stacking gel mixture was prepared by mixing, AccuGel™ 29:1 acrylamide, Protogel® Stacking buffer and distilled water in the indicated volumes (Table 2.8). Once the resolving gel was polymerised, the distilled water above it was poured away. The indicated volume of APS and TEMED (Table 2.8) were added to the stacking gel solution to initiate polymerisation. The stacking gel solution was mixed gently and applied on top of the polymerised resolving gel. The stacking gel allows protein accumulation at the interface of the resolving gel (Laemmli, 1970). Once the chamber had been filled with stacking gel solution, a comb of the correct thickness was quickly inserted into the non-polymerised gel mixture to generate the wells into which the samples would be loaded. The gel mixture was allowed to polymerise for 45 min, after which the comb was carefully removed and the wells were rinsed by flushing with running buffer to remove any trapped air bubbles prior to sample loading.

Table 2.7. Reagent volumes required for preparation of SDS-PAGE resolving gel for two mini gels

10 % (w/v) acrylamide resolving gel reagents	Volumes
40% (w/v) 29:1 AccuGel™ (Acrylamide stock)	5.0 ml
4x Protogel® Resolving buffer or (1.5 M Tris buffer, pH8.8 (5 ml), 10 % (w/v) SDS (100 µl))	5 ml
Distilled water	9.8 ml
10 % (w/v) APS	200 µl
TEMED	20 µl
Total volume	20 ml

Table 2.8. Reagent volumes required for preparation of SDS-PAGE stacking gel for two mini gels

4 % (w/v) acrylamide stacking gel reagents	Volumes
40% (W/V) 29:1 AccuGel™ (Acrylamide stock)	1 ml
Protogel® Stacking buffer	2.5 ml
Distilled water	6.4 ml
10 % (w/v) APS	100 µl
TEMED	20 µl
Total volume	10 ml

2.2.12.2 Preparation of protein samples for loading

Once the protein concentration had been determined (section 2.2.11.1), each cell lysate was mixed with sample loading buffer (4x Laemmli) in the ratio 1:3 and boiled at 100°C for 5 min prior to loading on the polyacrylamide gel. Precision Plus Protein™ Blue Colour Standards (2.5 µl) were applied to the first well to estimate the molecular weights of the separated proteins. This protein ladder comprised a three colour protein marker with 12 pre-stained proteins, in which the molecular weights ranged from 10 to 250 kDa. Equal amounts (µg) of protein from each sample were then loaded in order to obtain comparable results.

2.2.12.2.3 Separation of proteins in cell lysates by gel electrophoresis

Once the sample loading was complete, gels were placed vertically in the electrophoresis chamber which was then filled with running buffer to the required levels. The system was run first at 50 volts using a Bio-Rad PowerPac 300 for 10 min in order to organise the samples in the stacking gel. The voltage was then changed to 150 volts, allowing electrophoresis to continue until the dye front (bromophenol blue) reached the base of the resolving gel. After that, the power was switched off and the gel was carefully removed to avoid damage.

2.2.13 Western blotting**2.2.13.1 Western blotting materials****2.2.13.1.1 Primary antibodies**

Table 2.9. List of primary antibodies used for Western Blot and ELISA assay

Target antigen	Clone	Dilution	Species	Approximate molecular weight of interest (kDa)	Code	Supplier
Primary Antibodies for N2a cell lines						
MAP-2	H-300	1:1000	Mouse	140-200	sc-20172	Santa Cruz Biotechnology
β III tubulin	2G10	1:1000	Mouse	55	T8578	Sigma-Aldrich
Tau (a.a. 210-241)	TAU-5	1:1000	Mouse	45-68	MAB361	merckmillipore
Neurofilament heavy polypeptide, NF-H,	SMI 33	1:1000	Mouse	200	N0142	merckmillipore
Growth associated protein-43 (GAP43)	GAP-7B10	1:1000	Mouse	43	G-9264	Sigma-Aldrich
Primary Antibodies for C6 cell lines						
Glial fibrillary acidic protein (GFAP)	GA5	1:1000	Mouse	50	G3893	Sigma-Aldrich
Primary Housekeeping Antibodies for N2a and C6 cell lines						
GAPDH	6C5	1:1000	Mouse	37	sc-32233	Santa Cruz Biotechnology

2.2.13.1.2 Secondary antibodies**Table 2.10. Secondary antibodies for probing Western blot**

Secondary Antibody	Type	Dilution	Code	Supplier
Anti- mouse IgG	HRP	1:1000	A9044	Sigma-Aldrich
Anti- rat IgG	HRP	1:1000	P0450	DAKO-Cytomation
Anti- rabbit IgG	HRP	1:1000	A6154	Sigma-Aldrich

2.2.13.1.3 Other consumables

Hybond C nitrocellulose membrane of 0.45 μ m pore size and purchased from Amersham (Buckinghamshire, UK).

Continuous transfer buffer (CTB) was obtained from Geneflow Ltd. (UK), and consists a mixture of 0.25 M Tris and 1.92 M glycine at 10 times the making concentration, which is diluted with 7 volumes of water and 2 volumes of methanol prior to its use for electrophoretic transfer.

Enhanced chemiluminescence (ECL) reagent was purchased from Insight Biotechnology, Wembley, U.K. and was used to detect the binding of horseradish peroxidase (HRP) secondary antibody conjugate to primary antibodies on probed Western blots.

Whatman® filter paper of grade 3 MM filter paper was obtained from Sigma Aldrich.

2.2.13.2 Western blotting methods

2.2.13.2.1 Electroblotting

Once the protein separation by SDS-PAGE was complete, the separated proteins contained on the resolving gel were electrophoretically transferred onto the nitrocellulose membrane to facilitate binding of antibody to the investigated proteins (Towbin *et al.*, 1979). Briefly, the resolving gel was removed from the glass plate whilst the stacking gel was cut off.

Three pieces of filter paper (9 cm x 6 cm), nitrocellulose membranes and 6 mm thick sponges were soaked in CTB working solution (192 mM glycine, 25 mM Tris and 20 % (v/v) methanol) for 5 min to equilibrate. Methanol is a necessary component of CTB which removes any non-protein-bound SDS and also enhances the adsorption of protein to the nitrocellulose membrane. A transfer sandwich was built on the side of the transfer cassette with the membrane oriented between the gel and the anode plate (+), starting with a wet sponge, followed by three wetted filter papers, nitrocellulose membrane, the resolving gel, three additional pieces of pre-soaked filter papers and finally a second sponge. Any air bubbles between the different layers of the sandwich were removed by rolling a glass rod lightly across the sandwich assembly. When air bubbles are trapped between sandwich components, they can create blank spots on the membrane and impede protein transfer. The assembled sandwich was securely fixed in the transfer cassette, which was closed and immersed in the blotting chamber (Mini Trans-Blot^(R) Electrophoretic Transfer cell; Bio-Rad), containing CTB. The cell was connected to the power supply and the electrophoretic transfer performed at 30 volts overnight at room temperature.

2.2.13.2.2 Immunoprobings of Western blots

Nitrocellulose membranes containing the electrophoretically transferred proteins were incubated in 3 % (w/v) BSA in TBS for 1 h at room temperature to block all remaining protein binding sites on the membrane.

After that, membranes were incubated with appropriate dilutions of primary antibodies prepared in 3 % (w/v) BSA/TBS at 4°C overnight (Table 2.9). After incubation, probed membranes were washed to remove excess primary antibody which can otherwise cause high background. This washing was performed 6 times with constant agitation at room temperature using TBS containing 0.05 % (w/v) Tween-20 pH 7.4 over a period of 1 h, allowing 10 min each wash. Blots were then probed with appropriate dilution of the horseradish peroxidase (HRP) conjugated secondary antibodies diluted in 3 % (w/v) BSA/TBS (Table 2.10) for at least two hours at room temperature. This was followed by a further series of 6 washes to remove unbound secondary antibodies from the membrane as described above, with a final wash of TBS to remove possible traces of Tween 20.

2.2.13.2.3 Antibody reactivity visualisation

Antibody reactivity on the membrane was visualised with the enhanced chemiluminiscence (ECL) Western blotting detection reagent (Thermo Scientific, USA). The ECL reagents A and B were allowed to equilibrate at room temperature before they were mixed freshly in equal volumes and applied onto the blotted membranes to detect the band of interest. Digital images were captured using a G:BOX Chemi XT4 imager dark system (Syngene, Cambridge, UK), and band density was quantified by densitometric analysis using Advanced Image Data Analyser (AIDA) software (version 4.03) (Raytek GmbH, Straubenhardt, Germany). This software analyses band volumes, based on constant lane width and automatic band selection, from the raw data of pixel area and intensity that are independent of operator-altered contrast or brightness. All band densities were measured and corrected for background, then normalised to band densities for glyceraldehyde 3-phosphate dehydrogenase (GAPDH) reactivity, which was used as internal control for normalisation. Data are expressed as a percentage of the average value of the peak area compared to its corresponding control \pm SEM.

2.2.14 Enzyme linked immunosorbent assay (ELISA)

The effects of OPs on the levels of cytoskeletal proteins in N2a and C6 cell lines was further examined by using a cell-based enzyme linked immunosorbent assay (ELISA). This was based on the previous approach (Schmuck and Ahr, 1997) with modifications. The assay is based on the principle that antibodies will bind to very specific antigens to form antigen-antibody complexes, and an enzyme linked to an antibody can be used as a marker for the detection of a specific antigen or protein in sample. The conjugated enzyme reaction is stopped by the addition of H₂SO₄ producing a yellow colour product, which can be detected and measured at 405 nm by spectrophotometer. The intensity of the colour change is related to the amount of protein or antigen present in the sample.

2.2.14.1 Preparation of buffer and reagents

100 mM Sodium acetate buffer was prepared by dissolving 8.2 g sodium acetate in 900 ml of dH₂O at pH 6. The final volume made up to 1 litre with dH₂O

5 M Sulphuric acid (H₂SO₄) was prepared by adding a volume of 50 ml pure H₂SO₄ was added to 200 ml of dH₂O

3,3,5,5'-Tetramethylbenzidine (TMB)

A total of 10 mg of TMB was dissolved in 1 litre of DMSO (stock).

3 % (v/v) Hydrogen peroxide (H₂O₂)

Volume of 10 µl of 30 % (v/v) H₂O₂ (stock) was added to 90 µl of dH₂O

Developing substrate

The developing substrate was prepared by the addition of 150 µl of TMB stock solution and 30 µl of 3 % (v/v) H₂O₂ into 20 ml of 100 mM sodium acetate pH 6.

2.2.14.2 Assay procedure

The assay was performed in a sterile flat bottom 96-well plate. Cells were plated out at the density of 50,000 cells/ml for N2a and C6 cell lines in a total volume of 200 µl growth medium per well in four replicates and incubated overnight at 37°C in 5 % CO₂. After 24 h recovery, cells were induced to differentiate in the presence (1, 3, and 10 µM) and absence

of CPF, CPO and PSP for 24 h as described in section 2.2.6. After 24 h exposure time, the medium was carefully removed from each well and cells were fixed using 200 μ l/well of prewarmed 4 % (w/v) paraformaldehyde (Sigma-Aldrich, UK) for 10 min at room temperature. Fixative was removed and cells were washed 3 times with TBS allowing 5 min each wash. Cells were permeabilized by incubating with 0.05 % (v/v) Tween-20 in PBS for 15 min at room temperature, after which they were rinsed 3 times with TBS allowing 5 min each rinse. After rinsing, a volume of 300 μ l/well of 3 % (w/v) BSA/TBS (blocking buffer) was added for 1 h at room temperature to prevent non-specific binding. The blocking buffer was then removed and 100 μ l/well of primary antibodies diluted 1 to 1000 in blocking solution (Table 2.9) were added and incubated overnight at 4°C.

After that, the primary antibodies were removed and wells were washed three times with TBS/Tween20, followed by at least 2 h incubation at room temperature in 200 μ l/well of HRP conjugated secondary antibodies (diluted at 1:2000) in blocking buffer (Table 2.10). Following that, the antibodies were removed and the cells were washed with TBS/Tween20 three times allowing 5 min in each wash. Any remaining wash solution was removed completely from wells, as complete removal of liquid at each step is essential to good performance. The reaction was initiated by the addition of 100 μ l of developing substrate buffer into each well. After 5 min incubation at room temperature, a blue colour product was developed as a result of the reaction, which was then stopped by adding 100 μ l of 5 M H₂SO₄. The resultant yellow colour was detected and absorbance was measured spectrophotometrically using a micro plate reader (ASYS Expert 96, Biochrom, UK) set at 405 nm. Results were expressed as antibody binding in treated cells and presented as a percentage compared to untreated cells (set as 100 %) \pm SEM. The background level was estimated for correction by blank non populated wells. The specificity of antibody bindings was confirmed by non OP-treated cells incubated with the secondary antibody only.

2.2.15 Reverse transcription polymerase chain reaction (RT-PCR)

To investigate possible transcriptional responses to OP exposure, the expression of a few genes of interest was analysed in N2a, C6 and ReNcell CX cell lines after single treatment with the three OPs used throughout this study. Molecular biology grade laboratory reagents were used and they are listed in table 2.11.

Table 2.11. List of reverse transcription polymerase chain reaction reagents

Reagents	Code number	Supplier
Absolutely RNA Miniprep Kit.	400800	Agilent Technologies
SYBR TM Safe TM DNA Gel Stain.	VXS33102	Fisher Scientific UK Ltd
Quick-Load [®] 100 bp DNA Ladder (125 lanes).	N0467S	New England Biolabs Ltd.
Wizard [®] SV Gel and PCR Clean-Up System and x-tracta TM Gel Extraction Bundle.	A9283	Promega, UK.
PrimePCR TM SYBR [®] Green Assay: Rps18, Mouse, Rat.	100-25636	Bio-Rad, UK
PrimePCR TM SYBR [®] Green Assay: Gapdh, Mouse,Rat,Human.	100-25636	Bio-Rad, UK
dNTP Mix is a premixed solution containing sodium salts of dATP, dCTP, dGTP and dTTP at 100 mM each.	U1330	Promega, UK.
M-MLV Reverse Transcriptase kit.	M1701	Promega, UK.
iTaq TM Universal sybr green supermix.	172-5120	Bio-Rad, UK

2.2.15.1 Primer design for the genes of interest

To design specific primers, the cDNA sequences for each gene of interest were obtained from the Genome Browser (University of California, Santa Cruz (UCSC)). When a gene had more than one isoform, their sequences were aligned using the Multalin software and primers were designed in the common nucleotide regions between all the variants. The primers were designed using Primer-3 software (Untergasser *et al.*, 2012) and their qualities, including annealing temperature, size, presence of hairpins and GC content were checked before ordering. The BLAST software was used to select those primers which had the highest specificity with the desired gene.

2.2.15.1.1 Primer design criteria

- a) A 'GC' content between 40-60 %.
- b) Melting temperature (T_m) between 55-80°C.
- c) Primer size between 100-150bps.
- d) A and T mismatches were to be avoided at 3' ends.
- e) Self-complementarity of the sequences between forward and reverse primers was to be avoided.
- f) Self-hairpins of the sequences between forward and reverse primers were to be avoided.

2.2.15.2 Disruption and homogenization of brain tissues

Mouse and rat brains were used as positive controls to optimise the polymerase chain reaction (PCR) and to check the specificity of the designed primers to amplify the genes of interest. Total RNA was extracted from frozen rat and mouse brain tissue. After cleaning all equipment with 70% (v/v) ethanol, the brain tissues were removed from dry ice and approximately 40 mg were weighed and placed in a tube containing prepared Lysis Solution. A volume of 4.2 μ l β -mercaptoethanol (β -ME) had been freshly added to 600 μ l of lysis buffer, which was included in the Absolutely RNA Miniprep Kit. Then, the tissue was homogenised in the homogenizer Ultra Turrax (TR50) (Janke and Kunkel, IKA labortechnik). The homogenised samples were kept at -80°C for RNA isolation.

2.2.15.3 RNA extraction from cells and homogenised tissues

A T75 flasks were contained 40 ml of growth medium at cell density of 50,000 cells/ml of N2a cells and rat C6 glioma cells, or 100,000 cells/ml of ReNcell CX cell. When the cell monolayers were 80 - 90 % confluence, RNA extraction was performed according to the manufacturer's protocol (Absolutely RNA Miniprep Kit. Code number, 400800, Agilent Technologies) by the RNA binding column through a series of centrifugations then eluted in RNase free water as shown in figure 2.1. A volume of 4.2 μ β -mercaptoethanol (β -ME) had been freshly added to 600 μ l of lysis buffer, which was included in the Absolutely RNA Miniprep Kit.

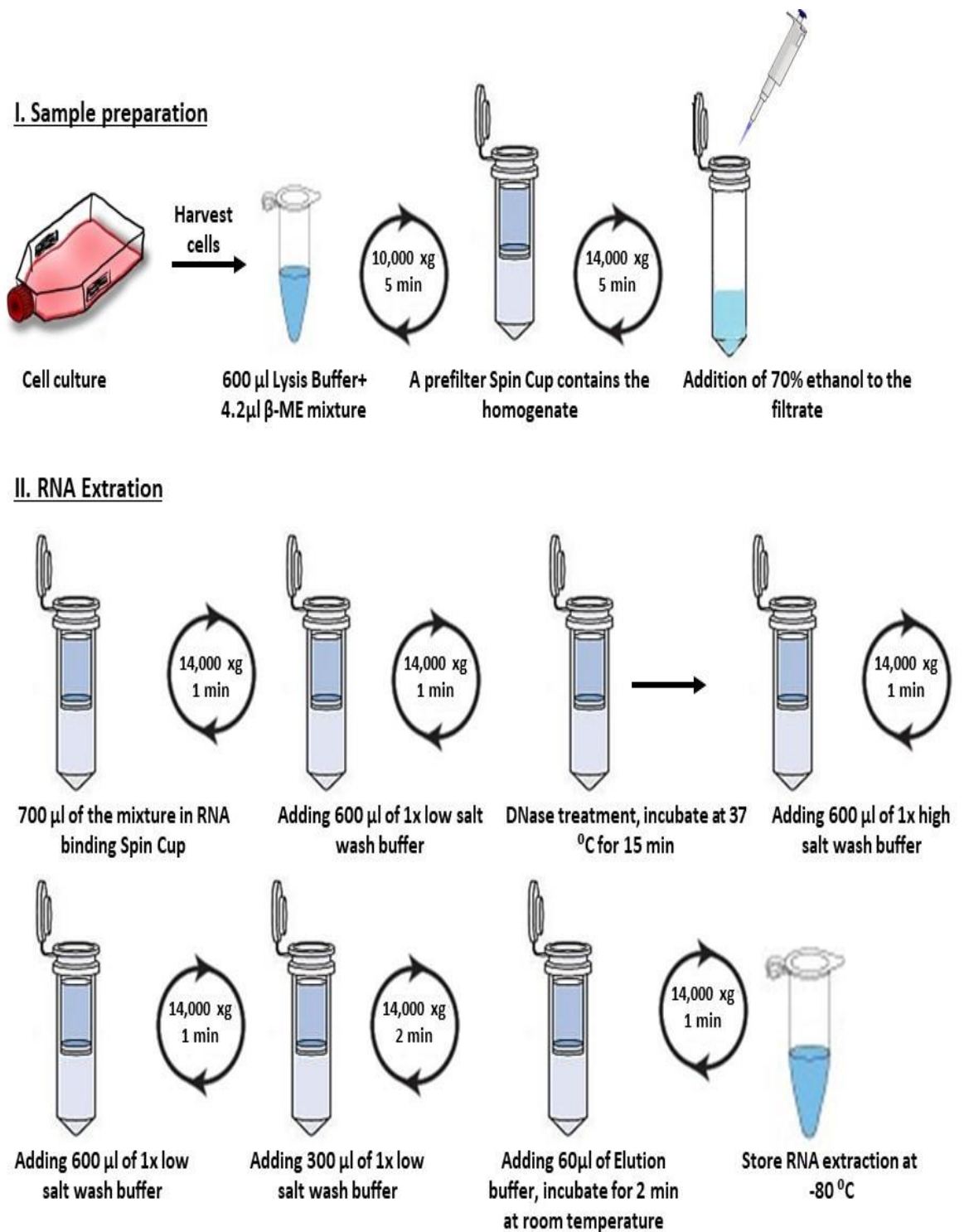


Figure 2.1. Graphical protocol of the steps involved in RNA extraction.

2.2.15.4 Quantification of RNA

The concentration of RNA in the samples was determined using a NanoDrop 8000 spectrophotometer (Thermo Fisher Scientific Inc). First, the samples pedestal of the

spectrophotometer were cleaned with wet lens tissue before setting the blank using either distilled water or elution buffer. For each RNA extract, 1 μ l was loaded into the pedestals and the absorbance readings taken at 260 and 280 nm. The NanoDrop then provides a value for the concentration and a ratio measurement that reflects the purity of the samples. According to the Beer-Lambert (or Beer's) Law, absorbance is proportional to concentration and nucleic acids concentrations can be determined with values of absorbance at 260 nm (Mayerhöfer *et al.*, 2016). RNA concentrations were adjusted to 1 μ g/ μ l to use in the reverse transcription reactions.

2.2.15.5 cDNA synthesis

First-strand cDNA synthesis from RNA samples was performed following the manufacturer's instructions (Promega,UK). A total of 2 μ g RNA, 0.5 μ g random primer and ddH₂O were added to a final volume of 15 μ l. Samples were then heated using a thermal cycler (Bio-Rad, T100) to 70°C for 5 min to melt secondary structures that could be present in the RNA. Then, samples were put on ice before the following components were added to each sample (Table 2.12).

Table 2.12. Final volumes and amounts of cDNA synthesis components

Components	Final volume (μ l)	Final amount
5x M-MLV buffer	5	200 units
dNTPs	2	10mM
M_MLV RT	1	200 units
RNasin ribonuclease inhibitor	0.5	25 units
Nuclease Free water	6.5	-

Samples were mixed gently and incubated for 70 min at 37°C in a thermal cycler. After incubation, samples were heated at 95°C for 5 minutes and immediately stored at -20°C to be ready for qPCR.

2.2.15.6 Optimisation of annealing temperature for the polymerase chain reaction (RT-PCR)

A volume of 1 μ l cDNA was added into PCR tubes containing 12.5 μ l Go taq green master mix (Promega, Catalogue no. M7122), upstream and downstream primers for the gene of

interest and nuclease free water (Table 2.13). PCR tubes were placed in a T100 thermal cycler (Bio-Rad, UK) to perform gene amplification under a gradient of temperature ranging from 55 to 62 °C. Thermal cycler settings are shown in the table 2.14.

Table 2.13. Volumes and final concentrations of the components for RT-PCR

Components	volume (µl)	Final concentration
GoTaq® Green Master Mix, 2X	12.5 µl	Provided
Upstream primer, 10 µM	0.25–2.5 µl	0.1–1.0 µM
Downstream primer, 10 µM	0.25–2.5 µl	0.1–1.0 µM
DNA template	1–5 µl	<250 ng
Nuclease-free water to	25 µl	-

Table 2.14. Settings of thermal cycler for PCR.

Steps						
Denaturation		Annealing	Extension			
1	2	3	4	5	6	7
95 °C	95 °C	Variant	72 °C		72 °C	12 °C
3:00 min.	0:30 sec.	0:30 sec.	0:45 sec.	Step 2	5:00min	-

← **34 X cycle**

2.2.15.7 Agarose gel electrophoresis

Agarose (1.5g) from Melford Biolaboratories Ltd, was added to 100 ml of 1x TAE buffer. The solution was boiled twice in order to improve the resolution of the gel. Syber safe (10 µl of a 10,000x stock) was then added to be able to visualise the DNA later. The solution was poured into a casting tray and a well comb was placed in it and left to cool down. After the gel had formed, it was covered by 1xTAE buffer which was prepared from 50x TAE buffer (242g Tris base, 57.1 ml glacial acetic acid, 0.5 M EDTA at pH8 and adjust pH of the buffer at 8.5). After 45 min, 20 µl of the PCR samples were loaded into the

wells, placing 10µl of the DNA ladder standard (Quick-Load® 100 bp DNA Ladder, NEB) in the first well, and the gel was run for 60 min at 85 V.

2.2.15.8 Visualization of bands on agarose gels

The agarose gel was removed from the tank when the electrophoresis was finished and placed in the G:BOX iChemi dark system (Bio-Rad,UK). The gel was exposed to ultraviolet light to reveal Sybr Safe-stained DNA bands and the images were captured by the camera. The sizes of the amplified band were determined by comparison to the DNA ladder used. The PCR conditions for those lanes showing single bands of the expected size product were considered positive and optimised.

2.2.15.9 PCR product confirmation by DNA sequencing

PCR products of the expected size were cut from the agarose gel and cleaned using Wizard® SV Gel and PCR clean-up system, A9281, Promega, following the manufacturer's guidelines. The extracted DNA was sent for sequencing to Source Bioscience, Nottingham, UK. The string of nucleotides received from the company was introduced in the Blast software to look for alignments with just the sequencing of our gene of interest. Those primers that amplified specific fragments of the expected size were then used in the quantitative PCR (qPCR) experiments.

2.2.16 Quantitative PCR (qPCR)

cDNA was obtained as described before and the reactions for qPCR were prepared in 0.1 ml of capped qPCR microtubes using the volumes and reagents described in table 2.15. The concentration of primers used was determined after the optimisation through the use of a primer matrix.

Table 2.15. Volumes and amounts of the components used in qPCR.


Component	Volume (μ l)	Final concentration
<i>iTaq</i> TM universal SYBR [®] Green supermix is 2x concentrated	6.5	Master mix
cDNA	1	
Forward primer	0.5	10 mM
Reverse primer	0.5	10 mM
Nuclease free water	4.5	


Then the qPCR microtubes (strips of four) were placed in the blue 72 rotor disc of Rotor Gene Q (Qiagen, 115H). Gene expression was obtained under the conditions in table 2.16.

Table 2.16. Quantitative RT-PCR protocol

Polymerase activation and DNA denaturation	Amplification			Melt curve analysis
	Denaturation	Annealing/Extension	Cycles	
95 °C 2 min	95 °C 5 sec	60 °C (or depending on annealing temperature of gene of interest) for 30 sec	40	95 °C 5 sec

When amplification was complete, Ct values were obtained and analysed following the delta-delta Ct method of Rao *et al.* (2013) as indicated below.

 $\Delta Ct = Ct (\text{Sample A -treated}) - Ct (\text{House keeping B-treated})$
 $\Delta Ct = Ct (\text{Sample A-control}) - Ct (\text{House keeping B-control})$
 $\Delta\Delta Ct = \Delta Ct (\text{treated}) - Ct (\text{control})$

 Normalized target gene expression level = $2^{(-\Delta\Delta Ct)}$

2.2.17 Histone deacetylases assay (HDAC)

2.2.17.1 Nuclei extraction buffers

Molecular biology grade reagents were used to prepare the buffers for the extraction (Table 2.17).

Table 2.17. List of nuclei extraction buffers for HDAC assay

Reagents	Supplier
Buffer A	
10 mM HEPES (pH7.9 at 4°C)	Sigma-Aldrich
1.5 mM Magnesium chloride (MgCl ₂)	Sigma-Aldrich
10 mM Potassium chloride (KCl)	Sigma-Aldrich
0.5mM 1,4-Dithiothreitol (DTT) [Add fresh]	Sigma-Aldrich
Buffer B	
0.3 M HEPES pH 7.9	Sigma-Aldrich
1.4 M KCl	Sigma-Aldrich
0.03 M MgCl ₂	Sigma-Aldrich
Buffer C	
20 mM HEPES pH 7.9	Sigma-Aldrich
25% v/v Glycerol	Sigma-Aldrich
0.42 M NaCl	Sigma-Aldrich
1.5 mM MgCl ₂	Sigma-Aldrich
0.2 mM EDTA	Sigma-Aldrich
0.5mM PMSF [Add fresh]	Sigma-Aldrich
0.5 mM DTT [Add fresh]	Sigma-Aldrich
Buffer D	
20 mM HEPES pH 7.9	Sigma-Aldrich
20% v/v Glycerol	Sigma-Aldrich
0.1 M KCl	Sigma-Aldrich
0.2 mM EDTA	Sigma-Aldrich
0.5 mM DTT [Add fresh]	Sigma-Aldrich
0.5 mM PMSF [Add fresh]	Sigma-Aldrich

2.2.17.2 Preparation of nuclear extraction for HDAC

According to Dignam *et al.* (1983), after washing the cells with ice cold PBS, they were scraped off the culture flask in 5 ml PBS ice-cold per flask. Then, cells were centrifuged at 448 × g for 10 min. The pellet was resuspended in 5 x volumes of Buffer A and kept on ice

for 10 min. and then centrifuged at $448 \times g$ for 10 min at 4°C . The pellet was resuspended in 2 volumes of buffer A. The mixture was homogenized with a glass Teflon homogeniser using around 20 strokes to break any intact plasma membranes. The destruction of the membranes was confirmed using a light microscope (Figure 2.2). Then, the extract was centrifuged at $448 \times g$ for 10 min at 4°C . The resultant pellet contained nuclei and was resuspended in 1 ml buffer B, then transferred to ultracentrifuge tubes and centrifuged at $25,000g$ at 4°C for 30 min. After resuspending the pellet in 0.6 ml buffer C, the mixture was homogenized, then, stirred with a magnet for 30 min at 4°C . It was then centrifuged at $25,000g$ for 30 min. The supernatant ($\sim 1\text{ml}$) was dialysed against buffer D for 5 hours and then centrifuged at $25,000g$, 4°C for 20 min. Then, the supernatant containing the nuclear proteins was kept at -20°C .

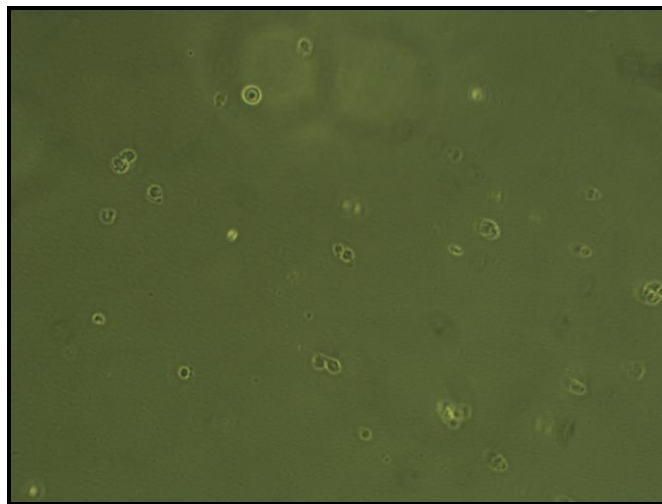


Figure 2.2. Phase contrast microscopy images of homogenised cells for nuclear extraction.

2.2.17.3 Histone deacetylation (HDAC) protocol

Total HDAC activity was performed in a microliter plate, and it was determined by using HDAC activity colorimetric assay kits (Catalogue No. 17-374, EMD Millipore, UK). HDAC assay was based on a two-step of colorimetric reaction. The first step was deacetylation of the incubated substrate with the samples. Then the substrate was sensitized as consequence of the activator solution that releases p-nitroanilide from the deacetylated substrate. Briefly, the protein was extracted after the fractionation of the

nucleus using the procedure mentioned above. Following BCA assay, as mentioned in 2.2.11.1, 20 µg of cell lysate of test sample, 20µg of HeLa nuclear extract (positive control), and 20µl of water (negative control) were each incubated with HDAC colorimetric substrate for 1 h at 37 °C, following the manufacturer’s instructions (Table 2.18). The absorbance was set at 405 nm by using a micro plate reader (ASYS Expert 96, Biochrom, UK), and it expressed as the relative O.D value per µg of protein.

Table 2.18. Assay incubation setup

	Negative Control	Positive Control	Test Sample
2X HDAC Assay Buffer	10 µl	10 µl	10 µl
Test sample/ µg the(s)	0 µl	20 µl	20 µl
4mM Substrate, colorimetric detection	10 µl	10 µl	10 µl
Water	20 µl	0	0
Activator Solution	20 µl	20 µl	20 µl
Total Assay Volume	60 µl	60 µl	60 µl

2.2.18 Statistical analysis

All data sets were generated from a minimum of 4 independent experiments and expressed as mean \pm SEM. GraphPad Prism (version 7) (GraphPad software, California, USA), was used for all statistical analysis. The significance of the differences between the average values for each treatment were compared to the corresponding controls or other treatment group by one-way analysis of variance (ANOVA) and comparison between means was analysed by a Sidak post hoc test, which takes into account multiple comparisons, with 95 % confidence interval. Results were considered to be significantly different when $P < 0.05$.

Chapter 3

**Cytotoxic Effects of Organophosphate
Compounds on Differentiating Mouse N2a
Neuroblastoma and C6 Glioma Cells**

3.1 Introduction

Organophosphate compounds are widely used as pesticides, but because they are non-selective for the target organism, their use has caused severe health damage and even death in humans and domestic animals (Murray *et al.*, 2005).

CPF remains one of the most commonly used OP insecticides around the world (Coronado *et al.*, 2006). In spite of its potential dangers to health and the imposed restrictions, CPF remains a major pesticide to use in both residential and in the industrial settings especially in many developing countries (Salyha, 2010). Moreover, tricresyl phosphate (from which the analogue of PSP is derived) has long been used in jet engine oils and jet hydraulic fluid, due to its anti-wear properties under extreme conditions (Liyasova *et al.*, 2011). It was linked to toxicity in both passengers and aircrew, with symptoms including muscle weakness, dizziness, nausea, disorientation and memory loss (Schopfer *et al.*, 2010; Liyasova *et al.*, 2011). A considerable effort has been made by the government, advocating control measures for prevention of potentially toxic organophosphate exposure, particularly amongst employees in manufacturing industries or those using or exposed to the compounds and in the most susceptible groups of the population, such as the young and the elderly. However, in a recent study, despite the suggestion by EPA that the use of all OPs should be banned not only in households but also in agriculture, it has not been well accepted, and OPs are still being used extensively (EPA, 2016; 2017).

As discussed previously in section 1.1.2, glial cells are specialized cells that do not transmit electrical signals but they are of major importance, in that they provide structural and metabolic support in the nervous system. They also play a key role in antioxidant activity, which is important for protection against potential effects of OPs on neural cells (Bagchi *et al.*, 1995). However, the cytotoxic effects of OPs may vary between neural and glial cells, the precise reasons remaining elusive as evidence keeps accumulating. One study has, however, suggested that, as glial cell development takes longer than that of neurons, the former may be more susceptible to prolonged exposure to CPF (Garcia *et al.*, 2002).

Substantial evidence has emerged from a number of epidemiological studies demonstrating that both CPF and CPO have the ability to induce neurotoxicity in developing organisms through their effects on developmental processes in the nervous system, such as neurite outgrowth (Campbell *et al.*, 1997; Crumpton *et al.*, 2000a; Flaskos, 2012).

Many studies have shown that OPs adversely affect most cell types in the nervous system, especially the neurons and glial cells (Sachana *et al.*, 2008; Flaskos *et al.*, 2011). The molecular basis of OP-induced neurotoxicity has been extensively studied and reported in both *in vivo* and *in vitro* models, as discussed in chapter 1 (Timofseeva and Gordon, 2002; Coronado *et al.*, 2006). The understanding of OP associated acute toxic effects, resulting from the inhibition of cholinesterase activity thereby causing accumulation of acetylcholine at nerve endings, has played a major part in providing a rationale for therapeutic and diagnostic approaches. Many *in vitro* studies on neural cell lines such as N2a and C6 have facilitated a better understanding of the cellular mechanism(s) involved in OP-induced cytotoxicity. For example, in viability assays such as MTT reduction, the IC₅₀ values for CPF and CPO were approximately 50 and 40 µM, respectively, and it was established that concentrations of 1-10 µM had no significant effect on the viability of differentiating C6 cells under the same experimental conditions as those used in the current study (Sachana *et al.*, 2008). Likewise, PSP was shown to inhibit the reduction of MTT in cultured mitotic N2a and hepatic (HepG2) cell lines, as indicated by their IC₅₀ values which were estimated to approximately 10-15 µM (Harris *et al.*, 2009a). This showed that the two cell lines exhibited similar trends in their sensitivity to PSP. Subsequent studies assessed the effects of PSP on MTT reduction in mitotic H9c2 cells at shorter time points than in the previous study (1, 2, 4, and 8 h) (Felemban *et al.*, 2015). The results showed that PSP-induced inhibition of MTT reduction was first evident at 4 h (IC₅₀ = 8.5 ± 5.5 µM), with comparable results obtained at 8 h exposure (IC₅₀ = 7.1 ± 4.7 µM). This suggests that PSP displays marked cytotoxicity towards mitotic H9c2 cells.

According to Sindi *et al.* (2016), the concentration of 3 µM CPF and CPO was chosen for studies of neurite retraction based on its ability to induce approximately 50 % reduction in both neurite outgrowth and in the number of pre-formed neurites in differentiating N2a cells. CPF at the sub-lethal concentration of 3µM had the ability to induce retraction of approximately 50 % of axon-like processes formed by differentiating N2a cells, as determined by light microscopy of Coomassie Brilliant Blue stained cells (Sachana *et al.*, 2001). In previous work by the same research group, it was found that the sub-lethal concentrations of OP pesticides such as CPF and diazinon (DZ) inhibited the outgrowth of axon-like processes in differentiating N2a cells (Sachana *et al.*, 2001; 2003; Flaskos *et al.*, 2007). Accordingly, a concentration range of (1-10 µM) was adopted for subsequent experiments in the current study.

Several *in vitro* and *in vivo* studies have shown that the adverse effects of CPF and CPO on the developing brain are not limited to inhibition of cholinesterase activity, but that it involves other potential targets (Slotkin, 2004). For example, CPF and CPO were found to interfere with the unique developmental process of the brain and the nervous system by causing several morphological changes in the formation of neurites, as discussed above. These neurites play key roles in axonal plasticity (Andrieux *et al.*, 2002; Wall, 2005). Neurite outgrowth is a unique morphological feature of neural development and has been investigated in several *in vitro* studies. Extension of neurites (axons and dendrites) during brain development is a crucial factor that determines neuronal connectivity (Radio *et al.*, 2008). Any interference with this critical cellular process, for example by OP exposure, may cause severe damage or could lead to neurodegenerative effects in developing organisms (Rice and Barone, 2000; Costa, 2006; Grandjean and Landrigan, 2006). As shown by *in vitro* studies, neurite outgrowth reflects many of the morphological and molecular changes that occur in axon outgrowth during nerve regeneration *in vivo* (Burgoyne, 1991; Berger-Sweeney and Hohmann, 1997). Neurotoxin-induced changes in this phenomenon may also reflect the ability of xenobiotics to cause axon retraction and/or inhibit nerve regeneration in adult animals (Burgoyne, 1991; Berger-Sweeney and Hohmann, 1997). Sub-lethal concentrations of PSP inhibited the outgrowth of axon-like processes in differentiating N2a cells (Hargreaves *et al.*, 2006). The mechanisms involved in OP-induced neurotoxicity may vary depending on the differentiation conditions used (Sachana *et al.*, 2001). Several developmental studies of OPs have been carried out under similar cell differentiation conditions, in which cells were treated with OPs at the point of induction of cell differentiation (Sachana *et al.*, 2008; Flaskos *et al.*, 2006; 2011; Sindi *et al.*, 2016). This method, also known as co-differentiation, forms a platform whereby the ability of OPs to inhibit the outgrowth of neurites can be studied. Also, reports have shown that CPF not only has the ability to inhibit neurite outgrowth but it can also cause the retraction of pre-formed neurites (Sachana *et al.*, 2001). This was demonstrated in a study that involved exposure of pre-differentiated N2a cells to a non-cytotoxic concentration of CPF at two different time points. The results showed that CPF caused a significant reduction in the number of axon-like processes in pre-differentiated N2a cells following 4 and 8 h exposure (Sachana *et al.*, 2001; Sachana *et al.*, 2005).

In the present study, in order to study the neurotoxic effects of CPF, CPO or PSP on neurite outgrowth in differentiating N2a cells, they were stained with Coomassie blue, after which neurites were quantified using manual counting. Although this method demonstrated

the ability of the compounds to induce changes in the process of neurite outgrowth, the limitation of this method is that the manual counting of neurite outgrowth is time-consuming. Therefore, high throughput screening (HTS) system was used to further measure the extent of neurite outgrowth in differentiating N2a cells exposed to CPF, CPO or PSP. This screening system was developed using fully automated integrated systems for cell imaging and data analysis (Abraham *et al.*, 2004; Smith and Eisenstein, 2005), which provides rapid measurements, time efficient and reliable of neurite outgrowth overcoming the common limitations of manual methods used in the earlier part of the current study and in previous research carried out at Nottingham Trent University. Additionally, HTS can assess the effects of a wide range of various chemicals and neurotoxicants on multiple parameters of neurite outgrowth including neurite number, neurite length, cell body area and the extent of neurite branching. Furthermore, high throughput assays can be used with different cellular models in order to compare and characterise the effects of several OPs or other chemicals on neurite outgrowth in multiple cell types (Mundy *et al.*, 2010). Earlier studies have validated the feasibility of this approach to evaluate the neurotoxicity potential of various chemicals on neurite outgrowth in neural cell lines under different exposure conditions (Radio *et al.*, 2008; Radio *et al.*, 2010; Harrill and Mundy, 2011; Wilson *et al.*, 2014; Sindi *et al.*, 2016).

3.2 Aims

The main aims of the present work were:

- (a) to investigate the cytotoxic effects of CPF, CPO and PSP on the viability of differentiating N2a and C6 cell lines. Cell viability was assessed by MTT reduction assay following exposure to the three OPs at 24 h. This was a preliminary study carried out to determine the time point of potential cytotoxicity.
- (b) to determine the effects of sub-lethal concentrations of the same 3 compounds on neurite outgrowth.

It was of particular interest to develop high throughput assays in order to examine the effects of a range of sub-lethal concentrations of OPs on multiple parameters of neurite outgrowth in a rapid quantitative analysis. Therefore, cells were fixed and stained by indirect immunofluorescence with antibodies against β -tubulin III (clone 2G10) and NFH (clones SMI 33) and monoclonal antibody of GFAP (clone GA5) and subsequently analysed by HTS.

3.3 Effects of CPF, CPO and PSP on the viability of differentiating N2a cells

The toxic effects of organophosphates of the current study on the two cell lines were further compared in terms of their IC₅₀ values, which is the concentration required to decrease the level of MTT reduction by 50 % compared to the non-organophosphate control. After 24h, an IC₅₀ value was not reached in both at 1-25 µM (Appendix 8.1, 8.2).

Mouse N2a neuroblastoma cells were induced to differentiate by the addition of 0.3 mM dbcAMP in the absence (0.5 % v/v DMSO control) or presence (1, 3, and 10 µM) of CPF, CPO or PSP for 24 h. To examine the viability of differentiated N2a cells after being exposed to the OPs, MTT reduction assays were performed, as described in section 2.2.7. As indicated in figures 3.1, the results showed no effect on the reduction of MTT by differentiating N2a cells when compared to its corresponding control after 24 h exposure to all three concentrations of CPF, CPO and PSP.

3.4 Effects of CPF, CPO and PSP on the viability of differentiating C6 cells

Similarly, mouse C6 glioma cells were induced to differentiate by the addition of 2 mM sodium butyrate in the absence (0.5 % v/v DMSO control) or presence (1, 3, and 10 µM) of CPF, CPO or PSP for 24 h. To determine the viability of differentiated C6 cells after being exposed to the OPs, MTT reduction assays were performed, as described in section 2.2.7. As indicated in figures 3.2, there was no significant change in the reduction of MTT by differentiating C6 cells when compared to its corresponding control after 24 h exposure to all the three concentrations of CPF, CPO or PSP.

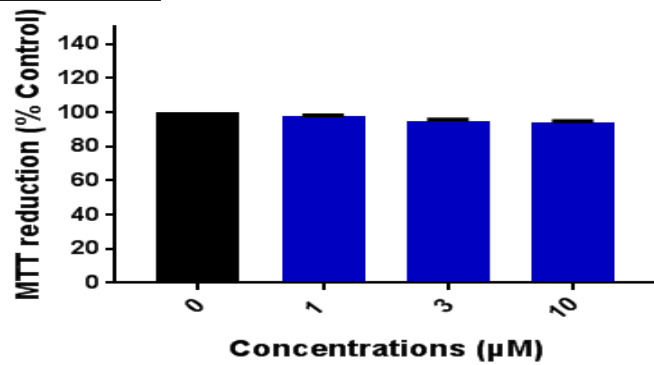
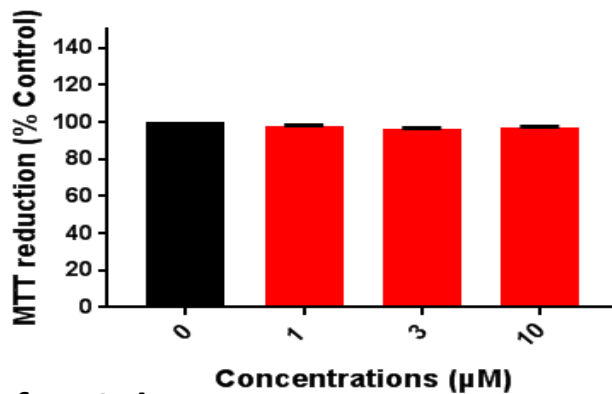
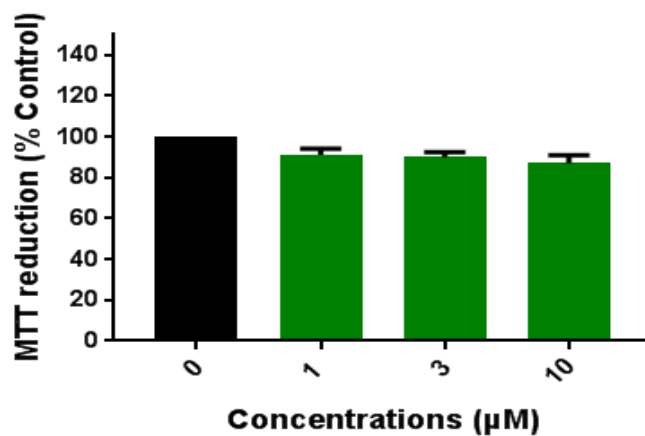
A. CPF in N2a after 24h**B. CPO in N2a after 24h****C. PSP in N2a after 24h**

Figure 3.1. Effects of CPF, CPO and PSP on MTT reduction in differentiating N2a cells after 24 h.

N2a cells were induced to differentiate in the absence and presence of different concentrations of CPF (panel A), CPO (panel B) and PSP (panel C) of induction of cell differentiation, and the levels of MTT reduction were measured to evaluate cell viability. Results are expressed as a mean percentage of the corresponding untreated control \pm SEM from five separate experiments. Statistical significance of data was analysed by using one way ANOVA.

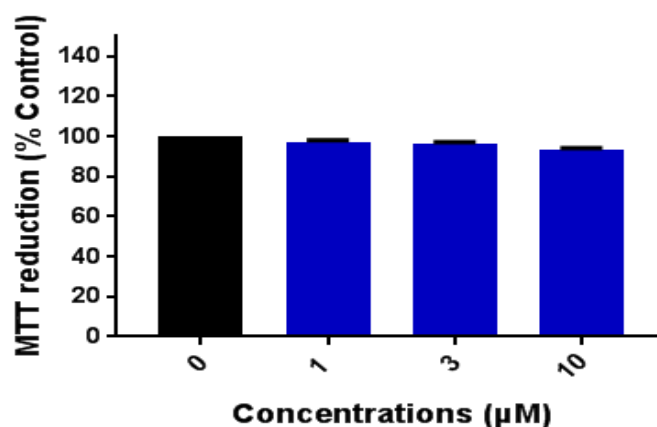
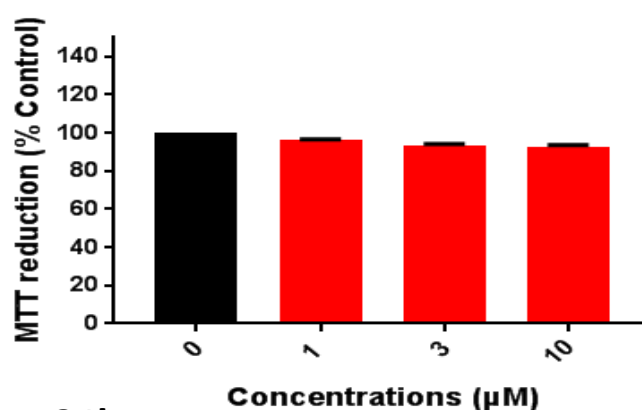
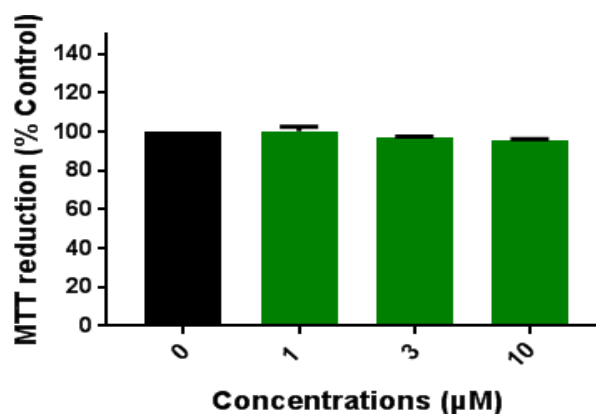
A. CPF in C6 after 24h**B. CPO in C6 after 24h****C. PSP in C6 after 24h**

Figure 3.2. Effects of CPF, CPO and PSP on MTT reduction in differentiating C6 cells after 24 h.

C6 cells were induced to differentiate in the absence and presence of different concentrations of CPF (A), CPO (B) and PSP (C) of induction of cell differentiation, and the reduction of MTT levels were measured to evaluate cell viability. Data are expressed as a mean percentage of the corresponding untreated control \pm SEM from five separate experiments. Statistical significance of data was analysed by using one way ANOVA. When SEM bar is not apparent means that error is smaller than the symbol size.

3.5 Effects of CPF, CPO and PSP on N2a and C6 cell growth

In order to further explore OP cytotoxicity on the growth of N2a and C6 cells, cell number and viability number were monitored at 24 h using a Trypan blue exclusion assay, and measured with the aid of an automated cell counter (TC20TM, Bio-Rad Laboratories Inc., Hemel Hempstead, UK) as described in materials and methods.

The results showed that neither the total cell number nor the percentage of viable cells was affected after 24 h exposure to all concentrations of CPF, CPO or PSP in N2a cells (Figure 3.3). Similarly, both cell number and viable cells were unaffected by all concentrations of CPF, CPO and PSP in C6 cells. However, the overall viable cell percentage was slightly but not significantly reduced under the same condition in C6 cells compared to the corresponding non CPO-treated control (Figure 3.4).

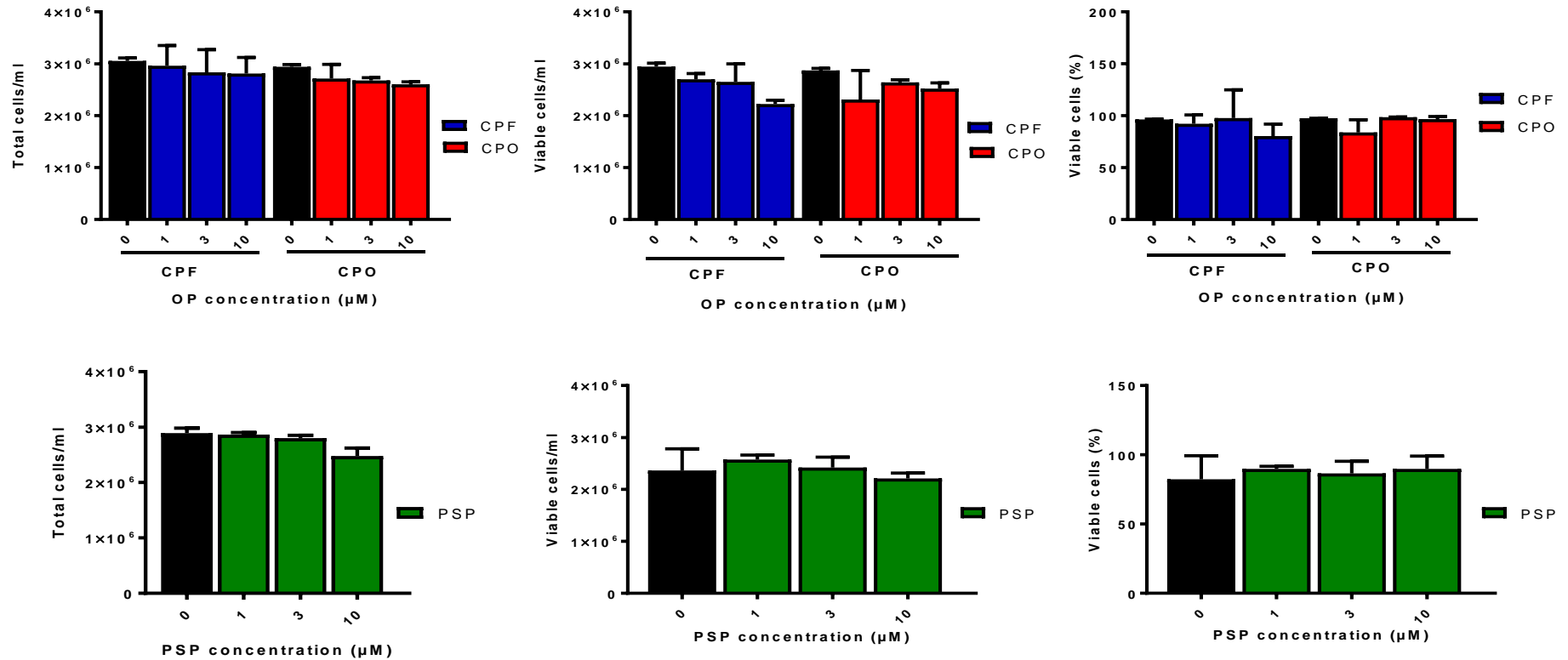


Figure 3.3. Effects of CPF, CPO or PSP on the cell number and viability of differentiating N2a cells.

N2a cells were induced to differentiate for 24h in the presence or absence of 1,3,10 μM CPF, CPO or PSP, before assessment of cell viability via the Trypan blue exclusion assay, as described in Materials and Methods. An average of four separate experiments is shown, and the results are presented as total cell count per ml, live cell count per ml and percentage (%) of live cell relative to the corresponding control. Statistical significance of data was analysed by using one way ANOVA. When SEM bars are not apparent means that error is smaller than the symbol size.

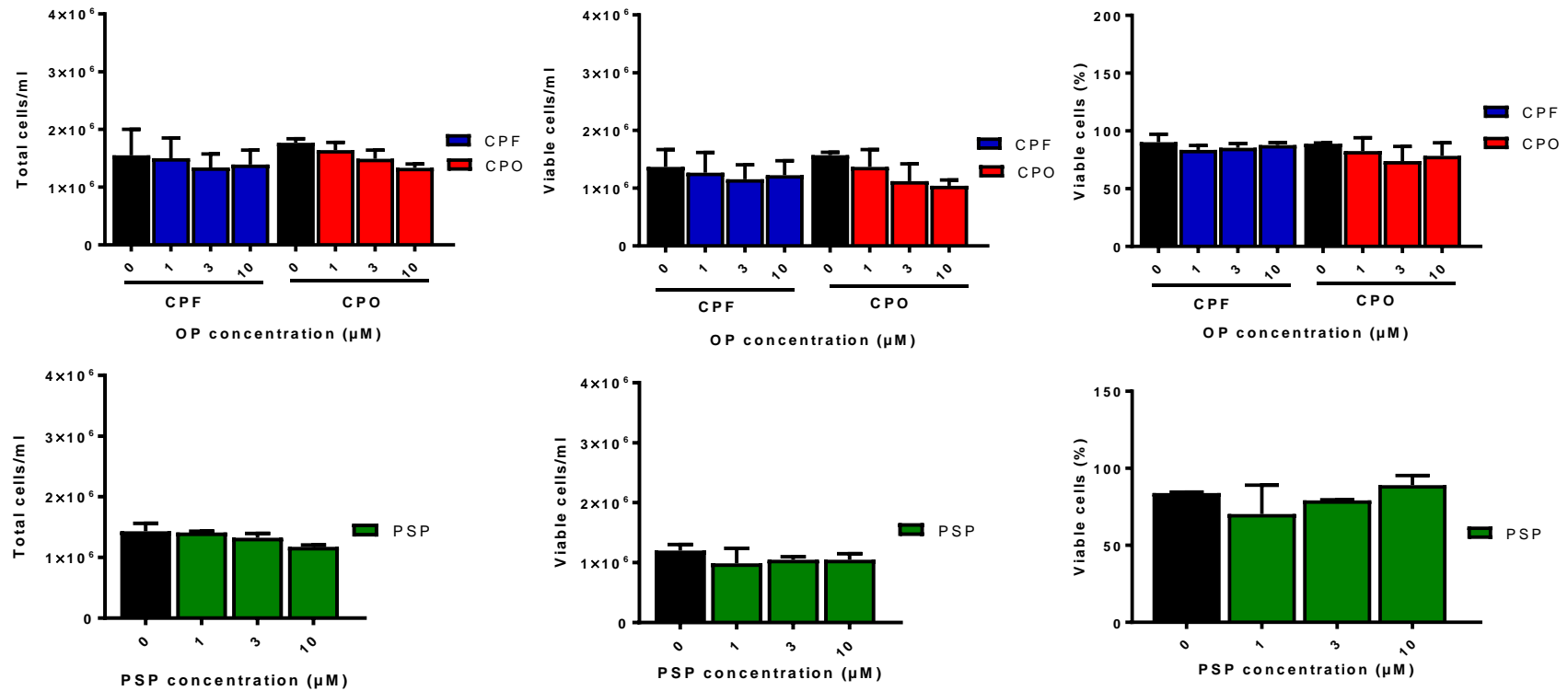


Figure 3.4. Effects of CPF, CPO or PSP on the number and viability of differentiating C6 cells.

C6 cells were induced to differentiate for 4h in the presence or absence of 1,3,10 μM CPF, CPO or PSP, before assessment of cell viability via the Trypan blue exclusion assay, as described in Materials and Methods. Four separate experiments are shown, and the results are presented as total cell count per ml, live cell count per ml and percentage (%) of live cell relative to the corresponding control. Statistical significance of data was analysed by using one way ANOVA.

3.6 Effects of CPF, CPO and PSP on N2a cell morphology

Morphological changes in differentiating N2a cells were assessed after 24 h exposure to different concentrations of CPF, CPO and PSP. Cells were incubated in the absence (0) or presence (1, 3 or 10) μM of CPF, CPO and PSP. They were then fixed and stained with Coomassie Brilliant Blue dye (Figure 3.5). By using light microscopy, the structural features that were studied included the 1) Extensions between half and 2 cell body diameters in length 2) axon, the latter being defined as a neurite outgrowth that is double the cell body diameter or longer. There were differences in the morphological changes in N2a cells exposed to varying concentrations of CPF, CPO and PSP after 24 h. The proportion of cells exhibiting clearly discernible extension was decreased with all concentrations of CPF and PSP after 24 h in N2a cells. The number of cell extensions was however unaffected by CPO.

Similarly, there was a decrease in axon-like neurite formation with all concentrations of CPF, CPO and PSP after 24 h exposure. The decrease was statistically significant except with 1 μM and 3 μM CPF and CPO, and the decrease was highly significant with 10 μM PSP (Table 3.1).

Table 3.1. Quantification of neurite outgrowth in differentiating N2a cells

OPs	Concentrations (μM)	Extension (%)	Axon (%)
CPF	0	45 \pm 1.2	15 \pm 0.4
	1	24 \pm 0.3*	14 \pm 1.00
	3	27 \pm 1.2*	14 \pm 1.2
	10	15 \pm 2.5**	7 \pm 0.8*
CPO	0	31 \pm 2.00	10 \pm 0.8
	1	26 \pm 0.3	7 \pm 0.3
	3	26 \pm 4.9	9 \pm 1.00
	10	23 \pm 1.4	6 \pm 0.5*
PSP	0	58 \pm 0.5	20 \pm 0.5
	1	26 \pm 3.2*	11 \pm 0.5**
	3	24 \pm 3.6*	11 \pm 0.7**
	10	21 \pm 4.2*	3 \pm 1.2****

N2a cells were induced to differentiate for 24 h in the presence of a range of CPF, CPO or PSP concentrations. Cells were fixed and stained with Coomassie blue prior to morphological measurements. Data are indicated to the number recorded per hundred cells \pm standard error from an average of four wells of cells cultured on four separate occasions for 24 h exposure.

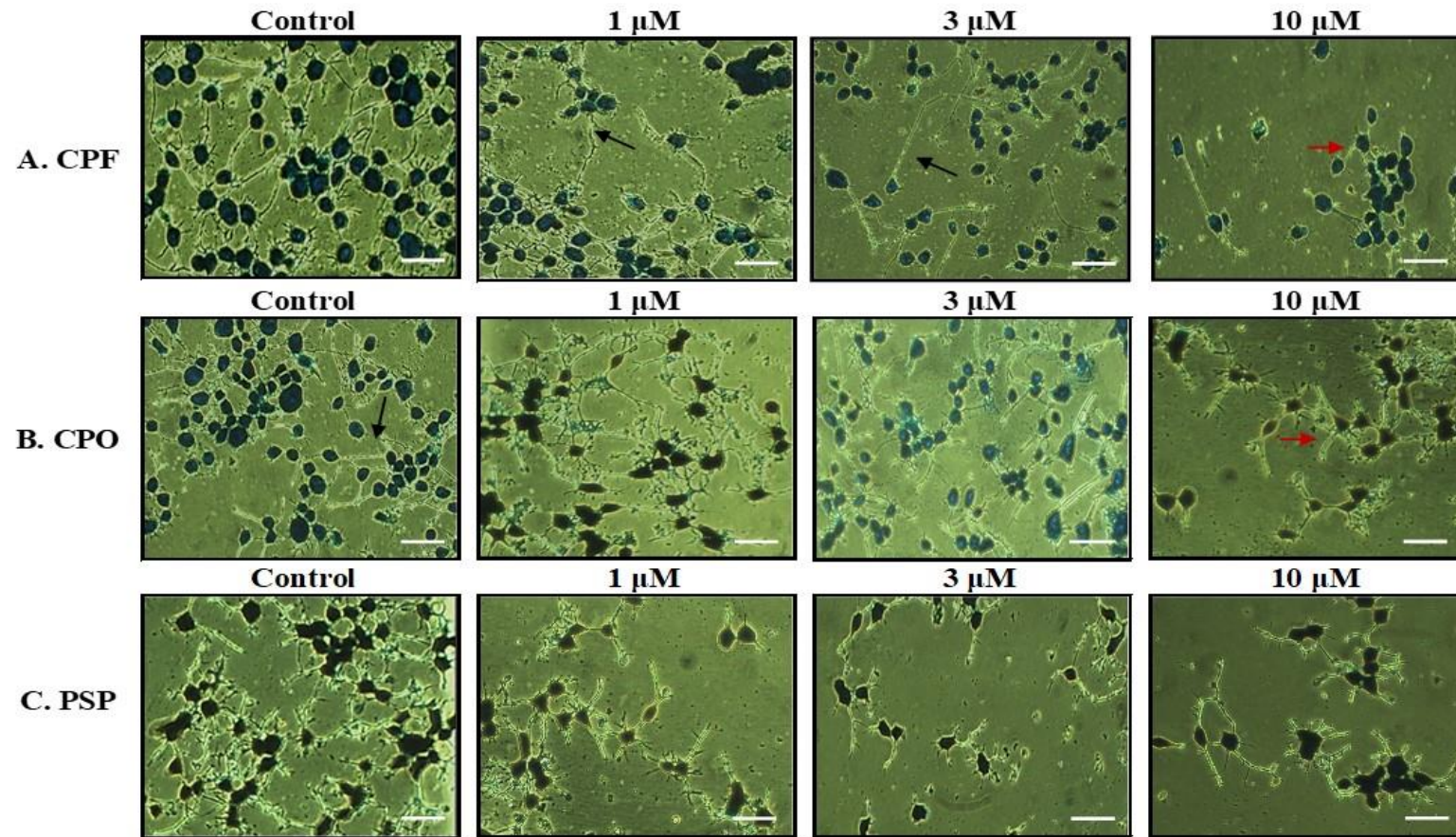


Figure 3.5. Effects of CPF, CPO or PSP on the morphology of differentiating N2a cells.

N2a cells were induced to differentiate for 24 h in the presence or absence of 1,3,10 μM CPF, CPO or PSP, as described in Materials and Methods. Shown are images of typical fields of cells viewed by phase contrast microscopy after 24 h differentiation by using an inverted light microscope following methanol fixation and staining with Coomassie blue after 24 h differentiation. Projecting from each individual N2a cell are outgrowth processes defined as (a) axon-like processes (if greater than 2 cell body diameters in length) (black arrows) or (b) extensions (shorter processes that are between 0.5 -2 cell body diameters in length) (red arrows) . Bar represents 25 μm .

3.7 Development of high content screening assay of neurite outgrowth

The neurotoxic effects of CPF, CPO and PSP on neurite outgrowth in differentiating N2a and C6 cells observed in the previous assay (sections 3.5, 3.6) were assessed using manual laboratory techniques, by which the number of axon-like processes was quantified per 100 cells following Coomassie and Trypan blue staining. Consistently, these methods demonstrated the ability of these compounds to impair the process of neurite outgrowth. However, the acquisition of microscopic images as well as the quantitative analyses was time-consuming and gave information only about neurites that were longer or shorter than two cell body diameters in length. The key aims of the work presented in this chapter was to develop medium to high throughput assays in order to examine the effects of multiple concentrations of CPF, CPO and PSP at 24 h on neurite outgrowth in differentiating N2a and C6 cells in a rapid quantitative analysis. This would, in turn validate the previous findings obtained from analysis of Coomassie Brilliant Blue staining of N2a and C6 cells induced to differentiate in the presence and absence of sub-lethal concentration of CPF, CPO and PSP.

For quantitative analysis of multiple parameters of neurite outgrowth in differentiating N2a and C6 cells following CPF, CPO and PSP exposure, cells were fixed and stained by indirect immunofluorescence with antibodies against their specific proteins. Anti- β III-tubulin (clone 2G10) and anti-neurofilament heavy chain NFH (clone SMI 33) antibodies were used for N2a cells while anti-GFAP (clone GA5) was used for C6 cells. The anti-tubulin antibody was expected to stain microtubules in axons, dendrites, cell bodies, and anti-NFH antibody was expected to preferentially stain mainly neurofilaments in axons of neuronal cells. These specific antibodies were used mainly because they detect neurite-enriched cytoskeletal proteins and thus facilitate the monitoring OP-induced effects on multiple parameters of neurite outgrowth to be investigated. Likewise, anti-GFAP was specifically selected for C6 cells because it detects a useful marker of astroglial neurotoxicity that is highly expressed by astrocytes (Harry *et al.*, 1998). Images of stained cell monolayers were acquired using the ImageXpress Micro Widefield High Content Screening System and neurite outgrowth analysis was performed using MetaXpress imaging and analysis software, as described by Sindi *et al.* (2016) and in section 2.2.10.

Shown in figure 3.6 is the segmentation of acquired images obtained by high throughput assays as previously described (section 2.2.10). As shown, all representative images are from non OP-treated controls stained with antibodies to β III tubulin, NFH and GFAP. The

procedure for image acquisition included using two fluorophores; FITC to detect cell body and neurites (green) and DAPI for all nuclei visualisation in a field (blue). The composite merged images showed staining distribution of FITC and DAPI within each neuronal cell. Following the image acquisition, image segmentation was performed and displayed as multicoloured masks tracking the neurites and cell bodies in the acquired image. For accurate image segmentation, the analysis settings of the integrated neurite outgrowth application mode were configured and optimised to capture maximum relevant detail with reduced background noise. The measurement and analysis of neurite outgrowth parameters were achieved by the use of mathematical algorithms and included the following:

- Average number of cells/field (total number of neural cell bodies averaged by the number of fields).
- Average cell body area/field (total area of cell bodies in square micron averaged by the number of fields).
- Percentage of cells with significant outgrowth (cells with at least one neurite $> 10 \mu\text{m}$ in length).
- Average number of neurites (total number of neurites produced from the cell bodies averaged by the number of fields).
- Maximum neurite length/cell (the length in microns of the longest neurite from the neuronal cell body to an extreme segment per cell).
- Average neurite length/cell (the total length in microns of all significant outgrowths averaged by the number of cells).
- Significant outgrowth (neurites longer than $10 \mu\text{m}$ in length).

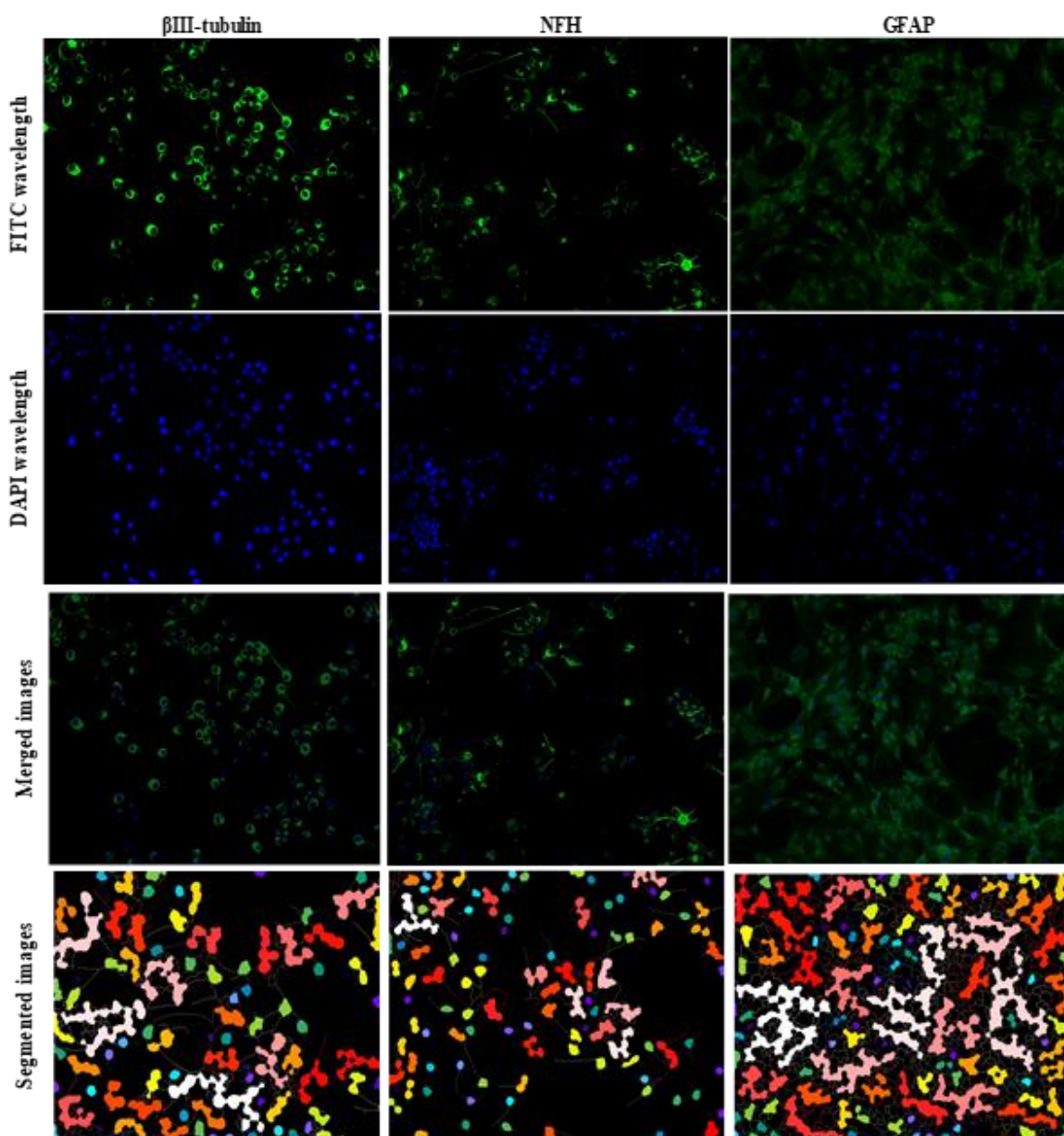


Figure 3.6. Segmentation of stained differentiating N2a and C6 cells using high throughput screening assay.

Cells were induced to differentiate for 24 h in the absence of OPs for 24 h. Cells were fixed and stained with antibodies recognising the neuronal marker of N2a cells β III-tubulin and NFH, and GFAP as glial neural marker for C6, followed by Alexa Fluor conjugated anti-IgG secondary antibodies, as described in Materials and Methods. The shown images were from a single field of view of untreated controls. Acquired images were obtained by using ImageXpress Micro system (10x objective) with two wavelengths; FITC to detect cell bodies and neurites and DAPI to detect nucleus counting. The multicoloured of segmented images with tracing masks on neurites and cell bodies were generated using the Neurite Outgrowth Module within the MetaXpress analysis software to monitor different parameters of neurite outgrowth including cell number, cell body area and outgrowth length for each identified cell.

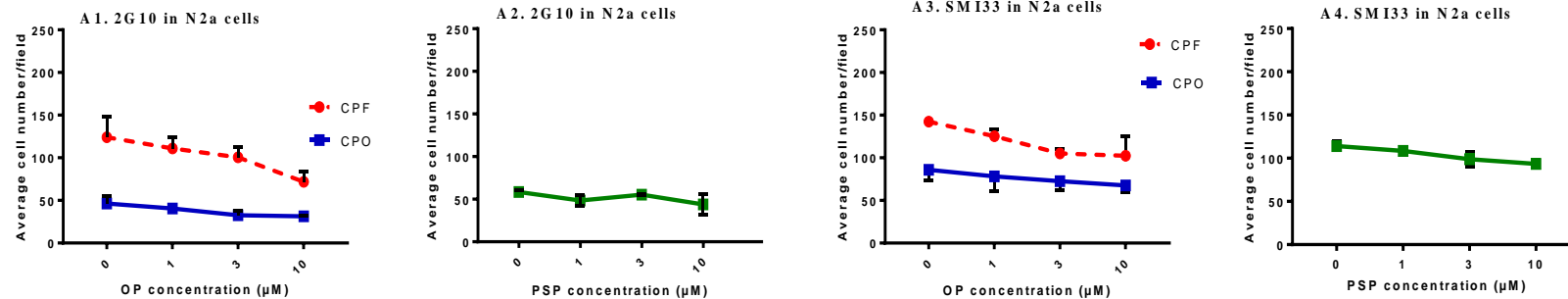
3.8 Monitoring multi-parameters of neurite outgrowth in differentiating N2a cells

The sub-lethal effects of CPF, CPO and PSP on neurite outgrowth in co-differentiated N2a cells were investigated following 24 h exposure using high throughput assay. The results of multi-parametric analysis of neurite outgrowth achieved by quantitation of β III tubulin and NFH staining are shown in Figures 3.7, 3.8, 3.9, 3.10.

Figure 3.7 shows the high content data for cell number and cell body area obtained by analysis of β III tubulin and NFH staining at 24 h exposure. The presented data show that all concentrations of CPF, CPO and PSP had no significant effects on the average neuronal cell number/field after 24 h exposure compared to the untreated controls (Figure 3.7, panel A1-A4). Similarly, both β III tubulin and NFH staining showed no significant effects on the measurements of cell body area/field of co-differentiated N2a cells following 24 h exposure to all the three OP treatments (Figure 3.7, panel B1-B4).

The effects of multiple concentrations of CPF, CPO and PSP on the average intensity of staining within the positive cells and the percentage of cells with significant outgrowth (neurites $> 10 \mu\text{m}$ in length) are shown in figure 3.8. The presented data show that all concentrations of CPF had no effects on the average intensity of staining/field after 24 h exposure compared to the untreated controls (Figure 3.8, panel A1, A3). As indicated in figure 3.8, panel A1, A3, no effects were observed on the average intensity of staining in cells treated with 1 and 3 μM CPO. In addition, exposure to the highest concentration (10 μM) of CPO and PSP resulted in significantly reduced intensity ($p < 0.05$), as with both β III tubulin and NFH staining. Exposure of cells to 3 μM PSP significantly reduced the average intensity of staining to 25 % of control values using anti-NFH stain (Figure 3.8, panel A4). The quantitative analysis of both stains for the average intensity of staining number of neurites/field in co-differentiated N2a cells showed that the exposure to 10 μM CPO and PSP caused 20 % and 25 % decline respectively, compared to the corresponding non OP-treated control (Figure 3.8).

A. Cell number



B. Cell body area

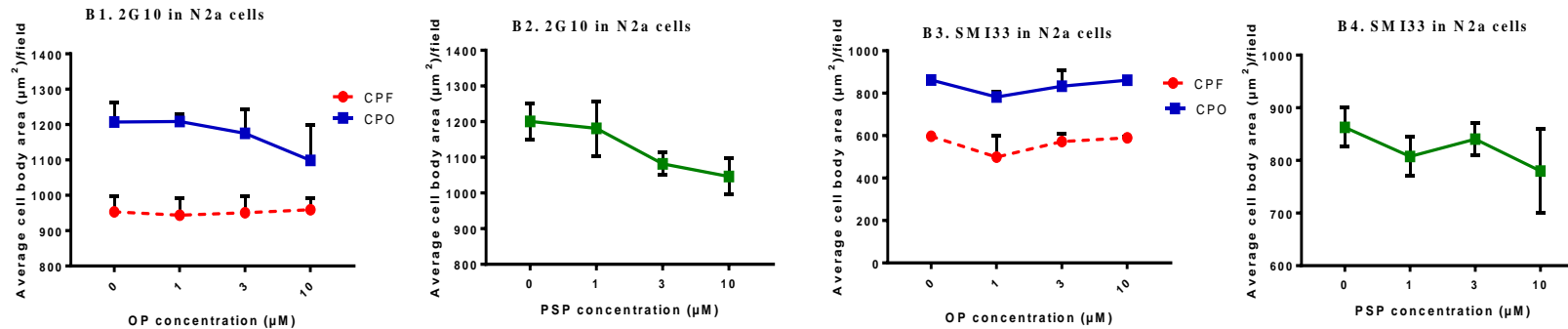


Figure 3.7. Effects of CPF, CPO and PSP on cell number and cell body area in differentiating N2a cells as assessed by high throughput assays.

Cells were fixed and stained with antibodies to β III tubulin and NFH, then data were acquired by using the ImageXpress Micro system, the cell number and cell body area were measured using MetaXpress imaging and analysis software. Data show the effects of CPF, CPO or PSP on the average cell number/field (panel A) and the average cell body area (μm^2)/field (panel B). High throughput data are represented as mean values \pm SEM from four independent experiments. Data were analysed using one-way ANOVA. The CPF effects are presented as red dashed lines; the CPO effects are presented as blue solid lines, whereas PSP effects are shown as green solid lines. When SEM bars are not apparent means that error is smaller than the symbol size.

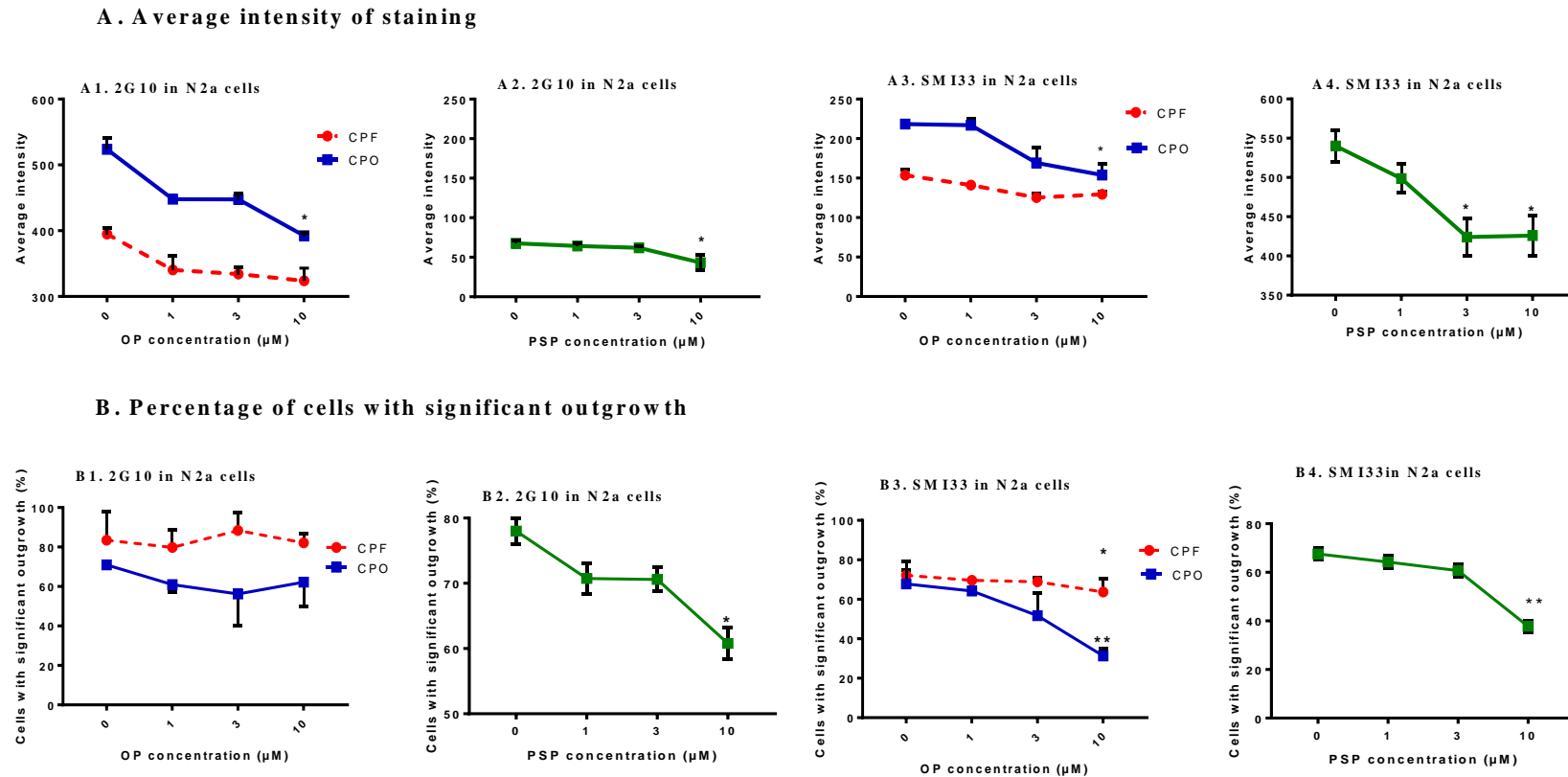


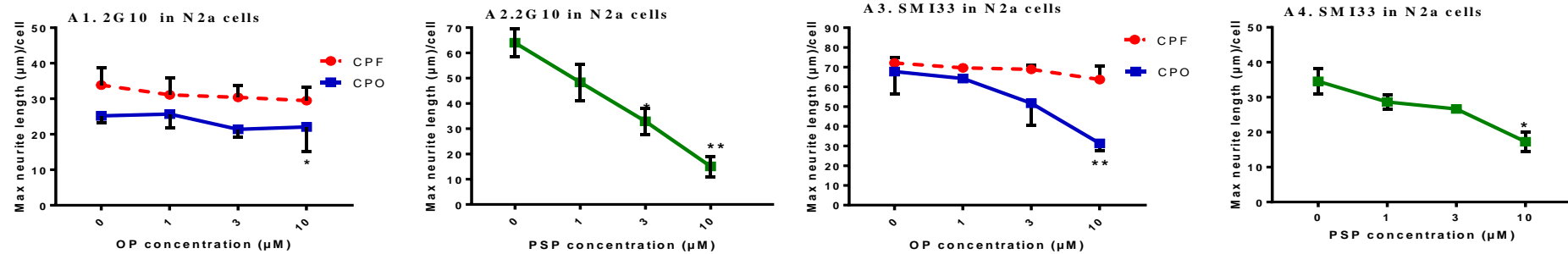
Figure 3.8. Effects of CPF CPO or PSP on average intensity of staining and percentage of cells with significant outgrowth in differentiating N2a cells as assessed by high throughput analysis.

Cells were stained with antibodies to β III tubulin and NFH, after which data were acquired using ImageXpress Micro system and measured using MetaXpress imaging and analysis software. Data show dose-related effects of CPF, CPO or PSP on the average intensity of staining/field (panel A) and the percentage of cells with significant outgrowth (panel B). Data are presented as mean values \pm SEM from four independent experiments. Data were analysed using one-way ANOVA. The CPF effects are presented as red dashed lines; the CPO effects are presented as blue solid lines, whereas PSP effects are showed as green solid lines. Asterisks indicate changes that are statistically different from the non OP-treated controls (* $p < 0.05$), (** $p < 0.01$). When SEM bars are not apparent, this means that error is smaller than the symbol size.

Figure 3.8 (panel B) quantitation of β III tubulin staining showed lack of detectable changes on the number of cells with significant outgrowth in differentiating N2a cells treated with multiple concentrations of CPF and CPO for 24 h. In contrast, this staining showed dose dependent decreases in this parameter in PSP-treated cells which was statistically significant at the highest concentration ($p < 0.05$). However, exposure to the highest concentration (10 μ M) of CPO and PSP significantly reduced the number of cells bearing neurites stained with anti-NFH ($p < 0.01$) staining (Figure 3.8, panel B3, B4). The quantitative analysis of NFH stain for the significant outgrowth in differentiating N2a cells showed that the treatment of 10 μ M CPF, CPO and PSP caused 20 %, 45 % and 65 % decline, respectively, compared to the corresponding non OP-treated control.

Further parameters of neurite outgrowth such as the maximum and average neurite length per neuronal cell were also assessed using high throughput assays. Following 24 h exposure, CPO ($p < 0.05$) and PSP ($p < 0.01$) significantly reduced maximum and average neurite length per neuronal cell, respectively, as indicated by anti- β III tubulin staining (Figure 3.9, panel B1). There was a dose-dependent decrease in both parameters of neurite outgrowth in PSP-treated cells compared to the non-treated controls. A significant concentration-related reduction ($p < 0.05$, $p < 0.01$) was observed in both parameters of neurite outgrowth at two concentrations (3 and 10 μ M) of PSP respectively, as indicated with anti- β III tubulin staining. Anti-NFH staining exhibited significant decreases in the maximum and average neurite length/cell following 10 μ M CPO and PSP treatments for 24 h. With regard to the measurement of maximum neurite length per neuronal cell were similar for both antibodies at around 25-65 μ m (Figure 3.9).

A. Maximum neurite length/cell



B. Average neurite length/cell

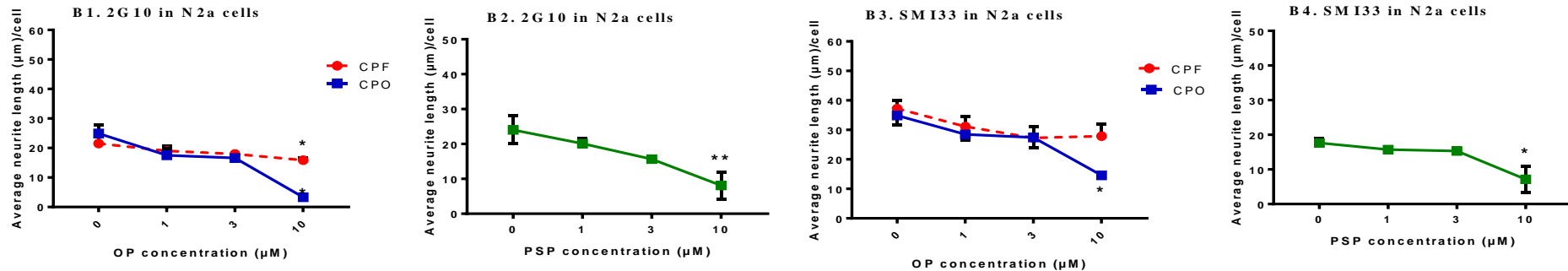


Figure 3.9. Effects of CPF, CPO or PSP on maximum and average neurite length/cell in differentiating N2a cells as assessed by high throughput analysis.

Cells were stained with antibodies to β III tubulin and NFH, after which data were acquired using ImageXpress Micro system and measured using MetaXpress imaging and analysis software. Data show dose-related effects of CPF, CPO or PSP on the maximum neurite length/cell (panel A) and the average neurite length/cell (panel B). Data are presented as mean values \pm SEM from four independent experiments. Data were analysed using one-way ANOVA. The CPF effects are presented as red dashed lines; the CPO effects are presented as blue solid lines, whereas PSP effects are showed as green solid lines. Asterisks show changes that are statistically different from the controls (* $p < 0.05$), (** $p < 0.01$). When SEM bars are not apparent, this means that error is smaller than the symbol size.

3.9 Monitoring multi-parameters of neurite outgrowth in differentiating C6 cells

Using high content throughput analysis, the effects of CPF, CPO and PSP were assessed over different concentrations (1, 3 and 10 μM) on the multi-parameters of neurite outgrowth in differentiating C6 cells after 24 h exposure. The parameters used to determine the impacts of these compounds on C6 cells were similar to those applied in N2a cell experiments, which included cell number, cell body area, and percentage of cells with significant outgrowth, maximum and average neurite length. Additionally, the average intensity of GFAP (clone GA5) staining within neurites and cell bodies of each antibody-positive cell were evaluated by high throughput assay, as described in section 2.2.10.

Figure 3.10 demonstrates the segmentation of acquired images obtained by high throughput assay employed for C6 cells in the current study. All procedures for image acquisition and image analysis were similar to those applied in N2a experiments. All representative images shown are from untreated control C6 cells from four single fields of view.

The high throughput data presented in Figure 3.10 show that all concentrations of CPF and PSP had no significant effect on either the average number of glial cells/field or on the average area of cell bodies/field after 24 h exposure compared to untreated controls, as indicated by the analysis of anti-GFAP staining (Figure 3.10, upper panels A1-B2). The average number of glial cells/field and the average area of cell bodies/field were, however, significantly ($p < 0.05$) reduced after 24 h exposure to the highest CPO concentration (Figure 3.10, panels A1 and B1). The average count of differentiated glial cells ranged between 110 to 150 cells/field in controls, as indicated by anti-GFAP staining (Figure 3.10, panels A1 and A2).

Figure 3.10 (lower panels C1-D2) displays the high throughput measurement of the average intensity of staining and the percentage of cells with significant outgrowth. The data demonstrated that CPF and CPO at all concentrations had no effect on either parameter following 24 h exposure, compared to non OP-treated controls. The average intensity of staining was, however, significantly ($p < 0.05$) reduced by all concentrations of PSP and the percentage of cells with significant outgrowth was significantly ($p < 0.05$) reduced following exposure to 10 μM PSP.

Measurements of glial cell extension length were also obtained using high throughput screening with GA5 staining. As illustrated in figure 3.11, while the maximum neurite length per cell in co-differentiated C6 cells was significantly ($P < 0.01$) reduced by 10 μM CPF and CPO following exposure for 24 h, there was a significant dose-dependent reduction in the average neural length per cell following PSP exposure for 24 h. As demonstrated in figure 3.11 (panels A1 and A2), the maximum length of astrocyte extensions/cell ranged between 35 to 58 μm in untreated controls. The data in figure 3.11 (panels B1 and B2) indicated that 24 h exposure to CPO at 1, 3 and 10 μM concentrations caused a significant reduction in the average neurite length/cell by 90 % at 10 μM ($p < 0.01$) compared to the untreated controls. However, the data show that all concentrations of PSP had no statistically significant effect on either parameter following 24 h exposure compared to non OP-treated controls, except the average neurite length per cell which was significantly reduced ($p < 0.05$) by exposure to 10 μM PSP.

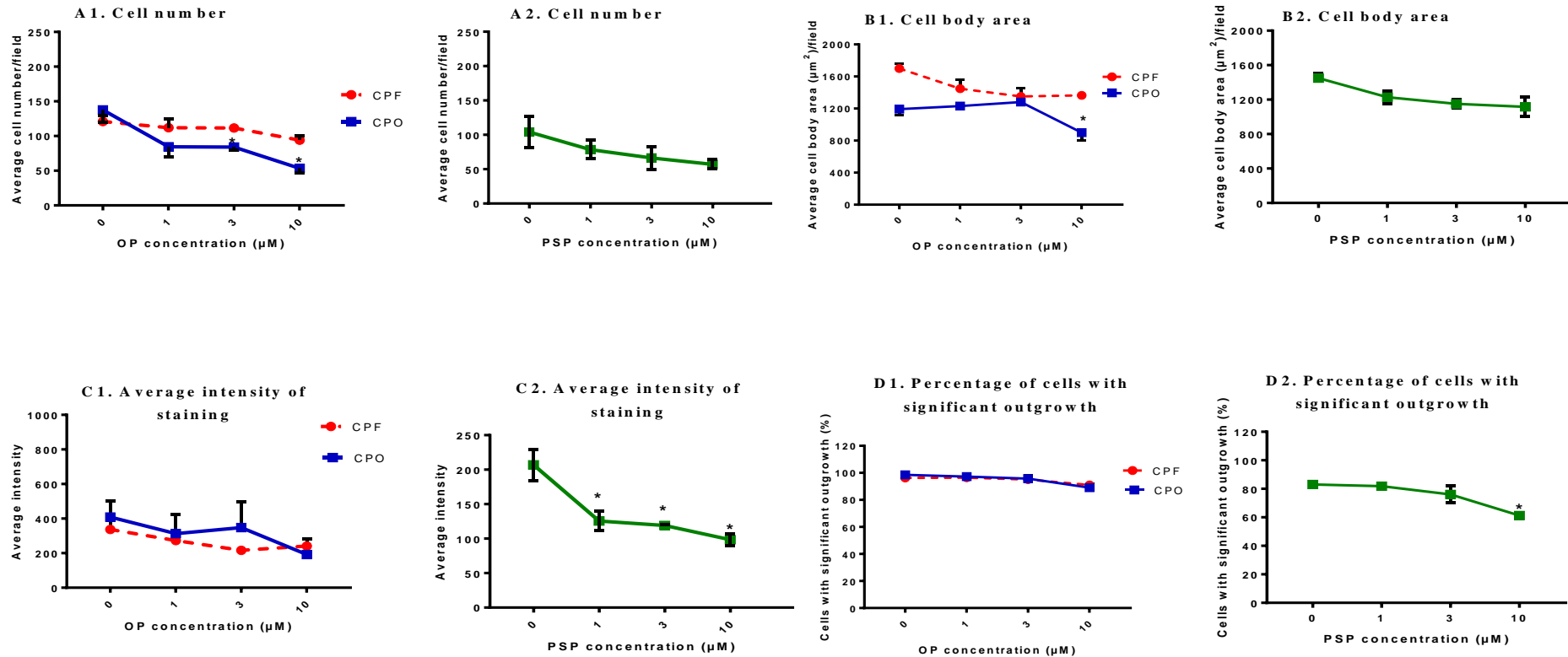


Figure 3.10. Effects of CPF CPO or PSP on multiple parameters in differentiating C6 cells as assessed by high throughput analysis.

Cells were stained with antibody to GFAP, after which data were acquired using ImageXpress Micro system and measured using MetaXpress imaging and analysis software. Data show dose-related effects of CPF, CPO or PSP on cell number (panel A), cell body area (panel B), the average intensity of staining (panel C) and percentage of cells with significant outgrowth (panel D). Data are presented as mean values \pm SEM from four independent experiments. Data were analysed using one-way ANOVA. The CPF effects are presented as red dashed lines; the CPO effects are presented as blue solid lines, whereas PSP effects are shown as green solid lines. Asterisks indicate changes that are statistically different from the non OP-treated controls (* $p < 0.05$). When SEM bars are not apparent, this means that error is smaller than the symbol size.

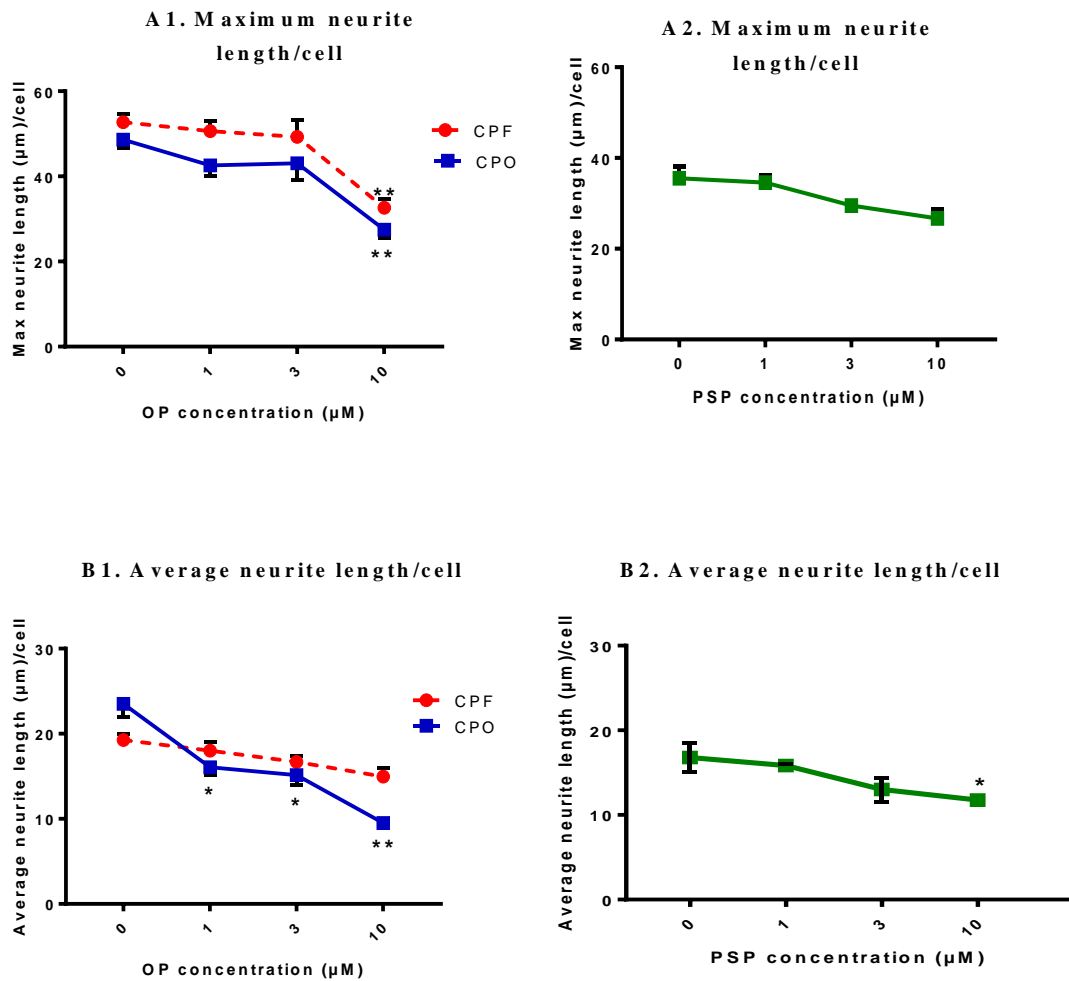


Figure 3.11. Effects of CPF CPO or PSP on multiple parameters in differentiating C6 cells as assessed by high throughput analysis.

Cells were stained with antibody to GFAP, after which data were acquired using ImageXpress Micro system and measured using MetaXpress imaging and analysis software. Data show dose-related effects of CPF, CPO or PSP on the maximum neurite length/cell (panel A), the average neurite length/cell (panel B). Data are presented as mean values \pm SEM from four independent experiments. Data were analysed using one-way ANOVA. The CPF effects are presented as red dashed lines; the CPO effects are presented as blue solid lines, whereas PSP effects are showed as green solid lines. Asterisks indicate changes that are statistically different from the non OP-treated controls (* $p < 0.05$), (** $p < 0.01$).

3.10 Effect of CPF, CPO and PSP on cytoskeletal organization in cultured differentiating N2a and C6 cells

In order to show whether the morphological changes observed in sections 3.6, and 3.7 reflected cytoskeletal disruption, cells from control and OP exposures were stained with antibodies to cytoskeletal proteins (β III tubulin, NFH and GFAP) by indirect immunofluorescence as described in Materials and Methods (section 2.2.9). The images in figures 3.12 – 3.17 show the effects of treatment of differentiating N2a cells with 1, 3 and 10 μ M CPF, CPO and PSP for 24 h on cytoskeletal networks as indicated by anti- β III tubulin (Clone 2G10) and anti-NFH (clone SMI33) staining.

Exposure to all of the OP concentrations modified the cells' cytoskeletal network after a 24 h treatment. This was mainly evident by some disruption in the microtubule and neurofilament networks in N2a cells showing cytoplasmic staining, which was reduced in intensity with treatments. Anti-tubulin staining was reduced and disrupted with OP treatments. The cytoplasmic staining was reduced compared to the control with CPF (Figures 3.12), CPO (Figures 3.13) and PSP (Figures 3.14) treatments, and the neurite outgrowth was visibly truncated in some cells with OP treatments.

Neurofilament staining intensity was also reduced in differentiating N2a cells with OP treatments, in particular with 3 and 10 μ M CPF (Figures 3.15), CPO (Figures 3.16) and PSP (Figures 3.17). The proportion of N2a cells exhibiting a clearly discernible neural outgrowth was visibly reduced with both concentrations of all the OP concentrations in N2a cell lines.

The images in Figures 3.18, 3.19 and 3.20 show that changes were observed in the staining intensity of GFAP in differentiating C6 cells with CPF and CPO treatments. However, in PSP treated C6 cells there was disruption in the GFAP staining, showing cytoplasmic staining, which was reduced in intensity compared to the non OP-treated control.

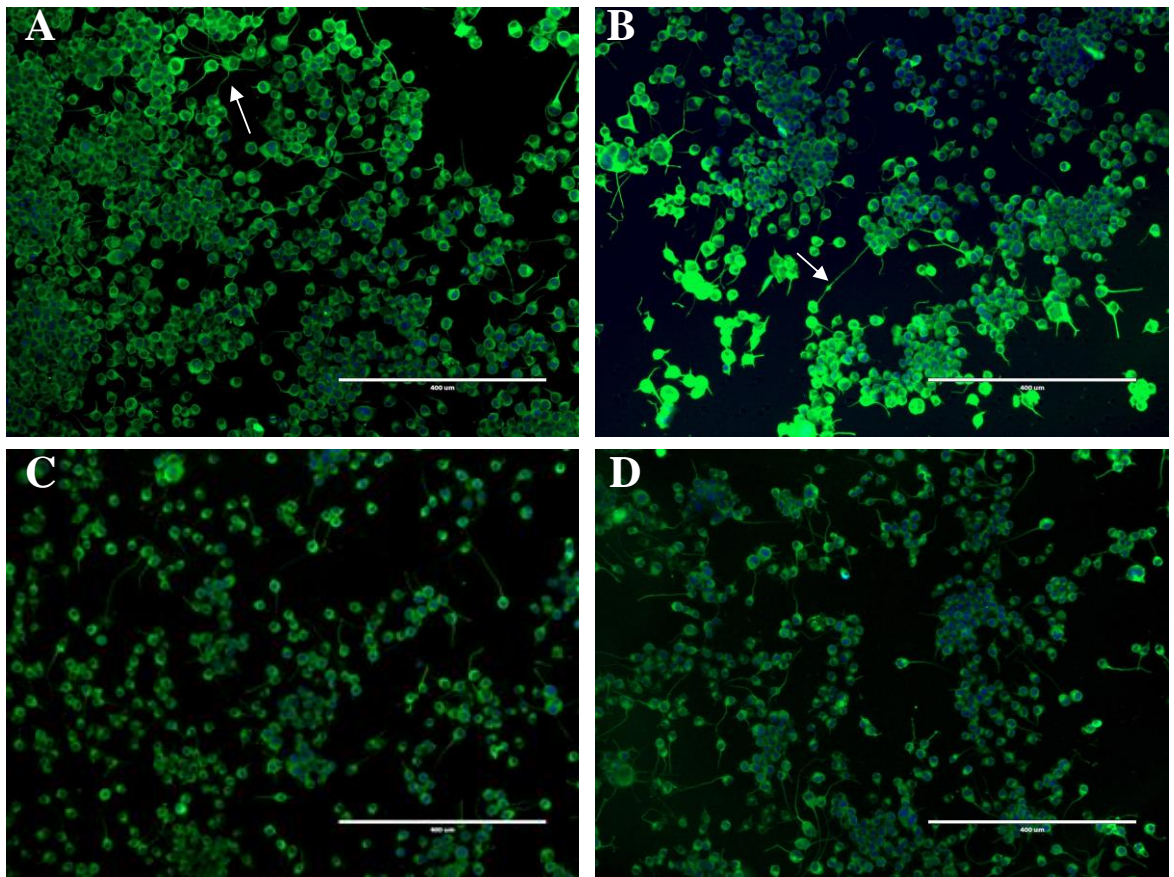


Figure 3.12. Indirect immunofluorescence staining of CPF effects on β III tubulin staining of differentiating N2a cells as detected by EVOS cell imaging system.

Shown are representative images of immunofluorescently stained cell monolayers with anti- β III tubulin. Cells were induced to differentiate for 24 h in the presence of 1 μ M (panel B), 3 μ M (panel C) and 10 μ M (panel D) or absence (panel A) of CPF for 24 h, then they were fixed and immunofluorescently stained for the neural marker of interest as described in Materials and Methods. The white arrow indicates to the axon. All Images shown were from a single representative field of view by using an EVOS FL cell imaging system (10x objective) with two channels; FITC for detecting cell bodies and neurites and DAPI for nucleus counting. Scale bar 400 μ m.

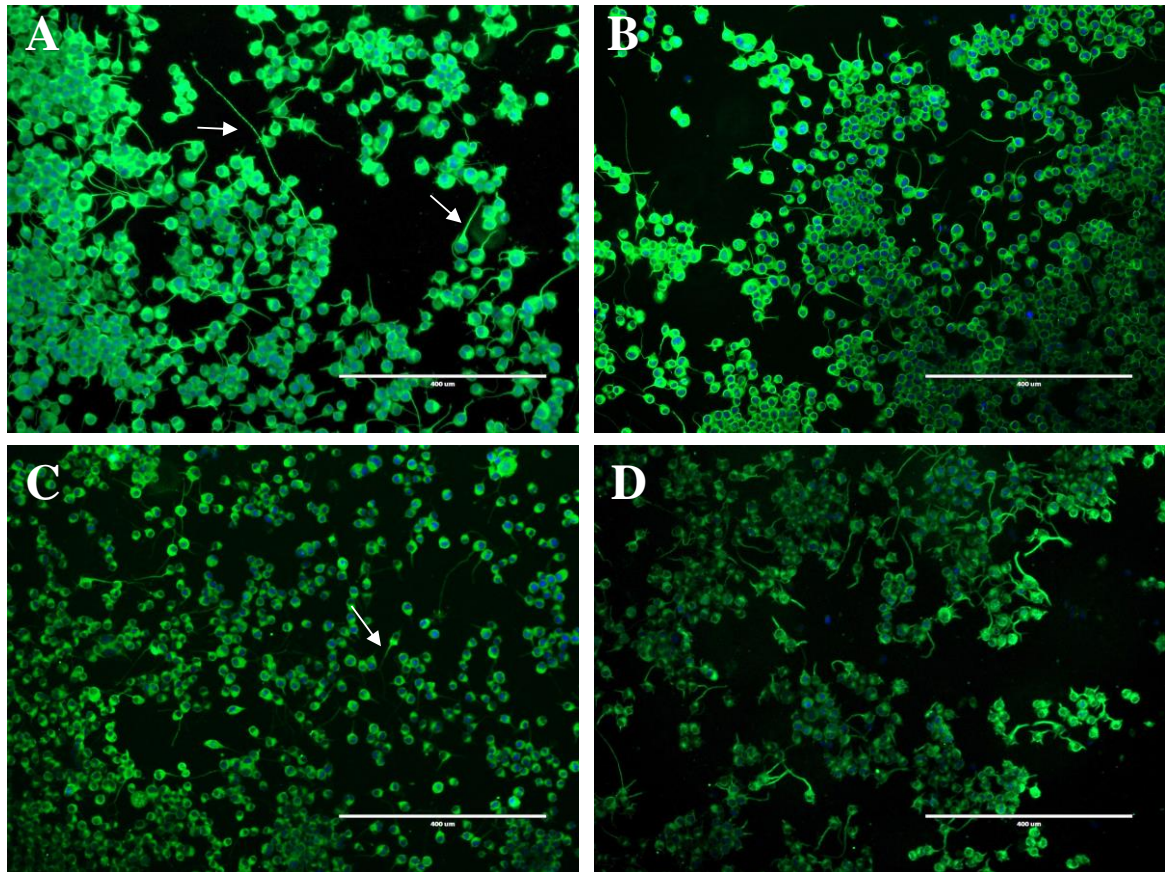


Figure 3.13. Indirect immunofluorescence staining of CPO effects on β III tubulin staining of differentiating N2a cells as detected by EVOS cell imaging system.

Shown are representative images of immunofluorescently stained cell monolayers with anti- β III tubulin. Cells were induced to differentiate for 24 h in the presence of 1 μ M (panel B), 3 μ M (panel C) and 10 μ M (panel D) or absence (panel A) of CPF for 24 h, then they were fixed and immunofluorescently stained for the neural marker of interest as described in Materials and Methods. The white arrow indicates to the axon. All Images shown were from a single representative field of view by using an EVOS FL cell imaging system (10x objective) with two channels; FITC for detecting cell bodies and neurites and DAPI for nucleus counting. Scale bar 400 μ m.

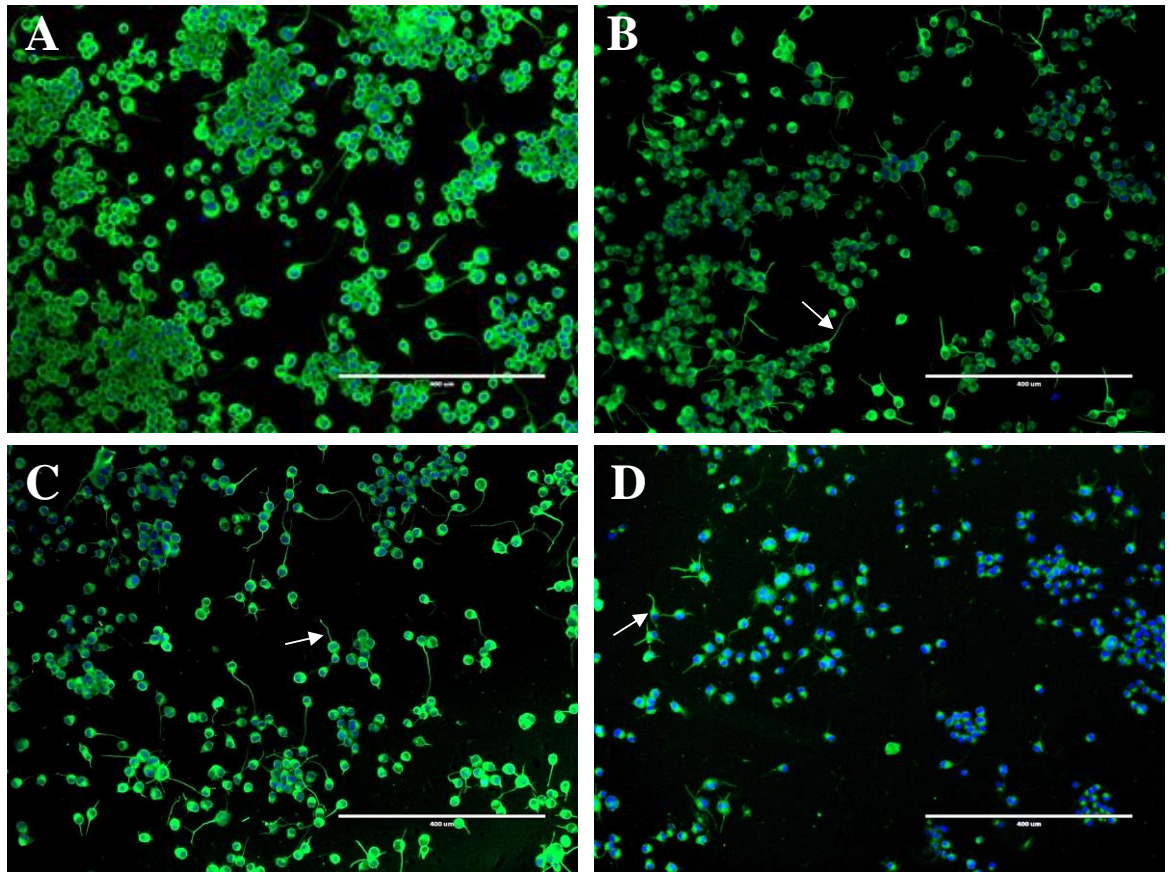


Figure 3.14. Indirect immunofluorescence staining of PSP effects on β III tubulin staining of differentiating N2a cells as detected by EVOS cell imaging system.

Shown are representative images of immunofluorescently stained cell monolayers with anti- β III tubulin. Cells were induced to differentiate for 24 h in the presence of 1 μ M (panel B), 3 μ M (panel C) and 10 μ M (panel D) or absence (panel A) of CPF for 24 h, then they were fixed and immunofluorescently stained for the neural marker of interest as described in Materials and Methods. The white arrow indicates to the axon. All Images shown were from a single representative field of view by using an EVOS FL cell imaging system (10x objective) with two channels; FITC for detecting cell bodies and neurites and DAPI for nucleus counting. Scale bar 400 μ m.

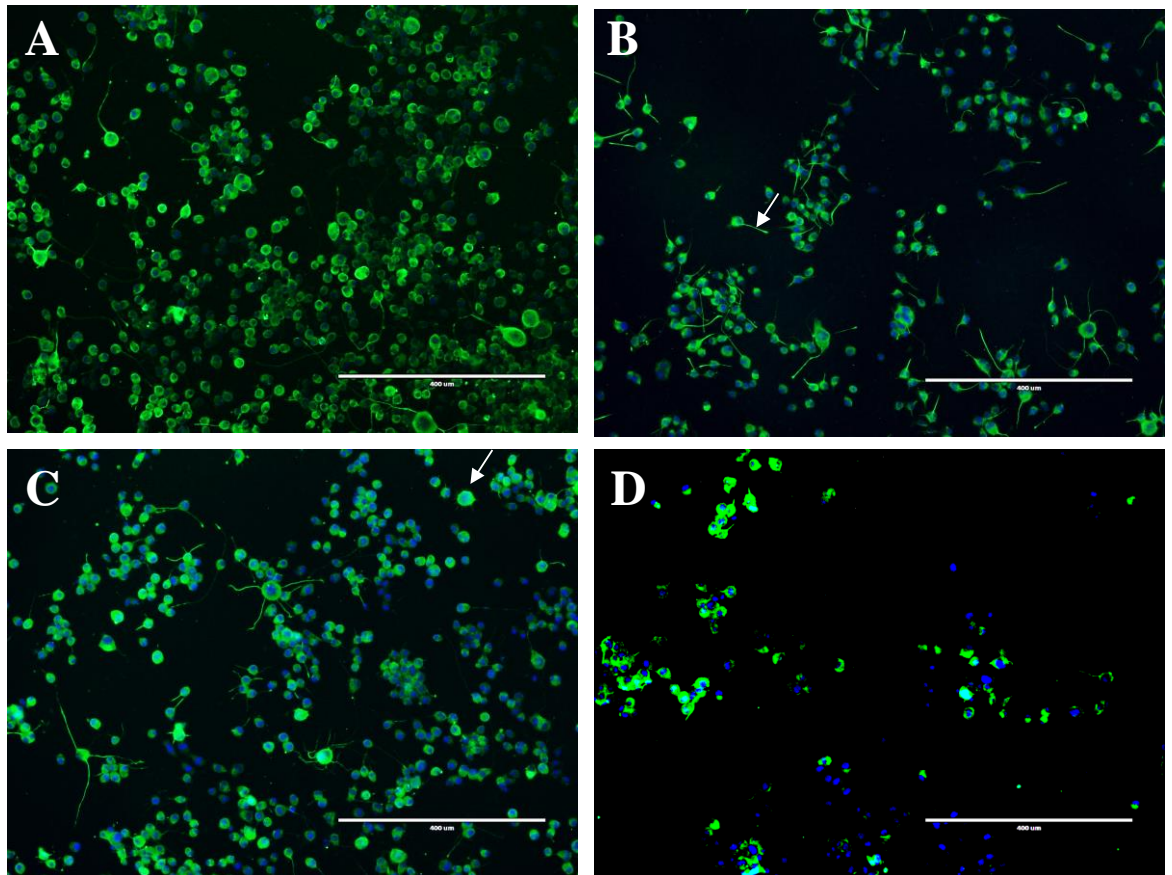


Figure 3.15. Indirect immunofluorescence staining of CPF effects on NFH staining of differentiating N2a cells as detected by EVOS cell imaging system.

Shown are representative images of immunofluorescently stained cell monolayers with anti-NFH (Clone SMI 33). Cells were induced to differentiate for 24 h in the presence of 1 μM (panel B), 3 μM (panel C) and 10 μM (panel D) or absence (panel A) of CPF for 24 h, then they were fixed and immunofluorescently stained for the neural marker of interest as described in Materials and Methods. The white arrow indicates to the axon. All Images shown were from a single representative field of view by using an EVOS FL cell imaging system (10x objective) with two channels; FITC for detecting cell bodies and neurites and DAPI for nucleus counting. Scale bar 400 μm .

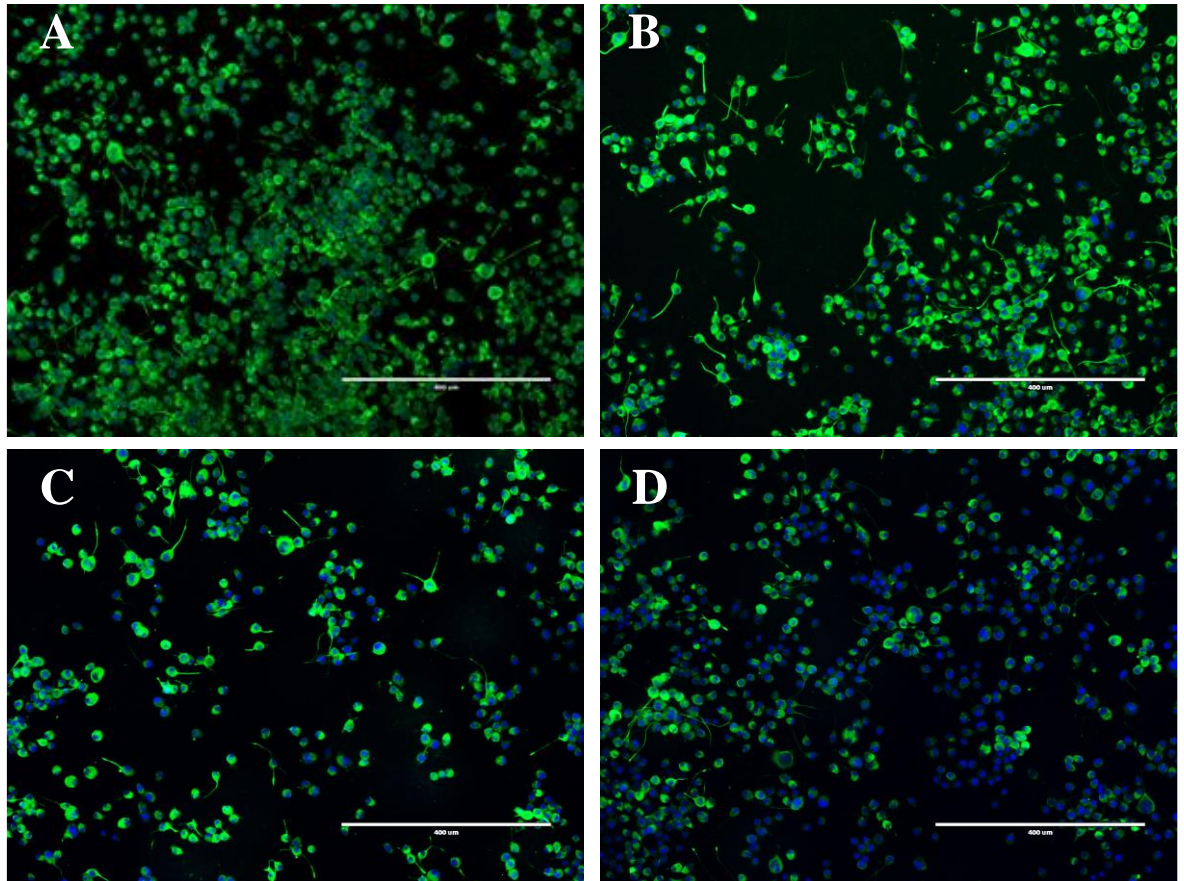


Figure 3.16. Indirect immunofluorescence staining of CPO effects on NFH staining of differentiating N2a cells as detected by EVOS cell imaging system.

Shown are representative images of immunofluorescently stained cell monolayers with anti-NFH (Clone SMI 33). Cells were induced to differentiate for 24 h in the presence of 1 μ M (panel B), 3 μ M (panel C) and 10 μ M (panel D) or absence (panel A) of CPF for 24 h, then they were fixed and immunofluorescently stained for the neural marker of interest as described in Materials and Methods. All Images shown were from a single representative field of view by using an EVOS FL cell imaging system (10x objective) with two channels; FITC for detecting cell bodies and neurites and DAPI for nucleus counting. Scale bar 400 μ m.

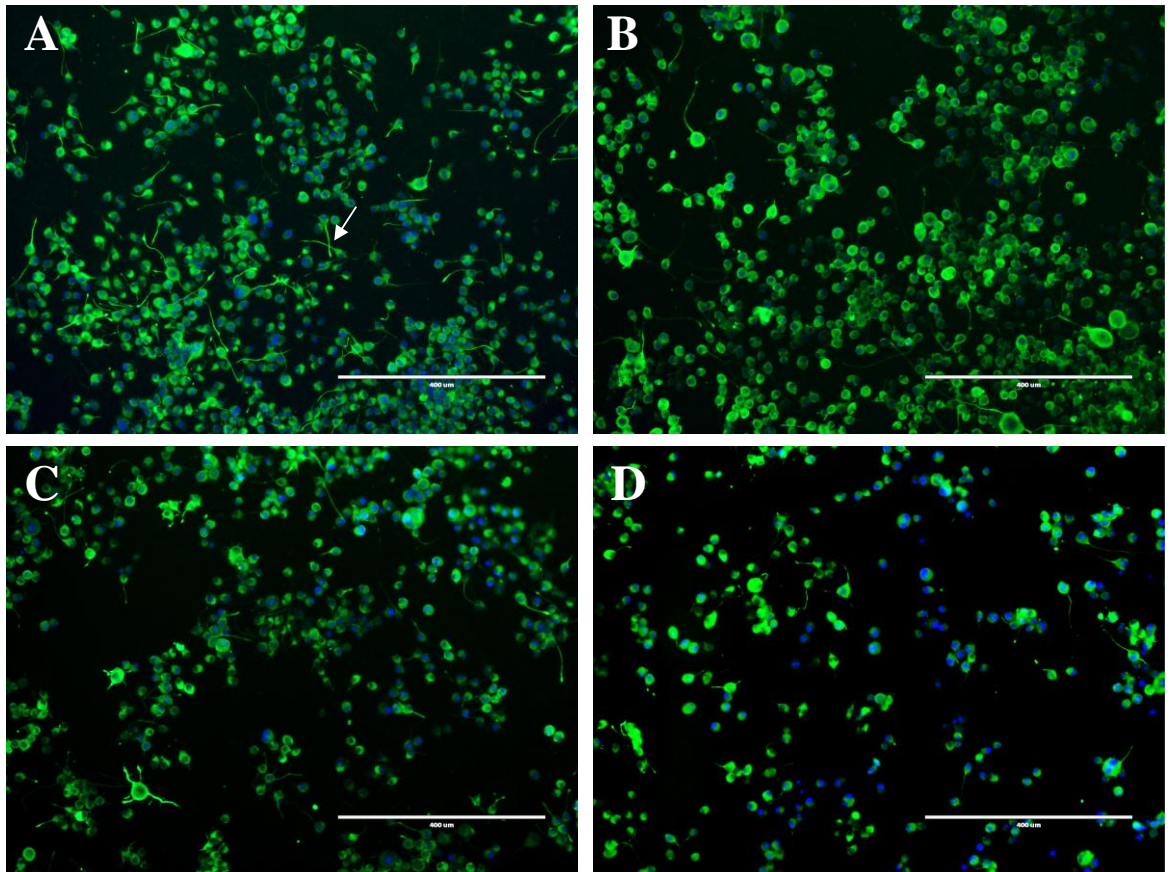


Figure 3.17. Indirect immunofluorescence staining of PSP effects on NFH staining of differentiating N2a cells as detected by EVOS cell imaging system.

Shown are representative images of immunofluorescently stained cell monolayers with anti-NFH (Clone SMI 33). Cells were induced to differentiate for 24 h in the presence of 1 μ M (panel B), 3 μ M (panel C) and 10 μ M (panel D) or absence (panel A) of CPF for 24 h, then they were fixed and immunofluorescently stained for the neural marker of interest as described in Materials and Methods. The white arrow indicates to the axon. All Images shown were from a single representative field of view by using an EVOS FL cell imaging system (10x objective) with two channels; FITC for detecting cell bodies and neurites and DAPI for nucleus counting. Scale bar 400 μ m.

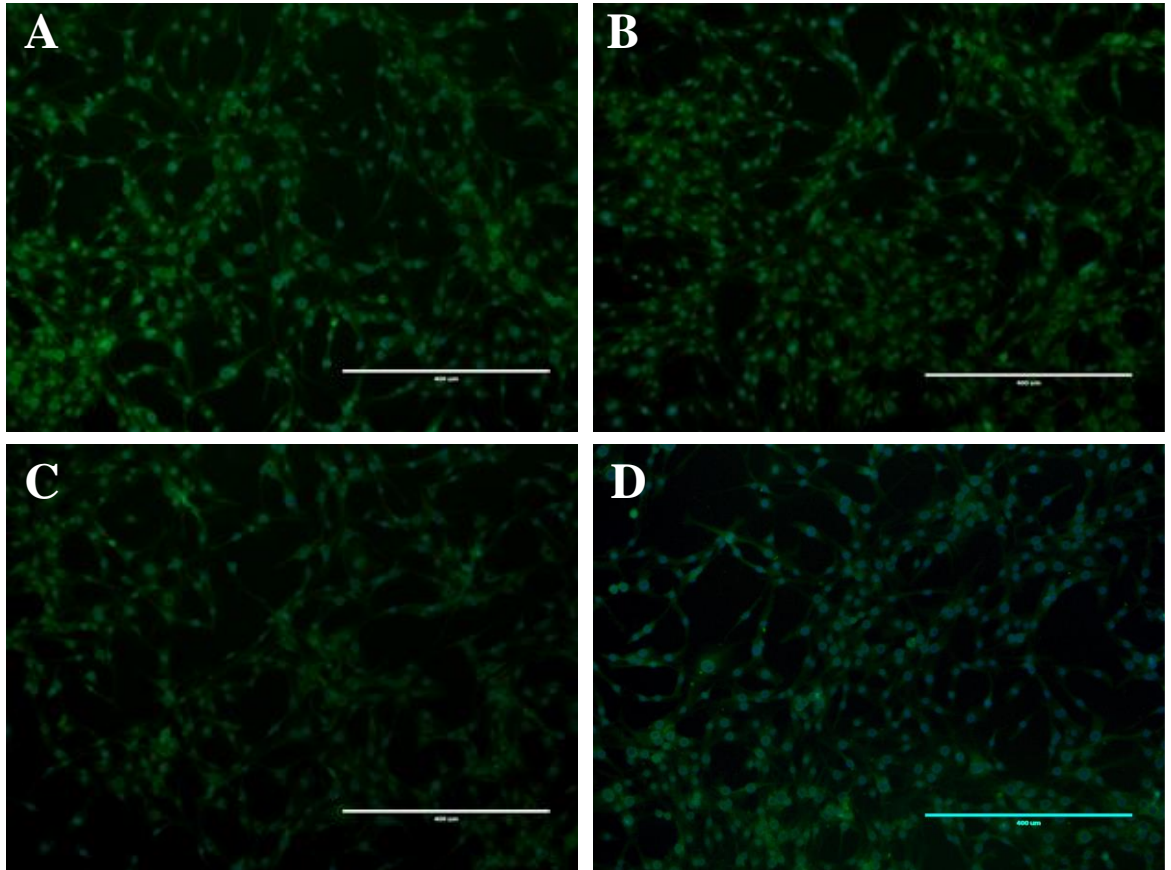


Figure 3.18. Indirect immunofluorescence of CPF effects on anti-GFAP staining differentiating C6 cells as detected by EVOS cell imaging system.

Shown are representative images of immunofluorescently stained with anti-GFAP (GA5). Cells were induced to differentiate for 24 h in the presence of 1 μM (panel B), 3 μM (panel C) and 10 μM (panel D) or absence (panel A) of CPF for 24 h, then they were fixed and immunofluorescently stained for GFAP as described in Materials and Methods. All Images shown were from a single representative field of view by using an EVOS FL cell imaging system (10x objective) with two channels; FITC for detecting cell bodies and neurites and DAPI for nucleus counting. Scale bar 400 μm .

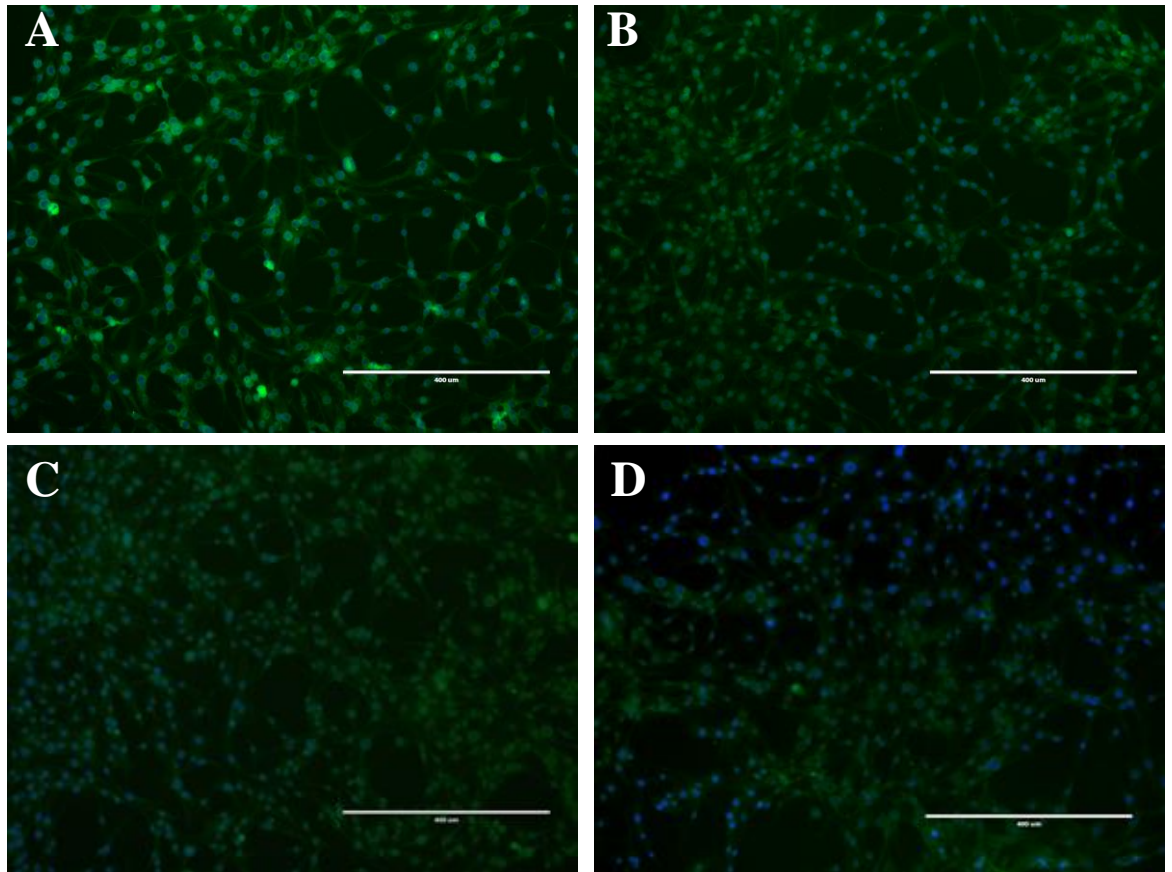


Figure 3.19. Indirect immunofluorescence of CPO effects on anti-GFAP staining differentiating C6 cells as detected by EVOS cell imaging system.

Shown are representative images of immunofluorescently stained with anti-GFAP (GA5) . Cells were induced to differentiate for 24 h in the presence of 1 μ M (panel B) ,3 μ M (panel C) and 10 μ M (panel D) or absence (panel A) of CPF for 24 h, then they were fixed and immunoflourescently stained for GFAP as described in Materials and Methods. All Images shown were from a single representative field of view by using an EVOS FL cell imaging system (10x objective) with two channels; FITC for detecting cell bodies and neurites and DAPI for nucleus counting. Scale bar 400 μ m.

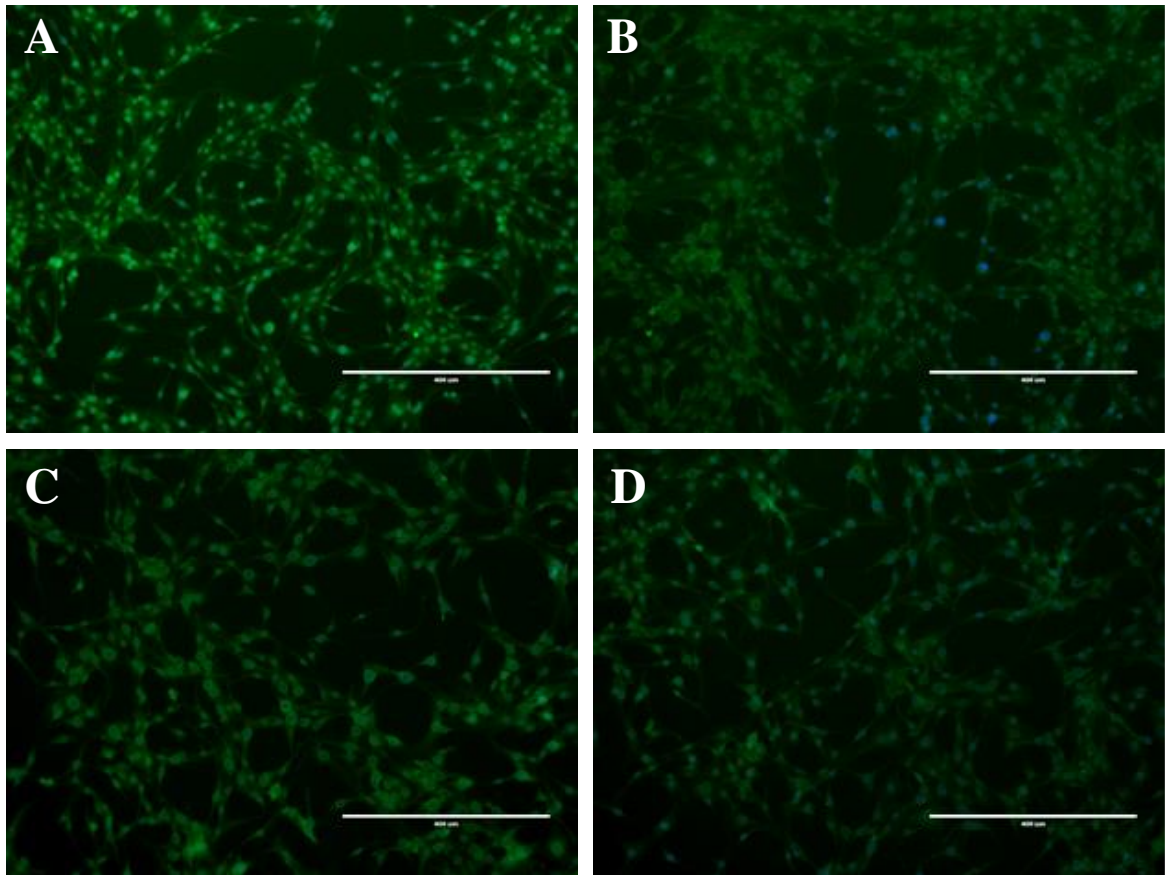


Figure 3. 20. Indirect immunofluorescence of PSP effects on anti-GFAP staining differentiating C6 cells as detected by EVOS cell imaging system.

Shown are representative images of immunofluorescently stained with anti-GFAP (GA5) . Cells were induced to differentiate for 24 h in the presence of 1 μ M (panel B) ,3 μ M (panel C) and 10 μ M (panel D) or absence (panel A) of CPF for 24 h, then they were fixed and immunoflourescently stained for GFAP as described in Materials and Methods. All Images shown were from a single representative field of view by using an EVOS FL cell imaging system (10x objective) with two channels; FITC for detecting cell bodies and neurites and DAPI for nucleus counting. Scale bar 400 μ m.

3.11 Discussion

There is a large amount of evidence highlighting the risks of OP exposure, which has led to restrictions being put in place over their use. However, CPF is still one of the most commonly used insecticides, especially in developing countries (Minton and Murray, 1988; Murray *et al.*, 2005; Coronado *et al.*, 2006; Salyha, 2010).

The current study investigated the effects of sub lethal concentrations (1, 3 and 10 μM), confirmed by MTT reduction and Trypan blue exclusion assays, of CPF, CPO or PSP on neurite outgrowth in differentiating N2a and C6 cells in order to extend findings from previous studies and allow the development of a high throughput screening system to study changes in neurite outgrowth much more comprehensively. The morphological effects of OPs on axon-like neurites were investigated initially by staining cells with Coomassie Brilliant Blue and manual quantification, then by developing a fully automated, HTS system to measure multiple parameters of neurite outgrowth in cells that were fixed and stained by indirect immunofluorescence with antibodies against NFH (clone SMI33) and β III tubulin (clone 2G10) in N2a cells, and in C6 cells stained with the monoclonal antibody to GFAP (clone GA5).

The results of the MTT assays showed that in N2a and C6 cells there was no significant decrease in MTT reduction after 24 h treatment with all 3 compounds. This finding fits well with previous MTT reduction studies in N2a and C6 cells, which have shown that concentrations of 1-10 μM CPF and CPO had no effect over 24 h, (Sachana *et al.*, 2008; Flaskos *et al.*, 2011). The PSP results in this study match the findings of previous investigations, which found higher concentrations of PSP inhibited the reduction of MTT in cultured N2a cells, but concentrations up to 10 μM had no effect (Hargreaves *et al.*, 2006; Harris *et al.*, 2009a). Further confirmation that the MTT reduction assay data indicated no effect of 24 h treatments on cell viability was obtained by Trypan blue exclusion assay using an automated cell counter to assess the effect of CPF, CPO and PSP on cell number and viability of differentiating N2a and C6 cells. Overall, the MTT and Trypan blue exclusion data suggest that the 1-10 μM OP concentration range is suitable to investigate sub-lethal effects on neurite outgrowth in N2a and C6 cells if used in combination with a 24 h time point.

The initial investigation into changes in morphology used Coomassie Brilliant Blue staining to allow the cell features of neurite outgrowth to be monitored. The results indicated that all 3 OPs could inhibit neurite outgrowth in both cell lines. These results

correlate with previous studies in C6 glioma cells that were exposed to sub-cytotoxic (1-10 μM) doses of CPF and CPO (Sachana *et al.*, 2008), studies in differentiating N2a cells that were exposure to sub-cytotoxic levels of CPF (Sachana *et al.*, 2001), and studies of differentiating neuroblastoma N2a cells exposed to PSP, which all produced inhibited neurite outgrowth (Hargreaves *et al.*, 2006; Flaskos *et al.*, 2007; Pomeroy-Black and Ehrich, 2012). These results suggest that this manual counting method is suitable for measuring changes in the parameters investigated, and confirmed that the OP treatments used do cause changes in neurite outgrowth. However, the application of this technique is limited in the detail it provides, and it is also time consuming and labour intensive.

In order to overcome the limitations of the manual counting method, a HTS approach using advanced technology was investigated, which is considered to be a novel and more powerful approach to determine the effects of OPs on differentiating mammalian cell lines. Previous studies have shown that high throughput assays can be used to compare the effects of different chemicals on neurite outgrowth in different cellular models of neural differentiation under a range of exposure conditions (Radio *et al.*, 2008; Mundy *et al.*, 2010; Radio *et al.*, 2010; Harrill and Mundy, 2011; Wilson *et al.*, 2014; Sindi, 2015).

A HTS approach used in a previous study with pre-differentiated N2a cells that were treated with or without 1, 3 and 10 μM CPF and CPO. Cells were then fixed and stained by indirect immunofluorescence with antibodies against NFH, βIII tubulin, and GFAP. Anti- βIII tubulin was chosen to stain microtubules in cell bodies, dendrites and axons anti-NFH was chosen to stain neurofilaments in axons of neuronal cells, and anti-GFAP was selected for use in C6 cells as it is an astro-glial marker (Sindi, 2015). The results for the indirect immunofluorescence staining showed good staining for all the antibodies and qualitative differences could be seen after some of the treatments, suggesting these were suitable markers for use in this study. By using the HTS system, multiple parameters of neurite outgrowth could be measured. The results for both cell types showed that the treatments had no significant effect on cell number, and only 10 μM CPO reduced cell body area in C6 cells stained for GFAP in agreement with metabolic and viability assays, and further confirming that the treatments did not cause cell death. The results agree with previous HTS studies which also showed no major changes to the number cells or cell body area at sub lethal concentrations. The reductions in staining intensity observed for anti- βIII tubulin and anti-NFH after treatment with 10 μM of all OPs, 3 μM PSP for anti-NFH, and all concentrations of PSP for anti-GFAP, suggest that the OPs, and especially PSP, are having

an effect on these protein levels and that this could be related to reduced neurite length, which is different to the results of previous studies where no changes in staining intensity were observed for these cell types, which is possibly due to the difference in exposure time between these studies, and the fact that they used different exposure starting points, as this study used a longer exposure time which would allow the differences on staining intensity to develop (Sindi, 2015).

For the N2a cells, the reductions observed by HTS in neurite length and neurite number per cell and the percentage of cells bearing neurites suggest that treatment with all 3 OPs inhibits neuronal cell differentiation as indicated by reductions the outgrowth of neurites that are positive for anti- β III tubulin and anti-NFH in a concentration dependent manner. For the C6 cells stained for GFAP, HTS analysis of differentiating C6 cells showed that the 3 OPs were also able to inhibit neurite outgrowth in glial cell differentiation, as indicated by concentration dependent reductions in the percentage of cells bearing neurites, the average number of neurites per cell and neurite length.

These results are in agreement with those found by Coomassie Brilliant Blue staining, and both approaches show impairment of neurite outgrowth due to treatment with the higher concentrations of all three OPs used. The HTS data also show that all of the OPs tested inhibited the formation of neurite extensions in neuronal and glial cells, which agree with previous studies that have shown outgrowth impairment in N2a cells after treatment at the point of induction with 3 μ M CPF (Sachana *et al.*, 2001; Sachana *et al.*, 2005), a similar concentration dependent response after treatment with CPO for 24 h (Flaskos *et al.*, 2011) and after treatment with PSP, with no significant effect on cell shape (Hargreaves *et al.*, 2006; Flaskos *et al.*, 2006). The results also agree with previous studies in glial cells which found an inhibitory effect on extension outgrowth of 24 h exposure to 1-10 μ M CPF and CPO in C6 cells (Sachana *et al.*, 2008).

Overall, the results correlate with the findings of previous studies that have shown that in differentiating neuronal cells, reduced neurite outgrowth is associated with neuronal degeneration and modification of axonal morphology, which are critical events in the development of OPIDN (Flaskos *et al.*, 1994; Ehrich and Jortner, 2001; Hargreaves *et al.*, 2006).

On the other hand, CPO caused the largest significant differences for some conditions, with the largest reduction in % cells with significant outgrowth for anti-NFH; the reduction

in maximum neurite length/cell was higher for CPO than PSP for NFH and CPO produced a similar response for NFH average neurite length/cell as PSP. The impairment of neurite outgrowth followed a similar pattern for anti-GFAP after treatment of C6 cells with CPO and CPF for maximum neurite length/cell; GFAP average neurite length/cell was affected more by CPO than PSP. These significant effects of CPO are mainly seen for anti-NFH and anti-GFAP staining, which suggests CPO exhibits potent effects on axon-like neurites and glial extensions more than cell bodies and dendrites, which is in agreement with previous studies which have shown CPO was more potent than CPF following 24 h exposure in pre-differentiated rat PC12 pheochromocytoma cells, and in differentiating N2a cells, causing inhibited neurite outgrowth, and a reduction in axonal length in embryonic derived primary cultures of sensory and sympathetic neurons (Das and Barone, 1999; Howard *et al.*, 2005; Yang *et al.*, 2008).

These results are also consistent with studies showing that CPO exposure can cause a reduction in NFH levels *in vitro* (Sidiropoulou *et al.*, 2009b; Flaskos *et al.*, 2011), that CPO can bind covalently to tubulin and disrupt polymerisation of bovine brain MT *in vitro* (Grigoryan and Lockridge, 2009), and disrupt the neurofilament network after 24 h treatment with non-cytotoxic neurite inhibitory concentrations of CPO (Flaskos *et al.*, 2011). The morphological changes observed after treatment with CPO occur at similar concentrations found *in vivo* in developing humans (Gupta, 1995; Ostrea *et al.*, 2002; Pelkonen *et al.*, 2006) and therefore can be linked to the developmental neurotoxicity observed (Bramanti *et al.*, 2010; Liu *et al.*, 2012).

The reduction in the staining intensity for β III tubulin and NFH after treatment with CPF, CPO and PSP could indicate a reduction in the protein levels of the neuron specific β III tubulin isoform and the axon enriched protein NFH, and changes, or a breakdown, in the NF networks, which would result in reduced axon stability (Sindi, 2015). The effects on neurite length depend on the OP and concentration used, which can easily be measured the sensitive high throughput assay, and these axon extensions play a key role in connecting single and multiple neurons (Hjorth *et al.*, 2014).

In summary, the data from this chapter show that sub-lethal concentrations of CPF, CPO and PSP impaired the outgrowth of neurites in differentiating N2a and C6 cells. The data also demonstrate that HTS was able to detect and quantify multiple changes in neurite outgrowth caused by the different OPs, and allowed a rapid analysis overcoming some of the disadvantages of manual methods, and validated the previous results obtained by the

Coomassie method both in this chapter and in other previous studies (Sachana *et al.*, 2001; Sachana *et al.*, 2005; Hargreaves *et al.*, 2006; Flaskos *et al.*, 2011). The results of this assay show there are inhibitory effects of all OPs on neurite number and length for the different markers measured, with each OP producing a slightly different pattern of effects. Based on the results of the studies presented in this chapter, further investigations into how CPF, CPO and PSP affected neurite outgrowth were planned. This included quantitative analysis of protein levels for a selection of key cytoskeletal and associated regulatory proteins MAP-2, β III tubulin, Tau, GAP-43, NFH and GFAP, which would be analysed for changes in the levels of expression in N2a and C6 cell lines differentiated with or without 1, 3 and 10 μ M of CPF, CPO or PSP by Western blotting analysis. The aims of this further study are to investigate how changes in expression of these key proteins are related to the morphological changes observed in this chapter, to help to elucidate the method of action of these OPs.

Chapter 4

**Effects of Organophosphates on
Cytoskeletal and Associated Regulatory
Proteins in Differentiating N2a
Neuroblastoma and C6 glial Cells**

4.1 Introduction

Having observed from the previous chapter, that changes in morphology of the two cell lines occurred as a result of exposure to sub-cytotoxic concentrations (1, 3 and 10 μM) of CPF, CPO and PSP, it was hypothesised that this might involve changes in the levels of cytoskeletal and associated regulatory proteins in rodent neural cell lines.

The neuronal cytoskeleton, particularly microtubules (MTs) and neurofilaments (NFs), is one of the most important endogenous factors that control normal neurodevelopment and stability including the process of axonal/neurite outgrowth (Cambray-Deakin, 1991). Disruption of the axonal cytoskeleton by OPs has often been associated with changes in neuronal cell morphology, particularly in cases of toxic neuropathies in which NFH which is one of the potential targets of OPs (Lee and Cleveland, 1994).

Impairment of neurite outgrowth following exposure to OPs has been linked with disruption of the expression levels of cytoskeletal proteins (Flaskos *et al.*, 1998; Sachana *et al.*, 2001; Sachana *et al.*, 2003; Sachana *et al.*, 2005; Hargreaves *et al.*, 2006; Flaskos *et al.*, 2007; Flaskos *et al.*, 2011; Sachana *et al.*, 2014; Sindi *et al.*, 2016).

Earlier reports evaluated the effects of CPF on a number of cytoskeletal and associated regulatory proteins in N2a cells under different differentiation and exposure conditions (Sachana *et al.*, 2001; Sachana *et al.*, 2005). Furthermore, the mechanisms underlying the ability of certain OPs to cause axon retraction and to inhibit axon outgrowth have been associated with some axon growth-associated proteins such as GAP-43, which is important in the regulation of axonal outgrowth and/or stabilization (Meiri *et al.*, 1986; 1998; Knoops and Octave, 1997).

Sachana and colleagues (2005) showed reduced levels of GAP-43 in pre-differentiated N2a cells that were subsequently treated with CPF. However, exposure of N2a cells to CPF for 4h at the point of induction of cell differentiation had no impact on GAP-43 expression (Sachana *et al.*, 2005). The findings of these previous studies suggest that the effects of CPF on the protein depend on the differentiation stage of the cells when exposure occurs. In another study, exposure of N2a cells at the point of induction of differentiation to 1-10 μM CPO caused reduced levels of GAP-43 and NF-H after 24 h (Flaskos *et al.*, 2011).

Exposure to 10 μM diazoxon and after differentiation for 24 h (DZO) decreased the expression of β III-tubulin and microtubule associated protein 1B (MAP1B) in

differentiating N2a cells. However, DZO had no effect on the expression of the microtubule associated protein Tau, NFL or NFM at the protein level. Thus, DZO disrupts the microtubule (MT) network affecting the expression and distribution of two specific MT proteins known to be important in neurite outgrowth (Sachana *et al.*, 2014). However, the effects of CPF, CPO and PSP on the levels of MAPs in N2a cells are not known.

There is a lack of quantitative data in the case of PSP treatment of C6 cells, as in early work it was suggested that PSP had no effect on C6 cell differentiation, as measured by neurite (extension) number (Fowler *et al.*, 2001). Given that the original data were preliminary and only involved a simple morphological assessment of Coomassie blue stained cells (i.e. a total count of extensions irrespective of length), further studies could be worthwhile. Moreover, the effects of PSP on cytoskeletal proteins in C6 cells have not been determined yet (Sachana *et al.*, 2001; 2005; 2008; 2014; Harris *et al.*, 2009a).

It was observed in a recent study that the levels of phosphorylated NFH (detected by the monoclonal antibody Ta51) were reduced significantly after 8 h exposure of pre-differentiated N2a cells to CPF and CPO, which corresponded to a collapse of the neurofilament network (Sindi *et al.*, 2016). Likewise, CPF and CPO can exert toxic effects directly on glial cell differentiation through disruption of the cytoskeleton and its associated proteins, and CPO in particular has a potent effect on the microtubule network (Sachana *et al.*, 2008). CPO was found to cause significant decreases in the levels of tubulin and MAP-1B in differentiating C6 cells after 24 h exposure by western blot analysis (Sachana *et al.*, 2008).

Inhibition of outgrowth of axon-like processes in differentiating N2a cells has been associated with exposure to sub-lethal concentrations of PSP (Hargreaves *et al.*, 2006). These morphological changes were associated with altered phosphorylation and levels of NFH protein detected on Western blots. Exposure of differentiating N2a cells to 2.5 μ M PSP increased the phosphorylation of NFH after 4 h as indicated by a relative increase in reactivity of the lysates with monoclonal antibody Ta51 (which recognises the phosphorylated form of NFH) compared to N52 (total NFH). However, 24 h exposure of differentiating N2a cells to the same compound resulted in decreases in both total and phosphorylated forms of NFH (Hargreaves *et al.*, 2006). Thus, there is clear evidence for cytoskeletal effects of the three OPs used in the current study on N2a cells but little data regarding molecular effects of PSP on cultured glial cells. As the current work is focussed on the cytoskeletal gene expression changes that might be associated with exposure to the

OPs it was important to show that known OP-induced protein changes could be reproduced in the N2a cells and to determine whether novel protein changes could be detected particularly in PSP-treated C6 cells.

4.2 Aims

Since a number of MT, NF and associated regulatory proteins are important in neurodevelopment and may be involved in neurite outgrowth and stability, a key aim of the work presented in this chapter was to examine the effects of CPF, CPO and PSP on the levels of expression of cytoskeletal and associated regulatory proteins involved in neural cell differentiation and survival in differentiating mouse N2a neuroblastoma cells and C6 glioma cells.

The molecular changes underlining the morphological effects of OPs on neurite outgrowth in N2a and C6 cell lines differentiated in the absence and presence of CPF, CPO and PSP (during differentiation) were studied by quantitative Western blotting. For immunoblotting, Western blots of lysates of N2a and C6 cells induced to differentiate in the absence and presence (1, 3 and 10 μ M) of CPF, CPO or PSP for 24 h were probed with antibodies against a range of proteins, including MAP-2, β III tubulin, Tau, GAP-43, NFH and GFAP, as described in section 2.2.13 and table 2.9.

4.3 Effects of CPF, CPO and PSP on the expression level of GAPDH in N2a and C6 cell lines

GAPDH levels were quantified by Western blot analysis. Western blots of lysates prepared from N2a and C6 cells differentiated in the presence (1, 3 and 10) μ M of CPF, CPO or PSP for 24 h were probed with antibodies against GAPDH, after which reactivity was detected using ECL reagent and was quantified densitometrically as described in Materials and Methods, section 2.2.13.

As indicated in figure 4.1 and table 4.1, the reactivity of anti-GAPDH with protein lysates from both cell lines showed no significant changes following exposure of cells to all the OPs and concentrations tested at 24 h. Therefore, the band intensities of all studied proteins were normalised to that for GAPDH in the same sample, which was used as internal control.

Table 4.1. Densitometric analysis of Western blots probed with antibody to GAPDH protein in N2a and C6 cell lines.

Antigen	Toxin (μM)	Densitometric peak (% control \pm SEM)		
		CPF	CPO	PSP
GAPDH of N2a cells	1	90 \pm 2	84 \pm 4	93 \pm 3
	3	103 \pm 7	86 \pm 13	92 \pm 4
	10	103 \pm 13	102 \pm 16	96 \pm 4
GAPDH of C6 cells	1	105 \pm 2	101 \pm 7	99 \pm 2
	3	104 \pm 3	98 \pm 10	100 \pm 6
	10	105 \pm 8	99 \pm 4	97 \pm 8

Western blots of cell lysates from N2a and C6 cells induced to differentiate in the absence and presence of CPF, CPO and PSP at the concentrations indicated, were probed with antibodies that recognise GAPDH. The antibody reactivity was then visualized with ECL reagents as described in Materials and Methods. Densitometric peak areas were quantified using AIDA software. Data represent means of four separate experiments and values are expressed as a percentage of corresponding non OP-treated control \pm SEM.

4.4 Effects of CPF, CPO and PSP on the expression levels of microtubule proteins in differentiating N2a cells

In order to determine the effects of OPs on the expression levels of microtubule proteins, Western blots of lysates prepared from cells differentiated in the absence and presence of 1, 3 and 10 μM of CPF, CPO or PSP for 24 h were probed with antibodies against a range of MT proteins which included MAP2, β III-tubulin and Tau as described in chapter 2. Changes were observed in the levels of antibody reactivity on Western blots of cell lysates from cell lines treated with OPs compared to the controls (Figures 4.1 and Table 4.2).

The three OP treatments showed significant effects on reactivity of lysates with anti-MAP2, which decreased significantly after exposure to 3 μM CPF ($p < 0.05$) and 10 μM CPF, CPO and PSP ($p < 0.05$). However, there was no statistically significant effect on the reactivity with same antibody in cell lysates for 1 μM CPF, 1 μM and 3 μM CPO and PSP.

Similarly, all OP treatments also showed significant effects on reactivity of lysates with anti- β III tubulin, which decreased significantly after exposure to 10 μM CPF ($p < 0.05$), CPO ($p < 0.05$) and PSP ($p < 0.01$).

Antibody cross reactivity of anti-Tau with whole cell lysate was significantly reduced after 24 h exposure to 3 and 10 μM concentrations of both CPF ($p < 0.01$) and PSP ($p < 0.05$) of 3 μM and ($p < 0.01$) of 10 μM . However, there was no statistically significant effect on reactivity with anti-tau in cells for any of the CPO concentrations tested.

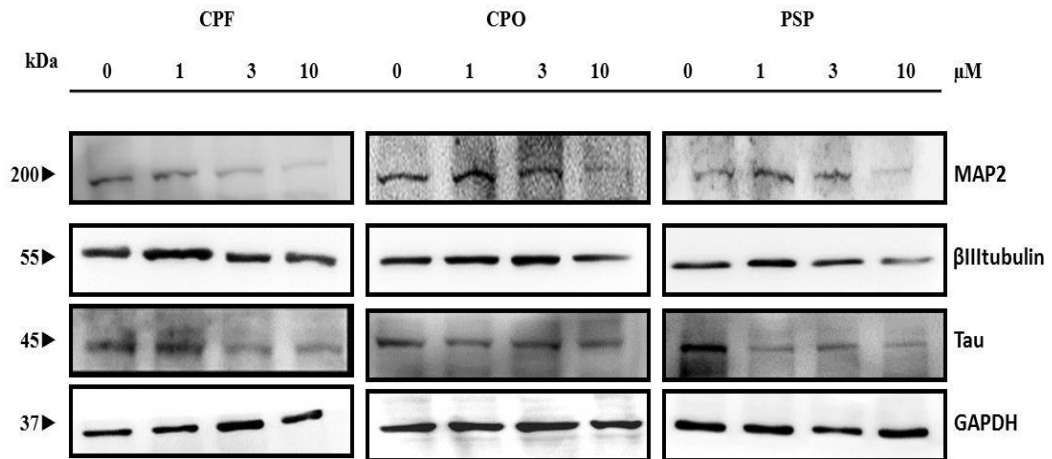


Figure 4.1. Detection of microtubule proteins by Western blots of differentiating N2a cell lysates.

N2a cells were induced to differentiate for 24 h with the treatment of (0, 1, 3, 10 μM) of CPF, CPO, PSP or without OP (Control 0 μM). Equal amounts of N2a cell lysates were loaded in SDS-PAGE and Western blotting as mentioned in the Material and Methods chapter. Shown are typical blots which probed with antibodies against MAP-2, β III tubulin and Tau followed by HRP-conjugated secondary antibodies and developed by ECL reagents. Blots probed with GAPDH were used as internal control.

Table 4.2. Densitometric analysis of Western blots probed with antibodies to microtubule proteins in N2a cell lines.

Antigen	Toxin (μM)	Densitometric peak (% control \pm SEM)		
		CPF	CPO	PSP
MAP-2	1	101 \pm 1	100 \pm 2	91 \pm 3
	3	75 \pm 6*	87 \pm 15	84 \pm 7
	10	69 \pm 7*	64 \pm 11*	72 \pm 6*
β III-tubulin	1	102 \pm 1	104 \pm 1	96 \pm 2
	3	90 \pm 5	76 \pm 17	89 \pm 3
	10	74 \pm 13*	64 \pm 12*	50 \pm 6**
Tau	1	85 \pm 3	101 \pm 1	95 \pm 1
	3	59 \pm 10**	100 \pm 1	78 \pm 9*
	10	35 \pm 4**	94 \pm 4	68 \pm 9**

Western blots of lysates from differentiating N2a cells were probed with antibodies that recognise MAP-2, β III-tubulin and Tau. The antibody reactivity was then visualized with ECL reagents as described in Materials and methods and densitometric peak areas were quantified using AIDA software. Data represent means of four separate experiments and values are expressed as a percentage of the corresponding control (band densities for all proteins were normalised to blots probed with GAPDH) \pm SEM; *P<0.05, **P<0.01, asterisks indicate significant differences compared to the corresponding untreated control.

4.5 Effects of CPF, CPO and PSP on the expression levels of neurofilament and growth associated proteins in N2a cells

To examine possible effects of the OP treatments on the levels of axonal intermediate filament and growth associated proteins in N2a cells, the immunoreactivity of antibodies with GAP43 and the core neurofilament forming protein NFH was quantified by Western blotting analysis.

For immunoblotting, Western blots of lysates prepared from cells induced to differentiate for 24 h in the absence and presence (1, 3 and 10 μM) of CPF, CPO or PSP were probed with antibodies against NFH and GAP43.

As indicated on figure 4.2 and table 4.3, there were no significant effects on the cross reactivity with the antibody that recognised NFH of lysates from differentiating N2a cells exposed to 1 μ M CPF, CPO or PSP for 24 h compared to control. However, probed Western blots of N2a cell lysates showed a significant decrease after exposure to 3 μ M CPF ($p<0.01$) and to 3 μ M PSP ($p<0.05$), while the decrease was high significant after exposure to 10 μ M CPF, CPO or PSP ($p<0.01$).

Similarly, GAP43 reactivity was unaffected following exposure to 1 μ M CPF, 1 μ M and 3 μ M CPO and PSP. However, probed Western blots of N2a cell lysates showed a significant decrease in antibody reactivity with GAP43 on exposure to 3 μ M CPF ($p<0.05$) and after exposure to 10 μ M CPF, CPO and PSP ($p<0.01$).

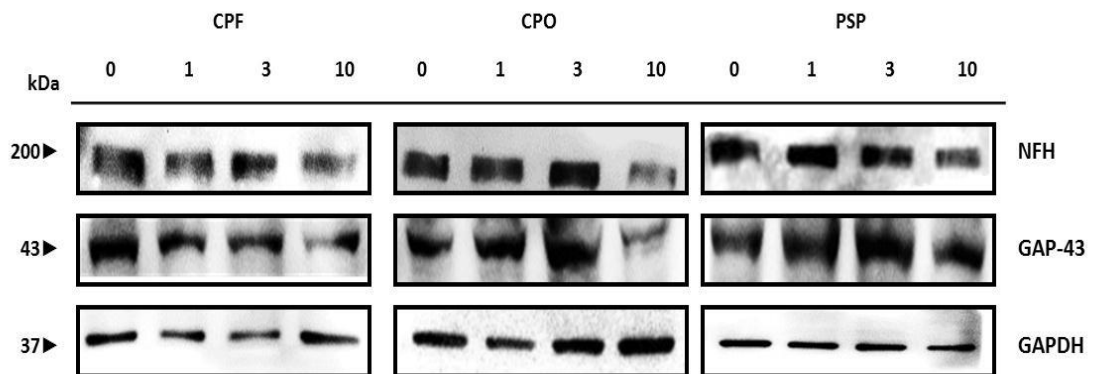


Figure 4.2. Detection of neurofilament and growth associated proteins by Western blots of differentiating N2a cell lysates.

N2a cells were differentiated for 24 h in the absence (0) and presence of 1, 3 and 10 μ M CPF, CPO or PSP. N2a cell lysates were separated by SDS-PAGE and Western blotting as explained in Material and Methods. Shown are typical blots which were probed with antibodies against NFH and GAP-43 followed by HRP-conjugated secondary antibodies and developed by ECL reagents. Blots probed with anti-GAPDH were used as internal control.

Table 4.3. Densitometric analysis of Western blots probed with antibodies to neurofilament and growth associated proteins in N2a cell lysates.

Antigen	Toxin (μM)	Densitometric peak (% control \pm SEM)		
		CPF	CPO	PSP
NFH	1	77 \pm 15	90 \pm 13	89 \pm 3
	3	48 \pm 2**	87 \pm 7	73 \pm 3*
	10	23 \pm 5**	38 \pm 4**	7 \pm 1**
GAP-43	1	96 \pm 12	99 \pm 3	89 \pm 9
	3	65 \pm 5*	86 \pm 11	88 \pm 7
	10	39 \pm 15**	45 \pm 16**	62 \pm 9**

Western blots probed with antibodies that recognise NFH and GAP43. The antibody reactivity was visualized with ECL reagents as described in Materials and Methods and densitometric peak areas were quantified using AIDA software. Data represent means of four independent experiments and values are expressed as a percentage of the corresponding non OP treated control (band densities for all proteins were normalised to blots probed with GAPDH) \pm SEM.; *P<0.05, **P<0.01, asterisks indicate significant differences compared to the corresponding untreated control.

4.6 Effects of CPF, CPO and PSP on the expression levels of glial fibrillary acid protein in C6 cells

To examine possible effects of the OP treatments on the levels of cytoskeletal in C6 cells, the immunoreactivity of antibodies with the core astrocyte intermediate filament forming protein GFAP was quantified by Western blot analysis. Interestingly, the cross reactivity of C6 cell lysates with anti GFAP antibody was significantly reduced after exposure to 10 μ M CPF, CPO and PSP ($p < 0.01$) and after exposure to 3 and 10 μ M of both CPO ($p < 0.01$) and PSP ($p < 0.05$) (Table 4.4). In addition, cross reactivity of cell lysates with anti GFAP antibody was unaffected by 1 and 3 μ M CPF and 1 μ M CPO and PSP (Figure 4.3 and Table 4.4).

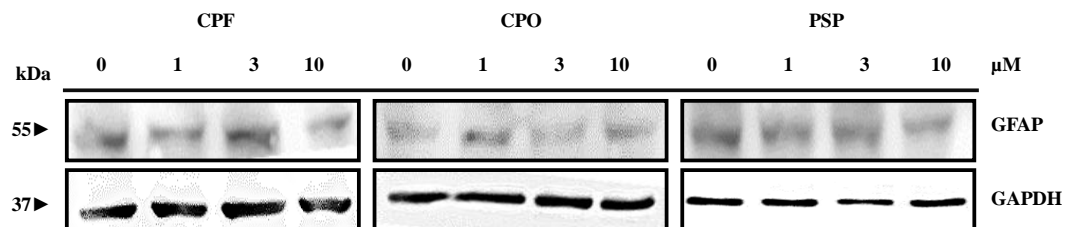


Figure 4.3. Detection of Glial fibrillary acidic protein by Western blots of differentiating C6 cell lysates.

C6 cells were differentiated for 24 h in the absence (0) and presence of 1, 3, 10 μ M of CPF, CPO, PSP. C6 cell lysates were separated by SDS-PAGE and Western blotting as explained in Chapter 2. Shown are typical blots, which were probed with antibodies against GFAP followed by HRP-conjugated secondary antibodies and developed by ECL reagents. Blots probed with anti-GAPDH were used as internal control.

Table 4.4. Densitometric analysis of Western blots probed with antibodies to glial fibrillary acid protein (GFAP) in C6 cells.

Antigen	Toxin (μM)	Densitometric peak (% control \pm SEM)		
		CPF	CPO	PSP
GFAP	1	103 \pm 1	100 \pm 3	87 \pm 1
	3	91 \pm 4	61 \pm 9**	72 \pm 4*
	10	39 \pm 4**	23 \pm 8**	51 \pm 7**

Western blots were probed with antibodies that recognise GFAP. The antibody reactivity was then visualized with ECL reagents as described in Materials and Methods and densitometric peak areas were quantified using AIDA software. Data represent means of four separate experiments and values are expressed as a percentage of the corresponding non OP treated control (band densities for all proteins were normalised to blots probed with anti GAPDH) \pm SEM.; *P<0.05, **P<0.01, asterisks indicate significant differences compared to the corresponding untreated control.

4.7 Determination of concentration-response effects of CPF, CPO and PSP on cytoskeletal and associated regulatory proteins using cell ELISA

The effects of multiple concentrations of CPF, CPO and PSP on cytoskeletal and associated regulatory proteins associated with their regulation in neurite outgrowth were further assessed in differentiating N2a and C6 cells using a cell ELISA technique, which could potentially facilitate rapid quantification. Cells were induced to differentiate in the absence (0) or presence of 1, 3 and 10 μM CPF, CPO and PSP as described in Materials and Methods. The differentiating cell monolayers were then fixed and changes in the binding levels of monoclonal antibodies against MAP-2, βIII tubulin, Tau, NFH, GAP-43 and GFAP were determined and quantified in controls and OP-treated cells following 24 h exposure, as described in section 2.2.14.

Figure 4.4 (panels A1 and A2) shows data from cell ELISA using a monoclonal antibody that recognises MAP-2. In figure 4.4 (panel A1), a dose-dependent decrease was seen in the level of MAP-2 binding in differentiating N2a cells treated with both CPF and CPO for 24 h. The decline in MAP-2 level was statistically significant at 3 μM of CPF and CPO ($p < 0.05$) and ($p < 0.01$) at 10 μM of CPF and CPO compared to that of non OP-treated controls. After 24 h treatment of differentiating N2a cells with all concentrations of PSP, there was a progressive reduction in the binding level of anti MAP-2 when compared to controls; however, the observed changes were not statistically significant (Figure 4.4, panel A2).

Quantification of anti- βIII tubulin cross reactivity by cell ELISA in differentiating N2a cells also showed a progressive reduction but this effect was not statistically significant for either CPF or CPO at the concentrations tested at 24 h (Figure 4.4, panel B1). However, in panel B2 of figure 4.4, a dose-dependent decrease was seen in the level of βIII tubulin binding in differentiating N2a cells treated with PSP for 24 h. The decline in βIII tubulin level was statistically significant at 10 μM concentration of PSP ($p < 0.05$), $p = 0.03$ compared to that the non OP-treated control (Figure 4.4, panel B2)

However, treatment with all concentrations of CPF and 1 and 3 μM of CPO showed no significant decrease on the binding levels of Tau compared to the untreated controls (Figure 4.4, panel C1). By contrast, in figure 4.4 panel C2, a dose-dependent reduction was observed with statistically significant changes in the level of anti-tau binding at 10 μM concentration of PSP ($p < 0.01$) compared to the non PSP-treated controls.

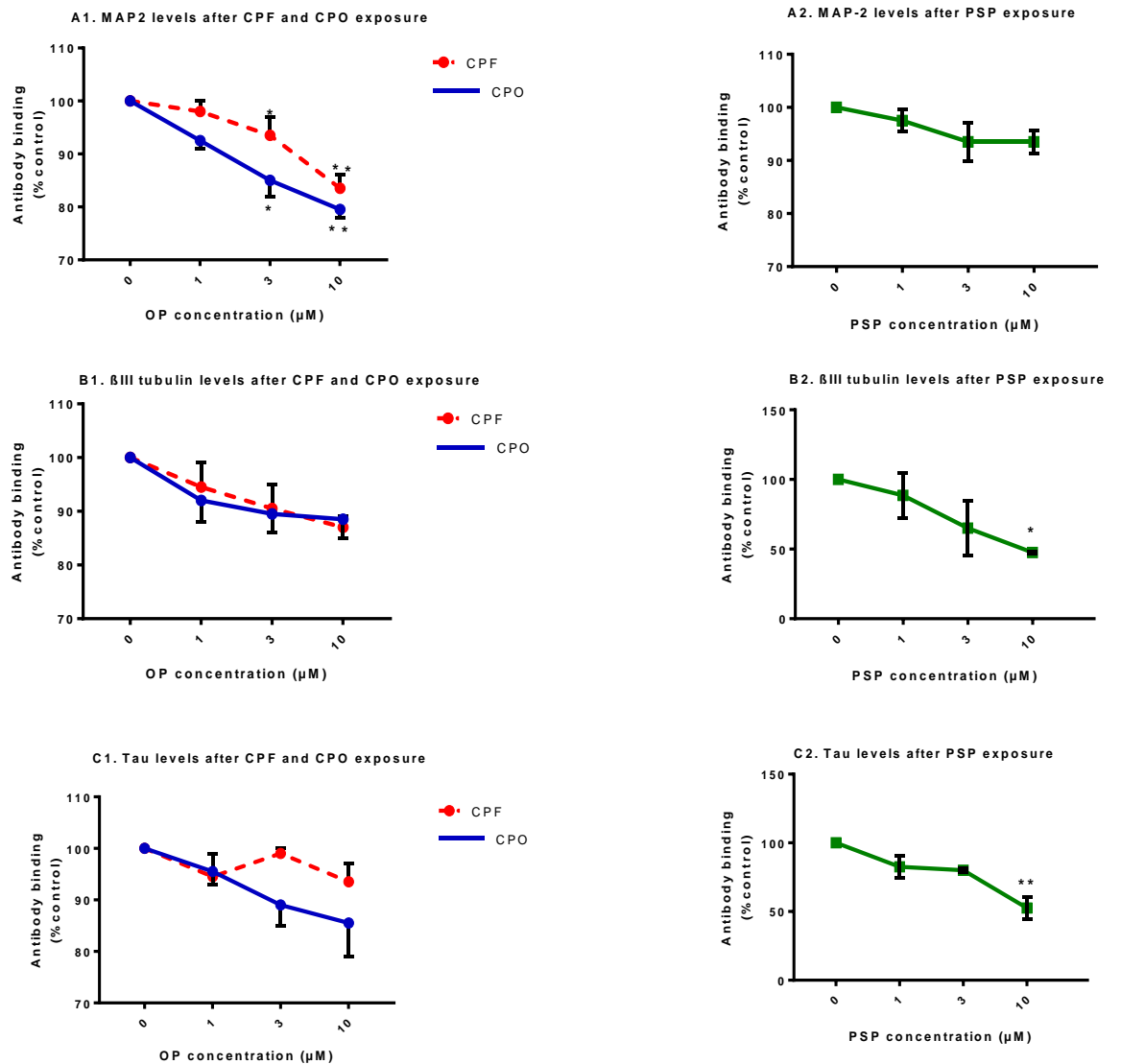


Figure 4.4. Effects of CPF, CPO and PSP on microtubule proteins in differentiating N2a cells as determined by cell ELISA.

N2a cells were induced to differentiate for 24 h either without (0) or with 1, 3 and 10 μM concentrations of CPF, CPO or PSP for 24 h. Changes in the binding levels of antibodies that recognise MAP-2 (panel A), βIII-tubulin (panel B) and Tau (in panel C) were quantified in controls and OP-treated cells using cell ELISA. Data are presented as a percentage of the non OP-treated control ± SEM (from 4 independent experiments). Data were analysed using one-way ANOVA, and Sidak post hoc test. The CPF effects are presented as red dashed lines; the CPO effects are presented as blue solid lines and PSP effects are presented as green solid lines with square symbols. Asterisks indicate changes that are statistically different from the non OP-treated controls (* $p < 0.05$) or (** $p < 0.01$). In cases where SEM bars are not apparent, the error is smaller than the symbol size.

Figure 4.5 (panels A1 and A2) shows dose-dependent decreases in the binding levels of anti-NFH with cell monolayers following the exposure to the three OPs used in the current study. The reduction was statistically significant ($p < 0.01$), $p = 0.001$ after exposure to 10 μM CPF (Figure 4.5, panel A1). After PSP exposure (Figure 4.5, panel A2), treatment of differentiating N2a cells with 1, 3 and 10 μM showed decreases in the binding levels of anti NFH but the changes were not statistically significant.

However, progressive decreases in the binding levels of anti GAP-43 with lysates of differentiating N2a cells following exposure to CPF, CPO and PSP can be observed in panels B1 and B2 of figure 4.5. Interestingly, in the case of CPF the reduction was statistically significant at 1 and 3 μM ($p < 0.05$), $p = 0.02$, and highly significant ($p < 0.01$) at 10 μM . However, the reductions in anti GAP-43 binding observed following CPO and PSP exposure were not statistically significant compared to non OP-treated controls at 24 h (Figure 4.5, panel B2).

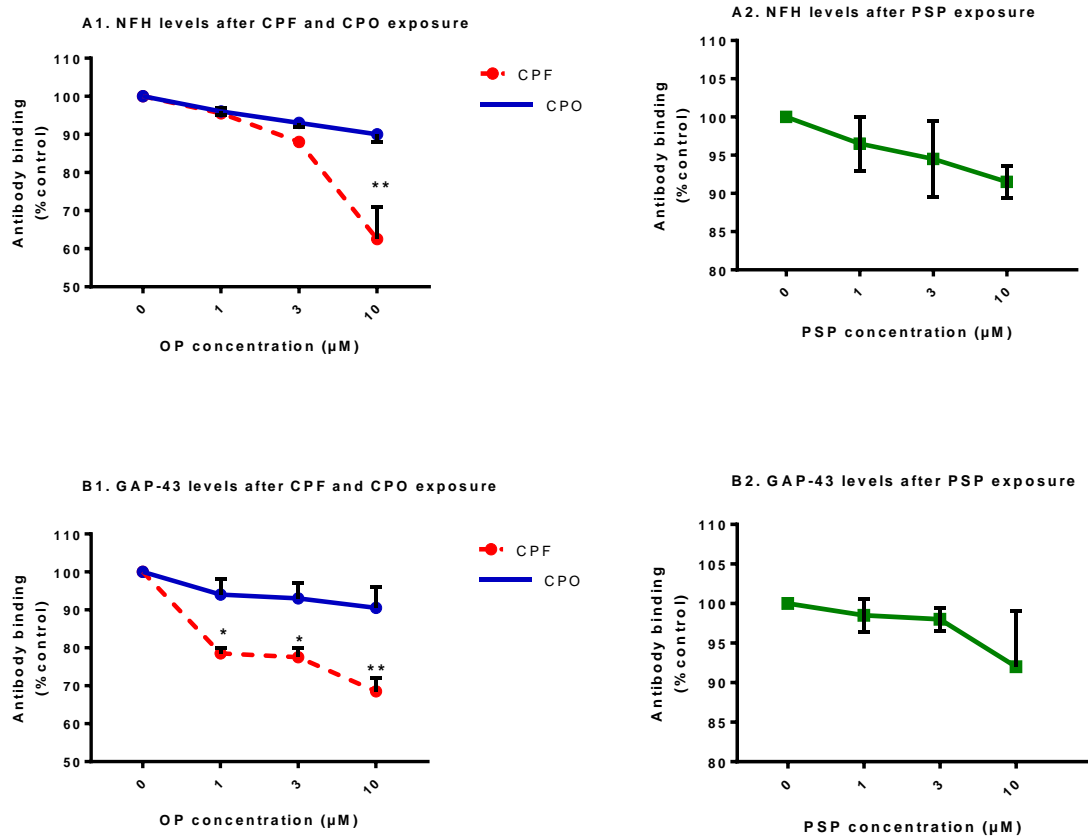


Figure 4.5. Effects of CPF, CPO and PSP on neurofilament and growth associated proteins in differentiating N2a cells as determined by cell ELISA.

N2a cells were induced to differentiate for 24 h either without (0) or with 1, 3 and 10 µM concentrations of CPF, CPO or PSP. Changes in the binding levels of antibodies that recognise NFH (SMI33) (panel A) and GAP-43 (panel B) were quantified in controls and OP-treated cells using cell ELISA. Data are presented as a percentage of the non OP-treated control \pm SEM (from four separate experiments). Data were analysed using one-way ANOVA, and Sidak post hoc test. The CPF effects are presented as red dashed lines; the CPO effects are presented as green solid lines; and PSP effects are presented as green solid lines with squares. Asterisks indicate changes that are statistically different from the non OP-treated controls (* $p < 0.05$) or (** $p < 0.01$). In cases where SEM bars are not apparent the error is smaller than the symbol size.

Since some dose-dependent changes were detected in the levels of binding cytoskeleton proteins in N2a cells, it was of interest to investigate the potential effects of the exposure to CPF, CPO or PSP on GFAP in the C6 glioma cell line used in the current study. Figure 4.6 (panel A) demonstrates the dose-response effects of both CPF and CPO on the levels of anti GFAP which caused similar concentration-dependent decreases, which was statistically significant at 1 μM ($p < 0.05$), 3 μM ($p < 0.05$) and 10 μM ($p < 0.01$) compared to non OP-treated controls. By contrast, compared to the control, no significant effects were detected in anti-GFAP cross reactivity with monolayers of differentiating C6 cells exposed to all 3 concentrations of PSP at 24 h (Figure 4.6, panel B).

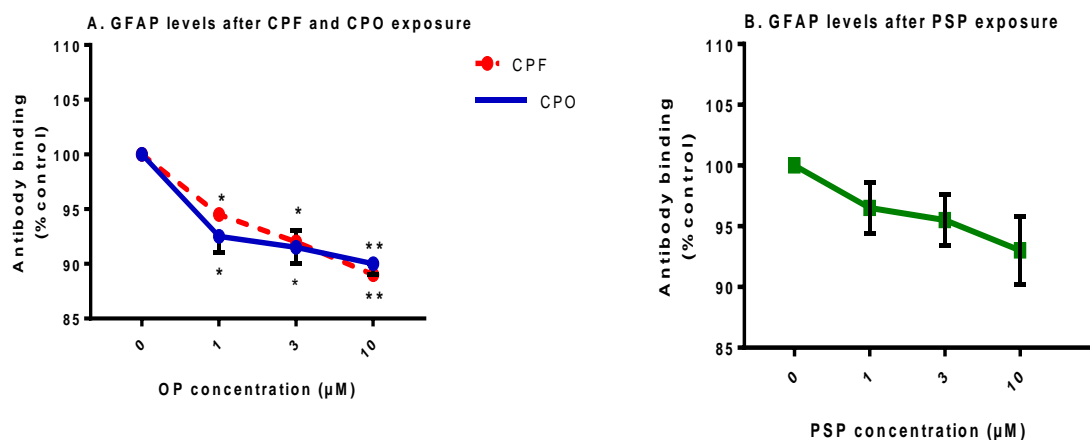


Figure 4.6. Effects of CPF, CPO and PSP on glial fibrillary acidic protein in differentiating N2a cells as determined by cell ELISA.

C6 cells were induced to differentiate for 24 h with incubation without (0) or with 1, 3 and 10 μM concentrations of CPF, CPO (panel A) or PSP (panel B) for 24 h. Changes in the binding levels of antibody that recognise GFAP quantified in controls and OP-treated cells using cell ELISA. Data are presented as a percentage of the non OP-treated control \pm SEM (from four separate experiments). Data were analysed in one-way ANOVA, and Sidak post hoc test. The CPF effects are presented as red dashed lines; the CPO effects are presented as blue solid lines; and PSP effects are presented as green solid lines with squares. Asterisks indicate changes that are statistically different from the non OP-treated controls (* $p < 0.05$) or (** $p < 0.01$). In cases where SEM bars are not apparent, the error is smaller than the symbol size.

4.8 Discussion

Based on the results of the previous chapter, which showed exposure to sub-cytotoxic concentrations of CPF, CPO and PSP caused morphological changes in N2a and C6 cells, the hypothesis that these changes may be due to alteration of cytoskeletal proteins was investigated in this chapter. Studies have shown that proteins, such as those of NFs and MTs, are key endogenous factors that control normal axonal and neurite outgrowth, neuro-stability and neurodevelopment. This investigation was supported by the evidence that disruption of the axonal cytoskeleton by OPs is associated with changes in neuronal cell morphology (Sachana *et al.*, 2001).

The aim of the work presented in this chapter was to examine the molecular changes underlining the morphological effects of CPF, CPO and PSP by analysing the expression levels of neural cell differentiation associated cytoskeletal and associated regulatory proteins, in differentiating mouse N2a neuroblastoma cells and rat C6 glioma cells. To achieve these aims, N2a and C6 cell lines were differentiated for 24 h with and without 1, 3 and 10 μM of CPF, CPO and PSP (co-differentiated), and changes in the key proteins MAP 2, Tau, β III tubulin, GAP-43, NFH and GFAP, were analysed by quantitative Western blotting and ELISA approaches.

MAP family members, such as MAP 2 and Tau, are important in central nervous system development; their roles include maintenance of the stability of growth cones, and the modulation of axonal and dendritic MT dynamics (Schoenfeld and Obar, 1994). They are involved in the stimulation of MT assembly, the cross-linking of MTs to other cytoskeletal elements, and interactions between IFs and actin filaments (Letierrier *et al.*, 1982; Nixon *et al.*, 1990; Cleveland, 1993). β -III tubulin plays an important role during nervous system development; it is one of earliest cytoskeletal proteins expressed in neurons and it has an essential role in neurite growth and cell differentiation (Easter *et al.*, 1993).

GAP-43, which is mainly found in elongating axons and growth cones in neurons, has been shown to play an important role in neurite outgrowth regulation (Skene, 1989; Perkiner *et al.*, 1996; Das *et al.*, 2004). It regulates many processes during neurodevelopment, including axon development, growth cone formation, and synapse plasticity (Benowitz and Routtenberg, 1997). NFH is usually found in mature neurons and axons, where they provide support during axonal extension, and regulate axonal development and growth, by forming cross bridges between extensions of the NF tail

domains and other cytoplasmic organelles (Hirokawa *et al.*, 1984; Lee and Cleveland, 1994). GFAP is found in mature astrocytes, and non-myelinating Schwann cells in the PNS, and glial cells of the digestive system, in which it provides structural support (Eng *et al.*, 2000; Yang and Wang, 2015). Increased levels of GFAP can be detected during glial development and differentiation (Bramanti *et al.*, 2010). The Western blot results for GAPDH showed there were no significant changes in expression following exposure of both cell types to all the concentrations of the different OPs tested at 24 h, which suggests this was a suitable internal control to use for normalisation of the band intensities of the other proteins under investigation.

The investigation of the effect of the OPs on the MT proteins MAP 2, β III-tubulin and Tau in N2a cells showed the different OPs did influence protein expression, with a reduction in expression seen for all three proteins with at least one OP treatment, but there were no differences seen for 1 μ M of any of the OPs. For MAP 2, there was a reduction in expression after treatment with 3 μ M CPF ($p < 0.05$) and 10 μ M CPF, CPO and PSP ($p < 0.05$), and no significant differences for 3 μ M CPO and PSP. For β III tubulin, there was a significant decrease in expression after treatment with 10 μ M CPF ($p < 0.05$), CPO ($p < 0.05$) and PSP ($p < 0.001$), but no significant differences were produced with 3 μ M of any of the OPs. The results for Tau show there was a significant reduction in expression after treatment with 3 and 10 μ M concentrations of CPF ($p < 0.01$) and PSP ($p < 0.05$), whereas CPO produced no significant differences, suggesting that there were differences in the cytoskeletal effects of the parent compound and its metabolite.

These results fit with the *in vivo* studies of Abou-Donia (1993), that showed OP exposure in hens disrupted the neural cytoskeleton and increased phosphorylation of cytoskeletal proteins including MAPs and tubulin (Abou-Donia, 1993). Further evidence to support these results come from structural and immunoreactivity studies in cultured rat brain slices; the results showed exposure to doses of CPO between 0.1 to 10 μ M after 24 h induced alterations in MAPs and MT ultra-structure, with a significant reduction in MAP 2 levels in each brain region investigated at concentrations as low as 0.1 μ M (Prendergast *et al.*, 2007). Similar results were also found in another study in that used single subcutaneous dose of chlorpyrifos (250 mg/kg) in Wistar rats for 15 days and detected a significant reduction of MAP 2 in the pre-frontal cortex (Ruiz-Muñoz *et al.*, 2011).

The results of the current investigation show some differences to those found by Sachana *et al.* (2008) who used Western Blot analysis to study the effects of sub lethal

concentrations (1–10 μM) of CPF and CPO on C6 cells. They found there was significant concentration-dependent reduction in antibody reactivity to α -tubulin by CPO after treatment for 24 h, which is similar to the response of β III-tubulin this study. However, in the Sachana *et al.* (2008) study there were no significant differences in α -tubulin expression after CPF treatment, and no significant differences in MAP2 expression seen for either treatment, which is different to the results of this study and may be due to the different cell types used (Sachana *et al.*, 2008). The effect of all 3 OPs on N2a cells in the current study is, however, similar to the results of Sachana *et al.* (2014) in a study that used differentiating N2a cells exposed to 10 μM DZO for 24 h, which decreased the expression of β III-tubulin in a similar way to this investigation, but their study showed DZO had no effect on Tau, which is different to our results for CPF and CPO (Sachana *et al.*, 2014). This suggests that some cytoskeletal effects of OPs may be cell type specific while others are compound specific.

To examine possible effects of the OP treatments on the levels of cytoskeletal axonal intermediate filament and growth associated proteins in differentiating N2a cells, the effects of 24 h exposure of CPF, CPO and PSP on NFH and GAP-43 were determined by Western blot analysis. As with results for the MT proteins, there were no significant differences seen after treatment with 1 μM of any of the OPs, suggesting this dose was too low to create a significant response at this time point. The results for NFH showed a significant decrease in expression after treatment with 3 μM CPF, 10 μM CPO and 3, 10 μM PSP. The results for GAP-43 were similar to NFH, in that there were significant decreases in expression after exposure to 3 μM CPF ($p < 0.05$) and 10 μM CPF, CPO and PSP ($p < 0.01$).

The results from this study agree with the results of other studies of the effects of CPF and CPO in N2a cells. Sachana *et al.* (2001) showed significantly reduced levels of NFH following 8 h exposure to 3 μM CPF. Flaskos *et al.* (2011) investigated the effect of 1-10 μM CPO for 24 h on N2a cells when added at the point of induction of differentiation and found reduced expression of both NFH and GAP-43, Sindi *et al.* (2016) found that exposure of pre-differentiated N2a cells to 3 μM CPF and CPO caused a transient reduction in GAP-43 expression after 4 h treatment, and a significant reduction in NFH expression after 8 h exposure, whereas Hargreaves *et al.* (2006) found treatment of differentiating N2a cells with 2.5 μM PSP for 24 h resulted in a significant reduction in NFH protein expression. Thus, taken together with previous data, the results in this chapter

suggest that reduced GAP-43 and NFH protein levels are effective markers of impaired neurite outgrowth following OP exposure.

The effects of CPF, CPO and PSP on cytoskeletal proteins in differentiating C6 cells were assessed by measuring changes in expression of GFAP by Western blot analysis. As with the other proteins measured, 1 μM of all the OPs produced no significant differences compared to the non OP-treated control. There was a significant reduction in GFAP expression after exposure to 10 μM CPF ($p < 0.05$), 3 and 10 μM of both CPO and PSP ($p < 0.05$). These results are similar to the *in vivo* studies in developing rats Garcia *et al.* (2002) which found that 4 days of subcutaneous CPF administration resulted in decreased in GFAP levels. These results are also supported by a study of the effects of 1-10 μM DZO for 24 h in differentiating rat C6 glioma cells, which reported a decrease in GFAP expression after treatment (Sidiropoulou *et al.*, 2009b). There are some similarities of these results to those found by Wang and Zhao (2017), who used purified astrocytes and Western blot analysis to investigate the effect of 25, 50, and 100 μM CPF combined with 1 $\mu\text{g}/\text{mL}$ LPS on GFAP expression.

Further assessment of the effect of the selected OPs on the cytoskeletal and associated regulatory proteins MAP-2, β III tubulin, Tau, NFH, GAP-43 and GFAP in differentiating N2a and C6 cells was carried out using a cell ELISA technique. Cells were induced to differentiate for 24 h in the absence (0) or presence of 1, 3 and 10 μM CPF, CPO and PSP and an ELISA was carried out on the fixed cell monolayer to detect changes in protein expression.

By comparing the treated cells to the relevant controls for the MT proteins, the results show that, as with the Western blot results, there were no differences seen for 1 μM of any of the OPs, and for most of the treatments there were also no significant differences observed for 3 μM of the OPs. For MAP 2 there was a significant decrease in expression detected by the ELISA after treatment with 10 μM CPF ($p < 0.05$), and 3 and 10 μM CPO ($p < 0.05$), when compared to the non OP-treated controls. For anti- β III tubulin and Tau, the result showed there was only a statistically significant decrease in protein levels after treatment with 10 μM PSP ($p < 0.05$, and $p < 0.01$, respectively) when compared to the non PSP-treated control. Thus, although these results show a similar pattern of decreased expression after OP treatment as observed by Western blot analysis, the ELISA only detects significant changes at the highest concentrations investigated, suggesting it is less sensitive than the Western blot.

By comparing the treated cells to the relevant controls for the NF and growth associated proteins, the results show a similar pattern to the ELISA results for the MT proteins. NFH protein levels were significantly reduced after treatment with 10 μM CPF ($p < 0.01$), when compared to the relevant control, and GAP-43 showed a statistically significant reduction in expression after treatment with 1, 3, and 10 μM CPF ($p < 0.05$, $p < 0.05$, and $p < 0.01$, respectively), when compared to the non OP-treated controls. This suggest the ELISA for GAP-43 is slightly more sensitive to changes in protein levels that the other proteins tested, but still not as sensitive as the Western blot analysis.

The expression levels of GFAP in C6 cells were also investigated by ELISA, and the results show that PSP treatment caused no significant differences in protein levels, whereas all three concentrations of CPF and CPO produced a statistically significant reduction in protein expression (1 μM $p < 0.05$, 3 μM $p < 0.05$. and 10 μM $p < 0.01$, for both) when compared to the untreated controls. Again, these results follow a similar pattern to those of the Western blot analysis as they all show decreases in protein expression after OP treatment, but the actual magnitude of the effect, and the OPs that cause it, show some differences between the detection methods. It may also reflect the fact that not all antibodies are equally suitable for ELISA and Western blot analysis.

Overall, the results of this investigation have shown that the OPs selected do influence the expression levels of the different cytoskeletal and regulatory proteins investigated, suggesting they may be important in the neurotoxic effects produced by OPs. Based on these results the aim of the next chapter is to investigate the genotoxic effects of these OPs on the expression level of selected cytoskeletal genes in differentiating N2a neuroblastoma and C6 cell lines.

Chapter 5

**Genotoxicity of Organophosphate
Compounds Chlorpyrifos, Chlorpyrifos
Oxon and Phenyl Saligenin Phosphate on
Differentiating Mammalian Cell Lines**

5.1 Introduction

CPF, CPO and PSP are known to induce neurological effects, as discussed in Chapter 1. While the neurodegenerative effect of these OPs on cell morphology and the expression of related proteins is widely established, their effect at the gene level remains to be fully elucidated. There have been relatively few studies performed to evaluate the genotoxic effect of CPF in models of neural cell differentiation including neural differentiation of mouse adipose tissue-derived stem cells (ADSCs) (Zarei *et al.*, 2016) and PC12 cells (Slotkin and Seidler, 2010). Despite the poor understanding of this action, genotoxic potential is considered a primary risk factor leading to long-term health effects. The concept of OP exposure causing malignant tumours as well as their effect on reproductive health has been accepted (Bolognesi, 2003).

Changes in genetic material, particularly DNA damage, were proposed as a useful measure of genotoxic properties of OPs (Kornuta *et al.*, 1996). As such, recent studies have aimed to understand the potential genotoxic effect of CPF (Sandhu *et al.*, 2013; Ismail *et al.*, 2014; Muller *et al.*, 2014; Wang *et al.*, 2014). These *in vivo* studies involved exposure of rats or fish to different concentrations of CPF followed by analysis of DNA damage using the Comet assay. Ismail *et al.* (2014) determined the acute LC₅₀ value for *L. rohita* fish exposed to various concentrations of CPF (73.8 – 221.4 µg/L for 96 h). Analysis of blood and gill samples showed that the amount of DNA damage was concentration and time dependent. Wang *et al.* (2014), who exposed zebrafish to CPF (0.01-1 mg/L) for 5 - 25 days, reported that the DNA damage had a clear dose-response relationship. Muller *et al.* (2014) gave Sprague-Dawley adult rats daily subcutaneous injections of CPF to model typical exposures of agricultural workers; a daily CPF dose of 10 mg/kg body weight was shown to induce DNA damage in blood samples. Using Wistar rats, Sandhu *et al.* (2013) administered oral CPF doses of 3 and 12 mg/kg. After 7 and 14 days, blood lymphocytes were harvested. In this case, CPF-induced DNA damage was observed at a concentration of 12 mg/kg. Overall, the studies described above confirm that even at sub lethal concentrations of CPF, DNA damage was occurring. However, the mechanism by which CPF induced cytotoxicity remains poorly understood. The observation of CPF binding to DNA and the outcome of DNA adducts has led to an increase in social concern about the CPF genotoxic risk in humans (Li *et al.*, 2015).

A variety of biological responses can be triggered by genotoxic stress, including the transcriptional activation of genes regulating DNA repair (Dickinson *et al.*, 2004).

Genotoxicity may also affect key structural genes, which is consistent with the morphological changes observed by the causative agent. Even though there are studies targeting DNA damage as a cytotoxicity marker, currently there are few studies examining this effect to further characterise the affected genes. As such, the use of real time PCR to analyse the effect of OPs on gene expression in mammalian neural cell lines provides a cutting edge approach to complement our understanding of the mechanism by which these compounds exhibit their toxicity. For example, as CPF, CPO and PSP cause morphological changes, understanding the gene expression patterns of related genes would open a new window towards exposing a new field in this area.

Another factor that could be involved in the genotoxicity of OPs is epigenetic changes. While there are numerous processes that are involved in epigenetic control of gene expression, histone acetylation is the most understood modification. The modification occurs at the histone epsilon amino group in specific lysine residues where an acetyl group is added. This reaction is catalysed by a class of enzymes that are known as histone acetyltransferases (HATs). The removal of the acetyl group is the reverse reaction and it is carried out by histone deacetylases (HDACs) (Altman-Price and Mevarech, 2009). There is a recognised correlation between transcription and histone acetylation levels, and it has been shown that modulating histone acetylation plays a pivotal role in regulating gene expression (Witt *et al.*, 2009). As such, histone deacetylation is considered as a tag for epigenetic repression. HDACs regulate many processes including DNA damage response and apoptosis (Urnov *et al.*, 2001). Aberrant HDACs are implicated in many diseases including cancer; consequently, it is important to analyse their activity in disease states, particularly where gene expression studies are targeted (Peng *et al.*, 2015).

The fact that HDACs were highlighted as important in a variety of diseases that are caused by mutagenesis, together with the recognised genotoxic effect of CPF, CPO and PSP, raises the question as to whether these OPs have epigenetic effects. And, if they do, does it influence the genes that encode proteins associated with the defects observed at the morphological and developmental levels in cellular models of OP toxicity? Studying the effect of HDAC activity in neuronal and glial cell lines in response to exposure to the OPs would be a novel approach in the field of OP neurotoxicity.

5.2 Aims

The aim of the work presented in this chapter was to study the effect of CPF, CPO, and PSP exposure on:

- 1) The expression level of selected cytoskeletal genes in differentiating N2a neuroblastoma and C6 cell lines. The targeted genes are involved in maintaining the cytoskeletal integrity of the cells. These include:-
 - *GAP43*; Growth associated protein 43
 - *MAP2*; Microtubule-associated protein 2
 - *MAPT*; Microtubule-associated protein Tau
 - *NEFH*; Neurofilament heavy chain
 - *TUBB3*; Tubulin β -III isoform
 - *GFAP*; Glial fibrillary acidic protein
- 2) HDAC activity in nuclear extracts of control and OP-treated cells and relate it to the changes in the expression levels of the genes of interest.

5.3 Results

5.3.1 Primer validation

The primers were designed using the Primer3 program and their specificities were tested prior to running the experiments. By means of conventional PCR, primers were used to amplify the targeted amplicons in cDNA which was reverse transcribed from the total RNA extracted from mouse and rat brain tissues (positive controls), as well as from mitotic and differentiated N2a and C6 cell lysates. The PCR conditions were initially optimised using RNA extracted from brain tissues, where the target genes were known to be expressed. Figure 5.1 and figure 5.3 illustrate that the primers were specific, as their cDNA amplification resulted in a single defined band at the expected size and showed no amplification product in the negative template control. To achieve that result, the annealing temperature was selected according to the properties of the primers' melting temperature and, where needed, a gradient PCR in the range of ± 5 °C of the mean (forward and reverse) melting temperature was used. The list of primers along with their corresponding annealing temperature and product size is shown in Table 5.1. The bands with N2a or C6 in Figure 5.1 and Figure 5.3 were excised and the amplified products were eluted and sequenced. Neither *NEFM* nor *NEFL* showed amplification in N2a cell extracts (Figure 5.2) which fits with the results of Hornburg *et al.* (2014). However, both sets of primers showed a clear band with the positive control. The sequences were blasted against the genome of *Mus musculus* or *Rattus norvegicus*, respectively. All sequenced PCR products were in a 100% alignment with their corresponding gene of interest (Appendix 8.3-8.8) accession numbers are listed in table.5.1.

Table 5.1. Designed primers targeting N2a and C6 cell lines neuronal markers.

Cells	Genes	Accession Number		Primer Sequence (5' to 3')	Annealing T (°C)	Product size (bp)		
N2a	<i>MAP2</i>	1. Isoform1 NM_001039934.1	Forward	AGATAGACTTAAGCCATGTGACATCCAAAT	63	100		
		2. Isoform2 NM_008632.2	Reverse	GTTTTACACTCTCAATTTTCACACGTCCAC				
		3. Isoform3 NM_001310634.1						
	<i>TUBB3</i>	NM_023279.2	Forward	CTATTCAGGCCCGACAACCTTTATCTTTGGTCA	68	131		
			Reverse	CAATTCTCACACTCTTTCCGCACGACATCTAG				
	<i>MAPT</i>	1. Isoform 1 NM_001038609.2 2. Isoform 2 NM_010838.4 3. Isoform 3 NM_001285454.1 4. Isoform 4 NM_001285455.1 5. Isoform 5 NM_001285456.1	Forward	GAGGAGGGAATAAGAAGATTGAAACCCACA	60	138		
			Reverse	CATTGCTGAGGTGCCGTGGAGATGTGT				
			Forward	CCATATCCACGCACATAAAAAGTCAA			60	100
			Reverse	ATCTCTTCTGTCTGTCCTTCTACAA				
			<i>NEFM</i>	NM_008691.2			Forward	AGGAGAGGATAGCAGTGATGATAAA
Reverse	GACGGTTACAGATTTGGTGATGTAT							
<i>NEFL</i>	NM_010910.1	Forward	GACACAATCAACAACTGGAGAATGAG	60	130			
		Reverse	GTTTTCTGTAAGCTGCAATCTCGATG					
<i>GAP43</i>	NM_008083.2	Forward	ACAGGTTGAAAAGAATGATGAGGAC	60.5	122			
		Reverse	TTTTCTTGTATGTGTCCACGGAA					
C6	<i>GFAP</i>	NM_017009.2	Forward	TTCTCCAACCTCCAGATCCG	60	123		
			Reverse	CGACTCCTTAATGACCTCGC				

MAP2; Microtubule-associated protein 2, *TUBB3*; Tubulin beta-3 chain, *MAPT*; Microtubule-associated protein tau, *NEFH*; Neurofilament heavy chain, *GAP43*; Growth associated protein 43, *GFAP*; Glial fibrillary acidic protein.

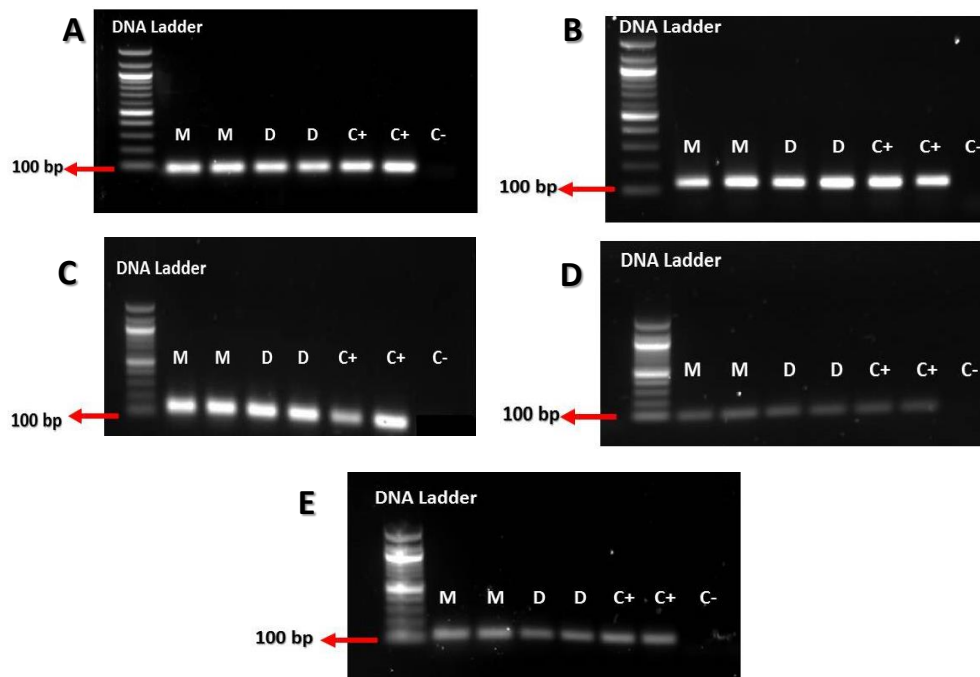


Figure 5.1. Analysis of genes of interest in mitotic and differentiating N2a cells by PCR.

A representation of PCR products amplified using **A-** Microtubule associated protein 2 (*MAP2*), **B-** β III tubulin (*TUBB3*), **C-** Microtubule associated protein tau (*MAPT*) **D-** Neurofilament Heavy chain (*NEFH*), and **E-** Growth associated protein-43(*GAP43*) primers. Bands were visualised after electrophoretic separation in a 1.5% agarose gel stained with SyberSafe. Mouse brain RNA extracts were used as a positive control (C+). RNA was obtained from mitotic (M) and differentiating (D) N2a cells and reverse transcribed into cDNA and analysed by PCR. Non-template controls were used as negative controls (C-). Amplified products are presented as a single defined band at size of approximately 100 base-pairs (bp).

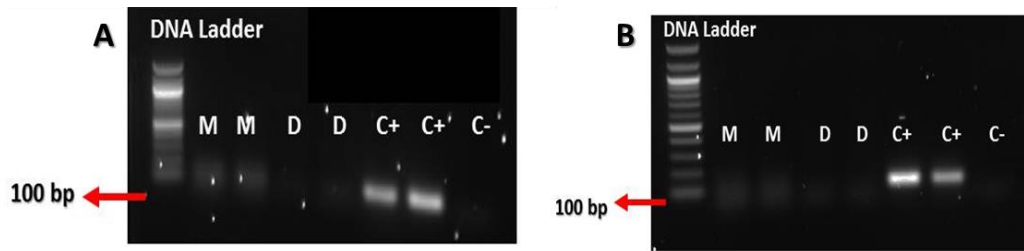


Figure 5.2. Analysis of other neurofilament genes of interest in mitotic and differentiating N2a cells by PCR.

A representation of PCR products amplified using **A-** Neurofilament medium chain (*NEFM*), **B-** Neurofilament light chain (*NEFL*) primers. Bands were visualised after electrophoretic separation in a 1.5% agarose gel stained with SyberSafe. Mouse brain RNA extracts were used as a positive control (C+). RNA was obtained from mitotic (M) and differentiating (D) N2a cells and reverse transcribed into cDNA and analysed by PCR. Non-template controls were used as negative controls (C-). Amplified products are presented as a single defined band at size of approximately 100 base-pairs (bp).

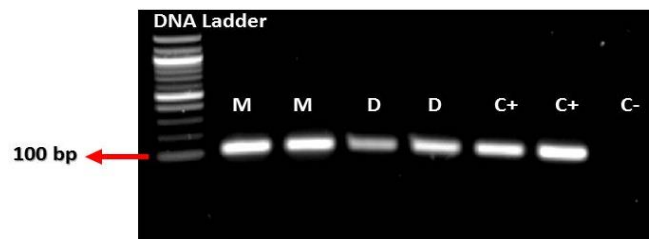


Figure 5.3. GFAP expression in mitotic and differentiating C6 cells.

Shown is a representation of PCR products amplified using primers for the gene encoding glial fibrillary acidic protein (*GFAP*) visualised on a 1.5% agarose gel stained with SyberSafe. Rat brain RNA extracts were used as a positive control (C+). RNA was obtained from mitotic (M) and differentiating (D) C6 cells and reverse transcribed into cDNA and analysed by PCR. Non-template reactions were used as negative controls (C-). Amplified products are presented as a single defined band at size of 100 base-pairs (bp).

5.3.2 Housekeeping genes

According to the literature, glyceraldehyde 3-phosphate dehydrogenase (*GAPDH*) and ribosomal protein S18 (*Rps18*) are frequently used as reference genes (Al-Bader and Al-Sarraf, 2005; Stephens *et al.*, 2011) since their expression levels are reported to be relatively stable when exposed to toxic compounds. As such, these two were selected as reference genes for the gene expression analysis in the current study. To assure their levels did not change across the studied groups, their expression was first analysed. Treatment

with CPF, CPO (Figure 5.4, panel A) and PSP (Figure 5.4, panel B) did not alter the expression of either *GAPDH* or *Rps18* in the N2a cell line (Figure 5.4, panel C and D).

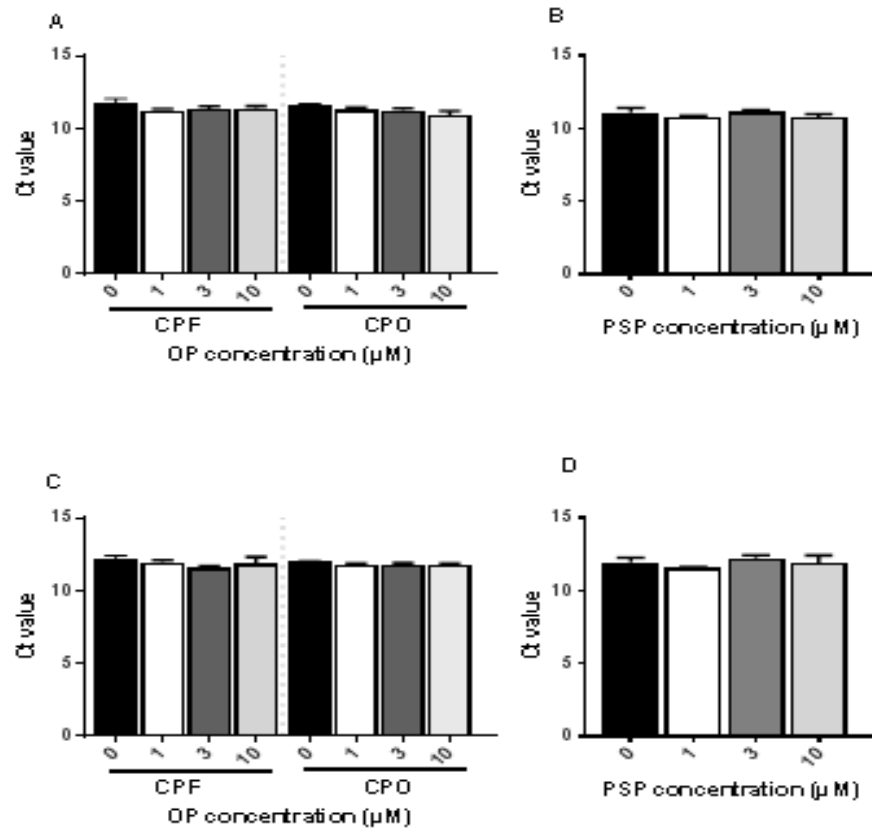


Figure 5.4. Ct values obtained for GAPDH and Rps18 expression (qPCR) in differentiating N2a cells after different OP treatments.

Shown is quantitative RT-qPCR analysis of the expression levels of *GAPDH* in N2a cells induced to differentiate for 24 h either in the absence (0) or presence of variable concentrations of CPF or CPO (panel A) and PSP (panel B), as well as the expression of *Rps18* N2a cell lysate treated with CPF or CPO (panel C) and PSP (panel D). Statistical analysis was by one-way ANOVA with Sidak post-hoc test comparing treatments to the control (0). Data are presented as mean \pm SEM for four independent experiments.

Their expression levels were also unaffected in the differentiating C6 cells across all the used concentrations of CPF, CPO (Fig.5.5, panel A and C) and PSP (Fig.5.5, panel B and C). As both genes exhibited similar patterns with no difference in their expression across all studied groups in both cell lines, they were both used independently to normalise the expression of targeted genes.

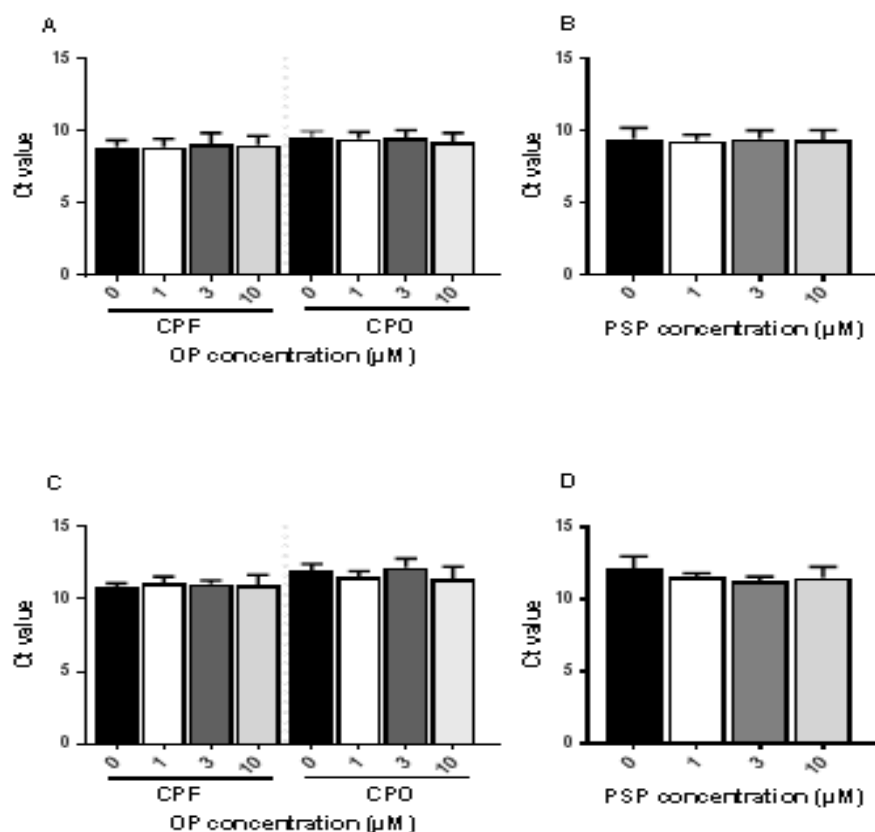


Figure 5.5. Ct values obtained for GAPDH and Rps18 expression in C6 cell line.

The expression level of *GAPDH* in differentiated C6 cell lysate for 24 h then exposed to 0, 1, 3 or 10 μM of CPF or CPO (panel A) and PSP (panel B) as well as the expression of *Rps18* in differentiated C6 cell lysate for 24hr then exposed to 0, 1, 3 or 10 μM of CPF or CPO (panel C) and PSP (panel D). Analysis was by one-way ANOVA with Sidak post-hoc test comparing treatments to the (0) control. Data is presented as mean ± SEM for four independent experiments.

5.3.3 Effect of CPF, CPO and PSP on neural markers in mammalian cell lines.

The mRNA expression level of neuronal marker genes including *MAP2*, *TUBB3*, *MAPT*, *NEFH* and *GAP43* was measured in differentiating N2a cells that were exposed to 1, 3 and 10 μM concentrations of CPF, CPO or PSP. Similarly, the mRNA expression of *GFAP* was measured in differentiating C6 cells after exposure to 1, 3 and 10 μM concentrations of CPF, CPO or PSP. All of these results are discussed in the next subsections.

5.3.3.1 Microtubule-associated protein 2 (MAP2).

The *MAP2* gene encodes the MAP2 protein. It is involved in microtubule assembly, which is considered as an essential step in neurite outgrowth, by promoting intracellular microtubule bundling and elaboration (Harada *et al.*, 2002). Due to its importance in neuritogenesis, the effect of the organophosphates on *MAP2* at the gene level was studied.

After the expression level of *MAP2* was normalised to the expression of *GAPDH*, it became apparent that *MAP2* expression was significantly reduced in N2a cells when exposed to 3 ($p = 0.017$) and 10 μM ($p = 0.014$) concentrations of CPF (Figure 5.6, panel A1). CPO and PSP had similar effects but the reduction was only significant at a concentration of 10 μM (Figure 5.6, panel A1 and A2). The expression of *MAP2* was then normalised to the expression of *Rps18* to further characterise it and, in this case, the statistical analysis corroborated that CPF induced a significant effect at both 3 ($p = 0.02$) and 10 μM ($p = 0.018$) (Figure 5.6, panel B1). *MAP2* expression was also significantly lower than its corresponding control when cells were exposed to 3 μM as well as 10 μM CPO and PSP when using *Rps18* (Figure 5.6, panel B1 and B2).

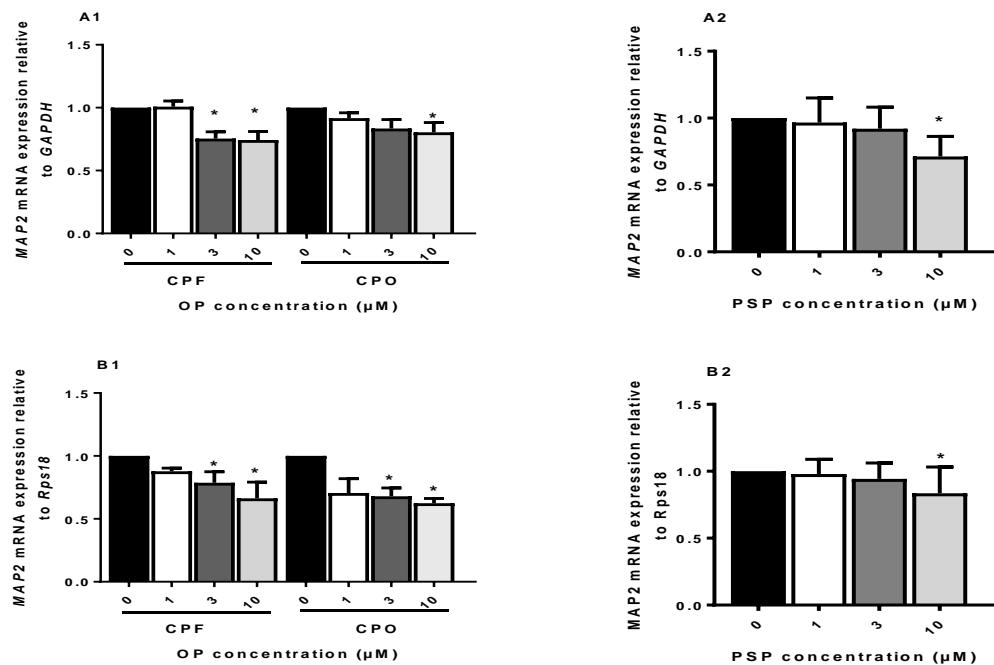


Figure 5.6. Relative expression of *MAP-2* mRNA in differentiating N2a cells after CPF, CPO and PSP exposure as determined by quantitative PCR.

N2a cells were induced to differentiate for 24 h incubation without (0) or with 1, 3 and 10 μM concentrations of CPF, CPO or PSP. Data were analysed using one-way ANOVA with Sidak post-hoc test comparing treatments to the (0) control. The normalization of data to the first housekeeping gene *GAPDH* is shown in panel A, whereas the normalisation to the second housekeeping gene *Rps18* is shown in panel B. Expression values are relative to the non-OP-treated control \pm SEM. Data presented are an average of four independent experiments, and all samples were amplified in triplicates. Asterisks indicate changes that are statistically different from the non-OP-treated controls (* $p < 0.05$) or (** $p < 0.01$).

5.3.3.2 Tubulin β III chain (TUBB3).

The *TUBB3* gene encodes the β III isotype of tubulin, which is abundant in neurons and involved in the development and maturation of neuronal cells the nervous system. While the mechanism by which it controls the neuronal development is not known, there is evidence showing that any alteration in its expression results in serious consequences to the cells' viability leading to diverse neurological syndromes (De Gendt *et al.*, 2011). Analysing its RNA expression level could help to form a better understanding of the β III tubulin protein changes described in chapter three.

The mRNA level of *TUBB3* relative to *GAPDH* was significantly reduced upon N2a cell exposure to 10 μ M CPF (p= 0.0237) and CPO (p= 0.0355) (Figure 5.7, panel A1). The pattern was similar when the expression was calculated relative to *Rsp18* with CPF, CPO having a significant effect apparent at an even lower concentration of 3 μ M (p=0.051) and 10 μ M (p= 0.003) (Figure 5.7, panel B1). PSP exposure also caused a significant drop in *TUBB3* RNA expression level normalised with either *GAPDH* (Figure 5.7, panel A2) or *Rps18* (Figure 5.7, panel B2).

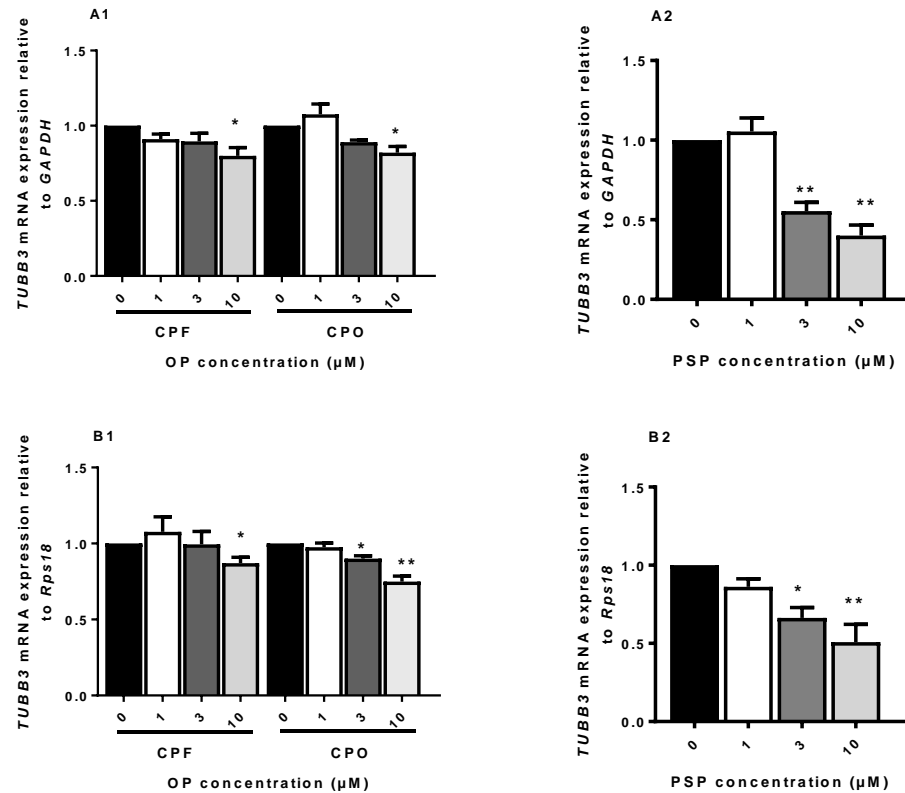


Figure 5.7. Relative expression of *TUBB3* mRNA in differentiating N2a cells after CPF, CPO and PSP exposure as determined by quantitative PCR.

N2a cells were induced to differentiate for 24 h incubation without (0) or with 1, 3 and 10 μM concentrations of CPF, CPO or PSP. Data were analysed using one-way ANOVA with Sidak post-hoc test comparing treatments to the (0) control. The normalization of data to the first housekeeping gene *GAPDH* is shown in panel A, whereas the normalisation to the second housekeeping gene *Rps18* is shown in panel B. Expression values are relative to the non-OP-treated control ± SEM. Data presented are an average of four independent experiments, and all samples were amplified in triplicates. Asterisks indicate changes that are statistically different from the non-OP-treated controls (*p < 0.05) or (**p < 0.01).

5.3.3.3 Microtubule-Associated Protein Tau (MAPT)

The main function of protein Tau, which is expressed by the *MAPT* gene, is to modulate the stability of axonal microtubules by Tau phosphorylation at Ser262 and Ser356. Furthermore, Tau plays an important role in maintaining the cytoskeletal structure of neurons. Abnormalities in its protein expression levels have been linked to neurodegenerative disease (Mietelska-Porowska *et al.*, 2014). Therefore, studying its RNA expression was of some importance as it would reflect the integrity of the neuronal cells and could help to explain the Tau protein changes observed in chapter 3.

CPF and CPO did not alter the RNA expression level of *MAPT* normalised with either *GAPDH* (Figure 5.8, panel A1) or *Rps18* (Figure 5.8, panel B1). However, PSP at a concentration of 3 and 10 μM induced a significant drop in its RNA expression independently of the housekeeping gene used for the normalisation (Figure 5.8, panel A2 and panel B2).

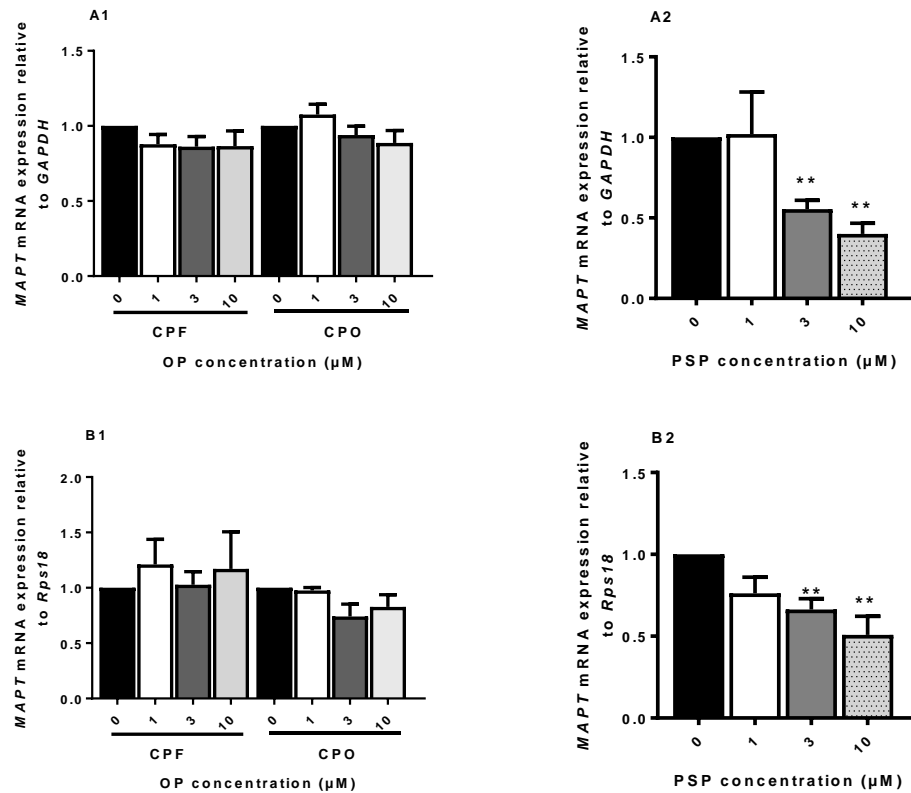


Figure 5. 8. Relative expression of *MAPT* (Tau) mRNA in differentiating N2a cells after CPF, CPO and PSP exposure as determined by quantitative PCR.

N2a cells were induced to differentiate for 24 h incubation without (0) or with 1, 3 and 10 μM concentrations of CPF, CPO or PSP. Data were analysed using one-way ANOVA with Sidak post-hoc test comparing treatments to the (0) control. The normalization of data to the first housekeeping gene *GAPDH* is shown in panel A, whereas the normalisation to the second housekeeping gene *Rps18* is shown in panel B. Expression values are relative to the non-OP-treated control \pm SEM. Data presented are an average of four independent experiments, and all samples were amplified in triplicates. Asterisks indicate changes that are statistically different from the non-OP-treated controls (** $p < 0.01$).

5.3.3.4 Neurofilament Heavy Chain (NEFH)

Studies on *NEFH*-null mice have showed that NF-H, encoded by the *NEFH* gene, plays an important role in determining the physical dimensions of axons and its role extends to maintaining a normal axonal conduction velocity (Yuan *et al.*, 2012). Understanding how

it behaves at the gene level when exposed to the OPs would help to further explain the changes observed in NFH protein levels in neural cells that underlie alterations in morphology following exposure to sub lethal concentrations of OPs.

When cells were exposed to 3 and 10 μM CPO, the relative RNA expression of *NEFH* was significantly decreased. These data were produced by normalizing either to *GAPDH* (Figure 5.9, panel A1) or *Rps18* (Figure 5.9, panel B1) and there was very little difference between the two sets. By contrast, CPF (Figure 5.9, panel A1) and PSP (Figure 5.9, panel A2 and B2) did not induce any significant effects on *NEFH* expression.

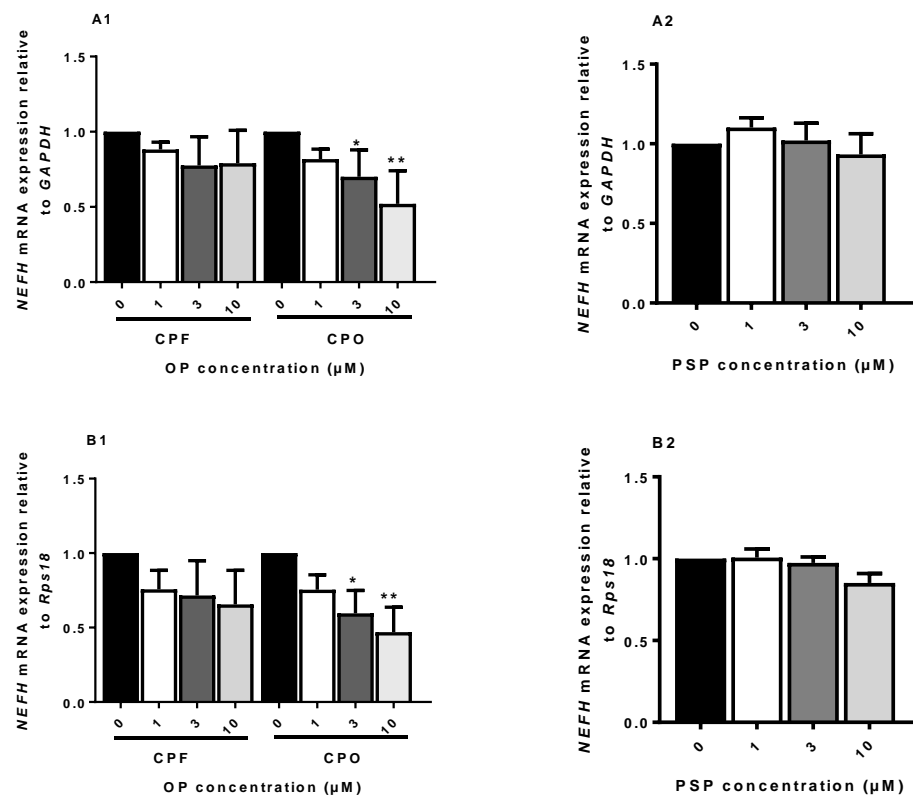


Figure 5. 9. Relative expression of *NEFH* mRNA in differentiating N2a cells after CPF, CPO and PSP exposure as determined by quantitative PCR.

N2a cells were induced to differentiate for 24 h incubation without (0) or with 1, 3 and 10 μM concentrations of CPF, CPO or PSP. Data were analysed using one-way ANOVA with Sidak post-hoc test comparing treatments to the (0) control. The normalization of data to the first housekeeping gene *GAPDH* is shown in panel A, whereas the normalisation to the second housekeeping gene *Rps18* is shown in panel B. Expression values are relative to the non-OP-treated control \pm SEM. Data presented are an average of four independent experiments, and all samples were amplified in triplicates. Asterisks indicate changes that are statistically different from the non-OP-treated controls (*p < 0.05) or (**p < 0.01).

5.3.3.5 Growth Associated Protein 43 (GAP43).

Like *NEFH*, *GAP43* has a role in the maintenance of axons particularly during CNS development. Null mutation of *GAP43* is lethal and causes death within days after birth as a consequent of defects in axon path finding (Routtenberg *et al.*, 2000). *GAP43* plays an important role in differentiating neurons as it is a component of the centrosome (Shen *et al.*, 2008). Its central role makes understanding the effect of the organophosphates on its expression level crucial.

The same trends were observed in the mRNA expression level of *GAP43* when normalised relative to both *GAPDH* and *Rps18*. Exposure to a concentration of 10 μM of CPF caused a significant reduction in its relative expression (Figure 5.10, panel A1 and B1). A reduction was observed at even lower concentrations of PSP: there was a significant reduction in its relative expression when cells were exposed to 3 μM as well as at 10 μM (Figure 5.10, panel A2 and B2). CPO did not exhibit any significant effects on *GAP43* mRNA expression level compared with the non OP-treated control (Figure 5.10, panel A1 and B1).

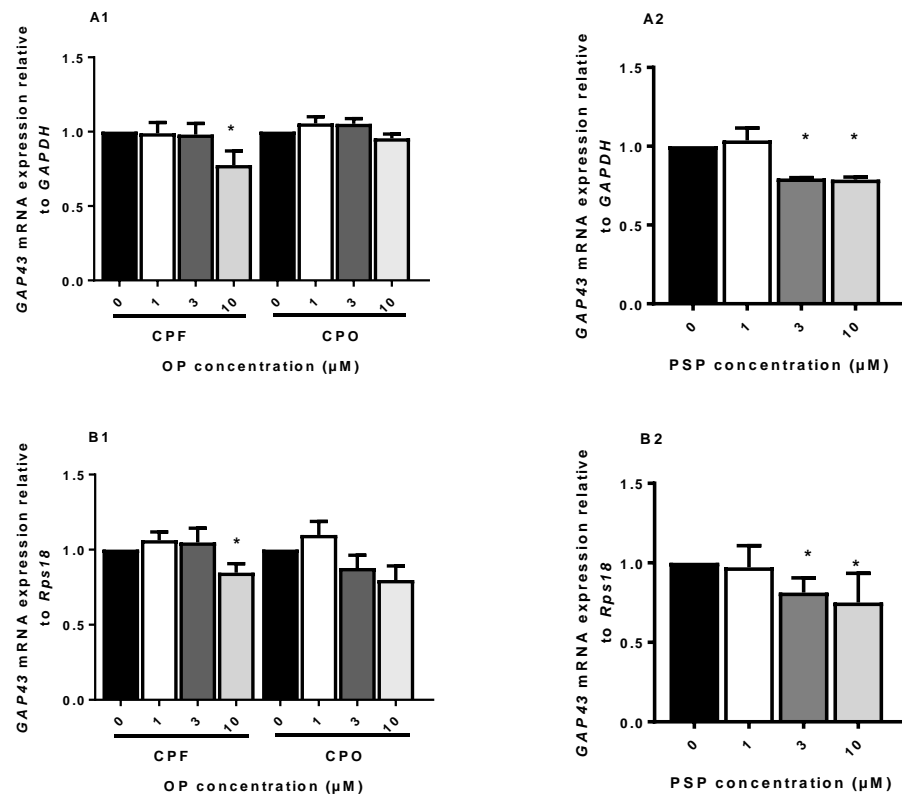


Figure 5. 10. Relative expression of GAP43 mRNA in differentiating N2a cells after CPF, CPO and PSP exposure as determined by quantitative PCR.

N2a cells were induced to differentiate for 24 h incubation without (0) or with 1, 3 and 10 μM concentrations of CPF, CPO or PSP. Data were analysed using one-way ANOVA with Sidak post-hoc test comparing treatments to the (0) control. The normalization of data to the first housekeeping gene *GAPDH* is shown in panel A, whereas the normalisation to the second housekeeping gene *Rps18* is shown in panel B. Expression values are relative to the non-OP-treated control \pm SEM. Data presented are an average of four independent experiments, and all samples were amplified in triplicates. Asterisks indicate changes that are statistically different from the non-OP-treated controls (* $p < 0.05$).

5.3.4 Effect of CPF, CPO and PSP on *GFAP* expression in differentiating C6 cells.

As mentioned previously in section (1.11.4), *GFAP* plays an important role in providing structural support in astrocytes. It also maintains important processes in the central nervous system including cell communication and blood brain barrier function. As such, studying the gene expression pattern of *GFAP* was of particular interest in order to determine whether this could be involved in the *GFAP* protein changes detected in the Western blots shown in chapter 3.

Normalizing to *GAPDH* or to *Rps18* produced comparable results. CPF, CPO as well as PSP treatments all caused switching off the gene as high significant decrease in *GFAP*

RNA expression level that ranged between 4 to 10 fold upon cell exposure to levels as low as 1 μM and as high as 10 μM (Figure 5.11, panel A1-B2).

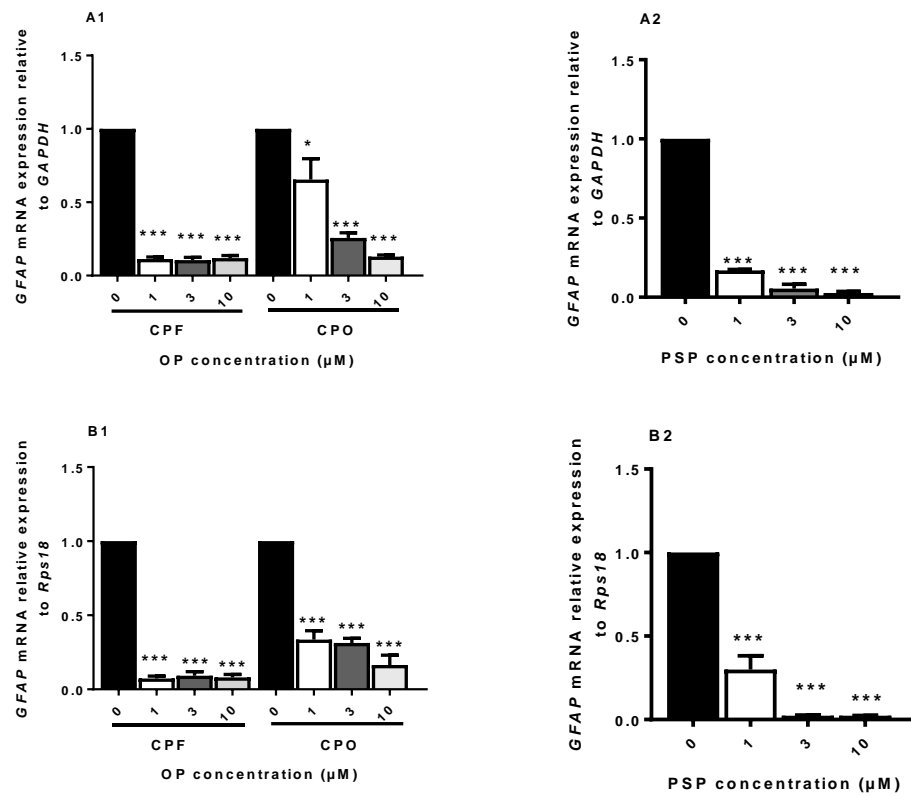


Figure 5. 11. Relative expression of *GFAP* mRNA in differentiating C6 cells after CPF, CPO and PSP exposure as determined by quantitative PCR.

C6 cells were induced to differentiate for 24 h incubation without (0) or with 1, 3 and 10 μM concentrations of CPF, CPO or PSP. Data were analysed using one-way ANOVA with Sidak post-hoc test comparing treatments to the (0) control. The normalization of data to the first housekeeping gene *GAPDH* is shown in panel A, whereas the normalisation to the second housekeeping gene *Rps18* is shown in panel B. Expression values are relative to the non-OP-treated control \pm SEM. Data presented are an average of four independent experiments, and all samples were amplified in triplicates. Asterisks indicate changes that are statistically different from the non-OP-treated controls (* $p < 0.05$) or (** $p < 0.001$).

Table 5.2. Summary of OP effects on neural marker gene expression relative to *GAPDH*

Cells	OPs	CPF			CPO			PSP		
	Conc. (μM)	1	3	10	1	3	10	1	3	10
N2a	<i>MAP2</i>	ns	-1.3↓ (0.017)	-1.34↓ (0.014)	ns	ns	-1.2↓ (0.018)	ns	ns	-1.23↓ (0.018)
	<i>TUBB3</i>	ns	ns	-1.25↓ (0.02)	ns	ns	-1.2↓ (0.03)	ns	-1.8↓ (0.003)	-2.5↓ (0.002)
	<i>MAPT</i>	ns	ns	ns	ns	ns	ns	ns	-1.7↓ (0.012)	-1.9↓ (0.005)
	<i>NEFH</i>	ns	ns	ns	ns	-1.2↓ (0.05)	-1.8↓ (0.003)	ns	ns	ns
	<i>GAP43</i>	ns	ns	-1.32↓ (0.04)	ns	ns	ns	ns	-1.26↓ (0.01)	-1.27↓ (0.01)
C6	<i>GFAP</i>	-8.8↓ (0.0001)	-9.5↓ (0.0001)	-8.4↓ (0.0001)	-1.5↓ (0.02)	-3.9↓ (0.0003)	-7.7↓ (0.0001)	-5.9↓ (0.0001)	-18.8↓ (0.0001)	-37.8↓ (0.0001)

Value are expressed as fold change relative to the control (0) with the p-value in the parenthesis. CPF; Chlorpyrifos, CPO; Chlorpyrifos oxon, PSP; Phenyl saligenin phosphate, *MAP2*; Microtubule-associated protein 2, *TUBB3*; Tubulin beta-3 chain, *MAPT*; Microtubule-associated protein Tau, *NEFH*; Neurofilament heavy chain, *GAP43*; Growth associated protein 43, *GFAP*; Glial fibrillary acidic protein.

5.3.5 Histone deacetylase (HDAC) activity upon exposure to CPF, CPO and PSP in differentiating neuronal cells.

Our qPCR results showed that the OP compounds can indeed significantly decrease the mRNA levels of some key genes involved in neuronal development (qPCR data are summarised in Table 5.2). Whilst it cannot be discounted that these compounds could affect RNA stability, leading to its decrease, an interesting possibility is that they could modulate gene expression through the regulation of transcription. This would mean that a series of transcription factors and chromatin remodelling complexes are specifically recruited to the promoter region of these genes. Once there, these complexes would be altering transcription rates by favouring DNA and/or histone modifications. And the acetylation and deacetylation of histones is one of the most widely studied changes controlling this process. In order to determine whether alterations in histone modifications could be involved in the genotoxic effects observed for the OPs studied in the current work, the analysis of HDAC activity was performed. As the genes studied exhibited reduced expression after exposure to CPF, CPO and PSP, and in general terms histone deacetylation is linked to transcriptional repression, it was felt that the HDAC activity could provide an insight to the mechanisms underlying the transcriptional changes observed. As such, the activity of HDAC was analysed using a colorimetric assay.

HDAC activity was measured in nuclear extracts prepared from differentiating N2a cells that were exposed to 1, 3 and 10 μM concentrations of CPF, CPO or PSP for 24 h. All three OPs caused a concentration dependent increase in the HDAC activity at concentrations of 1, 3 and 10 μM (Figure 5.12, panel A and B).

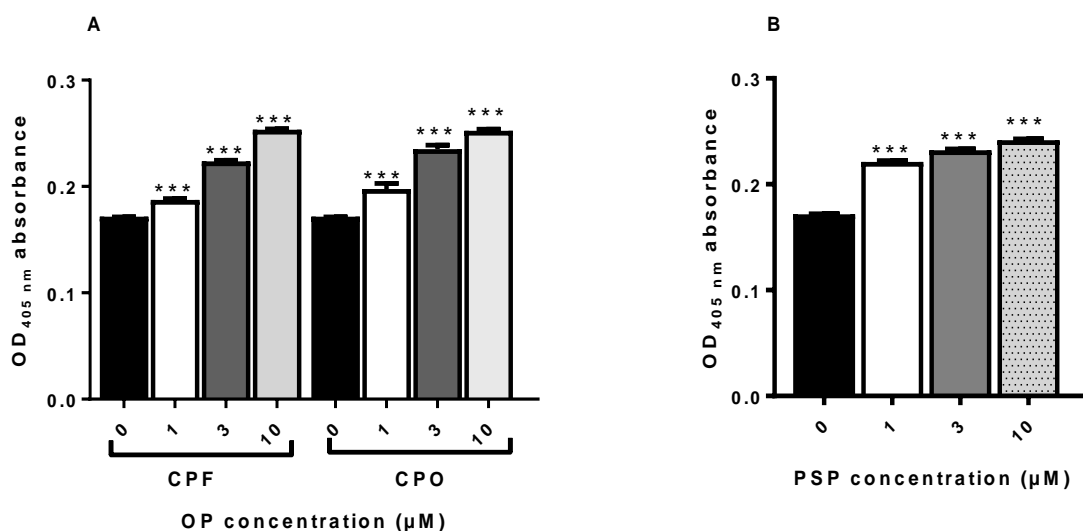


Figure 5.12. Effects of CPF, CPO and PSP on HDAC activity in differentiating N2a cells.

N2a cells were induced to differentiate for 24 h either without (0) or with 1, 3 and 10 μM concentrations of **A.** CPF and CPO or **B.** PSP. Data are presented as mean of the total HDAC activity of the non-OP-treated control ± SEM (from three independent experiments). Differences among different groups were determined by one way-ANOVA with Sidak post-hoc test comparing treatments to the (0) control. Asterisks indicate changes that are statistically different from the non-OP-treated controls (***) $p < 0.001$.

The experiment was also performed on nuclei prepared from differentiating C6 cells that were exposed or not to a concentration of 1, 3 and 10 μM of CPF, CPO or PSP for 24 h. The data were identical to those obtained for the N2a cells, where all three organophosphates caused statistically significant linear increases in the HDAC activity at concentrations of 1, 3 and 10 μM (Figure 5.13, panel A and B).

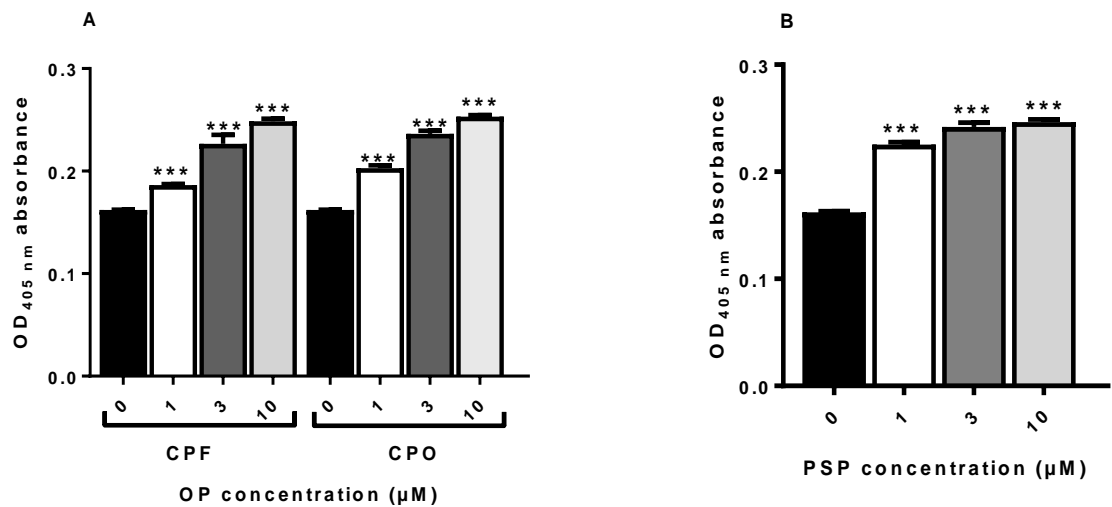


Figure 5.13. Effects of CPF, CPO and PSP on total HDAC activity differentiating C6 cells .

C6 cells were induced to differentiate for 24 h either without (0) or with 1, 3 and 10 μM concentrations of **A.** CPF and CPO or **B.** PSP. Data are presented as mean of the total HDAC activity of the non-OP-treated control ± SEM (from three independent experiments). Differences among different groups were determined by one way-ANOVA with Sidak post-hoc test comparing treatments to the (0) control. Asterisks indicate changes that are statistically different from the non-OP-treated controls (***) $p < 0.001$.

5.4 Discussion

The previous chapter investigated the effects of CPF, CPO and PSP on the expression levels of neural cell differentiation cytoskeletal and associated regulatory proteins (MAP 2, β III tubulin, Tau, NFH, GAP-43, and GFAP), in differentiating mouse N2a neuroblastoma cells and C6 glioma cells, and the results showed that the OPs selected influenced the expression levels of the proteins investigated, suggesting they may be important in the neurotoxic effects produced by OPs.

As we had observed significant changes in protein expression, this chapter investigated the genotoxic effect of CPF, CPO and PSP on the expression level of selected cytoskeletal genes in differentiating N2a neuroblastoma and C6 cell lines. There is some evidence that OPs can cause genotoxic effects; for example, studies into long-term effects of OPs have suggested that occupational exposure is linked to increased reports of cancers such as non-Hodgkin's lymphoma (Dreiherr *et al.*, 2005), and observations that CPF can bind to DNA and produce DNA adducts have led to increased concerns about CPF genotoxic risk in humans (Li *et al.*, 2015), but the actual effect of OPs at the genetic level is yet to be fully elucidated. Studies have shown that measuring changes to genetic material, such as DNA damage, can be a suitable measure of the genotoxic properties of OPs (Kornuta *et al.*, 1996), and genotoxicity may also affect key structural genes, which could then be linked to the changes observed at the protein level.

The aim of this chapter was to examine the effect of CPF, CPO, and PSP exposure on the expression level of selected cytoskeletal genes in differentiating N2a neuroblastoma and C6 cell lines. To achieve these aims, quantitative RT-PCR analysis of the RNA expression levels for the key proteins *GAP43*, *MAP2*, *MAPT*, *NFH*, *TUBB3*, and *GFAP* were measured after exposure to 1, 3 and 10 μ M CPF, CPO, and PSP, and normalised to the reference genes *GAPDH* and *Rps18*. To investigate if there were any significant effects due to epigenetic changes, a colorimetric test was used to evaluate HDAC activity.

The first stage of these experiments was the investigation of the specificity of the primer pairs designed to detect the selected genes. The primers were used in a PCR to amplify the targeted amplicon using cDNA from mouse and rat brain tissues as positive control, and then, using mitotic and differentiated N2a and C6 cell lysates. The results showed a single defined band at the expected size, and after excision and sequencing, all the PCR products were in a 100 % alignment with their corresponding gene of interest. These results

suggested the primers were suitable for use in detecting changes in gene expression after treatment with the selected OPs.

In order to understand gene expression in RNA samples, the selection of at least one 'housekeeping' gene is required. This is a gene whose expression does not change with the treatments and can be used to normalize the results. In this study, both *GAPDH* and *Rps18* gene expression was analysed as possible reference genes: they were both stable and presented with similar expression patterns. However, *GAPDH* had a lower coefficient of variance which meant higher stability, thus the results normalized to *GAPDH* have been used for the discussion (Table 5.2).

The results for the mRNA expression in the N2a cells showed that, as with the results for protein expression, there were no significant differences seen following exposure to 1 μM of any of the OPs. However, the *MAP2* results showed a significant reduction in expression after exposure to 3 and 10 μM CPF, 10 μM CPO, and 10 μM PSP. By comparing these results to those of the protein expression (Chapter 4), the data show the same pattern of reduced expression, which also agree with protein expression results of *in vivo* studies (Abou-Donia, 1993; Prendergast *et al.*, 2007; Ruiz-Muñoz *et al.*, 2011). As there is a good correlation between the mRNA levels and protein expression, these results suggest that the reduced protein levels are at least partly due to changes in gene expression.

The results for RNA expression for β III tubulin (*TUBB3*) normalised to *GAPDH* in N2a cells showed there was a significant reduction after exposure to 10 μM CPF, CPO and PSP, and 3 μM PSP. This is similar to the results for the protein levels, where there were significant reductions in expression after treatment with 10 μM of all the OPs, the only difference being there were no significant changes seen at 3 μM PSP. These results agree with previous studies, which show a reduction in tubulin protein expression after OP exposure (Sachana *et al.*, 2008; Sachana *et al.*, 2014), and would suggest the lower protein expression is driven by an altered gene expression.

The results for the mRNA expression for Tau (*MAPT*) normalised to *GAPDH* in N2a cells showed a significant reduction after exposure to 3 and 10 μM PSP, but not after treatment with any of the other OPs. These results are slightly different to those for the protein expression; here the treatment with 3 and 10 μM CPF as well as PSP caused a reduction in protein expression. As with the results for the protein expression levels, these results are different to those published in the literature for protein expression as they found that Tau

levels did not change after treatment with other OPs (Sachana *et al.*, 2014). However, it is worth remembering that mRNA changes and protein changes do not always correlate. Tau turnover is regulated through the proteasome activity and its half-life is 60 h in hippocampal neuronal cells (Poppek *et al.*, 2006). Taking this into account, the results obtained support a regulation of Tau protein levels through alteration of its proteasomal degradation rather than a modification of its gene expression. Changes in gene expression detected at 24 h, such as those of PSP treatment, would be detected at protein level only hours later than those covered in this study. Furthermore, as CPF treatment seems to modify Tau protein levels without affecting its gene expression levels, it would be interesting to study if it leads to post-translational modifications of Tau that could explain its increased degradation.

The results for the expression for *NFH* after normalisation to *GAPDH* showed a significant reduction after cells were exposed to 3 and 10 μM CPO, but no significant changes for the other OPs. This is similar to the results for the protein expression levels, but there were also reductions in protein expression after treatment with 3 and 10 μM CPF, and 10 μM PSP. This suggest that the treatment with CPO caused changes in gene expression which resulted in lower protein levels, but the lower protein levels seen after treatment with CPF and PSP were probably due to post-translational events. These results are consistent with the studies of the effects of OPs on protein levels for *NFH* in the literature, that have showed a reduction in expression of *NFH* after treatment of N2a cells with 3 μM CPF for 8 h (Sachana *et al.*, 2001; Sindi *et al.*, 2016), 3 μM CPO for 8 h (Sindi *et al.*, 2016), 1-10 μM CPO for 24 h (Flaskos *et al.*, 2011), and 2.5 μM PSP for 24 h (Hargreaves *et al.*, 2006).

The results for *GAP-43* normalised to *GAPDH* expression show that there was a significant reduction in expression after treatment with 10 μM of CPF, 3 μM and 10 μM PSP ($p < 0.05$ for all), but no significant differences were observed for CPO. These results have some similarities to the results for changes in protein expression; here there was a significant reduction in protein expression after exposure to 3 μM CPF and 10 μM of CPF, CPO and PSP ($p < 0.01$), which suggests the reduced protein expression for CPF and PSP are a result of an alteration in gene expression, but the changes in protein expression level for CPO are not due to changes in mRNA. As with the results for *NFH*, the results for *GAP-43* agree well with those in the literature, which reported a reduction in *GAP-43* protein expression in N2a cells after treatment with 3 μM CPF and CPO for 4 h (Sachana *et al.*, 2005; Sindi *et al.*, 2016), and 1-10 μM CPO for 24 h (Flaskos *et al.*, 2011).

The largest changes in mRNA expression after treatment with OPs were seen for *GFAP* in differentiating C6 cells. The results for RNA expression normalised to *GADPH* show that exposure to all concentrations of all the OPs resulted in a significant reduction in RNA expression; 1 μ M CPO ($p < 0.05$), 3 and 10 μ M CPO ($p < 0.001$), 1, 3 and 10 μ M CPF ($p < 0.001$), and 1, 3 and 10 μ M PSP ($p < 0.001$). This was a greater reduction than what was seen at the protein level, but the same trend was observed there: increasing concentrations of the OPs resulted in a reduced level of GFAP expression.

The results for the protein levels showed a significant reduction in expression after treatment with 10 μ M CPF ($p < 0.01$), 3 and 10 μ M of both CPO and PSP ($p < 0.01$), which suggest the changes in protein are possibly a result of reduced expression levels and that the gene expression is more sensitive to the OPs. As with the results for the changes in protein expression, the results for the changes in gene levels agree with the different studies published in the literature; both *in vivo* and cell line studies have reported a reduction in GFAP after treatment with certain combinations of CPF and DZO (Garcia *et al.*, 2002; Sidiropoulou *et al.*, 2009b; Wang and Zhao, 2017).

Garcia *et al.* (2001) indicated that CPF disrupted glial development *in vivo* of C6 glioma of the rat, by the disruption of signalling cascades, the inhibition of cell replication, disrupting the activity of nuclear transcription factors involved in cell differentiation and increasing the levels of reactive oxygen species. The results of the current study also fit with the work by Muñoz (2010), who found that 24 h treatment with 10 μ M CPO and CPF significantly reduced the expression of *GFAP* in differentiating C6 cells.

In addition, a study using RT-PCR to detect *GFAP* mRNA in neuroglia of the zebrafish brain to investigate cadmium cytotoxicity after treatment with 1 mg l⁻¹ cadmium chloride for 2, 7 and 16 days, found a considerable reduction in GFAP reactivity in the subependymal layer, the meninges and the outer surface of blood vessels (Monaco *et al.*, 2016). The reduced *GFAP* expression was not due to changes in transcript stability and/or transcription, but instead it was due a reduction of protein in the cells or a reduction in the number of cells (Monaco *et al.*, 2016). Thus, GFAP may be targetted differently at a molecular level by CdCl₂.

In a study of the effect of GFAP knock out, stable transfection of U-251 human astrocytoma cells with an antisense GFAP construct caused suppression of GFAP, and this resulted in a decreased ability to extend processes in response to neurons and a decrease in cell differentiation (Westermarck, 1973; Weinstein *et al.*, 1991). Furthermore, GFAP loss

could be an important step in glial tumour development, or the reduction in *GFAP* expression may signify the secondary loss of a differentiation marker, both of which are important in cancer progression, and can signal progression of the tumour to a more malignant and rapidly growing phenotype (Pekny *et al.*, 1998; Wilhelmsson *et al.*, 2003). Several studies indicated that many malignant astrocytic tumours are GFAP negative, and the majority of high-grade gliomas lose GFAP expression during their development (Jacque *et al.*, 1978; Van der Meulen *et al.*, 1978; Jacque *et al.*, 1979; Velasco *et al.*, 1980; Tascos *et al.*, 1982).

Overall, there is a good correlation between the reduced protein levels observed and the reduced the RNA expression of some but not all of the markers observed, which suggests the cause of the toxicity observed after OP treatment is partly due to genotoxic effects on the key genes, but possibly also due to posttranslational effects on gene products, leading to the morphological changes observed after OP exposure. The results for the expression of these genes agree with the more general studies into the genotoxic effects of OPs; *in vivo* studies in rats and fish have shown that exposure to sub lethal concentrations of CPF can cause DNA damage measured by the Comet assay, in a dose- and time- dependent manner (Sandhu *et al.*, 2013; Ismail *et al.*, 2014; Muller *et al.*, 2014; Wang *et al.*, 2014).

Studies have shown that a variety of biological responses can be induced by genotoxic stress, including transcriptional activation (Dickinson *et al.*, 2004). Histone acetylation is one of the best understood modifications of DNA involved in the epigenetic control of gene expression, and there is a correlation between transcription and histone acetylation levels. Therefore, having demonstrated that the RNA levels are often changed after OP treatments, it is a suitable target to check if OPs induce epigenetic changes (Allfrey *et al.*, 1964; Witt *et al.*, 2009). Histone deacetylases (HDACs) and histone acetyl transferases (HATs) are antagonistic enzymes that regulate gene expression through deacetylation and acetylation of histone proteins around which DNA is wrapped inside the eukaryotic cell nucleus (Ahmad Ganai *et al.*, 2016). Epigenetic modification of histones is an essential principle of how neurons regulate transcriptional responses and adapt to environmental signals (Cho and Cavalli, 2014). The post-translational modification of histones by histone deacetylases (HDACs) and chromatin-modifying enzymes histone acetyltransferases (HATs) shapes chromatin to regulate transcriptional profiles during neuronal development. The epigenetic control of HDACs and the cellular imbalance between HATs and HDACs dictate disease states and has been implicated in loss of memory, muscular dystrophy,

autistic disorders and neurodegeneration. Altering gene expression profiles through inhibition of HDACs is now emerging as a powerful technique (Ahmad Ganai *et al.*, 2016) and epigenetic events have been recently found to play important roles in regulating axon regeneration (Ahmad Ganai *et al.*, 2016). This is further supported by evidence that abnormal HDACs are involved in different diseases including cancer, suggesting analysing HDAC levels in combination with gene expression studies will provide a clearer picture of the effects of OPs (Peng *et al.*, 2015).

Therefore, to further investigate the genotoxic effects of the selected OPs, and to determine if epigenetic changes were involved in these changes, the analysis of HDAC activity in the nuclear extracts of differentiating N2a and C6 cells after treatment with CPF, CPO and PSP for 24 h was carried out using a colorimetric assay. The results showed that there was a significant increase in HDAC activity for all the concentrations of the different OPs, in both cell lines, which occurred in a dose-dependent manner.

The down regulation of gene expression mediated by the up regulating of HDAC activity found in this study is comparable to the published study on the HDAC inhibitor Trichostatin-A, which was found to induce the expression of GAP43, a neural marker for axonal regeneration. It should be noted however, that proteins other than histones can be modulated by acetylation of specific lysine residues. Therefore, HDACs have the potential to have repressive impact on gene expression, restricting transcription factor access to monitoring regions (Gregorette *et al.*, 2004; Haberland *et al.*, 2009). Therefore, the increased activity of HDAC can be correlated to the effects observed on the RNA expression; increased HDAC activity would result in higher levels of heterochromatin meaning less transcription and lower levels of RNA produced. This means that the genotoxic effect, when seen in OP toxicity is partly due the effects of OPs on epigenetic factors, which then causes the altered RNA and can be related to the altered protein levels and other morphological and developmental responses seen in the toxic effects of the OPs.

In the meantime, HDAC's function in neurons and the nervous system remains to be fully elucidated, which is a major impediment; hence, understanding the specific gene expression patterns alongside the accurate specificity and dosage will open a novel aspect in the field and trigger a new wave (Ahmad Ganai *et al.*, 2016).

Overall, the combined results from the mRNA and HDAC assays provide new information on how OPs produce their toxic effects: this occurs in part by altering the expression levels

of the genes investigated. Based on these results, the research could be taken forward by investigating other key genes using these techniques to help develop a better picture of the mechanisms involved in OP toxicity in more relevant human stem cells.

Chapter 6

Organophosphate Toxicity in a Human Neural Progenitor Stem Cell Model

6.1 Introduction

While the main aim of this thesis is to investigate the toxic effects of CPF, CPO and PSP on differentiating mouse and rat neural cell lines, testing the effects of these toxins on cell differentiation and evaluating the gene expression in human stem cell models would add value to this study and to the field. By using neural progenitor stem cells derived from humans, the cellular model will resemble cells of the developing human nervous system neurons *in situ* more closely, which can lead to more accurate predictions of chemical-related changes *in vivo* (Radio and Mundy, 2008).

The first neural stem cells were isolated from different regions of human embryonic brains (Vescovi *et al.*, 1999); however, recent advances have led to the isolation of neural progenitor stem cells from adult human particularly from the neocortex region of the nervous system (Richardson *et al.*, 2006). This makes human neural progenitor stem cells a valuable tool and exciting model for neuroscience research. Using human neural stem cells for evaluating xenobiotic toxicity could diminish the level of uncertainty that is associated with cells derived from animal models (Donato *et al.*, 2007).

Previous research using human neural progenitor stem cells was hampered by the short life span of stem cell cultures, as well as the limited facilities available to maintain both a stable phenotype and genotype across passages (Wright *et al.*, 2006; Donato *et al.*, 2007).

The development of immortalised human neural progenitor stem cells, achieved by using the myc oncogenic transcription factor, overcame these difficulties (Dang *et al.*, 1999; Kim, 2004). The cells' ability to self-renew, generating large numbers of cells, alongside their genomic stability is the fundamental core of immortalisation using myc technology. These characteristics have allowed the use of these cells for toxicity screening (Klemm and Schratzenholz, 2004).

The ReNcell CX cell line is one example of human immortalised neural progenitor stem cell lines that are commercially available (Merck Millipore). They were derived from a 14-week old human foetal brain cortex and, upon mitogen withdrawal in serum free defined medium, they have the ability to differentiate into a mixed population of neurons, astrocytes and oligodendrocytes (Donato *et al.*, 2007; Kornblum, 2007). Due to their immortalisation with myc oncogene transduction, these cells can self-renew, since they are multipotent, in addition to having phenotypic and genetic stability (Donato *et al.*, 2007).

Thus, the ReNcell CX cell line is a suitable model for the assessment of neurotoxicity *in vitro* (Breier *et al.*, 2008). Breier *et al.* (2008) employed ReNcell CX cells in an undifferentiated state, using HTS to measure the effects of chemicals such as lead acetate and methyl mercury chloride on the proliferation and viability of neural stem cells. However, chemical-induced changes in neurite outgrowth in differentiated ReNcell CX cells have yet to be studied. Nor have the underlying molecular effects of CPF, CPO and PSP been evaluated in differentiating human neural stem cell models.

Hence, it was of interest to study the potential effects of OPs using a human-relevant cell model. Furthermore, there was additional interest in determining whether this human neural progenitor stem cell line, which comprises a mixture of neuronal and glial cells at early stages of differentiation, was affected by OP compounds in a manner comparable to differentiating N2a cells described in chapters 3, 4 and 5.

To realize this goal, ReNcell CX cells were utilised as a cell model in co-differentiation exposure conditions similar to those applied to N2a and C6 cells. Cells were exposed to the same concentrations of CPF, CPO and PSP through 24h of differentiation.

MTT reduction assays were also used to assess the viability of cells after exposure to OP compounds. Furthermore, quantitative PCR was used to evaluate the effects of the OP compounds and to confirm the mRNA expression of the mature neural stem cell markers, including β III-tubulin, NF-H and GFAP. Finally, a histone deacetylation assay was carried out to further study the molecular mechanism underlying the genotoxic effects of the OPs of interest in differentiating ReNcell CX cells. The study of both gene expression and histone modification would be a valuable addition to the field of OP toxicity, as this study is the first to tackle these aspects particularly in the ReNcell CX cell model.

6.2 Results

6.2.1 Cell viability in the presence of organophosphates

A 3-(4,5-dimethylthiazol-2-yl)-2,5-diphenyltetrazolium bromide (MTT) reduction assay was used to assess the cells' viability upon exposure to toxins. ReNcell CX cells were differentiated for 24 h (as described in section 2.2.2) with simultaneous exposure to 1, 3 and 10 μM CPF, CPO or PSP. A slight but significant decrease ($P= 0.017$) in MTT reduction was observed with 1 μM CPO. The decrease was slightly more pronounced at 3 and 10 μM CPO ($P= 0.008$ and $P= 0.006$, respectively) (Figure.6.1, panel B). On the other hand, exposure to the same concentrations of CPF and PSP did not have any significant effect on MTT reduction.

In order to monitor any morphological changes, ReNcell CX cells line were assessed after 24 h exposure to different concentrations of CPF, CPO and PSP. Cells were incubated in the absence (0) or presence (1, 3 or 10) μM of CPF, CPO and PSP. They were then fixed and stained with Coomassie Brilliant Blue dyes (Figure 6.2). There were differences in the morphological changes in cells exposed to varying concentrations of CPF, CPO and PSP after 24 h. The proportion of cells exhibiting decreased with increasing concentrations of OPs, it was which difficult to determine changes using Coomassie blue stain, as there was no obvious change in cell density of the stained monolayers was.

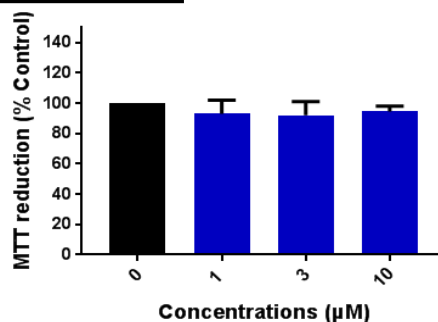
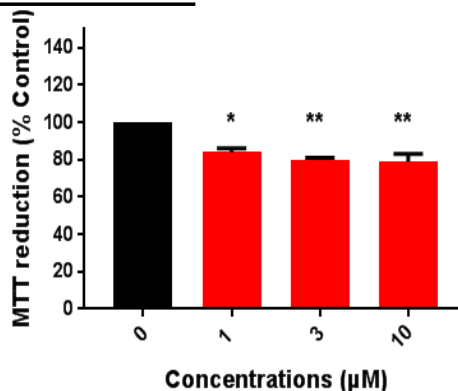
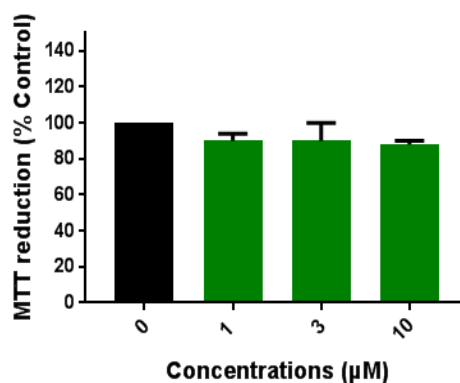
A. CPF in ReNcell CX cells after 24h**B. CPO in ReNcell CX cells after 24h****C. PSP in ReNcell CX cells after 24h**

Figure 6.1. Effects of CPF (A), CPO (B) and PSP (C) on MTT reduction in differentiating ReNcell CX cells.

ReNcell CX cells were exposed to different concentrations (1,3 and 10 µM) of OPs during 24 h of induction of cell differentiation, the levels of MTT reduction were measured to evaluate cell viability. Results are expressed as a mean percentage of the corresponding untreated control \pm SEM from five separate experiments. Statistical significance of data was analysed using one way ANOVA with Sidak post-hoc test comparing treatments to the (0) control (* $p < 0.05$, ** $p < 0.01$).

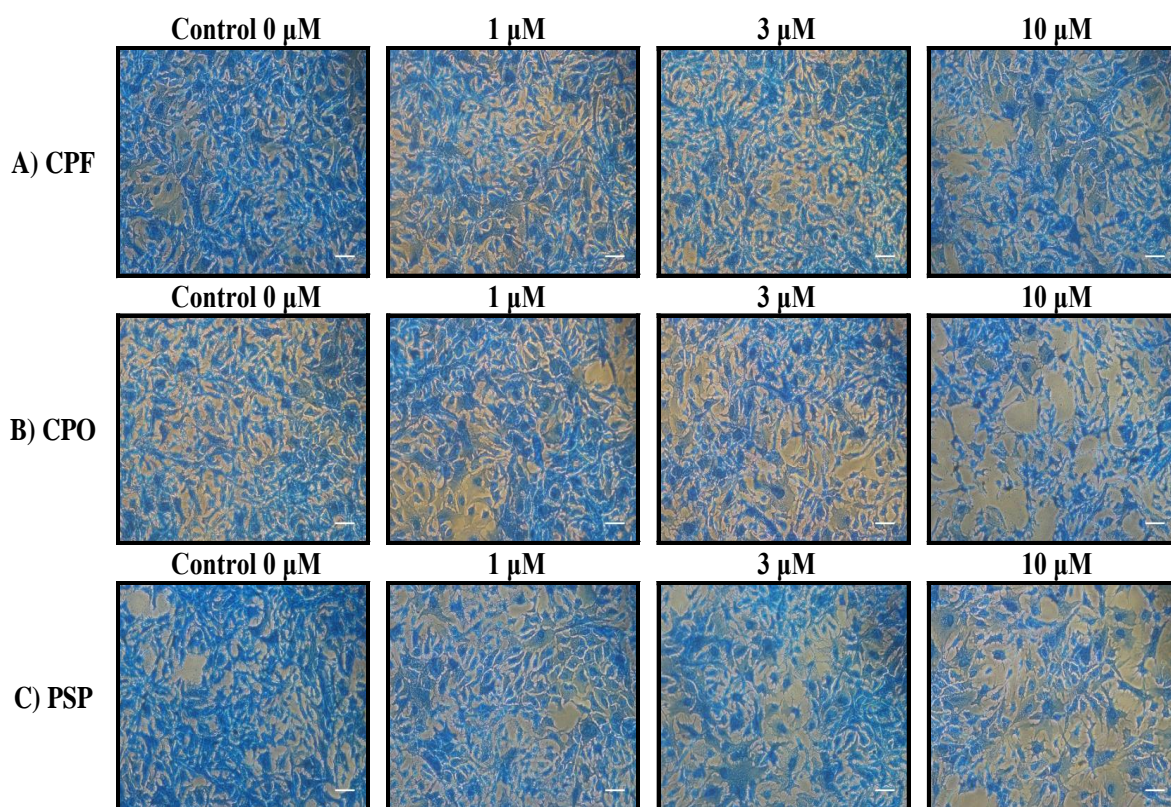


Figure 6.2. Effects of CPF, CPO or PSP on the morphology of differentiating ReNcell CX cells.

ReNcell CX cells were induced to differentiate for 24 h in the presence or absence of 1,3,10 μM CPF, CPO or PSP, as described in Materials and Methods. Shown are images of typical fields of cells viewed by phase contrast microscopy after 24 h differentiation by using an inverted light microscope following methanol fixation and staining with Coomassie blue. Bar represents 15 μm .

6.2.2 Primer validation

The designed primer pairs' specificities were tested prior to running the experiments. ReNcell CX cell total RNA was extracted and reversed transcribed to cDNA. The primers were used to amplify targeted amplicon in the constructed cDNA by conventional PCR.

Figure.6.3 illustrates the primers' specificities and table.6.1 shows the conditions that achieved the best amplification results. The amplified bands in Figure.6.3 were excised and the amplified products were eluted and sequenced then 'blasted' against the genome of *Homo sapiens*. The sequenced PCR products were in a 100% alignment with only their corresponding gene of interest (Appendix 8.9, 8.10), accession numbers are listed in table.6.1.

Table 6.1. Primer sequences and standardised PCR optimisation protocols for the amplification of specific neural markers genes

Gene	Variants	Primer Sequence (5' to 3')	Annealing Tm (C ⁰)	Product size
<i>TUBB3</i>	1. Isoform 1 NM_006086.3	Forward ATTTTCATCTTTGGTCAGAGTGGGGCC	65	121
	2. Isoform 2 NM_001197181.1	Reverse CAGTCGCAGTTTTTCACACTCCTTCC		
<i>NEFH</i>	NM_021076.3	Forward ACTCCCCAAAATTCCCTCTGTGTCC	61	121
		Reverse TTGGGTCTCCTCTGTCTGTTCTCC		
<i>GFAP</i>	1. Variant 1 NM_002055.4	Forward CAGAAGCTCCAGGATGAAACCAACC	63	119
	2. Variant 2 NM_001131019.2	Reverse GACTCAATCTTCCTCTCCAGATCCAGACG		
	3. Variant 3 NM_001242376.1			

GFAP; Glial fibrillary acidic protein, *NEFH*; Neurofilament heavy chain, *TUBB3*; Tubulin β III chain, and Tm; Melting temperature.

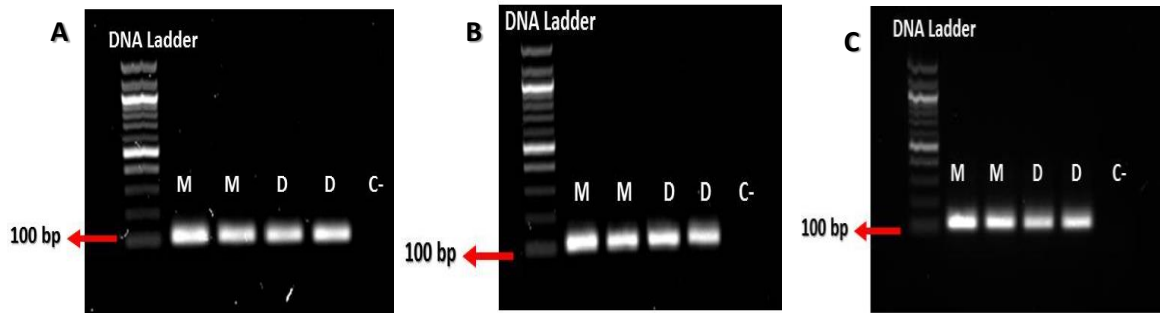


Figure 6.3. Confirmation of PCR for genes of interest in mitotic and differentiating ReNcell CX cells.

A- β III tubulin (*TUBB3*), B- *NEFH*, C-*GFAP*. RNA was obtained from mitotic (M) and differentiating (D) human stem cell and reverse transcribed into cDNA and analysed by PCR. Non-template controls were used as negative controls (C). Bands were visualised after electrophoretic separation in a 1.5% (w/v) agarose gel stained with SyberSafe. Amplified products are presented as a single defined band at size of approximately 100 base-pairs (bp).

6.2.3 Effect of CPF, CPO and PSP on neuronal markers in ReNcell CX cell line.

The mRNA expression level of neuronal markers including *TUBB3*, *NEFH* and *GFAP* was measured in differentiated ReNcell CX cells that were exposed to 1, 3 and 10 μ M concentrations of CPF, CPO and PSP.

Since the expression of neural marker genes in mammalian cell lines of the previous chapter were relative to glyceraldehyde 3-phosphate dehydrogenase (*GAPDH*), the same housekeeping gene was selected as reference gene in the gene expression analysis of differentiating ReNcell CX cells.

6.2.3.1 Tubulin beta-3 chain (*TUBB3*).

TUBB3 mRNA expression level relative to *GAPDH* was significantly reduced upon cells' exposure to 1 ($p= 0.0303$), 3 ($p= 0.0340$) and 10 μ M ($p= 0.0070$) CPF with 10 μ M causing the most significant effect. A concentration of 3 μ M ($p= 0.0005$) of CPO caused the most significant reduction in *TUBB3* mRNA levels. This reduction was also high at a concentration of 10 μ M ($p= 0.0019$) (Figure 6.4, panel A1). PSP exposure did not cause a significant effect until a concentration of 10 μ M ($p= 0.0074$), where the expression dropped in comparison to the control (Figure 6.4, panel A2).

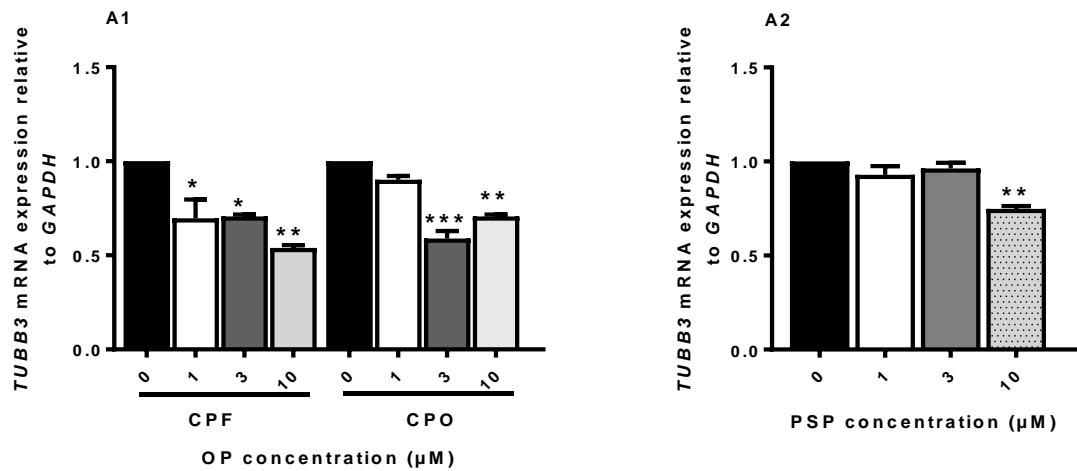


Figure 6.4. Expression of *TUBB3* mRNA in differentiating ReNcell CX cells after CPF, CPO and PSP exposure, as determined by quantitative qPCR.

ReNcell CX cells were induced to differentiate for 24 h with incubation without (0) or with 1, 3 and 10 μM concentrations of CPF, CPO or PSP. Data were analysed using one-way ANOVA with Sidak post-hoc test comparing treatments to the (0) control. The normalization of data was to the housekeeping gene *GAPDH*. Expression values are relative to the non-OP-treated control \pm SEM. Data presented are an average of four independent experiments, and all samples were amplified in triplicate. Asterisks indicate changes that are statistically different from the non-OP-treated controls (* $p < 0.05$, ** $p < 0.01$, or *** $p < 0.001$).

6.2.3.2 Neurofilament heavy chain (NEFH)

CPF did not cause a significant effect on *NEFH*'s mRNA expression levels. On the other hand, CPO caused a significant drop in its expression at a concentration of 3($p = 0.0031$) and 10 ($p = 0.0054$) μM (Figure 6.5, panel A1).

Low concentration of PSP (1 μM) elevated *NEFH* mRNA expression slightly but not significantly compared to the control; however, this effect was linearly reduced with increased PSP concentration but only significant at a concentration of 10 μM ($p = 0.0140$) (Figure 6.5, panel A2).

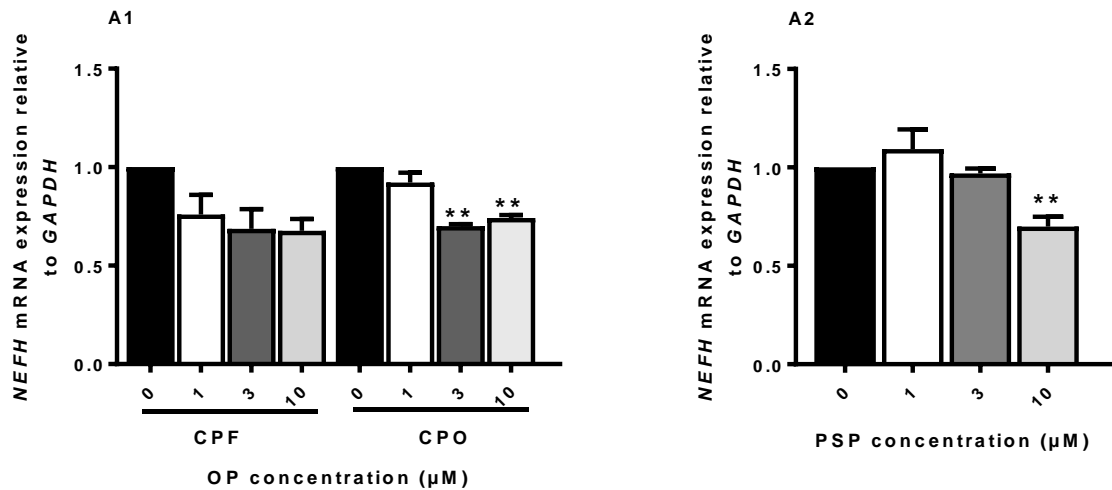


Figure 6. 5. Expression of *NEFH* mRNA in differentiating ReNcell CX cells after CPF, CPO and PSP exposure as determined by quantitative qPCR.

ReNcell CX cells were induced to differentiate for 24 h with incubation without (0) or with 1, 3 and 10 μM concentrations of CPF, CPO or PSP for 24 h. Data were analysed using one-way ANOVA with Sidak post-hoc test comparing treatments to the (0) control. The normalization of data was to the housekeeping gene *GAPDH*. Expression values are relative to the non-OP-treated control \pm SEM. Data presented are an average of four independent experiments, and all samples were amplified in triplicate. Asterisks indicate changes that are statistically different from the non-OP-treated controls (** $p < 0.01$).

6.2.4 Glial fibrillary acidic protein (GFAP)

Exposing the cells to 1 μM ($p=0.0433$) and 3 μM ($p=0.0374$) concentrations of CPF resulted in significant decreases in *GFAP* mRNA expression levels to approximately 50 % of control values. Higher CPF levels of 10 μM ($p=0.0125$) caused a drop in its expression to approximately 25 % of the corresponding control value (Figure 6.6, panel A1). CPO's effect was only significantly observed at a concentration of 10 μM ($p=0.0051$), where it caused an almost 50 % drop in *GFAP* expression (Figure 6.6, panel A1). Exposure to a concentration of 3 μM ($p=0.0123$) and 10 μM ($p=0.0074$) of PSP caused a similar effect to CPF exposure; it decreased *GFAP*'s mRNA expression by more than half of the control value (Figure 6.6, panel A2).

Data of OPs genotoxicity on ReNcell CX cells are summarised in table 6.2.

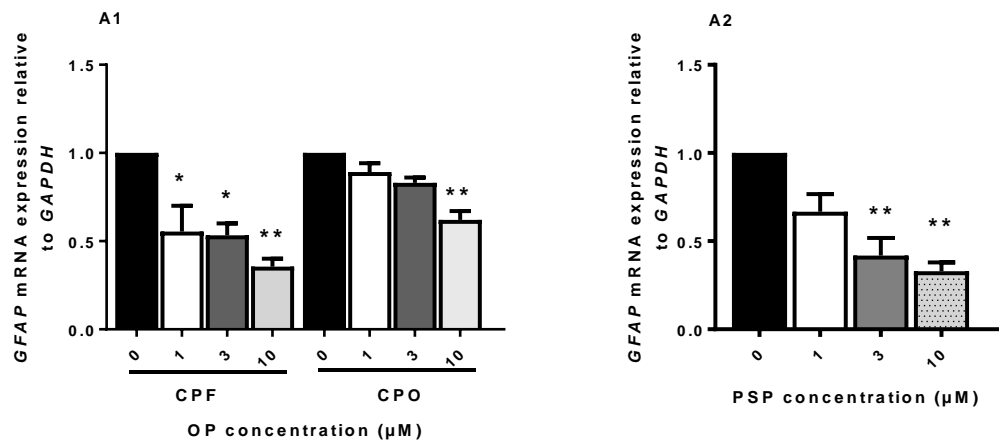


Figure 6.6. Expression of *GFAP* mRNA in differentiating ReNcell CX cells after CPF, CPO and PSP exposure as determined by quantitative qPCR.

ReNcell CX cells were induced to differentiate for 24 h with incubation without (0) or with 1, 3 and 10 μM concentrations of CPF, CPO or PSP for 24 h. Data were analysed using one-way ANOVA with Sidak post-hoc test comparing treatments to the (0) control. The normalization of data was to the housekeeping gene *GAPDH*. Expressions values are relative to the non-OP-treated control \pm SEM. Data presented are an average of four independent experiments, and all samples were amplified in triplicate. Asterisks indicate changes that are statistically different from the non-OP-treated controls (* $p < 0.05$) or (** $p < 0.01$).

Table 6.2. Summary of OP effects on human neural marker genes relative to *GAPDH*

Cells	OPs	CPF			CPO			PSP		
	Conc. (μ M)	1	3	10	1	3	10	1	3	10
ReNcell CX	<i>TUBB3</i>	-1.4↓ (0.03)	-1.4↓ (0.034)	-1.8↓ (0.007)	ns	-1.7↓ (0.0005)	-1.4↓ (0.0019)	ns	ns	-1.3↓ (0.0074)
	<i>NEFH</i>	ns	ns	ns	ns	-1.4↓ (0.0031)	-1.3↓ (0.0054)	ns	ns	-1.4↓ (0.014)
	<i>GFAP</i>	-1.8↓ (0.043)	-1.9↓ (0.037)	-2.8↓ (0.012)	ns	ns	-1.6↓ (0.0051)	ns	-2.4↓ (0.01)	-3.03↓ (0.007)

Value are expressed as fold change relative to the control (0) with the p-value in the parentheses, CPF; Chlorpyrifos, CPO; Chlorpyrifos oxon, PSP; Phenyl saligenin phosphate, *TUBB3*; Tubulin beta-3 chain, *NEFH*; Neurofilament heavy chain, *GFAP*; Glial fibrillary acidic protein.

6.2.5 Histone deacetylases (HDAC) activity upon exposure to CPF, CPO and PSP in differentiating RenCellCX cells.

HDAC activity was measured in differentiating ReNcell CX cells that were exposed to 1, 3 and 10 μM concentrations of CPF, CPO or PSP for 24 h. While different concentrations of both CPF, CPO (Figure 6.7, panel A) and PSP (Figure 6.7, panel B) exposure caused changes in HDAC activity relative to the non OP-treated control, a concentration of 3 μM and 10 μM ($p < 0.05$) of CPF, CPO and PSP (Figure 6.7, panel A) significantly increased its activity.

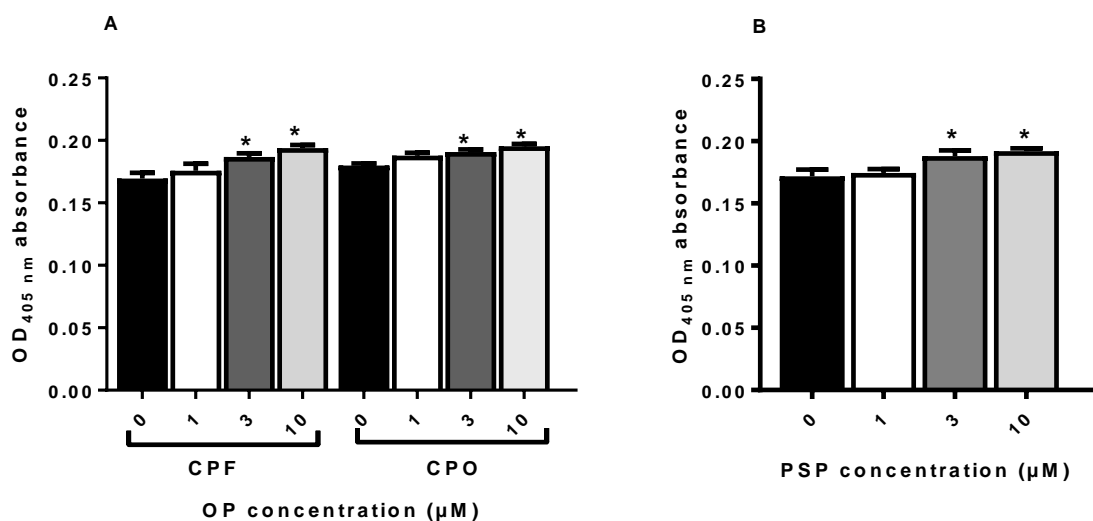


Figure 6.7. Effects of CPF, CPO and PSP on HDAC activity in differentiating ReNcell CX cells.

ReNcell CX cells were induced to differentiate for 24 h with incubation without (0) or with 1, 3 and 10 μM concentrations of CPF, CPO (panel A) or PSP (panel B). Data are presented as mean of the total HDAC activity \pm SEM (from three independent experiments). The significance of differences among different groups was determined by one way-ANOVA with Sidak post-hoc test comparing treatments to the (0) control. Asterisks indicate changes that are statistically different from the non-OP-treated controls ($*p < 0.05$).

6.3 Discussion

The previous chapters in this thesis have shown that in the N2a and C6 cell lines, the selected OPs (CPF, CPO and PSP) at sub-cytotoxic doses (1, 3 and 10 μM) can cause morphological changes to neurite outgrowth without cell death (Chapter 3), which can be linked to changes in the levels of selected cytoskeletal and associated regulatory proteins (MAP 2, Tau, β III tubulin, GAP-43, NFH and GFAP) (Chapter 4), and in turn this can be related to genotoxic effects from reduced mRNA expression of key genes (*MAP2*, *MAPT*, *TUBB3*, *NEFH*, *GAP43* and *GFAP*) and epigenetic changes measured by HDAC activity (Chapter 5).

The use of cell lines can provide a good insight into the effects of the OPs on individual cell types, but they do not provide information as to how the different cell types are affected in the presence of the other cell types; therefore a different system needs to be used to allow the interaction of these cell types to be observed. One such way of doing this is to use a stem cell line, such as ReNcell CX cells. These cells can be induced to differentiate to form a co-culture of different glial and neuronal cell types, which means they offer advantages over the C6 and N2a cell lines as the dendrites and axons formed by ReNcell CX cells have similar complex interactions to those found in developing human neural cells (Bal-Price *et al.*, 2008; Radio and Mundy, 2008). ReNcell CX cells have previously been used in toxicology studies. For example, proliferation and viability assays were used in a high throughput methodology approach to assess 16 compounds, including several that were known to cause developmental neurotoxicity, and the study found this cell line could successfully be used to detect changes in proliferation that were not linked to changes in cell viability (Breier *et al.*, 2008). Further high throughput toxicity screening studies in ReNcell CX cells have involved using the ToxCast Phase I library of 309 chemicals, initially at a dose of 40 μM , then in the range 1 nM–40 μM , in a study that measured proliferation and cytotoxicity compared to the rat PC12 cell line (Radio *et al.*, 2015). The results showed that ReNcell CX cells detected activity in 126 (41 %) of the chemicals with 63 chemicals selectively inhibiting proliferation, and the PC12 cells detected 46 (15 %) chemicals, with similar results between the different doses investigated, highlighting the sensitivity and suitability of the ReNcell CX cell type for this type of study (Radio *et al.*, 2015).

The aims of this chapter were to study the effects of the selected OPs (CPF, CPO and PSP) on a human-relevant cell model to investigate if similar results were obtained as in the N2a

and C6 cell lines. Identical conditions to the cell line studies (1, 3 and 10 μ M CPF, CPO and PSP) were used to treat the differentiating ReNcell CX cells for 24 h before cell viability was measured using MTT reduction assay, and quantitative PCR was used to measure mRNA expression of key markers (*TUBB3*, *NEFH* and *GFAP*), and epigenetic changes were measured by HDAC activity assays.

The results of the MTT assay showed that CPO had a slight inhibitory effect on MTT reduction, with a significantly lower level observed after 24 h treatment with 1, 3 and 10 μ M CPO, yet there were no significant differences for the other OPs. This suggests that there are some differences between the ReNcell CX cells and the N2a and C6 cell types, in that the ReNcell CX are more sensitive to reduced metabolic activity following CPO exposure than are the rodent cell lines. Further work would help to determine if this reflects an effect of CPO on metabolic activity of ReNCell CX cells only, or reduced cell proliferation and viability.

The next step in investigating the effects of the OPs in ReNcell CX cells was to check the specificity of the primer pairs designed to detect β III tubulin (*TUBB3*), *NEFH* and *GFAP*. The primers were used in PCR to amplify the target amplicon in cDNA reverse transcribed from ReNcell CX cells total RNA, and the results produced single defined band of the expected size. After excision and sequencing, all the PCR products were in a 100 % alignment with their corresponding *Homo sapiens* gene of interest, suggesting the primers were suitable for use in detecting changes in the expression of their target genes after treatment with the selected OPs.

The results for the mRNA expression levels show that all of the markers were reduced by at least one concentration of the selected OPs, which is similar to the results from the N2a and C6 cell lines. The results for β III tubulin (*TUBB3*), show that, when normalised to *GAPDH*, there was a significant reduction in mRNA levels after treatment with 1, 3 and 10 μ M CPF; 3 and 10 μ M CPO, and 10 μ M PSP. This has some similarities to the results in the N2a cells, as 10 μ M CPF, CPO and PSP all caused a reduction in mRNA in the N2a cells, but 3 μ M PSP also caused a reduction in mRNA. This suggests that *β III tubulin* mRNA in the ReNcell CX cells is more sensitive to CPF and CPO than in it is the N2a cells.

The results for *NEFH*, when compared to the relevant controls, showed there was a highly significant reduction in mRNA levels after treatment with 3 and 10 μ M CPO and 10 μ M

PSP. This was similar to the results for the N2a cell line, which showed a reduction after CPO treatment, except that in N2a cells there was no significant difference after PSP treatment. This suggests that in the ReNcell CX cells the production of *NEFH* mRNA is more sensitive to PSP than it is in N2a cells.

The results for *GFAP* mRNA levels in ReNCell CX cells, after correction to *GAPDH* levels, show there was a significant reduction after treatment with 1, 3 and 10 μM CPF, 3 and 10 μM PSP, and 10 μM CPO. These results are similar to those for *GFAP* in C6 cells, except that the C6 cells showed a slightly higher sensitivity, as all the concentrations of all 3 OPs produced a significant reduction in mRNA levels.

These results can be compared to those of a previous study that used ReNcell CX cells to investigate the changes in multi-parameters of neurite outgrowth using high throughput analysis for β III tubulin, pNFH and GFAP, and protein levels for β III tubulin and pNFH using ELISA after 8 h exposure to 1-10 μM CPF and CPO (Sindi, 2015).

In order to further investigate if the changes in mRNA were due to epigenetic factors, HDAC activity was monitored in the ReNcell CX cells after treatment with the selected OPs. The results indicated that there was a significant increase in HDAC activity after treatment with 3 and 10 μM CPF. Despite, the increase was also statistically significant with CPO and PSP exposure and, the significance with rodent cell lines were much higher than human ReNcell CX cells. It may be that in a mixed population of cells (e.g. differentiating ReNCell CX cells) not all sub-populations of cells (e.g. neurons, glia and undifferentiated stem cells) are similarly affected in terms of their HDAC activity by OP exposure, thus making a significant increase in HDAC activity more difficult to detect. In this respect, further work at longer exposure times in this cell model would be worthwhile. It could also be that, as suggested by Sindi (2015) some OPs (e.g. CPO) may be detoxified in the ReNCell system. The observed diversity could also be partly due to the distinct origins of the cells. For example, N2a cells are derived from the mouse C1300 tumour (neuroblastoma) (Klebe and Ruddle, 1969), C6 cells are derived a rat glial tumour (Benda *et al.*, 1968) and ReNcell CX cells were produced from human foetal cortex (Donato *et al.*, 2007).

Nevertheless, the trends revealed in this chapter are similar of those observed in the N2a and C6 cells, where there were statistically significant, dose-dependent increases in HDAC activity after treatment with all concentrations of the OP . Increased HDAC activity could

result in higher levels of heterochromatin and less transcription. In addition, my findings are in agreement with the study of Ahmad Ganai *et al.* (2016) in which HDAC inhibitors were found to play protective as well as toxic roles in cells, as it would show whether HDAC upregulation alone was responsible for the changes in mRNA levels observed.

The ReNcell CX results are similar to some other studies in the literature; for example sulforaphane, an organo-sulphur compound, has been shown to inhibit HDAC activity in human prostate cancer cell lines and colon cancer cell lines, resulting in increased expression of key inflammatory markers (Myzak *et al.*, 2004; 2005). Overall, the current work and the above mentioned studies suggest histone acetylation may be one of the key epigenetic changes in neuronal cells during the development of neurotoxicity.

Taken together, these findings could be explained by the fact that N2a and C6 cells are monocultures, whereas ReNcell CX cells are a co-culture of neuronal and glial cells, which might influence the outcome. For example, glial cells produce and secrete neurotrophins such as glial derived neurotrophic factor (Lin, 1996). In a study by the host research group, it was found that conditioned medium from glial cells, and specifically GDNF, protected against the neurite outgrowth inhibitory effect of diazinon in differentiating N2a cells (Harris *et al.*, 2009a). Moreover, the protective effect was found to involve attenuation of the ability of diazinon exposure to reduce the protein levels of NF-H, as detected by densitometric analysis of Western blots probed with the monoclonal antibody N52. It would be interesting to determine whether comparable effects were observed at the mRNA level.

Chapter 7

General Discussion

7.1 General Discussion

OPs, have been widely used as pesticides, and in industrial applications, as their use increased it became apparent that these compounds caused neurotoxicity with the effects seen depending on the dose, age and route of exposure to the OP. Although there are extensive studies highlighting the fact that OPs can cause effects on AChE inhibition, which is the primary acute toxicity target for many of them, there are several other cellular proteins that are proposed targets for OP neurotoxicity, including cytoskeletal proteins, axon growth associated proteins and other proteins involved in cell signalling pathways (Flaskos, 2014). Some developmental processes of the nervous system are controlled by the neuronal cytoskeleton, including proliferation, cell migration, differentiation, morphogenesis, neurite outgrowth, elongation of axons, branching of dendrites, steering of growth cones, and also apoptosis (Hargreaves, 1997; Flaskos, 2014). Hence, the disruption of cytoskeletal proteins can result in serious neural development damage (Flaskos, 2014). Therefore, further studies needed to focus on identifying non-cholinergic targets of OPs, in order to clarify the molecular mechanisms involved in OP-induced toxicity.

Based on previous studies showing that sub-lethal concentrations of CPF and CPO in differentiating mouse N2a neuroblastoma cells inhibited axon outgrowth and disrupted the cytoskeleton (Sachana *et al.*, 2001; Sindi *et al.*, 2016), the overall aims of this thesis were to investigate the effects of sub-cytotoxic concentrations (1, 3 and 10 μM) of CPF, CPO and PSP on differentiating N2a, C6 and ReNcell CX cell lines in terms of cell viability, neurite outgrowth, effects on expression of cytoskeletal proteins, expression of genes encoding key cytoskeletal proteins, and epigenetic regulation of gene expression.

The initial investigations of this thesis involved confirming previous reports of the toxicity of the selected OPs using MTT reduction assays and Trypan blue exclusion for cell viability, and the effects on neurite outgrowth using a manual Coomassie Brilliant Blue assay in differentiating N2a and C6 cells (Sachana *et al.*, 2001; Hargreaves *et al.*, 2006; Sachana *et al.*, 2008; Flaskos *et al.*, 2011; Sindi, 2015). Having confirmed previous results using these approaches, a strong basis was established for the development of a high throughput screen for multiple parameters of neurite outgrowth using differentiating cell monolayers that were

fixed and stained by indirect immunofluorescence with antibodies against NFH and β III tubulin in N2a cells, and GFAP in C6 cells. In this respect, indirect immunofluorescence showed good staining for all the antibodies selected, with differences visible after some of the treatments, suggesting these antigens were suitable markers for use in this study.

The development of high throughput platforms has enabled researchers to evaluate and quantify the neurotoxin exposure effects in a variety of neural cell lines. The observation that 10 μ M CPO reduced cell body area in differentiating C6 cells stained for GFAP after 24 h exposure, is consistent with previous high throughput screening studies in which C6 cells differentiated for 24 h before exposure to 10 μ M CPO for 8 h exhibited reduced cell body area (Sindi, 2015), indicating that one effect of CPO was to induce C6 cells to become more compact. The observed reduction in antibody staining intensity for β III tubulin, NFH and GFAP after treatment with the OPs could be related to reduce neurite length, and is different to the results of previous studies where no changes in staining intensity were observed for these cell types (Sindi, 2015). One reason for these differences could be the longer exposure time (24 h) in the current study compared to the work of Sindi (2015) and the fact that the latter involved the use of pre-differentiated cells as opposed to treatment throughout the course of differentiation in the present work.

The results for the neurite outgrowth markers in the high content assay were similar to the Coomassie blue staining results, as they both indicate reductions in neurite outgrowth due to treatment with the higher concentrations of all three OPs used, which agrees with previous studies that have shown neurite outgrowth impairment in N2a cells after treatment for up to 8h from the point of induction of differentiation with 3 μ M CPF (Sachana *et al.*, 2001; Sachana *et al.*, 2005). A similar concentration dependent response was observed after treatment with CPO for 24 h (Flaskos *et al.*, 2011). After 24 h treatment with PSP, there was no significant effect on cell shape but a concentration dependent reduction in neurite outgrowth in differentiating N2a cells (Hargreaves *et al.*, 2006; Flaskos *et al.*, 2006). The results were also consistent with previous studies in differentiating glial cells which found an inhibitory effect on extension outgrowth following 24 h exposure to 1-10 μ M CPF and CPO in C6 cells (Sachana *et al.*, 2008).

PSP reduced the percentage of cells with significant outgrowth for all markers; for anti- β III tubulin it also caused a significant reduction in maximum and average neurite length/cell (with a greater significant difference than for CPF). For anti-NFH it significantly reduced maximum neurite length and average neurite length/cell. For anti-GFAP it significantly reduced average neurite length/cell which were also affected by CPF but to a lesser extent. These results suggest PSP can affect all the markers investigated with a different response for each marker, and indicate that axon-like processes are most sensitive to PSP, causing disruption of neurofilaments, and that in differentiating neuronal cells PSP caused reduced neurite outgrowth associated with neuronal degeneration and modification of axonal morphology, which are critical events in both neural development and in the induction of OPIDN as mentioned in the literature (Flaskos *et al.*, 1994; Ehrlich and Jortner, 2001; Hargreaves *et al.*, 2006).

CPO treatment produced the largest inhibitory effect in anti-NFH positive (axon-like) neurites for the percentage of cells with significant outgrowth, maximum neurite length/cell, and had a similar effect to PSP on the average neurite length/cell, and in anti-GFAP staining for maximal neurite length/cell, it had a greater effect than PSP on average neurite length/cell. The fact that CPO produced a significant effect on NFH and GFAP suggests it has a relatively potent inhibitory effect on axon-like neurites and glial extensions, which is in agreement with previous studies which have shown CPO was more potent than CPF following 24 h exposure in pre-differentiated rat PC12 pheochromocytoma cells, and in co-differentiated N2a cells, causing inhibited neurite outgrowth, and a reduction in axonal length in embryonic derived primary cultures of sensory and sympathetic neurons (Das and Badone, 1999; Howard *et al.*, 2005; Yang *et al.*, 2008). These results also correlate with studies that have shown CPO can cause a reduction in NFH levels *in vitro* (Flaskos *et al.*, 2011), that CPO can bind tubulin and disrupt polymerisation in bovine brain MT *in vitro* (Grigoryan and Lockridge, 2009), and disrupt the neurofilament network after 24 h treatment with non-cytotoxic neurite inhibitory concentrations of CPO (Flaskos *et al.*, 2011). The morphological changes observed after treatment with CPO occur at similar concentrations found *in vivo* in developing humans (Gupta, 1995; Ostrea *et al.*, 2002; Pelkonen *et al.*, 2006) and therefore can be linked to the developmental neurotoxicity observed (Bramanti *et al.*, 2010; Liu *et al.*, 2012).

CPF caused significant reductions for β III tubulin in average neurite length/cell; for NFH in the percentage of cells with significant outgrowth; and in GFAP for maximal neurite length. CPF caused reduced levels of NFH and can be linked to the ability of CPF to inhibit protein and DNA synthesis. These findings correlate with previous studies (Song *et al.*, 1998; Sachana *et al.*, 2003; 2005; Flaskos *et al.*, 2007).

The reduction in β III tubulin and NFH after treatment with CPF, CPO and PSP could indicate a disruption in the neuronal MT network, and changes, or a breakdown, in the NF networks, which would result in reduced axon stability (Sindi, 2015). The effects on neurite length depend on the OP and dose used, which can easily be measured via the sensitive high content throughput assay, and these axon extensions play a key role in connecting single and multiple neurons (Hjorth *et al.*, 2014).

Based on the preliminary data and the high content analysis, further investigations into how CPF, CPO and PSP exert their effects were planned to investigate if the changes in neurite outgrowth observed were due to changes in expression of neural cell differentiation cytoskeletal and associated regulatory proteins, to help to elucidate the mechanism of action of these OPs more fully. Protein expression for MAP 2, β III tubulin, Tau, NFH, GAP-43 and GFAP, were analysed by quantitative Western blotting and cell ELISA approaches. Studies have shown that proteins, such as NFs and MTs, involved in the neuronal cytoskeletal are key endogenous factors that control normal axonal and neurite outgrowth, neuro-stability and neurodevelopment (Cambray-Deakin, 1991). Previous studies have shown that disruption of the axonal cytoskeleton by OPs is associated with changes in neuronal cell morphology (Lee and Cleveland, 1994).

The investigation of the effect of the OPs on the selected proteins in N2a and C6 cells showed that the OPs did influence protein expression, with a reduction in levels seen for all proteins with at least one OP treatment, but there were no significant differences produced with 1 μ M of any of the OPs, which is different to the morphological results where some of the OPs did cause an effect at this concentration. The levels of protein expression were also investigated by cell ELISA, which produced decreased expression after OP treatment with some similarities to the results of the Western blots, with differences appearing in

sensitivity for some of the markers investigated and the OPs that produced a response.

In that there were reductions in the protein levels of β III tubulin, NFH, GAP-43 and GFAP after treatment with at least one concentration of PSP, CPO and CPF seen in both sets of data. This suggests that the morphological changes observed could be linked to reduce cytoskeletal protein expression levels after treatment with the different OPs, which helps to explain how these OPs produce the neurotoxic effects observed.

The data obtained in this study may reflect the potential impacts of CPF and CPO on memory, since information acquisition and memory storage in the mammalian nervous system which are mainly dependent on changes in the synapses and their protein contents. Increased levels of GAP43 are vital for axonal outgrowth and neuronal connectivity by facilitating the formation of new synapses. GAP43 plays an essential role in synaptic transmission and plasticity (Holtmaat *et al.*, 1995). It has been validated that decreased levels of GAP43 were associated with memory impairment *in vivo* (Rekart *et al.*, 2005). Therefore, the protein changes observed in the current thesis could have induced structural and functional alterations in synaptic plasticity, which represents a cellular mechanism of memory and learning processes (Mansuy and Shenolikar, 2006). Thus, the cytoskeletal disruption observed in cell lines of the current study following OP exposure could reflect a potential to induce cognitive deficits and memory disorders related with aging, dementias or neurodegenerative disease.

The obtained findings for GFAP in the C6 cells are also similar to those previously published, as 24 h treatment with the organophosphorothioate pesticide DZO caused a decrease in GFAP expression (Sidiropoulou *et al.*, 2009b). The findings in this study did produce some differences to those previously published, in that earlier studies found no significant differences in expression for MAP2 after treatment with CPF and CPO in C6 cells, which may be due to the cell type used; and no effect on Tau or NFH of 24 h treatment of differentiating N2a cells with DZO, which highlights the possible differences in OP specificity (Sachana *et al.*, 2008; Sachana *et al.*, 2014).

As the results of the investigations into the effects of the selected OPs on morphological features correlated with the results from the investigations into the changes in expression of the selected cytoskeletal and associated regulatory proteins, the next step in this thesis was to examine if the reductions in expressed protein could be linked to reduced mRNA levels, which would indicate if the OPs caused a genotoxic effect, or whether they were only acting at the protein level. Based on the protein expression results, the key genes *MAP2*, *TUBB3*, *MAPT*, *GAP-43*, *NEFH* and *GFAP*, which encode those proteins, were measured after 24 h exposure to CPF, CPO, and PSP (1, 3 and 10 μ M), and normalised to the reference gene *GAPDH* in differentiating N2a neuroblastoma and C6 cell lines by qPCR analysis of the mRNA expression. To further investigate the actual mechanism of any genotoxicity of these OPs, any significant effects due to epigenetic changes were measured using a colorimetric test to evaluate HDAC activity.

After the initial tests confirmed that the primer pairs amplified the correct genes and *GAPDH* was stably present in the samples, the actual changes in mRNA after treatment with the OPs for 24 h were investigated. The results for the N2a cell line showed that the OPs did affect mRNA levels, but there were no significant differences after treatment with 1 μ M of any of the OPs, which correlates with their effects at the protein level from the Western blot results. In the N2a cell line mRNA changes for *MAP 2* and *TUBB3* correlate well with the reduced protein expression observed in this thesis and the literature from either *in vivo* studies of *MAP 2* (Abou-Donia, 1993; Prendergast *et al.*, 2007; Ruiz-Muñoz *et al.*, 2011), or *in vitro* studies for β III tubulin (Sachana *et al.*, 2008; Sachana *et al.*, 2014), which would suggest that the reduced protein levels are due to changes in gene expression. The N2a cell line mRNA results for *MAPT*, *NEFH* and *GAP-43* show some similarities to the protein level results from this thesis.

According to the important roles of glial cell as mentioned in section 1.1.2, any damage to glial cells and their extensions can severely impede nerve cell function and genesis or alter the integrity of these barriers, which would change the brain micro-environment and affect complex nervous system activity. Astrocytes are a sub set of glial cells and the primary component of the cytoskeletal intermediate filaments (IFs) in these cells is *GFAP* (Pekny *et al.*, 1999). Studies have shown

that GFAP can be substituted by other IF proteins in most situations; however, if IFs are absent in astrocytes, then this can lead to prolonged and impaired healing following injury to the central nervous system (Eliasson *et al.*, 1999). In the current study, we determined that exposure to CPF, CPO and PSP caused reduced expression of *GFAP* possibly due to switching off the gene. Indeed, the largest changes in mRNA expression were observed for *GFAP*, as a significant reduction in expression was observed after treatment with all concentrations of all the OPs. However, the *GFAP* mRNA changes were much greater than those for protein expression, but they both followed a concentration-dependent trend. These protein and mRNA results correlate with the literature results that have shown *in vivo* or *in vitro* reductions in GFAP protein after treatment with CPF, DZO, and CPO (Garcia *et al.*, 2002; Sidiropoulou *et al.*, 2009b; Muñoz, 2010; Wang and Zhao, 2017). Studies on *GFAP*^{-/-} mice have shown there were generally no gross structural CNS, behavioural, or neurologic abnormalities, with astrocytes found in a normal distribution. However, there were changes in myelination, which could lead to reduced contact between myelin sheaths and astrocytes, or oligodendrocytes and astrocytes. This highlights the importance of GFAP in brain development (Gomi *et al.*, 1995; Pekny *et al.*, 1995; Shibuki *et al.*, 1996; Liedtke *et al.*, 1996).

Normally, IFs are depolymerized before cell division, and this process is controlled, in part, by phosphorylation (Ku *et al.*, 1996). Studies have shown that some of the kinases that are involved in cell cycle regulation, such as cell-division cycle 2 (*cdc2*) and protein kinase C, also play a key role in IF phosphorylation (Inagaki *et al.*, 1990; Dalton, 1992; Yong, 1992; Tsujimura *et al.*, 1994). This means that, if the IFs are absent, then there may be an increased availability of these cell cycle kinases to act on their usual substrates that are involved in the cell cycle, which can result in increased proliferation of cells. This is supported by studies that have shown that cultured cells without GFAP, or within astrocytoma that contain both GFAP-positive and GFAP-negative cells, the GFAP-negative fraction have a higher proliferation rate than cells that are GFAP positive, and GFAP negative astrocytes were often found to be a less-mature, blastic and more aggressive cell state (Hara *et al.*, 1991; Weinstein *et al.*, 1991; Kajiwara *et al.*, 1992; Rutka *et al.*, 1994; Pekny *et al.*, 1998; Lee *et al.*, 2005). This is evident in glioblastoma multiforme, which is the most malignant and common form of glioma; it is highly invasive with rapid growth and low GFAP expression, whereas

high expression of GFAP is associated with low-grade astrocytomas (Lee *et al.*, 2005). Also, primary cultures of GFAP^{-/-} astrocytes have been shown to produce a higher final cell saturation density (Pekny *et al.*, 1998). However, *in vivo*, the loss of GFAP does not appear to produce an increase in the transformability of astrocytes (Weinstein *et al.*, 1991; Rutka *et al.*, 1994; Pekny *et al.*, 1998).

The mRNA results showed there were reductions in mRNA levels after treatment with the some of the selected OPs; therefore, to determine if epigenetic changes were involved, the nuclear extracts of differentiating N2a and C6 cells treated with CPF, CPO and PSP for 24 h were analysed for HDAC activity using a colorimetric assay. One of the key epigenetic gene regulation mechanisms in mammals is the control of histone acetylation; this process is carefully balanced by the activity of histone acetyl transferases (HATs) to increase histone acetylation, which is involved in the regulation of gene transcription. It is linked to the activity of histone deacetylase (HDAC), which induce histone hypoacetylation, causing gene silencing (Gallinari, 2007; Ropero and Esteller, 2007). HDACs have also been shown to regulate gene expression in other ways; they can join with nuclear receptors to form corepressor complexes in the absence of a ligand, or they can interact directly with transcription factors, including the retinoblastoma protein (Rb), p53, TFIIE, NF-kB, Stat3, and E2f, to regulate the expression of a large number of genes (Robertson *et al.*, 2000; Lin *et al.*, 2006; Gallinari, 2007).

Studies have shown HDAC1 and HDAC2 are involved with transcription factors, and play a role in transcriptional repression regulated by Rb (Robertson *et al.*, 2000). Tumour development has been linked to mutations and altered expression of HDAC controlling genes, as changes in these genes can affect the transcription of genes that are important in apoptosis, cell-cycle regulation, and cell proliferation, which are all important in regulating crucial cellular functions (Gallinari, 2007; Ropero and Esteller, 2007). The activities of HDACs are tightly regulated through many mechanisms as they are vital cellular regulators, including modulation of deacetylase activity by protein-protein interactions, recruitment of different co-repressor complexes, and by post-translational modifications (Gallinari, 2007). HDACs are not only involved in histone deacetylation, they can also cause the deacetylation of other non-histone proteins as well as regulation of transcription and other biological processes. For example, HDAC1 has been shown to deacetylate p53 (the tumour suppressor) *in vitro* and *in vivo* which can be

important in cancer (Juan *et al.*, 2000; Luo *et al.*, 2000; Gallinari, 2007). Under stress conditions, p53 is usually phosphorylated and acetylated, with the acetylated p53 lysine residues overlapping with the ubiquitination site; acetylation increases protein activation and stability, which is important in permanent cell-division arrest, cell death and checkpoints in the cell-division cycle (Juan *et al.*, 2000; Luo *et al.*, 2000). Due to these roles, HDAC inhibitors are currently being designed and studied as a potential therapy for the treatment of cancer (Ropero and Esteller, 2007).

The findings of the current work showed that there was a significant, dose-dependent increase in HDAC activity in both cell lines for all 3 concentrations of the 3 OPs, which would result in higher levels of heterochromatin meaning less transcription and lower levels of mRNA produced, and this can be linked to the reduced mRNA expression observed for some of the selected markers. Thus, HDACs have repressive effect on gene expression through restricting transcription factor access to monitoring regions (Gregoretto *et al.*, 2004; Haberland *et al.*, 2009).

There are some differences between the mRNA levels and the HDAC results; all the OPs caused changes in HDAC activity, but only some of the OPs affected the mRNA levels of the markers investigated, which suggests that the OPs do affect epigenetic factors and thereby cause the genotoxic effects observed, but the changes in the mRNA may not be solely due to the effects on HDAC.

Overall, for the markers that matched for changes in mRNA and protein expression, the results suggest that the changes in protein were due at least partly to genotoxic effects, which could be due the effects of OPs on epigenetic factors, and that these changes produced the morphological differences observed, which provides new information about how OPs produce their toxic effects.

Based on the results in the N2a and C6 cell lines, experiments were designed to investigate if similar effects of the OPs could be detected in the stem cell line ReNcell CX. The individual cell lines have provided a good insight into how the selected OPs affect cell viability, protein expression, mRNA and HDAC activity, but they don't allow the interactions of the different neural cell types to be examined, whereas ReNcell CX cells can be induced to differentiate to form a co-

culture of different glial and neuronal cell types, allowing the effects of the OPs to be studied in a more human-relevant system.

Interestingly, after 24 h treatment, all concentrations of CPO lowered MTT reduction in the ReNcell CX cells, whereas there were no differences in this parameter for the N2a and C6 cells, which suggests the ReNcell CX cells are more sensitive than N2a or C6 cells to CPO. Whether or not this represents a metabolic effect rather than an effect on cell viability requires further investigation.

After confirming the specificity of the human specific primers, mRNA expression for *TUBB3*, *NEFH* and *GFAP* was investigated in this human neural progenitor stem cell line. The OPs' impact on neural markers genes share some similarities with the N2a and C6 cells, with *TUBB3* in the ReNcell CX cells being more sensitive to CPF and CPO and less sensitive to PSP than in the N2a cells. On the other hand, *NEFH* in the ReNcell CX cells was more sensitive to PSP than it was in the N2a cells, and *GFAP* in C6 cells was more sensitive to all the OPs than it was the ReNcell CX cells. This suggests that the co-culture reacts differently in terms of the response of the individual cell types. A study of the cellular composition of the differentiating stem cell population would help to establish the extent to which the cells are differentiating at this time point in the human cell model, as undifferentiated stem cells may respond differently to establish rodent cell lines with predominantly one cell type. It may also be that different exposure and differentiation conditions are required to simulate a similar state of differentiation in RenCell CX cells as that attained by C6 and N2a cells.

As there was evidence of changes in epigenetic factors in the N2a and C6 cells, the activity of HDAC was also investigated in differentiating ReNcell CX cells. The data obtained suggest that HDAC activity was increased with increasing the OP concentration but that the differences were not statistically significant in the human model. This suggests that in the rodent cell lines there was a general decrease in transcription which resulted in reduced levels of mRNA. The weaker effect in RenCell CX cells may reflect the complexity of the stem cell model, which requires investigation under a wider range of experimental conditions as discussed above.

7.2 Conclusions

In conclusion the data reported in this thesis have established that:

- Sub-lethal concentrations of CPF, CPO and CPF inhibit the outgrowth of neurites in differentiating N2a, C6 and RenCellCX cells;
- Neurite inhibitory effects are associated with reduced levels of key cytoskeleton proteins in the axons and dendrites of differentiating N2a cells and of the intermediate filament protein GFAP in differentiating C6 cells;
- Changes in mRNA levels account at least in part for changes in protein expression;
- Inhibition of HDAC activity may contribute to the genotoxic effect of OPs with known developmental neurotoxicity;
- Similar changes in mRNA levels for β II tubulin, NF-H and GFAP were confirmed in a more human relevant model;
- Thus, the OPs tested not only act through inhibition of AChE to produce neurotoxicity, but they also act through suppression of key cytoskeletal protein expression via genotoxic effects. The combination of the cell types in the ReNcell CX cell line provides a more human relevant response to the OPs as the two cell types can interact, and therefore this cell line is suitable for use in further studies to help elucidate the mechanisms of how OPs cause neurotoxicity (Figure 7.1).

7.3 Future work

Overall the work presented in this thesis that has shown the selected OPs can produce a neurotoxic effect, involving disruption of cytoskeletal proteins/genes that are important in neural development. The results also confirm that AChE inhibition is not the only way that OPs produce a neurotoxic effect. To further enhance these results, there are several areas that could be considered for future work:

- Two-dimensional PAGE and MALDI-TOF mass spectrometry could be used after exposure to sub-cytotoxic concentrations of CPF, CPO and PSP, as

this would help identify the further changes in protein expression and identify any interacting proteins.

- The levels of DNA damage after treatment with sub-cytotoxic concentrations of CPF, CPO and PSP could be determined using the Comet assay, as this would help to clarify the genotoxic effects of these OPs by combining these results with the changes in mRNA levels and epigenetic results.
- It would also be of interest to investigate the ability of these OPs at sub-cytotoxic concentrations to alter histone acetylation using anti-acetylated histone antibodies or to cause changes in other epigenetic factors, such as DNA methylation.
- It would be interesting to analyse the promoter regions of those genes whose mRNA changes in the presence of OPs - to see if all those genes are controlled by the same transcription factors (as a possible mechanism: OP modifies transcription factor activity and, therefore, all genes dependent on that transcription factor are affected).
- Studies have shown that about 5 % of CPF is converted to CPO in humans (Eyer *et al.*, 2009; therefore the effects on neurite outgrowth of exposure to a mixture of CPF at a similar concentration to that used in this study with a much smaller amount of CPO, for example using a ratio of 1:20 CPO:CPF, together with longer exposure times merits investigation.
- Longer differentiation times could be applied to achieve a more comprehensive model of developmental toxicity. Extending the exposure time with lower concentrations or using repeat exposures could also have an effect on the extent of neurotoxicity both *in vitro* and *in vivo*.
- Similar approaches could also be used in N2a, C6 or ReNcell CX cells to investigate the effects of CPF, CPO and PSP on other neural markers such as (e.g. cofilin), which regulate microfilament dynamics in neural development , as such targets were found to be affected by diazinon exposure in previous work (Harris *et al.*, 2009).

- Further studies could be carried out in the ReNcell CX cells by using the high throughput analysis system described in this thesis. The system could be optimised for other important biomarkers, such as choline acetyl transferase to detect changes in cholinergic neurons, tyrosine hydroxylase to detect changes in dopaminergic neurons, and myelin basic proteins to detect changes in oligodendrocytes exposure to CPF, CPO and PSP, and in comparison to non-differentiated neural stem cells identified from monolayers counter-stained with anti-nestin antibodies.
- Further studies could be performed on the mechanisms of “switching off” of *GFAP* expression or the level of regulations of transcription factors after OPs exposure on various of neural developmental models.
- Further studies are also desirable with co-cultures or 3D culture models to enhance cell-cell interactions to simulate in vivo tissue organisation more closely.

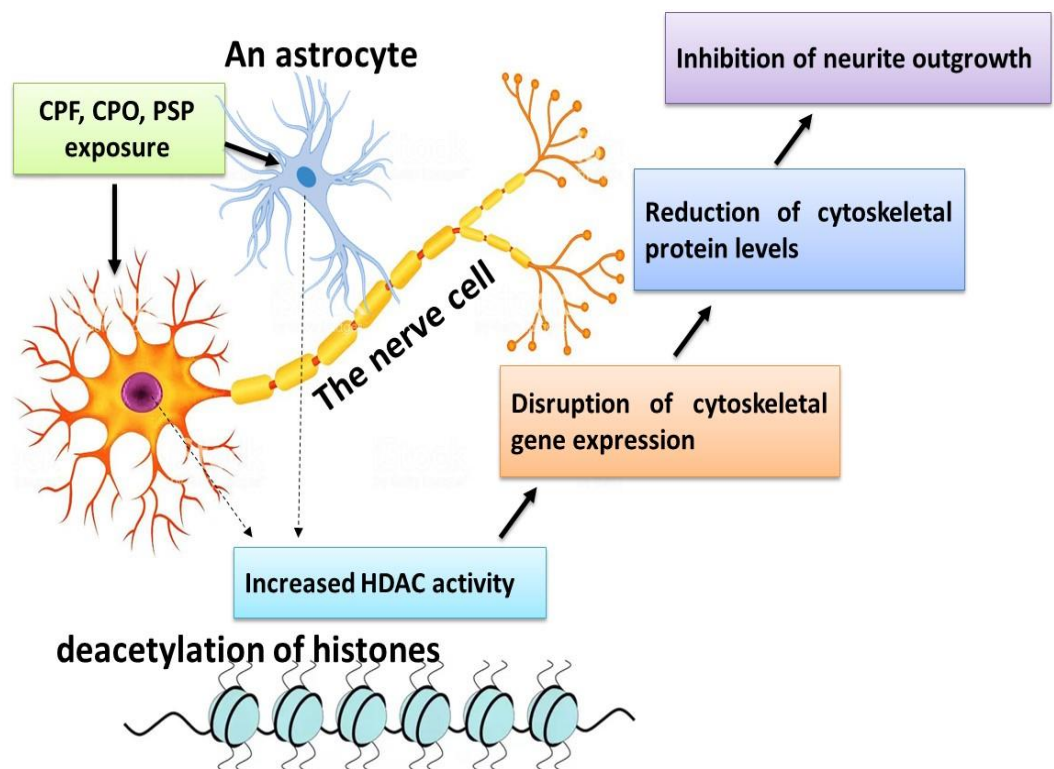


Figure 7.1. Schematic diagram of common CPF, CPO and PSP impacts on neural cells.

- OPs have been widely used as pesticides and in industrial applications.
- These compounds caused neurotoxicity with the effects seen depending on the dose, age and route of exposure to the OP.
- Sub-lethal concentrations of CPF, CPO and PSP inhibited axon outgrowth, disrupted the cytoskeleton in differentiating mouse N2a neuroblastoma cells.



Synopsis of PhD thesis

- What are the impacts of CPF, CPO or PSP on mammalian cell lines and human stem cells?
- Are the alterations in proteins expression of neural markers associated with genotoxic effects of OPs?
- Could OPs cause epigenetic impacts on the tested cell lines?
- Are these changes responsible for the morphological differences or neurodegenerative effects?

The objectives

Evaluate the effects of the selected OPs on: **1)** disruption of neurite outgrowth, **2)** expression of cytoskeletal proteins, **3)** their associated gene expression levels, and **4)** to investigate the molecular mechanism(s) involved in altered gene expression changes by analysing histone deacetylation in cell models using differentiating N2a, C6 and ReNcell CX cell lines.

Cell viability	Neurite outgrowth	Expression of cytoskeletal proteins	Expression of genes	Epigenetic regulation
<ul style="list-style-type: none"> • No changes in cell number, suggesting any changes observed cell morphology after the sub-lethal exposure were due to the effect of the OP and not cell death. 	<ul style="list-style-type: none"> • Disruption of axons, neurite outgrowth and neurodevelopment. • Reduced axon stability as result of βIII tubulin and NFH reduction which indicate a disruption in the MT network and changes in the NF network. • Reduced the neurite length and the average of neural length following OP exposure with anti GFAP in glial astrocyte cells. • Reduction in staining intensity for βIII tubulin, NFH and GFAP after treatment of the OPs, which could be related to reduced neurite length. • Changes in neural cell morphology 	<ul style="list-style-type: none"> • Reduction in the protein level of neural markers proteins. • reduced GFAP levels caused disruption of astrocyte intermediate filaments. 	<ul style="list-style-type: none"> • Alterations gene expression of the selected neural markers. 	<ul style="list-style-type: none"> • HDACs have the potential to have repressive impact on gene expression. • OPs affect the epigenetic factors and can cause the genotoxic effects observed.

References

- Abdollahi, M. and Karami-Mohajeri, S. (2012). A comprehensive review on experimental and clinical findings in intermediate syndrome caused by organophosphate poisoning. *Toxicology and Applied Pharmacology*, 258(3), pp.309-314.
- Abou-Donia, M. B. (1995). Involvement of cytoskeletal proteins in the mechanism of organophosphorus ester-induced delayed neurotoxicity. *Clinical and Experimental Pharmacology and Physiology*, 22(5), pp.358-359.
- Abou-Donia, M.B. (1981). Organophosphorus ester-induced delayed neurotoxicity. *Annual Review of Pharmacology and Toxicology*, 21(1), pp.511-548.
- Abou-Donia, M.B. (1993). The cytoskeleton as a target for organophosphorus ester-induced delayed neurotoxicity (OPIDN). *Chemico-Biological Interactions*, 87(1-3), pp.383-393.
- Abou-Donia, M.B. (2003). Organophosphorus ester-induced chronic neurotoxicity. *Archives of Environmental Health: An International Journal*, 58(8), pp.484-497.
- Abou-Donia, M.B. and Lapadula, D.M. (1990). Mechanisms of organophosphorus ester-induced delayed neurotoxicity: type I and type II. *Annual Review of Pharmacology and Toxicology*, 30(1), pp.405-440.
- Abou-Donia, M.B., Lapadula, D.M. and Suwita, E. (1988). Cytoskeletal proteins as targets for organophosphorus compound and aliphatic hexacarbon-induced neurotoxicity. *Toxicology*, 49(2-3), pp.469-477.
- Abraham, V.C., Taylor, D.L. and Haskins, J.R. (2004). High content screening applied to large-scale cell biology. *Trends in Biotechnology*, 22(1), pp.15-22.
- Ackerley, S., Thornhill, P., Grierson, A.J., Brownlees, J., Anderton, B.H., Leigh, P.N., Shaw, C.E. and Miller, C.C. (2003). Neurofilament heavy chain side arm phosphorylation regulates axonal transport of neurofilaments. *The Journal of Cell Biology*, 161(3), pp.489-495.
- ACP, A. C. O. P. (2002). ACP annual reports. Chlorpyrifos. *London*.
- AgroNews (2013). 2012 China`s major pesticides varieties trackingchlorpyrifos. [Online]. Available: <http://news.agropages.com/news/newsdetail8993.htm>.
- Ahmad Ganai, S., Ramadoss, M. and Mahadevan, V. (2016). Histone Deacetylase (HDAC) Inhibitors-emerging roles in neuronal memory, learning, synaptic plasticity and neural regeneration. *Current Neuropharmacology*, 14(1), pp.55-71.
- Akassoglou, K., Malester, B., Xu, J., Tessarollo, L., Rosenbluth, J. and Chao, M.V. (2004). Brain-specific deletion of neuropathy target esterase/Swiss cheese results in neurodegeneration. *Proceedings of the National Academy of Sciences*, 101(14), pp. 5075-5080.
- Alarcon, W.A., Calvert, G.M., Blondell, J.M., Mehler, L.N., Sievert, J., Propeck, M., Tibbetts, D.S., Becker, A., Lackovic, M., Soileau, S.B. and Das, R. (2005). Acute illnesses associated with pesticide exposure at schools. *Jama*, 294(4), pp.455-465.
- Al-Bader, M.D. and Al-Sarraf, H.A. (2005). Housekeeping gene expression during fetal brain development in the rat—validation by semi-quantitative RT-PCR. *Developmental Brain Research*, 156(1), pp.38-45.
- Albers, J.W., Berent, S., Garabrant, D.H., Giordani, B., Schweitzer, S.J., Garrison, R.P. and Richardson, R.J. (2004). The effects of occupational exposure to chlorpyrifos on the neurologic examination of central nervous system function: a prospective cohort study. *Journal of Occupational and Environmental Medicine*, 46(4), pp. 367-378
- Alberts, B., Bray, D., Lewis, J., - Raff, M., Roberts, K and Watson, J. D. (1983). *Molecular biology of the cell* (2nd Edition), Garland Publishing Inc., *New York*.

- Alexander, J.E., Hunt, D.F., Lee, M.K., Shabanowitz, J., Michel, H., Berlin, S.C., Macdonald, T.L., Sundberg, R.J., Rebhun, L.I. and Frankfurter, A. (1991). Characterization of posttranslational modifications in neuron-specific class III beta-tubulin by mass spectrometry. *Proceedings of the National Academy of Sciences*, 88(11), pp.4685-4689.
- Allen, N.J. and Barres, B.A. (2009). Neuroscience: glia—more than just brain glue. *Nature*, 457(7230), p.675.
- Allfrey, V. G., Faulkner, R. and Mirsky, A. E. (1964). Acetylation and methylation of histones and their possible role in the regulation of RNA synthesis. *Proceedings of the National Academy of Sciences of the United States of America*, 51(5), pp. 786-794.
- Altman-Price, N. and Mevarech, M. (2009). Genetic evidence for the importance of protein acetylation and protein deacetylation in the halophilic archaeon *Haloferax volcanii*. *Journal of Bacteriology*, 191(5), pp.1610-1617.
- Amer, S.M. and Fahmy, M.A. (1982). Cytogenetic effects of pesticides: I. Induction of micronuclei in mouse bone marrow by the insecticide Dursban. *Mutation Research/Genetic Toxicology*, 101(3), pp.247-255.
- Amer, S.M., Fahmy, M.A. and Donya, S.M. (1996). Cytogenetic effect of some insecticides in mouse spleen. *Journal of Applied Toxicology*, 16(1), pp.1-3.
- Andrieux, A., Salin, P.A., Vernet, M., Kujala, P., Baratier, J., Gory-Fauré, S., Bosc, C., Pointu, H., Proietto, D., Schweitzer, A. and Denarier, E. (2002). The suppression of brain cold-stable microtubules in mice induces synaptic defects associated with neuroleptic-sensitive behavioral disorders. *Genes and Development*, 16(18), pp.2350-2364.
- Antel, J. (2006). Oligodendrocyte/myelin injury and repair as a function of the central nervous system environment. *Clinical Neurology and Neurosurgery*, 108(3), pp.245-249.
- Antonijevic, B. and Stojiljkovic, M.P. (2007). Unequal efficacy of pyridinium oximes in acute organophosphate poisoning. *Clinical Medicine and Research*, 5(1), pp.71-82.
- Aschner, M., Allen, J., Kimelberg, H., LoPachin, R. and Streit, W. (1999). Glial cells in neurotoxicity development. *Annual Review of Pharmacology and Toxicology*, 39(1), pp.151-173.
- Aspelin, A. (1997). Pesticides industry sales and usage. Washington, DC: Biological and Economic Analysis Division, Office of Pesticide Programs, Office of Prevention, Pesticides and Toxic Substances, U.S. Environmental Protection Agency.
- Atherton, K.M., Williams, F.M., Egea González, F.J., Glass, R., Rushton, S., Blain, P.G. and Mutch, E. (2009). DNA damage in horticultural farmers: a pilot study showing an association with organophosphate pesticide exposure. *Biomarkers*, 14(7), pp.443-451.
- Atherton, K.M., Williams, F.M., Jameson, S. and Mutch, E. (2006). DNA damage by dichlorvos and repair profiles in human lymphocytes, *in vitro*. *Toxicology*, 226(1), p.53.
- Bagchi, D., Bhattacharya, G., and Stohs, S. (1996). *In vitro* and *in vivo* induction of heat shock (stress) protein (Hsp) gene expression by selected pesticides. *Toxicology*, 112(1), pp.57-68.
- Bagchi, D., Hassoun, E.A., Bagchi, M., Muldoon, D.F. and Stohs, S.J. (1995). Oxidative stress induced by chronic administration of sodium dichromate [Cr (VI)] to rats. *Comparative Biochemistry and Physiology Part C: Pharmacology, Toxicology and Endocrinology*, 110(3), pp.281-287.
- Baker, P.E., Cole, T.B., Cartwright, M., Suzuki, S.M., Thummel, K.E., Lin, Y.S., Co, A.L., Rettie, A.E., Kim, J.H. and Furlong, C.E. (2013). Identifying safer anti-wear triaryl phosphate additives for jet engine lubricants. *Chemico-Biological Interactions*, 203(1), pp.257-264.

- Bal-Price, A.K., Suñol, C., Weiss, D.G., van Vliet, E., Westerink, R.H. and Costa, L.G. (2008). Application of *in vitro* neurotoxicity testing for regulatory purposes: symposium III summary and research needs. *Neurotoxicology*, 29(3), pp.520-531.
- Bamburg, J.R., Bray, D. and Chapman, K. (1986). Assembly of microtubules at the tip of growing axons. *Nature*, 321 (6072), pp. 788-790 .
- Banker, G. and Goslin, K. eds. (1998). Culturing nerve cells. MIT press.
- Barone, J.S., Das, K.P., Lassiter, T.L. and White, L.D. (2000). Vulnerable processes of nervous system development: a review of markers and methods. *Neurotoxicology*, 21(1-2), pp.15-36 .
- Barra, H.S., Arce, C.A. and Argaraña, C.E. (1989). Posttranslational tyrosination/detyrosination of tubulin. In *Molecular Neurobiology*, pp. 133-153. Humana Press
- Barres, B. and Barde, Y. (2000). Neuronal and glial cell biology. *Current Opinion in Neurobiology*, 10(5), pp.642-648.
- Benda, P., Lightbody, J., Sato, G., Levine, L. and Sweet, W. (1968). Differentiated rat glial cell strain in tissue culture. *Science*, 161(3839), pp.370-371.
- Benowitz, L.I. and Routtenberg, A. (1997). GAP-43: an intrinsic determinant of neuronal development and plasticity. *Trends in Neurosciences*, 20(2), pp.84-91.
- Bergen, L.G. and Borisy, G.G. (1980). Head-to-tail polymerization of microtubules *in vitro*. Electron microscope analysis of seeded assembly. *The Journal of Cell Biology*, 84(1), pp.141-150.
- Berger-Sweeney, J. and Hohmann, C.F. (1997). Behavioral consequences of abnormal cortical development: insights into developmental disabilities. *Behavioural Brain Research*, 86(2), pp.121-142.
- Berridge, V.M. and Tan, S.A. (1992). Characterization of the cellular reduction of 3-(4,5-dimethylthiazol-2-yl)-2,5-diphenyltetrazolium bromide (MTT): subcellular localization, substrate dependence, and involvement of mitochondria electron transport in MTT reduction. *Archives of Biochemistry and Biophysics*, 303(2), pp.474-482.
- Betancourt, A.M. and Carr, R.L. (2004). The effect of chlorpyrifos and chlorpyrifos-oxon on brain cholinesterase, muscarinic receptor binding, and neurotrophin levels in rats following early postnatal exposure. *Toxicol Sci*, 77(1), pp. 63-71.
- Binder, L.I., Frankfurter, A. and Rebhun, L.I. (1985). The distribution of tau in the mammalian central nervous system. *The Journal of Cell Biology*, 101(4), pp.1371-1378.
- Bjørning-Poulsen, M., Andersen, H.R. and Grandjean, P. (2008). Potential developmental neurotoxicity of pesticides used in Europe. *Environmental Health*, 7(1), p.50.
- Black, M.M. and Greene, L.A. (1982). Changes in the colchicine susceptibility of microtubules associated with neurite outgrowth: studies with nerve growth factor-responsive PC12 pheochromocytoma cells. *The Journal of Cell Biology*, 95(2), pp.379-386.
- Black, M.M. and Lasek, R.J. (1980). Slow components of axonal transport: two cytoskeletal networks. *The Journal of Cell Biology*, 86(2), pp.616-623.
- Bolognesi, C. (2003). Genotoxicity of pesticides: a review of human biomonitoring studies. *Mutat Res*, 543(3), pp. 251-72.
- Bramanti, V., Tomassoni, D., Avitabile, M., Amenta, F. and Avola, R. (2010). Biomarkers of glial cell proliferation and differentiation in culture. *Front Biosci (Schol Ed)*, 2, pp.558-570.

- Breier, J.M., Gassmann, K., Kayser, R., Stegeman, H., De Groot, D., Fritsche, E. and Shafer, T.J. (2010). Neural progenitor cells as models for high-throughput screens of developmental neurotoxicity: state of the science. *Neurotoxicology and Teratology*, 32(1), pp.4-15.
- Breier, J.M., Radio, N.M., Mundy, W.R. and Shafer, T.J. (2008). Development of a high-throughput screening assay for chemical effects on proliferation and viability of immortalized human neural progenitor cells. *Toxicological Sciences*, 105(1), pp.119-133.
- Brown, A. G. (1991). An introduction to neuroscience in nerve cells and the nervous system. Springer-Verlag, London, pp. 117-125.
- Burgoyne, R. D. (1991). The neuronal cytoskeleton, New York, Wiley-Liss Inc.
- Caceres, A., Banker, G., Steward, O., Binder, L. and Payne, M. (1984). MAP2 is localized to the dendrites of hippocampal neurons which develop in culture. *Developmental Brain Research*, 13(2), pp.314-318.
- Calvert, G.M., Plate, D.K., Das, R., Rosales, R., Shafey, O., Thomsen, C., Male, D., Beckman, J., Arvizu, E. and Lackovic, M. (2004). Acute occupational pesticide-related illness in the US, 1998–1999: Surveillance findings from the SENSOR-pesticides program. *American Journal of Industrial Medicine*, 45(1), pp.14-23.
- Cambray-Deakin, M.A. (1991). Cytoskeleton of the growing axon. *The Neuronal Cytoskeleton*, pp.233-255.
- Campbell, C.G., Seidler, F.J. and Slotkin, T.A. (1997). Chlorpyrifos interferes with cell development in rat brain regions. *Brain Research Bulletin*, 43(2), pp.179-189.
- Carlson, K. and Ehrich, M. (2001). Organophosphorus compounds alter intracellular F-actin content in SH-SY5Y human neuroblastoma cells. *Neurotoxicology*, 22(6), pp.819-827.
- Carlson, K., Jortner, B.S. and Ehrich, M. (2000). Organophosphorus compound-induced apoptosis in SH-SY5Y human neuroblastoma cells. *Toxicology and Applied Pharmacology*, 168(2), pp.102-113.
- Carlton, E.J., Moats, H.L., Feinberg, M., Shepard, P., Garfinkel, R., Whyatt, R. and Evans, D. (2004). Pesticide sales in low-income, minority neighborhoods. *Journal of Community Health*, 29(3), pp.231-244.
- Carrington, C.D., Carrington, M.N. and Abou-Donia, M.B. (1985). Neurotoxic esterase in cultured cells: an *in vitro* alternative for the study of organophosphorous compound-induced delayed neurotoxicity. *Alternative Methods In Toxicology*, USA.
- Chambers, J.E. (2004). Organophosphates, Serine Esterase Inhibition, and Modeling of Organophosphate Toxicity. *Toxicological Sciences*, 77(2), pp.185-187.
- Chan, W.Y., Kohsaka, S. and Rezaie, P. (2007). The origin and cell lineage of microglia—New concepts. *Brain research reviews*, 53(2), pp.344-354
- Chen, X., Foote, A.G. and Thibeault, S.L. (2017). Cell density, dimethylsulfoxide concentration and needle gauge affect hydrogel-induced bone marrow mesenchymal stromal cell viability. *Cytotherapy*, 19(12), pp.1522-1528.
- Cho, Y. and Cavalli, V. (2014). HDAC signaling in neuronal development and axon regeneration. *Current Opinion in Neurobiology*, 27, pp.118-126.
- Choi, S.H., Kim, Y.H., Hebisch, M., Sliwinski, C., Lee, S., D’Avanzo, C., Chen, H., Hooli, B., Asselin, C., Muffat, J. and Klee, J.B. (2014). A three-dimensional human neural cell culture model of Alzheimer’s disease. *Nature*, 515(7526), p.274.

- Choudhary, S., Verma, K., Raheja, G., Kaur, P., Joshi, K., and Gill, D. (2006). The l-type calcium channel blocker Nimodipine mitigates cytoskeletal proteins phosphorylation in Dichlorvos-Induced delayed Neurotoxicity in rats. *Basic and Clinical Pharmacology and Toxicology*, 98(5), pp.447-455.
- Clegg, D.J. and Van Gemert, M. (1999a). Determination of the reference dose for chlorpyrifos: proceedings of an expert panel. *Journal of Toxicology and Environmental Health Part B: Critical Reviews*, 2(3), pp.211-255.
- Clegg, D.J. and Van Gemert, M. (1999b). Expert panel report of human studies on chlorpyrifos and/or other organophosphate exposures. *Journal of Toxicology and Environmental Health Part B: Critical Reviews*, 2(3), pp.257-279.
- Cleveland, D. W. (1993). Tubulin and associated proteins. In: KREIS, T. and VALE, R. (eds.) Guidebook to the cytoskeletal and motor proteins Oxford: Oxford University Press .
- Colborn, T. (2006). A Case for Revisiting the Safety of Pesticides: A Closer Look at Neurodevelopment. *Environmental Health Perspectives*, 114(1), pp.10-17.
- Compston, A., Zajicek, J., Sussman, J., Webb, A., Hall, G., Muir, D., Shaw, C., Wood, A. and Scolding, N. (1997). Review: Glial lineages and myelination in the central nervous system. *Journal of Anatomy*, 190(2), pp.161-200.
- Cooper, G.M. and Hausman, R.E. (2000). The cytoskeleton and cell movement. The cell: a molecular approach, 2nd edn. ASM Press; Sinauer Associates, Washington, DC Sunderland, Mass., pp xxiv, 689.
- Coronado, G.D., Vigoren, E.M., Thompson, B., Griffith, W.C. and Faustman, E.M. (2006). Organophosphate pesticide exposure and work in pome fruit: evidence for the take-home pesticide pathway. *Environmental Health Perspectives*, 114(7), p.999.
- Costa, L.G. (2006). Current issues in organophosphate toxicology. *Clinica Chimica Acta; International Journal of Clinical Chemistry*, 366(1-2), pp. 1-13 .
- Costa, L.G., Giordano, G., Cole, T.B., Marsillach, J. and Furlong, C.E. (2013). Paraoxonase 1 (PON1) as a genetic determinant of susceptibility to organophosphate toxicity. *Toxicology*, 307, pp.115-122.
- Costa, L.G., Vitalone, A., Cole, T.B. and Furlong, C.E. (2005). Modulation of paraoxonase (PON1) activity. *Biochemical Pharmacology*, 69(4), pp. 541-550 .
- Cox, C. (1994). Chlorpyrifos, part 1: toxicology. *Journal of Pesticide Reform*, 14(4), pp.15-20.
- Craig, A. M. and Banker, G. (1994). Neuronal polarity. *Annual Review of Neuroscience*, 17, 267-310 .
- Croom, E.L., Wallace, A.D. and Hodgson, E. (2010). Human variation in CYP-specific chlorpyrifos metabolism. *Toxicology*, 276(3), pp.184-191.
- Crumpton, T., Seidler, F. and Slotkin, T. (2000a). Developmental neurotoxicity of chlorpyrifos *in vivo* and *in vitro*: effects on nuclear transcription factors involved in cell replication and differentiation. *Brain Research*, 857(1-2), pp.87-98.
- Crumpton, T., Seidler, F. and Slotkin, T. (2000b). Is oxidative stress involved in the developmental neurotoxicity of chlorpyrifos?. *Developmental Brain Research*, 121(2), pp.189-195.
- Cui, Y., Guo, J., Xu, B. and Chen, Z. (2006). Potential of chlorpyrifos and cypermethrin forming DNA adducts. *Mutation Research/Genetic Toxicology and Environmental Mutagenesis*, 604(1), pp.36-41.

- Dalton, S. (1992). Cell cycle regulation of the human *cdc2* gene. *The EMBO Journal*, 11(5), pp.1797-1804.
- Dang, C.V., Resar, L.M., Emison, E., Kim, S., Li, Q., Prescott, J.E., Wonsey, D. and Zeller, K., (1999). Function of the c-Myc oncogenic transcription factor. *Experimental Cell Research*, 253(1), pp.63-77.
- Das, K., and Barone, S. (1999). Neuronal Differentiation in PC12 Cells Is Inhibited by Chlorpyrifos and Its Metabolites: Is Acetylcholinesterase Inhibition the Site of Action?. *Toxicology and Applied Pharmacology*, 160(3), pp.217-230.
- Das, K.P., Freudenrich, T.M. and Mundy, W.R. (2004). Assessment of PC12 cell differentiation and neurite growth: a comparison of morphological and neurochemical measures. *Neurotoxicology and Teratology*, 26(3), pp.397-406.
- De Camilli, Á., Miller, P.E., Navone, F., Theurkauf, W.E. and Vallee, R.B. (1984). Distribution of microtubule-associated protein 2 in the nervous system of the rat studied by immunofluorescence. *Neuroscience*, 11(4), pp.819-846.
- De Gendt, K., Denolet, E., Willems, A., Daniels, V. W., Clinckemalie, L., Denayer, S., Wilkinson, M. F., Claessens, F., Swinnen, J. V. and Verhoeven, G. (2011). Expression of Tubb3, a Beta-Tubulin Isotype, Is Regulated by Androgens in Mouse and Rat Sertoli Cells. *Biology of Reproduction*, 85(5), pp. 934-945.
- de la Torre, J. C. (2002). Vascular basis of Alzheimer's pathogenesis. *An. N Y Aca. Sci*, 977, pp.196–215.
- Diaz-Nido, J., Serrano, L., Lopez-Otin, C., Vandekerckhove, J. and Avila, J. (1990). Phosphorylation of a neuronal-specific beta-tubulin isotype. *Journal of Biological Chemistry*, 265(23), pp.13949-13954.
- Dickinson, D. A., Warnes, G. R., Quievryn, G., Messer, J., Zhitkovich, A., Rubitski, E. and Aubrecht, J. (2004). Differentiation of DNA reactive and non-reactive genotoxic mechanisms using gene expression profile analysis. *Mutat Res*, 549(1-2), pp. 29-41.
- Dignam, J., Lebovitz, R. and Roeder, R. (1983). Accurate transcription initiation by RNA polymerase II in a soluble extract from isolated mammalian nuclei. *Nucleic Acids Research*, 11(5), pp.1475-1489. <http://dx.doi.org/10.1093/nar/11.5.1475>
- Doering, L. C. (1993). Probing modifications of the neuronal cytoskeleton. *Molecular Neurobiology*, 7(3-4), pp.265-291.
- Donato, R., Miljan, E.A., Hines, S.J., Aouabdi, S., Pollock, K., Patel, S., Edwards, F.A. and Sinden, J.D. (2007). Differential development of neuronal physiological responsiveness in two human neural stem cell lines. *BMC Neuroscience*, 8(1), p.36.
- Dragunow, M. (2008). High-content analysis in neuroscience. *Nat Rev Neurosci*, 9, pp.779-88.
- Dreiherr, J., Novack, V., Barachana, M., Yerushalmi, R., Lugassy, G. and Shpilberg, O. (2005). Non-Hodgkin's lymphoma and residential proximity to toxic industrial waste in southern Israel. *Haematologica*, 90(12), pp.1709-1710.
- Drubin, D.G. and Kirschner, M.W. (1986). Tau protein function in living cells. *The Journal of Cell Biology*, 103(6), pp.2739-2746.
- Du Toit, P.W., Muller, F.O., Van Tonder, W.M. and Ungerer, M.J. (1981). Experience with the intensive care management of organophosphate insecticide poisoning. *S Afr Med j*, 60(6), pp.227-229.

- Easter, S.S., Ross, L.S. and Frankfurter, A. (1993). Initial tract formation in the mouse brain. *Journal of Neuroscience*, 13(1), pp.285-299.
- Eaton, D.L., Daroff, R.B., Autrup, H., Bridges, J., Buffler, P., Costa, L.G., Coyle, J., McKhann, G., Mobley, W.C., Nadel, L. and Neubert, D. (2008). Review of the toxicology of chlorpyrifos with an emphasis on human exposure and neurodevelopment. *Critical Reviews in Toxicology*, 38(2), pp.1-125.
- EC, E. C. (2005). Monitoring of pesticide residues in products of plant origin in the European Union, Norway, Iceland and Liechtenstein. Commission staff working document.
- Eddleston, M., Buckley, N. A., Eyer, P. and Dawson, A. H. (2008). Management of acute organophosphorus pesticide poisoning. *Lancet*, 371(9612), 597–607. [http://doi.org/10.1016/S0140-6736\(07\)61202-1](http://doi.org/10.1016/S0140-6736(07)61202-1)
- Ehrich, M. (1995). Using neuroblastoma cell lines to address differential specificity to organophosphates. *Clinical and Experimental Pharmacology and Physiology*, 22(4), pp.291-292.
- Ehrich, M. and Jortner, B. S. (2001). Delayed Neuropathy. In: Handbook of Pesticide Toxicology, Elsevier, 2, 987-1012.
- Ehrich, M., Correll, L. and Veronesi, B. (1994). Neuropathy target esterase inhibition by organophosphorus esters in human neuroblastoma cells. *NeuroToxicology*, 15 (2), pp.309-314.
- Ehrich, M., Correll, L. and Veronesi, B. (1997). Acetylcholinesterase and neuropathy target esterase inhibitions in neuroblastoma cells to distinguish organophosphorus compounds causing acute and delayed neurotoxicity. *Toxicological Sciences*, 38(1), pp.55-63.
- Elerssek, T. and Filipic, M. (2011). Organophosphorous pesticides-mechanisms of their toxicity. In Pesticides-The Impacts of Pesticides Exposure. InTech.
- El-Fawal, H.A. and Ehrich, M.F. (1993). Calpain activity in organophosphorus-induced delayed neuropathy (OPIDN): Effects of a phenylalkylamine calcium channel blocker. *Annals of the New York Academy of Sciences*, 679(1), pp.325-329.
- El-Fawal, H.A. and McCain, W.C. (2008). Antibodies to neural proteins in organophosphorus-induced delayed neuropathy (OPIDN) and its amelioration. *Neurotoxicology and Teratology*, 30(3), pp.161- 166.
- Eliasson, C., Sahlgren, C., Berthold, C.H., Stakeberg, J., Celis, J.E., Betsholtz, C., Eriksson, J.E. and Pekny, M. (1999). Intermediate filament protein partnership in astrocytes. *Journal of Biological Chemistry*, 274(34), pp.23996-24006.
- Eng, L.F., Ghirmikar, R.S. and Lee, Y.L. (2000). Glial fibrillary acidic protein: GFAP-thirty-one years (1969–2000). *Neurochemical Research*, 25(9-10), pp.1439-1451.
- EPA, U. S. E. P. A. (1992). prevention, pesticides and toxic Substances. Pesticides in groundwater database: A compilation of monitoring studies: 1971-1991, *Washington, DC: USEPA*.
- EPA, U. S. E. P. A. (1994). Office of prevention, pesticides and toxic substances. Review of poison control center data call in. Memo from J. Blondell, Health Statistician Health Effects Division, to Steve Knott, Section Head, and Larry Dorsey, Chief. *Washington, DC,USA*.
- EPA, U. S. E. P. A. (1997). Office of prevention, pesticides and toxic substances. Review of chlorpyrifos poisoning data. *Washington, DC,USA*.
- EPA, U. S. E. P. A. (1999). Occupational/residential handler and postapplication residential risk assessment for chlorpyrifos. *Washington, DC,USA*.

- EPA, U. S. E. P. A. (2000). Chlorpyrifos revised risk assessment and agreement with registrants prevention, pesticides and toxic substances. *Washington, DC: USEPA.*
- EPA, U. S. E. P. A. (2013). Chlorpyrifos: Preliminary evaluation of the potential risks from volatilisation. *Washington, DC, USA.*
- EPA, U. S. E. P. A. (2016). Chlorpyrifos: Revised human health risk assessment for registration review. *Washington, DC, USA.*
- EPA, U. S. E. P. A. (2017). EPA Administrator Pruitt denies petition to ban widely used pesticide. *Washington, DC, USA.*
- Eriksson, J.E., Dechat, T., Grin, B., Helfand, B., Mendez, M., Pallari, H.M. and Goldman, R.D. (2009). Introducing intermediate filaments: from discovery to disease. *The Journal of Clinical Investigation*, 119(7), pp.1763-1771.
- Fedalei, A. and Nardone, R.M. (1983). An *in vitro* alternative for testing the effect of organophosphates on neurotoxic esterase activity. *Alternative Methods in Toxicology*, 1, pp.252-267 .
- Felemban, S.G., Garner, A.C., Smida, F.A., Boocock, D.J., Hargreaves, A.J. and Dickenson, J.M. (2015). Phenyl Saligenin Phosphate Induced Caspase-3 and c-Jun N-Terminal Kinase Activation in Cardiomyocyte-Like Cells. *Chemical Research in Toxicology*, 28(11), pp.2179-2191.
- Fiedler, N., Kipen, H., Kelly-McNeil, K. and Fenske, R. (1997). Long-term use of organophosphates and neuropsychological performance. *American Journal of Industrial Medicine*, 32(5), pp.487-496.
- Flanagan, L.A., Rebaza, L.M., Derzic, S., Schwartz, P.H. and Monuki, E.S. (2006). Regulation of human neural precursor cells by laminin and integrins. *Journal of Neuroscience Research*, 83(5), pp.845-856.
- Flaskos, J. (1995). The use of neuronal cell cultures in the study of delayed organophosphate action: *In 33d International Congress on Forensic and first on Environmental Toxicology*, 27-31.
- Flaskos, J. (2012). The developmental neurotoxicity of organophosphorus insecticides: A direct role for the oxon metabolites. *Toxicology Letters*, 209(1), 86-93.
- Flaskos, J. (2014). The neuronal cytoskeleton as a potential target in the developmental neurotoxicity of organophosphorothionate insecticides. *Basic and Clinical Pharmacology and Toxicology*, 115(2), pp.201-208.
- Flaskos, J., Harris, W., Sachana, M., Munoz, D., Tack, J. and Hargreaves, A.J. (2007). The effects of diazinon and cypermethrin on the differentiation of neuronal and glial cell lines. *Toxicology and Applied Pharmacology*, 219(2-3), pp.172-180.
- Flaskos, J., McLean, W., Fowler, M. and Hargreaves, A. (1998). Tricresyl phosphate inhibits the formation of axon-like processes and disrupts neurofilaments in cultured mouse N2a and rat PC12 cells. *Neuroscience letters*, 242(2), pp.101-104.
- Flaskos, J., McLean, W.G. and Hargreaves, A.J. (1994). The toxicity of organophosphate compounds towards cultured PC12 cells. *Toxicology Letters*, 70(1), pp.71-76.
- Flaskos, J., Nikolaidis, E., Harris, W., Sachana, M. and Hargreaves, A.J. (2011). Effects of sub-lethal neurite outgrowth inhibitory concentrations of chlorpyrifos oxon on cytoskeletal proteins and acetylcholinesterase in differentiating N2a cells. *Toxicology and Applied Pharmacology*, 256(3), pp.330-336.

- Flaskos, J., Sachana, M., Pen, M., Harris, W.C. and Hargreaves, A.J. (2006). Effects of phenyl saligenin phosphate on phosphorylation of pig brain tubulin *in vitro*. *Environmental Toxicology and Pharmacology*, 22(1), pp.70-74.
- Fotakis, G. and Timbrell, J.A. (2006). *In vitro* cytotoxicity assays: comparison of LDH, neutral red, MTT and protein assay in hepatoma cell lines following exposure to cadmium chloride. *Toxicology Letters*, 160(2), pp.171-177.
- Fourest-Lieuvain, A., Peris, L., Gache, V., Garcia-Saez, I., Juillan-Binard, C., Lantez, V. and Job, D. (2006). Microtubule regulation in mitosis: tubulin phosphorylation by the cyclin-dependent kinase Cdk1. *Molecular Biology of the Cell*, 17(3), pp.1041-1050.
- Fowler, M.J., Flaskos, J., McLean, W.G. and Hargreaves, A.J. (2001). Effects of neuropathic and non-neuropathic isomers of tricresyl phosphate and their microsomal activation on the production of axon-like processes by differentiating mouse N2a neuroblastoma cells. *Journal of Neurochemistry*, 76(3), pp.671-678.
- Gallinari, P., Di Marco, S., Jones, P., Pallaoro, M. and Steinkühler, C. (2007). HDACs, histone deacetylation and gene transcription: from molecular biology to cancer therapeutics. *Cell Research*, 17(3), p.195.
- Garcia, S.J., Seidler, F.J., Crumpton, T.L. and Slotkin, T.A. (2001). Does the developmental neurotoxicity of chlorpyrifos involve glial targets? Macromolecule synthesis, adenylyl cyclase signaling, nuclear transcription factors, and formation of reactive oxygen in C6 glioma cells. *Brain Research*, 891(1-2), pp.54-68.
- Garcia, S.J., Seidler, F.J., Qiao, D. and Slotkin, T.A. (2002). Chlorpyrifos targets developing glia: effects on glial fibrillary acidic protein. *Developmental Brain Research*, 133(2), pp.151-161.
- Gavrilescu, M., Demnerová, K., Aamand, J., Agathos, S. and Fava, F. (2015). Emerging pollutants in the environment: present and future challenges in biomonitoring, ecological risks and bioremediation. *New Biotechnology*, 32(1), pp.147-156.
- Gearhart, D.A., Sickles, D.W., Buccafusco, J.J., Prendergast, M.A. and Terry Jr, A.V. (2007). Chlorpyrifos, chlorpyrifos-oxon, and diisopropylfluorophosphate inhibit kinesin-dependent microtubule motility. *Toxicology and Applied Pharmacology*, 218(1), pp.20-29.
- Gelfand, V.I. and Bershadsky, A.D. (1991). Microtubule dynamics: mechanism, regulation, and function. *Annual Review of Cell Biology*, 7(1), pp.93-116.
- Gennari, P., Heyman, A. and Kainu, M. (2015). FAO Statistical Pocketbook. World food and agriculture. Food and Agriculture Organization of the United Nations, Rome, Italy.
- Giacomotto, J. and Ségalat, L. (2010). High-throughput screening and small animal models, where are we?. *British Journal of Pharmacology*, 160(2), pp.204-216.
- Ginzburg, I. (1991). Neuronal polarity: targeting of microtubule components into axons and dendrites. *Trends in Biochemical Sciences*, 16, pp.257-261.
- Glynn, P. (1999). Neuropathy target esterase. *Biochemical Journal*, 344(3), pp.625-631.
- Glynn, P., Holton, J.L., Nolan, C.C., Read, D.J., Brown, L., Hubbard, A. and Cavanagh, J.B. (1998). Neuropathy target esterase: immunolocalization to neuronal cell bodies and axons. *Neuroscience*, 83(1), pp.295-302.
- Gollapudi, B.B., Mendrala, A.L. and Linscombe, V.A. (1995). Evaluation of the genetic toxicity of the organophosphate insecticide chlorpyrifos. *Mutation Research/Genetic Toxicology*, 342(1-2), pp.25-36.

- Gomi, H., Yokoyama, T., Fujimoto, K., Ikeda, T., Katoh, A., Itoh, T. and Itohara, S. (1995). Mice devoid of the glial fibrillary acidic protein develop normally and are susceptible to scrapie prions. *Neuron*, 14(1), pp.29-41.
- Gomi, H., Yokoyama, T., Fujimoto, K., Ikeda, T., Katoh, A., Itoh, T. and Itohara, S. (1995). Mice devoid of the glial fibrillary acidic protein develop normally and are susceptible to scrapie prions. *Neuron*, 14(1), pp.29-41.
- Grammas, P., Yamada, M. and Zlokovic, B. (2002). The cerebrovasculature: a key player in the pathogenesis of Alzheimer's disease. *Journal of Alzheimer's Disease*, 4(3), pp.217-223.
- Grandjean, P. and Landrigan, P.J. (2006). Developmental neurotoxicity of industrial chemicals. *Lancet*, 368, pp. 2167–2178.
- Gregorette, I., Lee, Y.M. and Goodson, H.V. (2004). Molecular evolution of the histone deacetylase family: functional implications of phylogenetic analysis. *Journal of Molecular Biology*, 338(1), pp.17-31.
- Griffith, L.M. and Pollard, T.D. (1978). Evidence for actin filament-microtubule interaction mediated by microtubule-associated proteins. *The Journal of Cell Biology*, 78(3), pp.958-965.
- Grigoryan, H., and Lockridge, O. (2009). Nanoimages show disruption of tubulin polymerization by chlorpyrifos oxon: implications for neurotoxicity. *Toxicology and Applied Pharmacology*, 240(2), pp.143-148.
- Guerri, C., and Renau-Piqueras, J. (1997). Alcohol, astroglia, and brain development. *Molecular Neurobiology*, 15(1), pp.65-81. <http://dx.doi.org/10.1007/bf02740616>
- Gunnell, D., Eddleston, M., Phillips, M.R. and Konradsen, F. (2007). The global distribution of fatal pesticide self-poisoning: systematic review. *BMC Public Health*, 7(1), p.357.
- Gupta, R.C. (1995). Environmental agents and placental toxicity: anticholinesterases and other insecticides. In *Placental Toxicology*, pp. 257-278. CRC Press Boca Raton, FL.
- Gupta, R.C. (2006). Classification and uses of organophosphates and carbamates. In *Toxicology of Organophosphate and Carbamate Compounds*, pp. 5-24.
- Gupta, S.C., Mishra, M., Sharma, A., Balaji, T.D., Kumar, R., Mishra, R.K. and Chowdhuri, D.K. (2010). Chlorpyrifos induces apoptosis and DNA damage in *Drosophila* through generation of reactive oxygen species. *Ecotoxicology and Environmental Safety*, 73(6), pp.1415-1423.
- Haberland, M., Montgomery, R.L. and Olson, E.N. (2009). The many roles of histone deacetylases in development and physiology: implications for disease and therapy. *Nature Reviews Genetics*, 10(1), p.32.
- Haffke, S.C. and Seeds, N.W. (1975). Neuroblastoma: the *Escherichia coli* of neurobiology. *Life Sciences*, 16(11), pp.1649-1658.
- Hara, A., Sakai, N., Yamada, H., Niikawa, S., Ohno, T., Tanaka, T. and Mori, H. (1991). Proliferative assessment of GFAP-positive and GFAP-negative glioma cells by nucleolar organizer region staining. *Surgical Neurology*, 36(3), pp.190-194.
- Harada, A., Teng, J., Takei, Y., Oguchi, K. and Hirokawa, N. (2002). MAP2 is required for dendrite elongation, PKA anchoring in dendrites, and proper PKA signal transduction. *The Journal of Cell Biology*, 158(3), pp. 541-549.
- Hargreaves, A.J. (1997). The cytoskeleton as a target in cell toxicity. In *Advances in Molecular and Cell Biology* (Vol. 20, pp. 119-144). Elsevier.

- Hargreaves, A.J. (2012). Neurodegenerations induced by organophosphorous compounds. In *Neurodegenerative Diseases* (pp. 189-204). Springer, *New York, NY*.
- Hargreaves, A.J., Fowler, M.J., Sachana, M., Flaskos, J., Bountouri, M., Coutts, I.C., Glynn, P., Harris, W. and McLean, W.G. (2006). Inhibition of neurite outgrowth in differentiating mouse N2a neuroblastoma cells by phenyl saligenin phosphate: effects on MAP kinase (ERK 1/2) activation, neurofilament heavy chain phosphorylation and neuropathy target esterase activity. *Biochemical Pharmacology*, 71(8), pp.1240-1247.
- Harrill, J. A. and Mundy, W. R. (2011). Quantitative assessment of neurite outgrowth in PC12 cells. *Methods Mol Biol*, 758, pp.331-48.
- Harris, W., Munoz, D., Bonner, P. L. and Hargreaves, A.J. (2009a). Effects of phenyl saligenin phosphate on cell viability and transglutaminase activity in N2a neuroblastoma and HepG2 hepatoma cell lines. *Toxicology in Vitro*, 23(8), pp.1559-63.
- Harris, W., Sachana, M., Flaskos, J. and Hargreaves, A.J. (2009b). Neuroprotection from diazinon-induced toxicity in differentiating murine N2a neuroblastoma cells. *Neurotoxicology*, 30(6), pp.958-964.
- Harry, G.J., Billingsley, M., Bruinink, A., Campbell, I.L., Classen, W., Dorman, D.C., Galli, C., Ray, D., Smith, R.A. and Tilson, H.A., (1998). *In vitro* techniques for the assessment of neurotoxicity. *Environmental Health Perspectives*, 106(1), p.131.
- Hasan, M., Maitra, S.C. and Ali, S.F. (1979). Organophosphate pesticide DDVP-induced alterations in the rat cerebellum and spinal cord an electron microscopic study. *Experimental Pathology*, 17(2), pp.88-94.
- Hassel, B., Bachelard, H., Jones, P., Fonnum, F. and Sonnewald, U. (1997). Trafficking of amino acids between neurons and glia *in vivo*. Effects of inhibition of glial metabolism by fluoroacetate. *Journal of Cerebral Blood Flow and Metabolism*, 17(11), pp.1230-1238.
- Heidemann, S.R., Landers, J.M. and Hamborg, M.A. (1981). Polarity orientation of axonal microtubules. *J Cell Biol*, 91(3), pp.661-665.
- Heimann, R., Shelanski, M.L. and Liem, R.K. (1985). Microtubule-associated proteins bind specifically to the 70-kDa neurofilament protein. *Journal of Biological Chemistry*, 260(22), pp.12160-12166.
- Henschler, D., Schmuck, G., van Aerssen, M. and Schiffmann, D. (1992). The inhibitory effect of neuropathic organophosphate esters on neurite outgrowth in cell cultures: A basis for screening for delayed neurotoxicity. *Toxicology in Vitro*, 6(4), pp.327-335.
- Hertz, L., Dringen, R., Schousboe, A. and Robinson, S.R. (1999). Astrocytes: glutamate producers for neurons. *Journal of Neuroscience Research*, 57(4), pp.417-428.
- Hirokawa, N., Glicksman, M.A. and Willard, M.B. (1984). Organization of mammalian neurofilament polypeptides within the neuronal cytoskeleton. *The Journal of Cell Biology*, 98(4), pp.1523-1536.
- Hjorth, J.J., van Pelt, J., Mansvelder, H.D. and van Ooyen, A. (2014). Competitive dynamics during resource-driven neurite outgrowth. *PLoS One*, 9(2), p.e86741.
- Holtmaat, A.J., Dijkhuizen, P.A., Oestreicher, A.B., Romijn, H.J., Van der Lugt, N.M., Berns, A., Margolis, F.L., Gispén, W.H. and Verhaagen, J. (1995). Directed expression of the growth-associated protein B-50/GAP-43 to olfactory neurons in transgenic mice results in changes in axon morphology and extraglomerular fiber growth. *Journal of Neuroscience*, 15(12), pp.7953-7965.

- Hornburg, D., Drepper, C., Butter, F., Meissner, F., Sendtner, M. and Mann, M. (2014). Deep proteomic evaluation of primary and cell line motoneuron disease models delineates major differences in neuronal characteristics. *Molecular and Cellular Proteomics*, 13(12), pp.3410-3420.
- Howard, A.S., Bucelli, R., Jett, D.A., Bruun, D., Yang, D. and Lein, P.J. (2005). Chlorpyrifos exerts opposing effects on axonal and dendritic growth in primary neuronal cultures. *Toxicology and Applied Pharmacology*, 207(2), pp.112-124.
- Inagaki, M., Gonda, Y., Nishizawa, K., Kitamura, S., Sato, C., Ando, S., Tanabe, K., Kikuchi, K., Tsuiki, S. and Nishi, Y. (1990). Phosphorylation sites linked to glial filament disassembly in vitro locate in a non-alpha-helical head domain. *Journal of Biological Chemistry*, 265(8), pp.4722-4729.
- Inui, K., Mitsumori, K., Harada, T. and Maita, K. (1993). Quantitative analysis of neuronal damage induced by tri-ortho-cresyl phosphate in Wistar rats. *Fundamental and Applied Toxicology*, 20(1), pp.111-119.
- Ismail, M., Khan, Q. M., Ali, R., Ali, T. and Mobeen, A. (2014). Genotoxicity of chlorpyrifos in freshwater fish *Labeo rohita* using Alkaline Single-cell Gel Electrophoresis (Comet) assay. *Drug Chem Toxicol*, 37(4), pp. 466-71.
- Jacque, C.M., Kujas, M., Poreau, A., Raoul, M., Collier, P., Racadot, J. and Baumann, N. (1979). GFA and S 100 protein levels as an index for malignancy in human gliomas and neurinomas. *Journal of the National Cancer Institute*, 62(3), pp.479-483.
- Jacque, C.M., Vinner, C., Kujas, M., Raoul, M., Racadot, J. and Baumann, N.A. (1978). Determination of glial fibrillary acidic protein (GFAP) in human brain tumors. *Journal of the Neurological Sciences*, 35(1), pp.147-155.
- Jakel, R.J., Schneider, B.L. and Svendsen, C.N. (2004). Using human neural stem cells to model neurological disease. *Nature Reviews Genetics*, 5(2), p.136.
- Jamal, G.A. (1995). Long term neurotoxic effects of chemical warfare organophosphate compounds (Sarin). *Adverse Drug Reactions and Toxicological Reviews*, 14(2), pp. 83-84 .
- Janke, C. and Kneussel, M. (2010). Tubulin post-translational modifications: encoding functions on the neuronal microtubule cytoskeleton. *Trends in Neurosciences*, 33(8), pp.362-372.
- Janke, C.(2014). The tubulin code: molecular components, readout mechanisms, and functions. *J Cell Biol*, 206(4), pp.461-472.
- Jessen, K. (2004). Glial cells. *The International Journal of Biochemistry and Cell Biology*, 36(10), pp.1861-1867.
- Jett, D.A., Navoa, R.V., Beckles, R.A. and McLemore, G.L. (2001). Cognitive function and cholinergic neurochemistry in weanling rats exposed to chlorpyrifos. *Toxicology and Applied Pharmacology*, 174(2), pp. 89-98 .
- Johnson, M.K. (1969). The delayed neurotoxic effect of some organophosphorus compounds. Identification of the phosphorylation site as an esterase. *The Biochemical Journal*, 114(4), pp. 711-717 .
- Johnson, M.K. (1970). Organophosphorus and other inhibitors of brainneurotoxic esterase'and the development of delayed neurotoxicity in hens. *Biochemical Journal*, 120(3), p.523.
- Johnson, M.K. (1990). Organophosphates and delayed neuropathy--is NTE alive and well?. *Toxicology and Applied Pharmacology*, 102(3), pp. 385-399 .

- Jokanovic, M., Kosanovic, M., Brkic, D. and Vukomanovic, P. (2011). Organophosphate induced delayed polyneuropathy in man: an overview. *Clinical Neurology and Neurosurgery*, 113(1), pp. 7-10 .
- Jones, A.L. and Karalliedde, L. (2006). Poisoning. In: Boon, N.A., Colledge, N.R., Davidson, S.S. and Walker, B.R., Eds., *Davidson's Principles and Practice of Medicine*, 20th Edition, Churchill Livingstone, *Edinburgh*, pp.203-226.
- Juan, L.J., Shia, W.J., Chen, M.H., Yang, W.M., Seto, E., Lin, Y.S. and Wu, C.W. (2000). Histone deacetylases specifically down-regulate p53-dependent gene activation. *Journal of Biological Chemistry*, 275(27), pp.20436-20443.
- Kajiwara, K., Orita, T., Nishizaki, T., Kamiryo, T., Nakayama, H. and Ito, H. (1992). Glial fibrillary acidic protein (GFAP) expression and nucleolar organizer regions (NORs) in human gliomas. *Brain Research*, 572(1-2), pp.314-318.
- Kamel, F., Rowland, A.S., Park, L.P., Anger, W.K., Baird, D.D., Gladen, B.C., Moreno, T., Stallone, L. and Sandler, D.P. (2003). Neurobehavioral performance and work experience in Florida farmworkers. *Environmental Health Perspectives*, 111(14), pp. 1765-1772 .
- Kaplan, D. (1995). Life and death in the nervous system: Role of Neurotrophic factors and their receptors. *Elsevier Science* ,73(2), pp.37-53.
- Karalliedde, L. (1999). Organophosphorus poisoning and anaesthesia. *Anaesthesia*, 54(11), pp. 1073-1088.
- Karalliedde, L. (2006). Carbon monoxide poisoning. *Int J Clin Pract*, 60, 1523-4.
- Karki, P., Ansari, J., Bhandary, S. and Koirala, S. (2004). Cardiac and electrocardiographical manifestations of acute organophosphate poisoning. *Singapore Medical Journal*, 45(8), pp.385-389.
- Keilbaugh, S. A., Prusoff, W. H. and Simpson, M. V. (1991). The PC 12 as a model for studies of the mechanism of induction of peripheral neuropathy by anti-HIV-1 dideoxynucleoside analogs. *Biochemical Pharmacology*, 42(1), pp. R5-R8.
- Kerssemakers, J.W., Munteanu, E.L., Laan, L., Noetzel, T.L., Janson, M.E. and Dogterom, M. (2006). Assembly dynamics of microtubules at molecular resolution. *Nature*, 442(7103), p.709.
- Kim, S.U. (2004). Human neural stem cells genetically modified for brain repair in neurological disorders. *Neuropathology*, 24(3), pp.159-171.
- Kirschner, M.W. and Mitchison, T.I.M. (1986). Microtubule dynamics. *Nature*, 324(6098), pp.621-621.
- Klebe, R.J. and Ruddle, R.H. (1969). Neuroblastoma-Cell culture analysis of a differentiating stem cell system. In *Journal of Cell Biology*, 43(2), p.2, p. A69.
- Klemm, M. and Schratzenholz, A. (2004). Neurotoxicity of active compounds--establishment of hESC-lines and proteomics technologies for human embryo-and neurotoxicity screening and biomarker identification. *Altex*, 21, pp.41-48.
- Knoops, B. and Octave, J.N. (1997). α 1-tubulin mRNA level is increased during neurite outgrowth of NG 108-15 cells but not during neurite outgrowth inhibition by CNS myelin. *Neuroreport*, 8(3), pp.795-798.
- Koelle, G.B. (1992). Erythrocyte and tissue AChE inhibition. *Journal of Applied Toxicology : JAT*, 12(4), pp. 305 .

- Kolarova, M., García-Sierra, F., Bartos, A., Rícný, J. and Ripova, D. (2012). Structure and pathology of tau protein in Alzheimer disease. *International Journal of Alzheimer's Disease*.
- Kornblum, H.I. (2007). Introduction to neural stem cells. *Stroke*, 38(2), pp.810-816.
- Kornuta, N., Bagley, E. and Nedopitanskaya, N. (1996). Genotoxic effects of pesticides. *J Environ Pathol Toxicol Oncol*, 15(2-4), pp. 75-8.
- Kosik, K.S., Orecchio, L.D., Bakalis, S., Duffy, L. and Neve, R.L. (1988). Partial Sequence of MAP2 in the Region of a Shared Epitope with Alzheimer Neuronbrillary Tangles. *Journal of Neurochemistry*, 51(2), pp.587-598.
- Ku, N.O., Liao, J., Chou, C.F. and Omary, M.B. (1996). Implications of intermediate filament protein phosphorylation. *Cancer and Metastasis Reviews*, 15(4), pp.429-444.
- Laemmli, U.K. (1970). Cleavage of structural proteins during the assembly of the head of bacteriophage T4. *Nature*, 227(5259), p.680.
- Lauder, J.M. and Schambra, U.B. (1999). Morphogenetic roles of acetylcholine. *Environmental Health Perspectives*, 107(1), pp. 65-69 .
- LeDizet, M. and Piperno, G. (1987). Identification of an acetylation site of Chlamydomonas alpha-tubulin. *Proceedings of the National Academy of Sciences*, 84(16), pp.5720-5724.
- Lee, K., Jeon, K., Kim, J.M., Kim, V.N., Choi, D.H., Kim, S.U. and Kim, S. (2005). Downregulation of GFAP, TSP-1, and p53 in human glioblastoma cell line, U373MG, by IE1 protein from human cytomegalovirus. *Glia*, 51(1), pp.1-12.
- Lee, M.K. and Cleveland, D.W. (1994). Neurofilament function and dysfunction: involvement in axonal growth and neuronal disease. *Current Opinion in Cell Biology*, 6(1), pp.34-40.
- Leterrier, J.F., Liem, R.K. and Shelanski, M.L. (1982). Interactions between neurofilaments and microtubule-associated proteins: a possible mechanism for intraorganellar bridging. *The Journal of Cell Biology*, 95(3), pp.982-986.
- Levin, H.S., Rodnitzky, R.L. and Mick, D.L. (1976). Anxiety associated with exposure to organophosphate compounds. *Archives of General Psychiatry*, 33(2), pp. 225-228 .
- Lewis, S.A. and Cowan, N.J. (1986). Anomalous placement of introns in a member of the intermediate filament multigene family: an evolutionary conundrum. *Molecular and Cellular Biology*, 6(5), pp.1529-1534.
- Li, D., Huang, Q., Lu, M., Zhang, L., Yang, Z., Zong, M. and Tao, L. (2015). The organophosphate insecticide chlorpyrifos confers its genotoxic effects by inducing DNA damage and cell apoptosis. *Chemosphere*, 135, pp. 387-93.
- Liedtke, W., Edelmann, W., Bieri, P.L., Chiu, F.C., Cowan, N.J., Kucherlapati, R. and Raine, C.S. (1996). GFAP is necessary for the integrity of CNS white matter architecture and long-term maintenance of myelination. *Neuron*, 17(4), pp.607-615.
- Liedtke, W., Edelmann, W., Bieri, P.L., Chiu, F.C., Cowan, N.J., Kucherlapati, R. and Raine, C.S. (1996). GFAP is necessary for the integrity of CNS white matter architecture and long-term maintenance of myelination. *Neuron*, 17(4), pp. 607-615 .
- Lin, H.Y., Chen, C.S., Lin, S.P., Weng, J.R. and Chen, C.S. (2006). Targeting histone deacetylase in cancer therapy. *Medicinal Research Reviews*, 26(4), pp.397-413.
- Lin, L.F. (1996). Glial cell line-derived neurotrophic factor (GDNF): A comprehensive review. *Neural Notes*, 2, pp.3-7.

- Liu, C., Li, Y., Lein, P.J. and Ford, B.D. (2012). Spatiotemporal patterns of GFAP upregulation in rat brain following acute intoxication with diisopropylfluorophosphate (DFP). *Current Neurobiology*, 3(2), pp. 90-97 .
- Liu, Y., Peterson, D.A., Kimura, H. and Schubert, D. (1997). Mechanism of cellular 3-(4, 5-dimethylthiazol-2-yl)-2, 5-diphenyltetrazolium bromide (MTT) reduction. *Journal of Neurochemistry*, 69(2), pp.581-593.
- Liyasova, M., Li, B., Schopfer, L.M., Nachon, F., Masson, P., Furlong, C.E. and Lockridge, O. (2011). Exposure to tri-o-cresyl phosphate detected in jet airplane passengers. *Toxicology and Applied Pharmacology*, 256(3), pp.337-347.
- Lodish, H., Berk, A., Zipursky, S. L., Matsudaira, P., Baltimore, D. and Darnell, J. (2000a). The actin cytoskeleton.
- Lodish, H., Berk, A.Z.S.L., Zipursky, S.L., Matsudaira, P., Baltimore, D. and Darnell, J. (2000b). Protein structure and function. Molecular Cell Biology, 4th Edition WH Freeman, New York.
- Lotti, M. (1992). The pathogenesis of organophosphate polyneuropathy. *Critical Reviews In Toxicology*, 21(6), pp.465-487.
- Lotti, M. and Moretto, A. (1993). The search for the physiological functions of NTE: Is NTE a receptor?. *Chemico-Biological Interactions*, 87(1-3), pp.407-416.
- Lotti, M. and Moretto, A. (2005). Organophosphate-induced delayed polyneuropathy. *Toxicological Reviews*, 24(1), pp. 37-49 .
- Lotti, M., Moretto, A., Zoppellari, R., Dainese, R., Rizzuto, N. and Barusco, G. (1986). Inhibition of lymphocytic neuropathy target esterase predicts the development of organophosphate-induced delayed polyneuropathy. *Archives of Toxicology*, 59(3), pp. 176-179 .
- Ludueno, R.F. (1993). Are tubulin isotypes functionally significant?. *Molecular Biology of The Cell*, 4(5), pp. 445-457 .
- Luo, J., Su, F., Chen, D., Shiloh, A. and Gu, W. (2000). Deacetylation of p53 modulates its effect on cell growth and apoptosis. *Nature*, 408(6810), p.377.
- Mandell, J.W. and Banker, G.A. (1995). The microtubule cytoskeleton and the development of neuronal polarity. *Neurobiology of Aging*, 16(3), pp.229-237.
- Mansuy, I.M. and Shenolikar, S. (2006). Protein serine/threonine phosphatases in neuronal plasticity and disorders of learning and memory. *Trends in Neurosciences*, 29(12), pp.679-686.
- Margolis, R.L. and Wilson, L. (1978). Opposite end assembly and disassembly of microtubules at steady state *in vitro*. *Cell*, 13(1), pp.1-8.
- Martin, M.A., Osmani, S.A. and Oakley, B.R. (1997). The role of gamma-tubulin in mitotic spindle formation and cell cycle progression in *Aspergillus nidulans*. *Journal of Cell Science*, 110(5), pp.623-633.
- Massicotte, C., Jortner, B. and Ehrich, M. (2003). Morphological effects of neuropathy-inducing organophosphorus compounds in primary dorsal root ganglia cell cultures. *Neurotoxicology*, 24(6), pp.787-796.
- Mattingly, J.E., Sullivan, J.E., Spiller, H.A. and Bosse, G.M. (2003). Intermediate syndrome after exposure to chlorpyrifos in a 16-month-old girl. *Journal of Emergency Medicine*, 25(4), pp.379-381.

- Matus, A. (1988). Neurofilament protein phosphorylation-where, when and why. *Trends in Neurosciences*, 11(7), pp.291-292.
- Mayerhöfer, T., Mutschke, H. and Popp, J. (2016). Employing Theories Far beyond Their Limits-The Case of the (Boguer-) Beer-Lambert Law. *ChemPhysChem*, 17(13), pp.1948-1955.
- McGough, A. and Chiu, W. (1999). ADF/cofilin weakens lateral contacts in the actin filament. *Journal of Molecular Biology*, 291(3), pp. 513-519 .
- Mearns, J., Dunn, J. and Lees-Haley, P. (1994). Psychological effects of organophosphate pesticides: A review and call for research by psychologists. *Journal of Clinical Psychology*, 50(2), pp.286-294.
- Meiri, K.F., Pfenninger, K.H. and Willard, M.B. (1986). Growth-associated protein, GAP-43, a polypeptide that is induced when neurons extend axons, is a component of growth cones and corresponds to pp46, a major polypeptide of a subcellular fraction enriched in growth cones. *Proceedings of the National Academy of Sciences*, 83(10), pp.3537-3541.
- Meiri, K.F., Saffell, J.L., Walsh, F.S. and Doherty, P. (1998). Neurite outgrowth stimulated by neural cell adhesion molecules requires growth-associated protein-43 (GAP-43) function and is associated with GAP-43 phosphorylation in growth cones. *Journal of Neuroscience*, 18(24), pp.10429-10437.
- Michaelis, S. (2011). Contaminated aircraft cabin air. *The journal of Biological Physic*, 11(3), pp.132- 145.
- Mietelska-Porowska, A., Wasik, U., Goras, M., Filipek, A. and Niewiadomska, G. (2014). Tau protein modifications and interactions: their role in function and dysfunction. *International Journal of Molecular Sciences*, 15(3), pp. 4671-4713.
- Millecamps, S. and Julien, J.P. (2013). Axonal transport deficits and neurodegenerative diseases. *Nature Reviews Neuroscience*, 14(3), p.161.
- Minton, N.A. and Murray, V.S. (1988). A review of organophosphate poisoning. *Medical Toxicology and Adverse Drug Experience*, 3(5), pp.350-375.
- Monaco, A., Grimaldi, M.C. and Ferrandino, I. (2016). Neuroglial alterations in the zebrafish brain exposed to cadmium chloride. *Journal of Applied Toxicology*, 36(12), pp.1629-1638.
- Moser, M., Stempfl, T., Li, Y., Glynn, P., Büttner, R. and Kretzschmar, D. (2000). Cloning and expression of the murine sws/NTE gene. *Mechanisms of Development*, 90(2), pp.279-282.
- Mosmann, T. (1983). Rapid colorimetric assay for cellular growth and survival: application to proliferation and cytotoxicity assays. *Journal of Immunological Methods*, 65(1-2), pp.55-63.
- Muller, M., Hess, L., Tardivo, A., Lajmanovich, R., Attademo, A., Poletta, G., Simoniello, M. F., Yodice, A., Lavarello, S., Chialvo, D. and Scremin, O. (2014). Neurologic dysfunction and genotoxicity induced by low levels of chlorpyrifos. *Neurotoxicology*, 45, pp. 22-30.
- Mundy, W.R., Radio, N.M. and Freudenrich, T.M. (2010). Neuronal models for evaluation of proliferation *in vitro* using high content screening. *Toxicology*, 270(2-3), pp.121-130.
- Muñoz, D. (2010). Effects of organophosphates on neural and purified liver tissue transglutaminase. PhD thesis, Nottingham Trent University.
- Muñoz-Quezada, M.T., Iglesias, V., Lucero, B., Steenland, K., Barr, D.B., Levy, K., Ryan, P.B., Alvarado, S. and Concha, C. (2012). Predictors of exposure to organophosphate pesticides in schoolchildren in the Province of Talca, Chile. *Environment International*, 47, pp.28-36.

- Murphy, D.B. and Borisy, G.G. (1975). Association of high-molecular-weight proteins with microtubules and their role in microtubule assembly *in vitro*. *Proceedings of the National Academy of Sciences*, 72(7), pp.2696-2700.
- Murphy, D.B., Vallee, R.B. and Borisy, G.G. (1977). Identity and polymerization-stimulatory activity of the nontubulin proteins associated with microtubules. *Biochemistry*, 16(12), pp.2598-2605.
- Murray, A., Rathbone, A.J. and Ray, D.E. (2005). Novel protein targets for organophosphorus pesticides in rat brain. *Environmental Toxicology and Pharmacology*, 19(3), pp.451-454.
- Muscarella, D.E., Keown, J.F. and Bloom, S.E. (1984). Evaluation of the genotoxic and embryotoxic potential of chlorpyrifos and its metabolites *in vivo* and *in vitro*. *Environmental and Molecular Mutagenesis*, 6(1), pp.13-23.
- Mutch, E. and Williams, F. (2006). Diazinon, chlorpyrifos and parathion are metabolised by multiple cytochromes P450 in human liver. *Toxicology*, 224(1-2), pp.22-32.
- Myzak, M.C., Hardin, K., Wang, R., Dashwood, R.H. and Ho, E. (2005). Sulforaphane inhibits histone deacetylase activity in BPH-1, LnCaP and PC-3 prostate epithelial cells. *Carcinogenesis*, 27(4), pp.811-819.
- Myzak, M.C., Karplus, P.A., Chung, F.L. and Dashwood, R.H. (2004). A novel mechanism of chemoprotection by sulforaphane: inhibition of histone deacetylase. *Cancer Research*, 64(16), pp.5767-5774.
- Nakamura, Y. (2002). Regulating factors for microglial activation. *Biological and Pharmaceutical Bulletin*, 25(8), pp.945-953.
- NCFAP, N. C. F. F. A. A. P. (2000). Pesticide use in U.S. crop production: 1997 national summary report. In: LEONARD P, G. A. M. B. M. (ed.). *Washington, DC, USA*.
- Nikkhah, G., Tonn, J.C., Hoffmann, O., Kraemer, H.P., Darling, J.L., Schachenmayr, W. and Schönmayr, R. (1992). The MTT assay for chemosensitivity testing of human tumors of the central nervous system. *Journal of Neuro-Oncology*, 13(1), pp.13-24.
- Nixon, R.A., Fischer, I. and Lewis, S.E. (1990). Synthesis, axonal transport, and turnover of the high molecular weight microtubule-associated protein MAP 1A in mouse retinal ganglion cells: tubulin and MAP 1A display distinct transport kinetics. *The Journal of Cell Biology*, 110(2), pp.437-448.
- Nomeir, A.A. and Abou-Donia, M.B. (1986). Studies on the metabolism of the neurotoxic tri-*o*-cresyl phosphate. Distribution, excretion, and metabolism in male cats after a single, dermal application. *Toxicology*, 38(1), pp.15-33.
- Nostrandt, A., Rowles, T. and Ehrich, M. (1992). Cytotoxic effects of organophosphorus esters and other neurotoxic chemicals on cultured cells. *In Vitro Toxicology*, 5(3), pp.127-136.
- O'Callaghan, J.P. (1988). Neurotypic and gliotypic proteins as biochemical markers of neurotoxicity. *Neurotoxicology and Teratology*, 10(5), pp. 445-452 .
- Odell, I.D. and Cook, D. (2013). Immunofluorescence techniques. *The Journal of Investigative Dermatology*, 133(1), p.e4.
- Ogrodnik, M., Salmonowicz, H., Brown, R., Turkowska, J., Średniawa, W., Pattabiraman, S., Amen, T., Abraham, A.C., Eichler, N., Lyakhovetsky, R. and Kaganovich, D. (2014). Dynamic JUNQ inclusion bodies are asymmetrically inherited in mammalian cell lines through the asymmetric partitioning of vimentin. *Proceedings of the National Academy of Sciences*, 111(22), pp.8049-8054.

- Okabe, S. and Hirokawa, N. (1988). Microtubule dynamics in nerve cells: analysis using microinjection of biotinylated tubulin into PC12 cells. *The Journal of Cell Biology*, 107(2), pp.651-664.
- Olmsted, J.B. (1986). Microtubule-associated proteins. *Annual Review of Cell Biology*, 2(1), pp.421-457.
- Omary, M.B., Ku, N.O., Tao, G.Z., Toivola, D.M. and Liao, J. (2006). "Heads and tails" of intermediate filament phosphorylation: multiple sites and functional insights. *Trends in Biochemical Sciences*, 31(7), pp. 383-394 .
- Orkand, R.K., Nicholls, J.G. and Kuffler, S.W. (1966). Effect of nerve impulses on the membrane potential of glial cells in the central nervous system of amphibia. *Journal of neurophysiology*, 29(4), pp.788-806.
- Osborn, M. and Weber, K. (1986). Intermediate filament proteins: a multigene family distinguishing major cell lineages. *Trends in Biochemical Sciences*, 11(11), pp.469-472.
- Osterloh, J., Lotti, M. and Pond, S.M. (1983). Toxicologic studies in a fatal overdose of 2, 4-D, MCP, and chlorpyrifos. *Journal of Analytical Toxicology*, 7(3), pp.125-129.
- Ostrea Jr, E.M., Morales, V., Ngoumna, E., Prescilla, R., Tan, E., Hernandez, E., Ramirez, G.B., Cifra, H.L. and Manlapaz, M.L. (2002). Prevalence of fetal exposure to environmental toxins as determined by meconium analysis. *Neurotoxicology*, 23(3), pp.329-339.
- Paz-y-Miño, C., Dávalos, M.V., Sánchez, M.E., Arévalo, M. and Leone, P.E. (2002). Should gaps be included in chromosomal aberration analysis?: evidence based on the comet assay. *Mutation Research/Genetic Toxicology and Environmental Mutagenesis*, 516(1), pp.57-61.
- Pekiner, C., Dent, E.W., Roberts, R.E., Meiri, K.F. and McLean, W.G. (1996). Altered GAP-43 immunoreactivity in regenerating sciatic nerve of diabetic rats. *Diabetes*, 45(2), pp.199-204.
- Pekny, M., Eliasson, C., Chien, C.L., Kindblom, L.G., Liem, R., Hamberger, A. and Betsholtz, C. (1998). GFAP-Deficient Astrocytes Are Capable of Stellation in Vitro When Cocultured with Neurons and Exhibit a Reduced Amount of Intermediate Filaments and an Increased Cell Saturation Density. *Experimental Cell Research*, 239(2), pp.332-343.
- Pekny, M., Johansson, C.B., Eliasson, C., Stakeberg, J., Wallén, Å., Perlmann, T., Lendahl, U., Betsholtz, C., Berthold, C.H. and Frisén, J. (1999). Abnormal reaction to central nervous system injury in mice lacking glial fibrillary acidic protein and vimentin. *The Journal of Cell Biology*, 145(3), pp.503-514.
- Pekny, M., Leveen, P., Pekna, M., Eliasson, C., Berthold, C.H., Westermarck, B. and Betsholtz, C. (1995). Mice lacking glial fibrillary acidic protein display astrocytes devoid of intermediate filaments but develop and reproduce normally. *The EMBO Journal*, 14(8), pp.1590-1598.
- Pelkonen, O., Vähäkangas, K. and Gupta, R.C. (2006). Placental toxicity of organophosphate and carbamate pesticides. *In Toxicology of Organophosphate and Carbamate Compounds*, pp. 463-479.
- Peng, L., Yuan, Z. and Seto, E. (2015). Histone deacetylase activity assay. *Methods Mol Biol*, 1288, pp. 95-108.
- Peraica, M., Capodicasa, E., Moretto, A. and Lotti, M. (1993). Organophosphate polyneuropathy in chicks. *Biochemical Pharmacology*, 45(1), pp.131-135.
- Pernigo, S., Lamprecht, A., Steiner, R.A. and Dodding, M.P. (2013). Structural basis for kinesin-1: cargo recognition. *Science*, p.1232807.

- Pomeroy-Black, M. and Ehrich, M. (2012). Organophosphorus compound effects on neurotrophin receptors and intracellular signaling. *Toxicology in Vitro: An International Journal Published in Association with BIBRA*, 26(5), pp.759-65.
- Pope, C.N. (1999). Organophosphorus pesticides: do they all have the same mechanism of toxicity?. *Journal of Toxicology and Environmental Health Part B: Critical Reviews*, 2(2), pp.161-181.
- Poppek, D., Keck, S., Ermak, G., Jung, T., Stolzing, A., Ullrich, O., Davies, K.J. and Grune, T. (2006). Phosphorylation inhibits turnover of the tau protein by the proteasome: influence of RCAN1 and oxidative stress. *Biochemical Journal*, 400(3), pp.511-520.
- Prendergast, M.A., Self, R.L., Smith, K.J., Ghayoumi, L., Mullins, M.M., Butler, T.R., Buccafusco, J.J., Gearhart, D.A. and Terry Jr, A.V. (2007). Microtubule-associated targets in chlorpyrifos oxon hippocampal neurotoxicity. *Neuroscience*, 146(1), pp.330-339.
- Qiao, D., Seidler, F.J. and Slotkin, T.A. (2001). Developmental neurotoxicity of chlorpyrifos modeled *in vitro*: comparative effects of metabolites and other cholinesterase inhibitors on DNA synthesis in PC12 and C6 cells. *Environmental Health Perspectives*, 109(9), p.909.
- Quincozes-Santos, A., Nardin, P., De Souza, D.F., Gelain, D.P., Moreira, J.C., Latini, A., Gonçalves, C.A. and Gottfried, C. (2009). The janus face of resveratrol in astroglial cells. *Neurotoxicity Research*, 16(1), pp.30-41.
- Radio, N.M. and Mundy, W.R. (2008). Developmental neurotoxicity testing in vitro: models for assessing chemical effects on neurite outgrowth. *Neurotoxicology*, 29(3), pp.361-376.
- Radio, N.M., Breier, J.M., Reif, D.M., Judson, R.S., Martin, M., Houck, K.A., Mundy, W.R. and Shafer, T.J. (2015). Use of neural models of proliferation and neurite outgrowth to screen environmental chemicals in the ToxCast phase I library. *Applied In Vitro Toxicology*, 1(2), pp.131-139.
- Radio, N.M., Breier, J.M., Shafer, T.J. and Mundy, W.R. (2008). Assessment of chemical effects on neurite outgrowth in PC12 cells using high content screening. *Toxicological Sciences*, 105(1), pp.106-118.
- Radio, N.M., Freudenrich, T.M., Robinette, B.L., Crofton, K.M. and Mundy, W.R. (2010). Comparison of PC12 and cerebellar granule cell cultures for evaluating neurite outgrowth using high content analysis. *Neurotoxicology and Teratology*, 32(1), pp.25-35.
- Rahman, M.F., Mahboob, M., Danadevi, K., Banu, B.S. and Grover, P. (2002). Assessment of genotoxic effects of chlorpyrifos and acephate by the comet assay in mice leucocytes. *Mutation Research/Genetic Toxicology and Environmental Mutagenesis*, 516(1), pp.139-147.
- Rao, M., Campbell, J., Yuan, A., Kumar, A., Gotow, T., Uchiyama, Y. and Nixon, R. (2003). The neurofilament middle molecular mass subunit carboxyl-terminal tail domains is essential for the radial growth and cytoskeletal architecture of axons but not for regulating neurofilament transport rate. *The Journal of Cell Biology*, 163(5), pp. 1021-1031. <http://dx.doi.org/10.1083/jcb.200308076>
- Rao, X., Lai, D., and Huang, X. (2013). A New Method for Quantitative Real-Time Polymerase Chain Reaction Data Analysis. *Journal of Computational Biology*, 20(9), pp.703-711.
- Rasoul, G.M.A., Salem, M.E.A., Mechael, A.A., Hendy, O.M., Rohlman, D.S. and Ismail, A.A. (2008). Effects of occupational pesticide exposure on children applying pesticides. *Neurotoxicology*, 29(5), pp.833-838.
- Ray, D. and Richards, P. (2001). The potential for toxic effects of chronic, low-dose exposure to organophosphates. *Toxicology Letters*, 120(1-3), pp.343-351.

- Reigart, J.R. and Roberts, J.R. (1999). Recognition and management of pesticide poisonings. Washington, DC: US EPA. Office of Prevention, Pesticides, and Toxic Substances. Field and External Affairs Division. Certification and Worker Protection Branch.
- Rekart, J.L., Meiri, K. and Routtenberg, A. (2005). Hippocampal-dependent memory is impaired in heterozygous GAP-43 knockout mice. *Hippocampus*, 15(1), pp.1-7.
- Rice, D. and Barone, S. (2000). Critical periods of vulnerability for the developing nervous system: evidence from humans and animal models. *Environmental Health Perspectives*, 108(3), pp.511-533 .
- Richardson, R. (1995). Assessment of the neurotoxic potential of chlorpyrifos relative to other organophosphorus compounds: A critical review of the literature. *Journal of Toxicology and Environmental Health*, 44(2), 135-165. <http://dx.doi.org/10.1080/15287399509531952>
- Richardson, W.D., Kessaris, N. and Pringle, N. (2006). Oligodendrocyte wars. *Nature Reviews Neuroscience*, 7(1), p.11.
- Road, D. (2010). Molecular toxicology of neuropathy, *Toxicology Letters*, 5(3), pp.109-120.
- Robertson, K.D., Ait-Si-Ali, S., Yokochi, T., Wade, P.A., Jones, P.L. and Wolffe, A.P. (2000). DNMT1 forms a complex with Rb, E2F1 and HDAC1 and represses transcription from E2F-responsive promoters. *Nature Genetics*, 25(3), p.338.
- Robson, R.M. (1989). Intermediate filaments. *Current Opinion in Cell Biology*, 1(1), pp.36-43.
- Rohlman, D.S., Arcury, T.A., Quandt, S.A., Lasarev, M., Rothlein, J., Travers, R., Tamulinas, A., Scherer, J., Early, J., Marín, A. and Phillips, J. (2005). Neurobehavioral performance in preschool children from agricultural and non-agricultural communities in Oregon and North Carolina. *Neurotoxicology*, 26(4), pp.589-598.
- Rohlman, D.S., Bailey, S.R., Anger, W.K. and McCauley, L. (2001). Assessment of neurobehavioral function with computerized tests in a population of Hispanic adolescents working in agriculture. *Environmental Research*, 85(1), pp.14-24.
- Rohlman, D.S., Lasarev, M., Anger, W.K., Scherer, J., Stupfel, J. and McCauley, L. (2007). Neurobehavioral performance of adult and adolescent agricultural workers. *Neurotoxicology*, 28(2), pp.374-380.
- Ropero, S. and Esteller, M. (2007). The role of histone deacetylases (HDACs) in human cancer. *Molecular Oncology*, 1(1), pp.19-25.
- Rosenstock, L., Keifer, M., Daniell, W.E., McConnell, R., Claypoole, K. and Pesticide Health Effects Study Group (1991). Chronic central nervous system effects of acute organophosphate pesticide intoxication. *The Lancet*, 338(8761), pp.223-227.
- Routtenberg, A., Cantalops, I., Zaffuto, S., Serrano, P. and Namgung, U. (2000). Enhanced learning after genetic overexpression of a brain growth protein. *Proc Natl Acad Sci U S A*, 97(13), pp. 7657-62.
- Ruiz-Muñoz, A.M., Nieto-Escamez, F.A., Aznar, S., Colomina, M.T. and Sanchez-Santed, F. (2011). Cognitive and histological disturbances after chlorpyrifos exposure and chronic A β (1–42) infusions in Wistar rats. *Neurotoxicology*, 32(6), pp.836-844.
- Rutka, J.T., Hubbard, S.L., Fukuyama, K., Matsuzawa, K., Dirks, P.B. and Becker, L.E. (1994). Effects of antisense glial fibrillary acidic protein complementary DNA on the growth, invasion, and adhesion of human astrocytoma cells. *Cancer Research*, 54(12), pp.3267-3272.
- Sachana, M. and Hargreaves, A.J. (2012). Toxicological testing: *in vivo* and *in vitro* models. In *Veterinary Toxicology (Second Edition)* (pp. 62-79).

- Sachana, M., Flaskos, J. and Hargreaves, A.J. (2005). Effects of Chlorpyrifos and Chlorpyrifos-Methyl on the Outgrowth of Axon-Like Processes, Tubulin, and GAP-43 in N2a Cells. *Toxicology Mechanisms and Methods*, 15(6), pp. 405-410 .
- Sachana, M., Flaskos, J., Alexaki, E. and Hargreaves, A.J. (2003). Inhibition of neurite outgrowth in N2a cells by leptophos and carbaryl: effects on neurofilament heavy chain, GAP-43 and HSP-70. *Toxicology in Vitro: an International Journal Published in Association with BIBRA*, 17(1), pp. 115-120 .
- Sachana, M., Flaskos, J., Alexaki, E., Glynn, P. and Hargreaves, A.J. (2001). The toxicity of chlorpyrifos towards differentiating mouse N2a neuroblastoma cells. *Toxicology in vitro: an international journal published in association with BIBRA*, 15(4-5), pp. 369-372 .
- Sachana, M., Flaskos, J., Sidiropoulou, E., Yavari, C. and Hargreaves, A. (2008). Inhibition of extension outgrowth in differentiating rat C6 glioma cells by chlorpyrifos and chlorpyrifos oxon: Effects on microtubule proteins. *Toxicology in Vitro*, 22(5), pp.1387-1391.
- Sachana, M., Sidiropoulou, E., Flaskos, J., Harris, W., Robinson, A.J., Woldehiwet, Z. and Hargreaves, A.J. (2014). Diazoxon disrupts the expression and distribution of betaIII-tubulin and MAP 1B in differentiating N2a cells. *Basic and Clinical Pharmacology and Toxicology*, 114(6), pp. 490-496 .
- Sagara, J.I., Miura, K. and Bannai, S. (1993). Maintenance of neuronal glutathione by glial cells. *Journal of Neurochemistry*, 61(5), pp.1672-1676.
- Salazar-Arredondo, E., de Jesús Solís-Heredia, M., Rojas-García, E., Hernández-Ochoa, I. and Quintanilla-Vega, B. (2008). Sperm chromatin alteration and DNA damage by methylparathion, chlorpyrifos and diazinon and their oxon metabolites in human spermatozoa. *Reproductive Toxicology*, 25(4), pp.455-460.
- Salto, R., Vílchez, J.D., Girón, M.D., Cabrera, E., Campos, N., Manzano, M., Rueda, R. and López-Pedrosa, J.M. (2015). β -Hydroxy- β -Methylbutyrate (HMB) promotes neurite outgrowth in Neuro2a cells. *PLoS One*, 10(8), p.e0135614.
- Salvi, R.M., Lara, D.R., Ghisolfi, E.S., Portela, L.V., Dias, R.D. and Souza, D.O. (2003). Neuropsychiatric evaluation in subjects chronically exposed to organophosphate pesticides. *Toxicological Sciences : an Official Journal of the Society of Toxicology*, 72(2), pp. 267-271 .
- Salyha, Y. (2010). Biological effects assessment of chlorpyrifos and some aspects of its neurotoxicity. Visnyk of Lviv University. *Biology Series*, 54, pp.3-14 .
- Sanchez-Santed, F., Canadas, F., Flores, P., Lopez-Grancha, M. and Cardona, D. (2004). Long-term functional neurotoxicity of paraoxon and chlorpyrifos: behavioural and pharmacological evidence. *Neurotoxicology and Teratology*, 26(2), pp. 305-317 .
- Sandhu, M. A., Saeed, A. A., Khilji, M. S., Ahmed, A., Latif, M. S. and Khalid, N. (2013). Genotoxicity evaluation of chlorpyrifos: a gender related approach in regular toxicity testing. *J Toxicol Sci*, 38(2), pp. 237-44.
- Sattilaro, R.F., Dentler, W.L. and LeCluyse, E.L. (1981). Microtubule-associated proteins (MAPs) and the organization of actin filaments *in vitro*. *The Journal of Cell Biology*, 90(2), pp.467-473.
- Savage, E.P., Keefe, T.J., Mounce, L.M., Heaton, R.K., Lewis, J.A. and Burcar, P.J. (1988). Chronic neurological sequelae of acute organophosphate pesticide poisoning. *Archives of Environmental Health*, 43(1), pp. 38-45 .
- Schmuck, G. and Ahr, H.J. (1997). Improved *in vitro* method for screening organophosphate-induced delayed polyneuropathy. *Toxicology in vitro*, 11(3), pp.263-270.

- Schoenfeld, T.A. and Obar, R.A. (1994). Diverse distribution and function of fibrous microtubule-associated proteins in the nervous system. In *International review of cytology* (Vol. 151, pp. 67-137). Academic Press.
- Schopfer, L.M., Grigoryan, H., Li, B., Nachon, F., Masson, P. and Lockridge, O. (2010). Mass spectral characterization of organophosphate-labeled, tyrosine-containing peptides: characteristic mass fragments and a new binding motif for organophosphates. *Journal of Chromatography B*, 878(17-18), pp.1297-1311.
- Schubert, D., Humphreys, S., Baroni, C. and Cohn, M. (1969). *In vitro* differentiation of a mouse neuroblastoma. *Proceedings of the National Academy of Sciences*, 64(1), pp.316-323.
- Seaberg, R.M. and van der Kooy, D. (2003). Stem and progenitor cells: the premature desertion of rigorous definitions. *Trends in Neurosciences*, 26(3), pp.125-131.
- Senanayake, N. and Karalliedde, L. (1987). Neurotoxic effects of organophosphorus insecticides. *New England Journal of Medicine*, 316(13), pp.761-763.
- Shelanski, M.L., Gaskin, F. and Cantor, C.R. (1973). Microtubule assembly in the absence of added nucleotides. *Proceedings of the National Academy of Sciences*, 70(3), pp.765-768.
- Shen, Y., Mishra, R., Mani, S. and Meiri, K. F. (2008). Both cell-autonomous and cell non-autonomous functions of GAP-43 are required for normal patterning of the cerebellum *in vivo*. *Cerebellum (London, England)*, 7(3), pp. 451-466.
- Shibuki, K., Gomi, H., Chen, L., Bao, S., Kim, J.J., Wakatsuki, H., Fujisaki, T., Fujimoto, K., Katoh, A., Ikeda, T. and Chen, C. (1996). Deficient cerebellar long-term depression, impaired eyeblink conditioning, and normal motor coordination in GFAP mutant mice. *Neuron*, 16(3), pp.587-599.
- Sidiropoulou, E., Sachana, M., Flaskos, J., Harris, W., Hargreaves, A.J. and Woldehiwet, Z. (2009a). Diazinon oxon affects the differentiation of mouse N2a neuroblastoma cells. *Archives of Toxicology*, 83(4), pp.373-380.
- Sidiropoulou, E., Sachana, M., Flaskos, J., Harris, W., Hargreaves, A.J. and Woldehiwet, Z. (2009b). Diazinon oxon interferes with differentiation of rat C6 glioma cells. *Toxicology in Vitro*, 23(8), pp.1548-1552.
- Silva, R.F.M., Falcao, A.S., Fernandes, A., Gordo, A.C., Brito, M.A. and Brites, D. (2006). Dissociated primary nerve cell cultures as models for assessment of neurotoxicity. *Toxicology Letters*, 163(1), pp.1-9.
- Sindi, R. (2015). Chlorpyrifos and chlorpyrifos oxon induce neurite retraction and cytoskeletal disruption in mouse N2a cells and human neural progenitor stem cells. PhD thesis, Nottingham Trent University.
- Sindi, R.A., Harris, W., Arnott, G., Flaskos, J., Mills, C.L. and Hargreaves, A.J. (2016). Chlorpyrifos-and chlorpyrifos oxon-induced neurite retraction in pre-differentiated N2a cells is associated with transient hyperphosphorylation of neurofilament heavy chain and ERK 1/2. *Toxicology and applied pharmacology*, 308, pp.20-31.
- Singh, G. and Khurana, D. (2009). Neurology of acute organophosphate poisoning. *Neurology India*, 57(2), p.119.
- Singh, S. and Sharma, N. (2000). Neurological syndromes following organophosphate poisoning. *Neurology India*, 48(4), p.308.
- Skene, J. (1989). Axonal Growth-Associated Proteins. *Annual Review of Neuroscience*, 12(1), 127-156. <http://dx.doi.org/10.1146/annurev.neuro.12.1.127>

- Sloboda, R.D., Dentler, W.L. and Rosenbaum, J.L. (1976). Microtubule-associated proteins and the stimulation of tubulin assembly *in vitro*. *Biochemistry*, 15(20), pp.4497-4505.
- Slotkin, T. A. and Seidler, F. J. (2010). Diverse neurotoxicants converge on gene expression for neuropeptides and their receptors in an *in vitro* model of neurodifferentiation: effects of chlorpyrifos, diazinon, dieldrin and divalent nickel in pc12 cells. *Brain research*, 1353, pp. 36-52.
- Slotkin, T.A. (2004). Cholinergic systems in brain development and disruption by neurotoxicants: nicotine, environmental tobacco smoke, organophosphates. *Toxicology and Applied Pharmacology*, 198(2), pp.132-151.
- Smith, C. and Eisenstein, M. (2005). Automated imaging: data as far as the eye can see. *Nature methods*, 2, pp.547-55.
- Song, X., Violin, J., Seidler, F., and Slotkin, T. (1998). Modeling the developmental neurotoxicity of chlorpyrifos *in vitro*: Macromolecule synthesis in PC12 cells. *Toxicology and Applied Pharmacology*, 151(1), pp.182-191.
- Sprague, G.L. and Castles, T.R. (1985). Estimation of the delayed neurotoxic potential and potency for a series of triaryl phosphates using an *in vitro* test with metabolic activation. *Neurotoxicology*, 6(1), pp.79-86.
- Steenland, K., Jenkins, B., Ames, R.G., O'Malley, M., Chrislip, D. and Russo, J. (1994). Chronic neurological sequelae to organophosphate pesticide poisoning. *American Journal of Public Health*, 84(5), pp.731-736
- Steevens, J.A. and Benson, W.H. (1999). Toxicological interactions of chlorpyrifos and methyl mercury in the amphipod, *Hyalella azteca*. *Toxicological Sciences: An Official Journal of The Society of Toxicology*, 52(2), pp.168-177.
- Stephens, A.S., Stephens, S.R. and Morrison, N.A. (2011). Internal control genes for quantitative RT-PCR expression analysis in mouse osteoblasts, osteoclasts and macrophages. *BMC research notes*, 4(1), p.410.
- Stephens, R., Spurgeon, A., Calvert, I., Beach, J., Levy, L., Harrington, J. and Berry, H. (1995). Neuropsychological effects of long-term exposure to organophosphates in sheep dip. *The Lancet*, 345(8958), pp.1135-1139.
- Strelkov, S.V., Herrmann, H. and Aebi, U. (2003). Molecular architecture of intermediate filaments. *Bioessays*, 25(3), pp.243-251.
- Tascos, N.A., Parr, J. and Gonatas, N.K. (1982). Immunocytochemical study of the glial fibrillary acidic protein in human neoplasms of the central nervous system. *Human Pathology*, 13(5), pp.454-458.
- Tata, A., Velluto, L., D'Angelo, C. and Reale, M. (2014). Cholinergic system dysfunction and neurodegenerative diseases: cause or effect?. *CNS & Neurological Disorders-Drug Targets .Formerly Current Drug Targets-CNS and Neurological Disorders*, 13(7), pp. 1294-1303 .
- Theriot, J. (1994). Regulation of the actin cytoskeleton in living cells. *Seminars in Cell Biology*, 5(3), 193-199. <http://dx.doi.org/10.1006/scel.1994.1024>
- Thiermann, H., Szinicz, L., Eyer, F., Worek, F., Eyer, P., Felgenhauer, N. and Zilker, T. (1999). Modern strategies in therapy of organophosphate poisoning. *Toxicology Letters*, 107(1-3), pp.233-239.

- Thoma, K. and Nicholson, B. (1989). Pesticide losses in runoff from a horticultural catchment in South Australia and their relevance to stream and reservoir water quality. *Environmental Technology Letters*, 10(1), pp.117-129.
- Tilney, L.G., Bryan, J., Bush, D.J., Fujiwara, K., Mooseker, M.S., Murphy, D.B. and Snyder, D.H. (1973). Microtubules: evidence for 13 protofilaments. *The Journal of Cell Biology*, 59(2), pp.267-275.
- Timchalk, C., Nolan, R.J., Mendrala, A.L., Dittenber, D.A., Brzak, K.A. and Mattsson, J.L. (2002). A physiologically based pharmacokinetic and pharmacodynamic (PBPK/PD) model for the organophosphate insecticide chlorpyrifos in rats and humans. *Toxicological Sciences*, 66(1), pp.34-53.
- Timofeeva, O. and Gordon, C. (2002). EEG spectra, behavioral states and motor activity in rats exposed to acetylcholinesterase inhibitor chlorpyrifos. *Pharmacology Biochemistry and Behavior*, 72(3), pp.669-679.
- Tischfield, M.A. and Engle, E.C. (2010). Distinct α - and β -tubulin isotypes are required for the positioning, differentiation and survival of neurons: new support for the 'multi-tubulin' hypothesis. *Bioscience Reports*, 30(5), pp.319-330.
- Towbin, H., Staehelin, T. and Gordon, J. (1979). Electrophoretic transfer of proteins from polyacrylamide gels to nitrocellulose sheets: procedure and some applications. *Proceedings of the National Academy of Sciences*, 76(9), pp.4350-4354.
- Tran, S., Puhar, A., Ngo-Camus, M. and Ramarao, N. (2011). Trypan Blue Dye Enters Viable Cells Incubated with the Pore-Forming Toxin HlyII of *Bacillus cereus*. *Plos ONE*, 6(9), e22876. <http://dx.doi.org/10.1371/journal.pone.0022876>
- Tsacopoulos, M. and Magistretti, P.J. (1996). Metabolic coupling between glia and neurons. *Journal of Neuroscience*, 16(3), pp.877-885.
- Tsujimura, K., Tanaka, J., Ando, S., Matsuoka, Y., Kusubata, M., Sugiura, H., Yamauchi, T. and Inagaki, M. (1994). Identification of phosphorylation sites on glial fibrillary acidic protein for cdc2 kinase and Ca²⁺-calmodulin-dependent protein kinase II. *The Journal of Biochemistry*, 116(2), pp.426-434.
- Untergasser, A., Cutcutache, I., Koressaar, T., Ye, J., Faircloth, B.C., Remm, M. and Rozen, S.G. (2012). Primer3—new capabilities and interfaces. *Nucleic Acids Research*, 40(15), pp.e115-e115.
- Urnov, F. D., Wolffe, A. P. and Guschin, D. (2001). Molecular mechanisms of corepressor function. *Curr Top Microbiol Immunol*, 254, pp. 1-33.
- Vallee, R. (1980). Structure and phosphorylation of microtubule-associated protein 2 (MAP 2). *Proceedings of the National Academy of Sciences*, 77(6), pp.3206-3210.
- Vallee, R.B. and Bloom, G.S. (1991). Mechanisms of fast and slow axonal transport. *Annual Review of Neuroscience*, 14(1), pp.59-92.
- Van der Meulen, J.D.M., Houthoff, H.J. and Ebels, E.J. (1978). Glial fibrillary acidic protein in human gliomas. *Neuropathol Appl Neurobiol*, 4(3), pp.177-190.
- Van Tienhoven, M., Atkins, J., Li, Y. and Glynn, P. (2002). Human neuropathy target esterase catalyzes hydrolysis of membrane Lipids. *Journal of Biological Chemistry*, 277(23), pp. 20942-20948.

- Vargas-Bernal, R., Rodríguez-Miranda, E. and Herrera-Pérez, G. (2012). Evolution and expectations of enzymatic biosensors for pesticides. In *Pesticides-Advances in Chemical and Botanical Pesticides*. InTech.
- Velasco, M.E., Dahl, D., Roessmann, U. and Gambetti, P. (1980). Immunohistochemical localization of glial fibrillary acidic protein in human glial neoplasms. *Cancer*, 45(3), pp.484-494.
- Veronesi, B. (1992). Organophosphorus-induced delayed neuropathy. *Clinical and Experimental Toxicology of Organophosphates and Carbamates*, p.114.
- Vescovi, A.L., Parati, E.A., Gritti, A., Poulin, P., Ferrario, M., Wanke, E., Frölichsthal-Schoeller, P., Cova, L., Arcellana-Panlilio, M., Colombo, A. and Galli, R. (1999). Isolation and cloning of multipotential stem cells from the embryonic human CNS and establishment of transplantable human neural stem cell lines by epigenetic stimulation. *Experimental neurology*, 156(1), pp.71-83.
- Walker, J.M. (2002). The bicinchoninic acid (BCA) assay for protein quantitation. In *The protein protocols handbook* (pp. 11-14). Humana Press.
- Wall, M.J. (2005). Short-term synaptic plasticity during development of rat mossy fibre to granule cell synapses. *European Journal of Neuroscience*, 21(8), pp.2149-2158.
- Wang, J., Zhu, L., Xie, H., Shao, B. and Hou, X. (2014). The enzyme toxicity and genotoxicity of chlorpyrifos and its toxic metabolite TCP to zebrafish *Danio rerio*. *Ecotoxicology*, 23(10), pp. 1858-69.
- Wang, P. and Zhao, L. (2017). The Expression change of GFAP and HMGB1 in primary cultured astrocytes exposed to chlorpyrifos and lipopolysaccharide. pp.161-169.
- Wauchope, R.D., Buttler, T.M., Hornsby, A.G., Augustijn-Beckers, P.W.M. and Burt, J.P. (1992). The SCS/ARS/CES pesticide properties database for environmental decision-making. In *Reviews of environmental contamination and toxicology* (pp. 1-155). Springer, *New York, NY*.
- Weingarten, M. D., Lockwood, A. H., Hwo, S-Y. and Kirschner, M. W. (1975). A protein factor essential for microtubule assembly. *Proceedings of the National Academy of Science of the United States of America*, 72 (5), pp.1858-1862.
- Weinstein, D.E., Shelanski, M.L. and Liem, R.K. (1991). Suppression by antisense mRNA demonstrates a requirement for the glial fibrillary acidic protein in the formation of stable astrocytic processes in response to neurons. *The Journal of Cell Biology*, 112(6), pp.1205-1213.
- Westermarck, B. (1973). The deficient density-dependent growth control of human malignant glioma cells and virus-transformed glia-like cells in culture. *International Journal of Cancer*, 12(2), pp.438-451
- Whang, J., Schomburg, C., Glotfelty, D. and Taylor, A. (1993). Volatilization of Fonofos, Chlorpyrifos, and Atrazine from Conventional and No-Till Surface Soils in the Field. *Journal of Environment Quality*, 22(1), p.173.
- Whitney, K.D., Seidler, F.J. and Slotkin, T.A. (1995). Developmental neurotoxicity of chlorpyrifos: cellular mechanisms. *Toxicology and Applied Pharmacology*, 134(1), pp.53-62.
- WHO (2001). Organophosphorus pesticides in the environment- Integrated risk assessment. *Geneva*.
- WHO (2008). The global burden of disease- 2004 updated. *Geneva*.

- Wilhelmsson, U., Eliasson, C., Bjerkvig, R. and Pekny, M. (2003). Loss of GFAP expression in high-grade astrocytomas does not contribute to tumor development or progression. *Oncogene*, 22(22), p.3407.
- Wilson, J. and Hunt, T. (2014). *Molecular biology of the cell: the problems book*. Garland Science.
- Wilson, M.S., Graham, J.R. and Ball, A.J. (2014). Multiparametric High Content Analysis for assessment of neurotoxicity in differentiated neuronal cell lines and human embryonic stem cell-derived neurons. *Neurotoxicology*, 42, pp.33-48.
- Winder, C. and Balouet, J.C. (2001). Aircrew Exposure to Chemicals in Aircraft: Symptoms of Irritation and Toxicity. *Journal of Occupational Health and Safety*, 17(2), pp.471-483.
- Witt, O., Deubzer, H. E., Milde, T. and Oehme, I. (2009). HDAC family: What are the cancer relevant targets?. *Cancer Lett*, 277(1), pp. 8-21.
- Wolfe, R.A., Sato, G.H. and McClure, D.B. (1980). Continuous culture of rat C6 glioma in serum-free medium. *The Journal of Cell Biology*, 87(2), pp.434-441.
- Wright, L.S., Prowse, K.R., Wallace, K., Linskens, M.H. and Svendsen, C.N. (2006). Human progenitor cells isolated from the developing cortex undergo decreased neurogenesis and eventual senescence following expansion *in vitro*. *Experimental cell research*, 312(11), pp.2107-2120.
- Yang, C.C. and Deng, J.F. (2007). Intermediate syndrome following organophosphate insecticide poisoning. *Journal of the Chinese Medical Association*, 70(11), pp.467-472.
- Yang, D., Howard, A., Bruun, D., Ajua-Alemanj, M., Pickart, C. and Lein, P.J. (2008). Chlorpyrifos and chlorpyrifos-oxon inhibit axonal growth by interfering with the morphogenic activity of acetylcholinesterase. *Toxicology and Applied Pharmacology*, 228(1), pp.32-41.
- Yang, Z. and Wang, K.K. (2015). Glial fibrillary acidic protein: from intermediate filament assembly and gliosis to neurobiomarker. *Trends in Neurosciences*, 38(6), pp.364-374.
- Yong, V.W. (1992). Proliferation of human and mouse astrocytes in vitro: signalling through the protein kinase C pathway. *Journal of the Neurological Sciences*, 111(1), pp.92-103.
- Yuan, A., Rao, M., Veeranna, and Nixon, R. (2012). Neurofilaments at a glance. *Journal of Cell Science*, 125(14), 3257-3263. <http://dx.doi.org/10.1242/jcs.104729>
- Zabik, J. and Seiber, J. (1993). Atmospheric Transport of Organophosphate Pesticides from California's Central Valley to the Sierra Nevada Mountains. *Journal of Environment Quality*, 22(1), p.80. <http://dx.doi.org/10.2134/jeq1993.00472425002200010011x>
- Zarei, M. H., Soodi, M., Qasemian-Lemraski, M., Jafarzadeh, E. and Taha, M. F. (2016). Study of the chlorpyrifos neurotoxicity using neural differentiation of adipose tissue-derived stem cells. *Environ Toxicol*, 31(11), pp. 1510-1519.
- Zhang, H.S., Xiao, J.H., Cao, E.H. and Qin, J.F. (2005). Homocysteine inhibits store-mediated calcium entry in human endothelial cells: evidence for involvement of membrane potential and actin cytoskeleton. *Molecular and Cellular Biochemistry*, 269(1), pp.37-47.
- Zhang, Z., Zoltewicz, J.S., Mondello, S., Newsom, K.J., Yang, Z., Yang, B., Kobeissy, F., Guingab, J., Glushakova, O., Robicsek, S. and Heaton, S. (2014). Human traumatic brain injury induces autoantibody response against glial fibrillary acidic protein and its breakdown products. *PloS One*, 9(3), p.e92698.
- Zhao, Q., Dourson, M. and Gadagbui, B. (2006). A review of the reference dose for chlorpyrifos. *Regulatory Toxicology and Pharmacology*, 44(2), pp.111-124.

Zonta, M., Angulo, M.C., Gobbo, S., Rosengarten, B., Hossmann, K.A., Pozzan, T. and Carmignoto, G. (2003). Neuron-to-astrocyte signaling is central to the dynamic control of brain microcirculation. *Nature Neuroscience*, 6(1), p.43.

Appendix

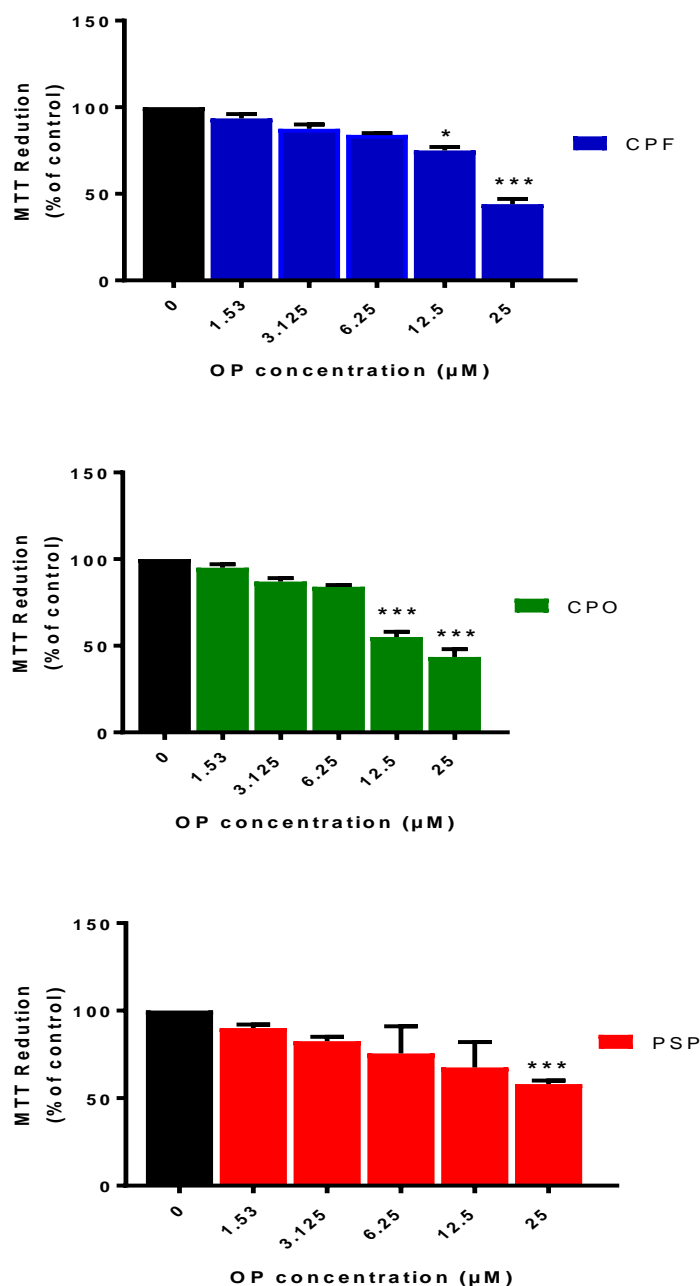


Figure 8.1. Dose estimation of the effects of CPF, CPO and PSP on MTT reduction in differentiating N2a cells after 24 h.

N2a cells were induced to different concentrations (1.53, 3.125, 6.25, 12.5, 25 µM) of CPF (panel A), CPO (panel B) and PSP (panel C), of induction of cell differentiation, and the levels of MTT reduction were measured to evaluate cell viability. Results are expressed as a mean percentage of the corresponding untreated control \pm SEM from five separate experiments. Statistical significance of data was analysed using one way ANOVA. When an SEM bar is not apparent, the error is smaller than the symbol size (* $p < 0.05$, *** $p < 0.001$).

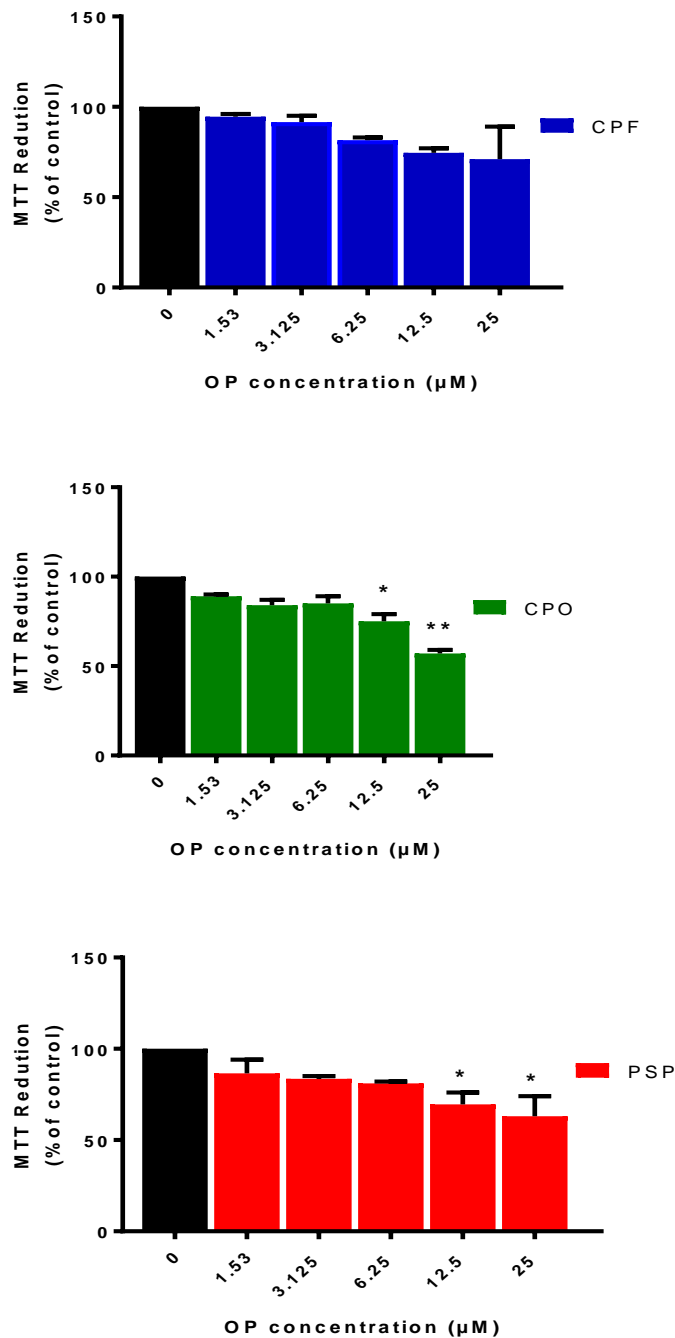


Figure 8.2. Dose estimation of the effects of CPF, CPO and PSP on MTT reduction in differentiating C6 cells after 24 h.

C6 cells were induced to different concentrations (1.53, 3.125, 6.25, 12.5, 25 µM) of CPF (panel A), CPO (panel B) and PSP (panel C), of induction of cell differentiation, and the levels of MTT reduction were measured to evaluate cell viability. Results are expressed as a mean percentage of the corresponding untreated control \pm SEM from five separate experiments. Statistical significance of data was analysed using one way ANOVA. When an SEM bar is not apparent, the error is smaller than the symbol size (* $p < 0.05$, *** $p < 0.001$).

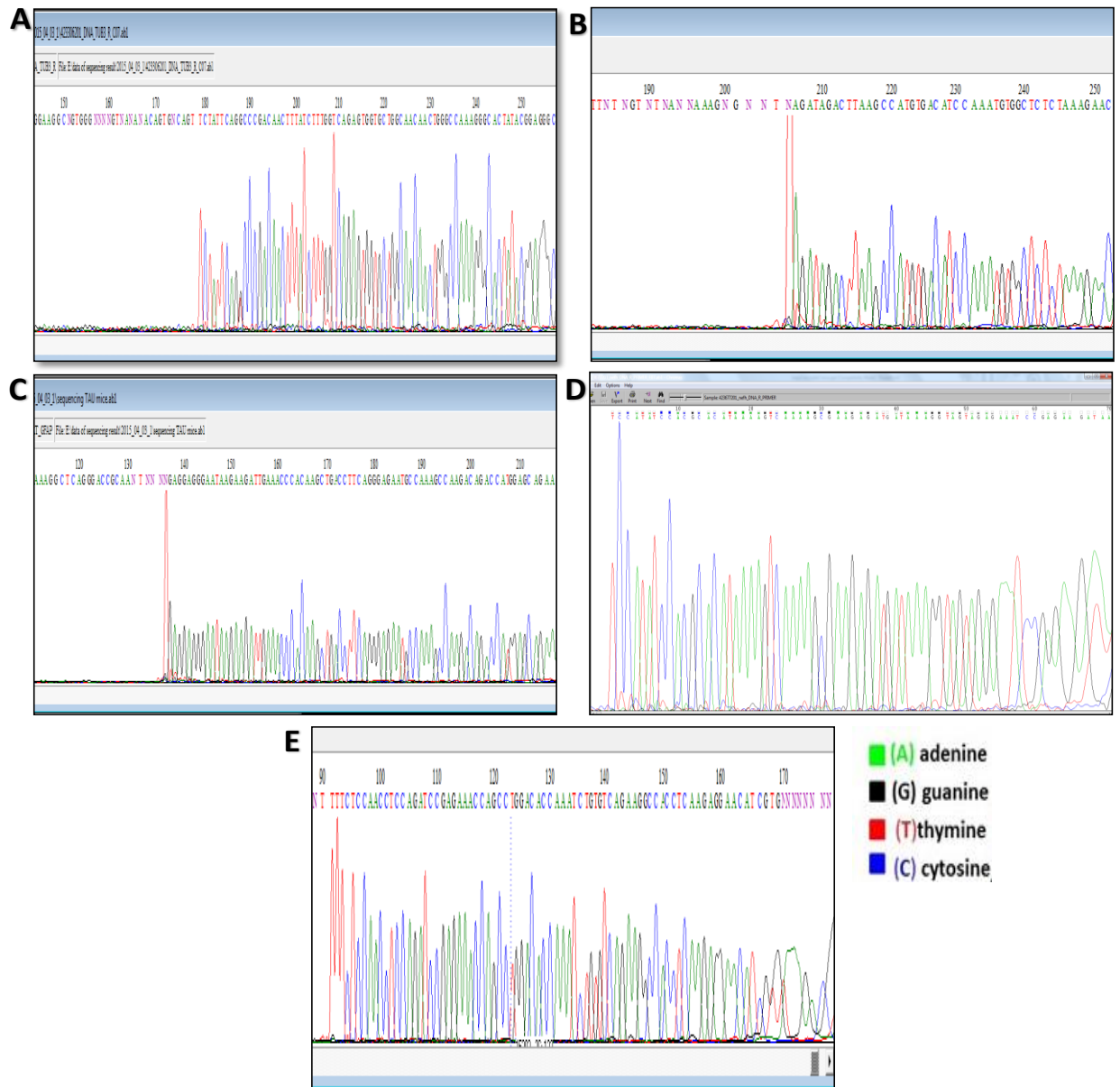


Figure 8.3. Electropherogram data for MAP2 (panel A), TUBB3 (panel B), MAPT (panel C), NEFH (panel D) and GAP43 (panel E) PCR sequenced product in N2a cell lines.

The bases represented by N (nucleotides) were replaced by the specific bases identified by coloured peaks (A) Adenine (Green), (G) Guanine (Black), (T) Thymine (Red), (C) Cytosine (Blue).

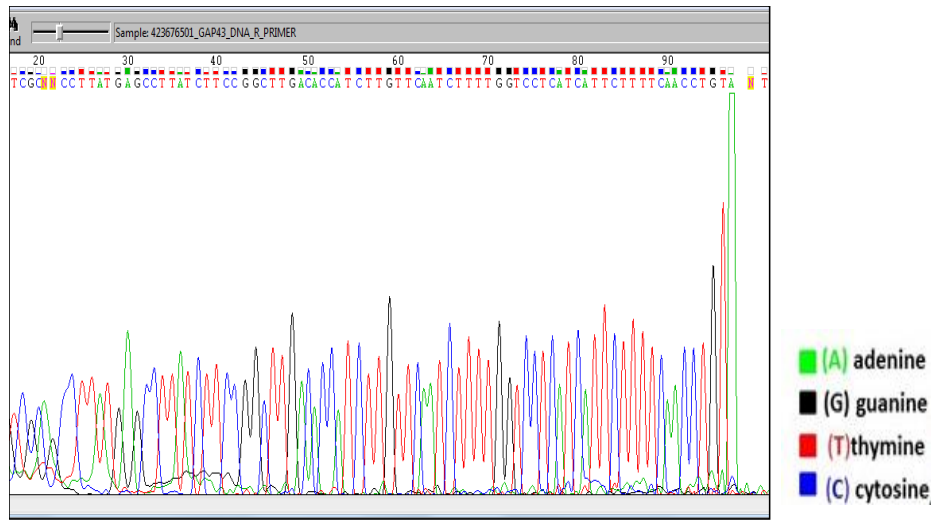


Figure 8.4. Electropherogram data for GFAP PCR sequenced product in C6 cell lines.

The bases represented by N (nucleotides) were replaced by the specific bases identified by coloured peaks (A) Adenine (Green), (G) Guanine (Black), (T) Thymine (Red), (C) Cytosine (Blue).

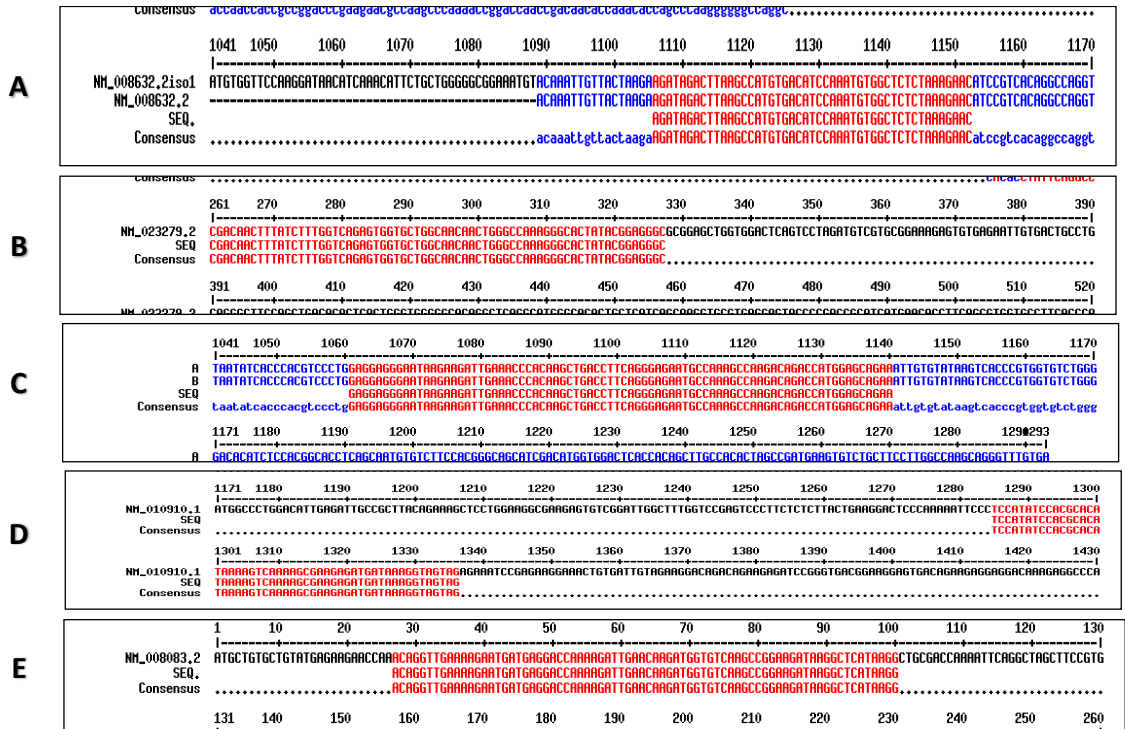


Figure 8.5. Sequences alignments.

Examples of alignments matching cDNA and sequencing data for the genes in N2a cell lines: *MAP2* (panel A), *TUBB3* (panel B), *MAPT* (panel C), *NEFH* (panel D) and *GAP43* (panel E).

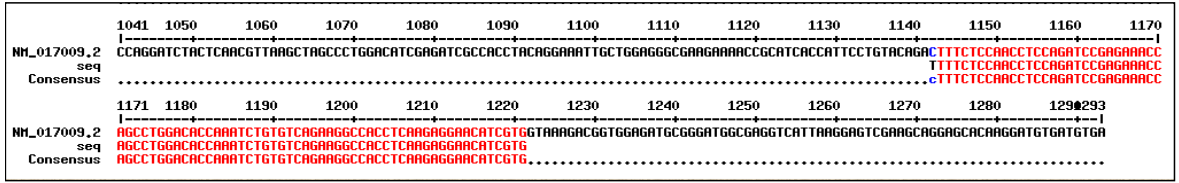


Figure 8.6. Sequences alignments.

Example of alignments matching between cDNA and sequencing data for *GFAP* in C6 cell line.

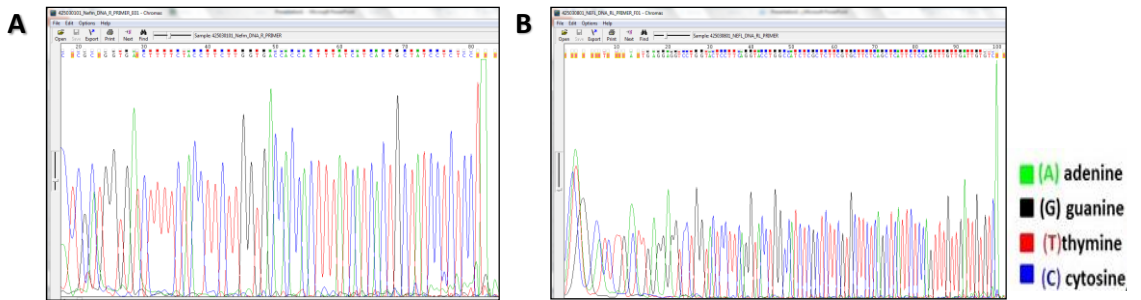


Figure 8.7. Electropherogram data for NEFM (panel A) and NEFL (panel B) PCR sequenced product in N2a cell lines.

The bases represented by N (nucleotides) were replaced by the specific bases identified by coloured peaks (A) Adenine (Green), (G) Guanine (Black), (T) Thymine (Red), (C) Cytosine (Blue).

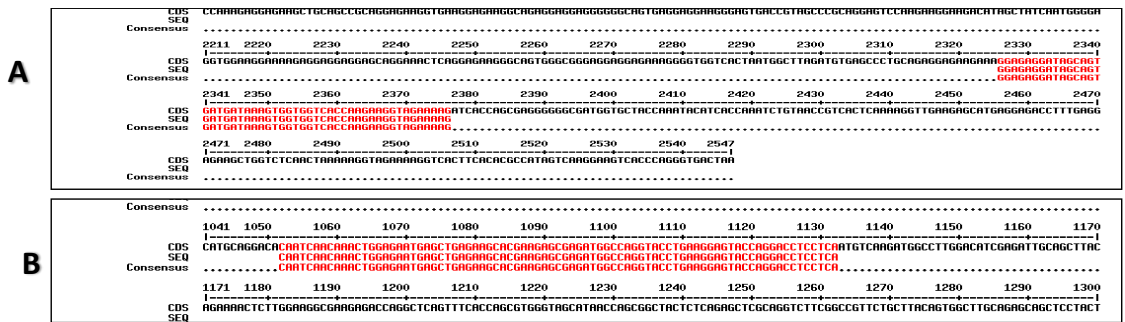
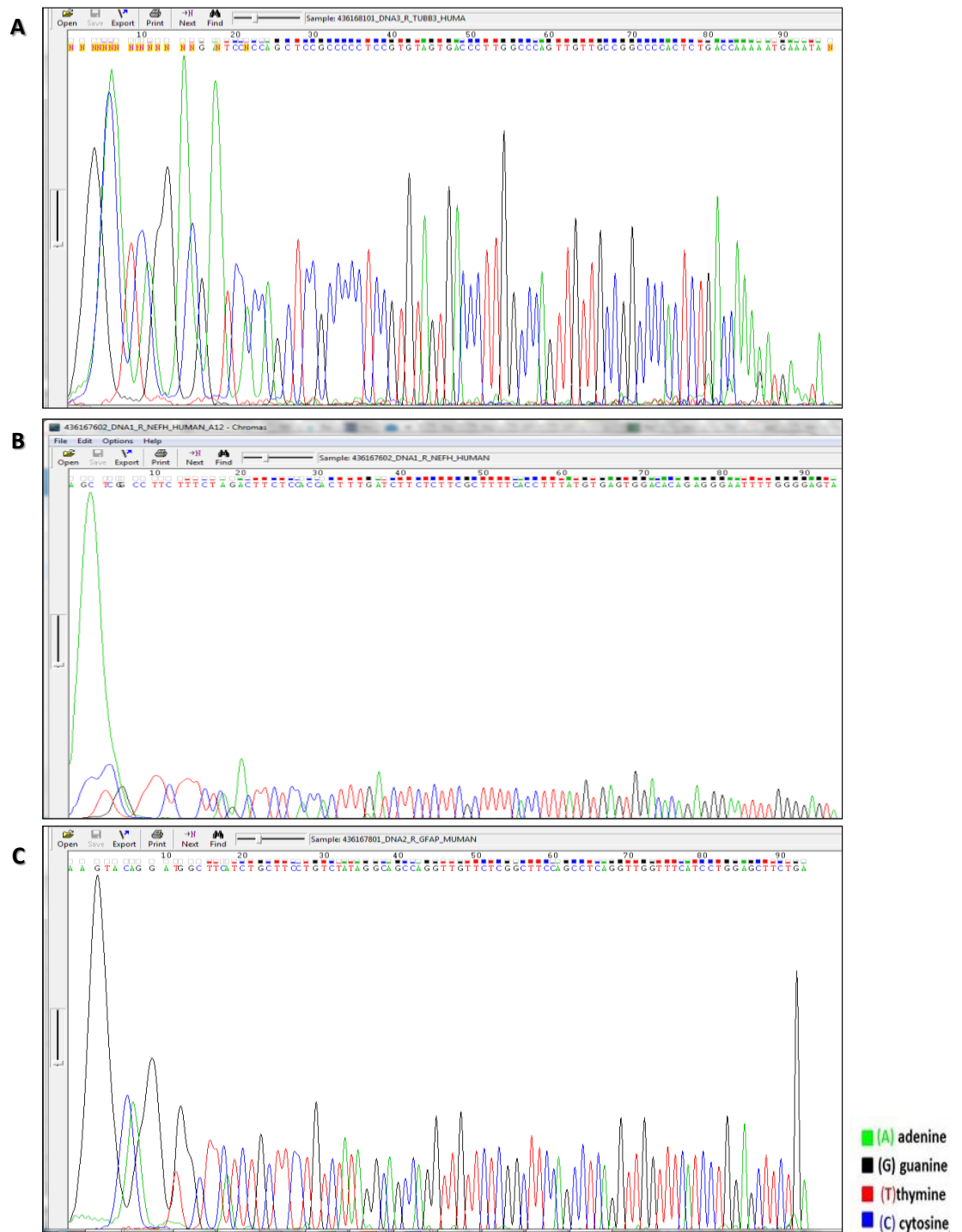


Figure 8.8. Sequences alignments.

Example of alignments matching between cDNA and sequencing data for the genes in N2a cell lines: *NEFM* (panel A) and *NEFL* (panel B).



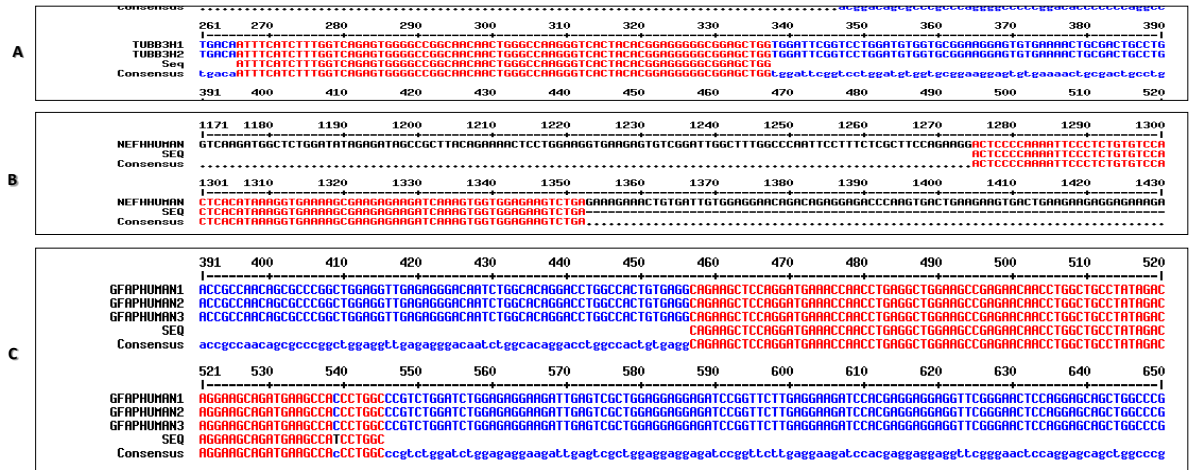


Figure 8. 2. Sequences alignments.

The alignments matching between cDNA and sequencing data for the genes in RenCells CX cell lines: *TUBB3* (panel A), *NEFH* (panel B), *GFAP* (panel C).